# CHARACTERISATION OF PROTEINS AND RNA EXPRESSED IN SYNCYTIOTROPHOBLAST MEMBRANE EXTRACELLULAR VESICLES (STB-EVs) IN PREECLAMPSIA

Dr Toluwalase Ayobami Awoyemi

Hertford college

A thesis submitted for the degree of Doctor of Philosophy

Hilary term 2022

44,138 words

This thesis is submitted to the University of Oxford in partial fulfilment of the Doctor of Philosophy degree requirements.

The thesis is my work and describes my research, except where otherwise stated.

Copyright © Toluwalase Ayobami Awoyemi

All rights reserved

**ACKNOWLEDGEMENTS**

Since I started my DPhil, I have pondered what to write on this page. Now that I am done, I still find it challenging to write. These past years have been filled with rapid growth. I have pushed myself harder, worked smarter, and longer dreamt more ambitiously, leapt instead of running, running instead of walking, and walked instead of crawling. This thesis is a testimony that dreams do not correlate with societal norms. Like they say in Nigeria, it is a story of a *small boy, big dreams, and a bigger God*. When I look back, what made a difference was the people I met during my DPhil, not necessarily how hard I worked. People who have gone out of their way to help me achieve my dreams.

To start with, my dad and role model, Dr Olatunbosun Oladeninde Awoyemi, is one of the most selfless men I have ever had the pleasure of knowing. The level of comfort he had to sacrifice to see me excel is beyond what words can describe. My family and siblings, Oluwatomisin, Oduntan, Ajulooluwa, and Towooluwa, are all incredible. I will never understand how tough it must have been to be unable to see me for three years but still be so supportive and loving.

Prof Manu Vatish, you are an angel in human form. I could not have done this without you. I can write another thesis on how incredible you are and how the world is better because you are in it. You have made yourself more than a supervisor. You became a father when I needed one, a brother when I needed one, a friend when I needed one, a hype-man when I needed one, a cheerleader when I needed one, a sounding board when I needed one and my conscience when I needed one. Professor Stephen Kennedy, you invested and believed in me more than anyone has ever done. You ensured I had everything I wanted. Nothing was ever too small or too big for me to accomplish because I knew you were by my side all the way. I am so lucky to have crossed paths with you and Manu. This is an experience I will always cherish.

Prof. Chris Redman, Dr Wei Zhang, and Dr Sofia Cerdeira, words fail me as I attempt to describe how your mentorship, guidance, friendship, and education have shaped me over the past years. You have taken great interest in my development as a scientist, clinician, and individual. Whenever I wanted to brainstorm or plan, your brains are my favourite to pick. I will fondly remember how generous you were to me. Dr Neva Kandzija taught me my first set of experiments and were my first friend in the group. I will always cherish my friendship and help when I was a novice. Dr Rannya Ri, for your friendship and help with discussions about clinical medicine. I am happy I met you. Babatomisin Adeniran, though I may not say it often, having another Nigerian as a friend in the department was one of the reasons, I was always excited while working. It was effortless to talk to you and discuss in Yoruba or Pidgin.

To the fantastic four; Shuhan Jiang, Maryam Rahbar, Prassana Logenthiran and Karanjit Das. You all made difficult days fun. It is difficult to imagine what science would mean without Maryam's marvelousness, Shuhan's selflessness, Prassana's collegiality, and Karan's inquisitiveness. Thank you to the fantastic team Manu, and Kennedy past and present, Carolina Motta Mejia, William Cooke, Emily Mazey, Emily Hyde, Yosuke Matsumiya, Gabriel Jones, Faheem Seedat, Catarina Dos Palmos, Yushi Abe, Josephine Agyeman-Duah, Wahyu Santosa, Shobana Nagraj, Abigail Takyi, Gavin Collett, Adele Winsey, Linda Holden, Fenella Roseman, and Lotoyah Carty. Thanks to my Thames office and friends, Magda Mareckova, Ruth Appeltant and Danielle Perro, all the exchange students who made my experience richer and more fun; Drs Daniela Iaccarino, Sina Raiss, Cathy Wang, Qing Cao, Ezekiel Musa, and Alice Buchan.

To the members of my inner circle and numerous friends, home and abroad, to name a few; Dr Eloho Olojakpoke, Dr Ayokunle Adenipekun, Dr Babatunde Ogunsanwo, Dr Olubukola Adedayo, Semilore Atere, my great (football and travel) friend; Dr Sonia Deatoni, mentors from University College Hospital, Dr Aje, Prof. Omigbodun, Dr Ogah, Dr Oladokun, Dr Adeoye, and Dr Adesina.

To my funding bodies; Rhode's trust, Rhodes West African selection committee, and friends of Rhodes West Africa, especially Ike Chioke, Andrew Nevin, Uma Kymal, Sangu Delle, Black Heart Foundation, Sidney Perry Foundation, Hertford College (Alan Locke Scholarship), Medical Sciences Division (Goodger and Schorstein Scholarship), Rhodes West Africa scholars; Emmanuelle Dankwa, Godwin Nwagele, Boluwatife Cole and Elizabeth Nwarueze.

To the research midwives, Linda Holden, Fenella Roseman and Lotoyah Carty and all the patients, who generously offered biological samples to complete this project.

Nations will come to my light, and kings (and queens) to the brightness of my dawn

Isiah 60:3

My patients who spurred me on to look for solutions to their afflictions and my dad; Dr Olatunbosun Awoyemi

## LIST OF ABBREVIATIONS

| | |
|---|---|
| ALIX | ALG-2 interacting protein X |
| BCA | Bicinchonic assay |
| Bio-M | BODIPY FL N-(2-Aminoethyl) Maleimide |
| CALX | Calnexin |
| CD63 | Cluster of differentiation 63 |
| cDNA | Complementary deoxyribonucleic acid |
| CHMP4 | Charged multivesicular body protein 4 |
| COL17A1 | Collagen 17 alpha1 |
| Cq | Quantification Cycle |
| CytC | Cytochrome C |
| DEG | Differentially expressed genes |
| DEM | Differentially expressed micro ribonucleic acids |
| DEP | Differentially expressed proteins |
| dNTP | Deoxynucleotide triphosphate |
| ESCRT | Endosomal sorting complexes required for transport |
| EV | Extracellular vesicles |
| FC | Fold change |
| FLT-1 | FMS like tyrosine kinase 1 |
| FLNB | Filamin B |
| FSC | Forward Scatter |
| fPBS | Filtered phosphate buffered saline |
| X g | centrifugal force |
| GGI | Gene-Gene Interaction |
| HRP | Horseradish peroxidase |

| | |
|---|---|
| HLA I/II | Human leukocyte antigen I /II |
| HUVEC | Human umbilical vein endothelial cells |
| LFC | Log 2 fold change |
| LFQ | Label free quantification |
| MAPK | Mitogen activated protein kinases |
| MESF | Molecules of equivalent soluble fluorochrome |
| mg | Milligrams |
| mL | Millilitres |
| M\L STB-EVs | Medium/Large syncytiotrophoblast membrane extracellular vesicles |
| mRNA | Messenger ribonucleic acid |
| miRNA | Micro ribonucleic acid |
| microRNA | Micro ribonucleic acid |
| NEP | Neprilysin |
| NP | Normal pregnancy |
| NTA | Nanoparticle tracking analysis |
| OR | Odds ratio |
| PAPP-A2 | Pappalysin A2 |
| PBS | Phosphate buffered saline |
| PE | Preeclampsia |
| PH | Placenta homogenate |
| PLAP | Placenta alkaline phosphatase |
| PL or P | Placenta lysate |
| PPI | Protein-Protein Interaction |
| PVDF | Polyvinylidene difluoride |
| RBC | Red blood cell |

| | |
|---|---|
| RNA | Ribonucleic acid |
| R-PE | R Phycoerythrin |
| RR | Relative Risk |
| RT-qPCR | Reverse transcription (quantitative) polymerase chain reaction |
| SSC | Side scatter |
| S STB-EVs | Small syncytiotrophoblast membrane extracellular vesicles |
| STB-EVs | Syncytiotrophoblast membrane extracellular vesicles |
| sRNA | Small ribonucleic acid |
| SR-BI | Scavenger receptor class B, type 1 |
| TEM | Transmission electron microscopy |
| TSG101 | Tumour susceptibility gene 101 |
| WB | Western blot |
| WBC | White blood cell |
| µg | Micrograms |
| µl | Microlitres |

# Table of Contents

**Abstract** ..... 16

**CHAPTER 1**

**1.1 Background** ..... 19

**1.2 Classification of Preeclampsia** ..... 20

**1.3 Risk factors of Preeclampsia** ..... 21

**1.4 Complications of Preeclampsia** ..... 22

**1.5 Mechanistic theories of Preeclampsia** ..... 23

**1.6 Syncytiotrophoblast membrane extracellular vesicle (STB-EVs)** ..... 25

**1.6.1 Classification of syncytiotrophoblast membrane extracellular vesicle (STB-EVs)** ..... **25**

**1.6.2 Isolation and enrichment of trophoblast derived membrane extracellular vesicles** ..... **26**

**1.6.3 Biodistribution of EVs and STB-EVs** ..... **28**

**1.6.4 Detection of STB-EVs in biofluids** ..... **29**

**1.6.5 Biogenesis of syncytiotrophoblast membrane extracellular vesicle (STB-EVs)** ..... **30**

**1.6.5.1 S STB-EVs (including exosomes) biogenesis** ..... 32

**1.6.5.2 M/L STB-EVs (including microvesicles) biogenesis** ..... 34

**1.6.5.3 Apoptotic bodies** ..... 35

**1.6.6 Preferential targeting and sorting molecules into syncytiotrophoblast membrane extracellular vesicles** ..... **36**

**1.6.7 Syncytiotrophoblast membrane extracellular vesicle cellular entry mechanisms** ..... **37**

**1.6.8 Diagnostic potential** ..... **38**

**1.6.8.1 Diagnostic potential: syncytiotrophoblast membrane extracellular vesicle expressed diagnostic microRNAs in preeclampsia** ..... 38

**1.6.8.2 Diagnostic potential: syncytiotrophoblast membrane extracellular vesicle expressed proteins in preeclampsia** ..... 39

**1.6.8.3 Diagnostic potential: syncytiotrophoblast membrane extracellular vesicle expressed diagnostic metabolites, messenger RNA, lipids, and DNA in preeclampsia** ..... 40

**1.6.9 Mechanisms of action of STB-EVs in preeclampsia** ..... **41**

**1.6.9.1 PE STB-EVs are inflammatory** ..... 41

**1.6.9.2 PE STB-EVs are anti-angiogenic and cause endothelial dysfunction** ..... 41

**1.6.9.3 PE STB-EVs promote abnormal coagulation** ..... 42

**1.6.10 Challenges of studying/researching STB-EVs in pregnancy and preeclampsia** ..... **42**

1.6.10.1 Nomenclature and universal STB-EV markers ..... 42

1.6.10.2 Source material ..... 43

**1.7 Preventive and therapeutic options in Preeclampsia** ..... 44

**1.7.1 Aspirin** ..... 44

**1.7.2 Sulfasalazine and antioxidants** ..... **44**
**1.7.3 Pravastatin** ..... **45**
**1.7.4 Metformin** ..... **46**
**1.7.5 Proton pump inhibitors** ..... **46**
**1.7.6 Nutritional supplements** ..... **46**
**1.7.7 Nanoparticles and nanocarriers** ..... **47**
**1.7.8 Other potential therapeutic agents** ..... **47**
**1.8 Conclusion** ..... 48

**CHAPTER 2**

**2.1 General methods** ..... 50
**2.1.1 Human Subjects** ..... **50**
**2.1.2 Introduction to and clarification of nomenclatures and terminologies used in this thesis** ..... **50**
**2.1.3 Enrichment of STB-EVs by placental *ex vivo* dual lobe perfusion and differential ultracentrifugation** ..... **51**
**2.1.4 Characterisation of STB-EVs generated by *ex vivo* dual lobe placental perfusion and differential ultracentrifugation** ..... **55**
**2.1.4.1 Transmission electron microscopy** ..... 55
**2.1.4.2 Flow cytometry** ..... 55
**2.1.4.3 Nanoparticle tracking analysis** ..... 57
**2.1.4.4 Western blot analysis** ..... 58
**2.1.5 Cell culture: Human endothelial umbilical vein cells as a positive control for Western blots** ..... **61**
**2.1.6 BCA protein assay** ..... **63**
**2.2 Methods for mRNA isolation, characterisation, and analysis** ..... 63
**2.2.1 RNA-sequencing library preparation and sequencing** ..... **63**
**2.3 Methods for bioinformatic and statistical analysis messenger RNA sequences** ..... 65
**2.3.1 Bioinformatic analysis of messenger RNA sequences** ..... **65**
**2.3.2 Differential expression analysis of messenger RNA data** ..... **66**
**2.3.3 Functional enrichment analysis of messenger RNA analysis** ..... **67**
**2.4 Methods for validation of selected mRNA with quantitative polymerase chain reaction (qPCR)** ..... 68
**2.4.1 Synctiotrophoblast membrane extracellular vesicles (STB-EVs) RNA extraction** ..... 68
**2.4.2 Complementary cDNA synthesis for mRNA synthesis** ..... 69
**2.4.3 Preamplification of complementary DNA samples** ..... 70
**2.4.4 Quantitative polymerase chain reaction (qPCR) for mRNA validation** ..... 70
**2.5 Methods for microRNA characterisation, and analysis** ..... 73

**2.5.1 RNA-Sequencing library preparation and sequencing ..... 73**
**2.6 Methods for bioinformatic and statistical analysis microRNA sequences** ..... 73
**2.6.1 Bioinformatic analysis of microRNA sequences..... 73**
**2.6.2 Differential expression analysis of microRNA data ..... 77**
**2.6.3 Functional enrichment analysis of microRNA analysis..... 77**
**2.7 Methods for validation of selected microRNA with quantitative polymerase chain reaction (qPCR)** ..... 78
**2.7.1 Complementary cDNA synthesis for microRNA synthesis ..... 78**
**2.7.2 Quantitative polymerase chain reaction (qPCR)** ..... 79
**2.8 Methods for protein isolation, characterisation, and analysis** ..... 81
**2.8.1 Sample preparation for mass spectrometric analysis and bioinformatic analysis of proteomic data from placenta tissue, medium/large, and small STB-EVs ..... 81**
**2.8.2 Selection of placenta enriched proteins for Western blot validation..... 82**
**2.8.3 Western Blotting for validation of identified differentially expressed STB-EV proteins in PE ..... 83**
**2.9 Methods for multi-omic correlation analysis**..... 84
**2.9.1 MicroRNA-messenger RNA correlation analysis ..... 84**
**2.9.2 mRNA-protein correlation analysis ..... 87**
**2.10 Methods for modular and clustering network analysis** ..... 87
**2.10.1 Protein-protein (PPI) and gene-gene interaction (GGI) network construction, hub genes, proteins and pathways, and cluster analysis ..... 87**
**2.11 Methods for discovery of potential therapeutic agents in preeclampsia using connectivity Map Analysis** ..... 89
**2.12 Results** ..... 91
**2.12.1 Patient demographics and clinical characteristics ..... 91**
**2.12.1 Characterisation of STB-EVs by transmission electron microscopy (TEM), nanoparticle tracking analysis (NTA), flow cytometry, and Western blot (WB)..... 94**
**2.13 Conclusion** ..... 99

**CHAPTER 3**

**3.1 Abstract**..... 101
**3.2 Introduction**..... 103
**3.3 Aims**..... 105
**3.4 Methods**..... 105
**3.5 Results** ..... 106
**3.5.1 Differentially expressed genes (DEGs) in placenta homogenate, M/L STB-EVs and S STB-EVs between PE and NP..... 106**
**3.5.2 Quantitative PCR (qPCR) Validation of selected genes ..... 108**

**3.5.3 Functional enrichment analysis and signalling pathway impact analysis (SPIA) of differentially expressed genes (DEGs) in Preeclampsia** ..... **112**

**3.5.3.1 Functionally enriched Gene Ontology Biological processes (GO: BP) in preeclampsia** ..... 112

**3.5.3.2 Functionally enriched Gene Ontology Molecular Function (GO: MF) in preeclampsia** ..... 116

**3.5.3.3 Functionally enriched Gene Ontology Cellular Component (GO: CC) in preeclampsia** ..... 119

**3.5.3.4 Functionally enriched KEGG Pathways in Preeclampsia** ..... 122

**3.5.3.5 Signalling pathway impact analysis (SPIA) in preeclampsia** ..... 125

**3.6 Discussion** ..... 128

**CHAPTER 4**

**4.1 Abstract** ..... 133

**4.2 Introduction** ..... 134

**4.3 Aims** ..... 136

**4.4 Methods** ..... 136

**4.5 Results** ..... 137

**4.5.1 General descriptive characteristics of small RNA sequencing in the placenta, medium/large STB-EVs and small STB-EVs** ..... **137**

**4.5.2 Differentially expressed MicroRNAs (DEMs) in Placenta, medium/large STB-EVs, and small STB-EVs in preeclampsia** ..... **139**

**4.5.3 Quantitative PCR (qPCR) validation of selected microRNAs** ..... **145**

**4.5.4 Functional enrichment analysis of differentially expressed microRNAs (DEMs) in Preeclampsia** ..... **148**

**4.5.5 MicroRNA and messenger RNA correlation in placenta homogenate, medium/large STB-EVs and small STB-EVs in Preeclampsia** ..... **151**

**4.6 Discussion** ..... 156

**CHAPTER 5**

**5.1 Abstract** ..... 161

**5.2 Introduction** ..... 162

**5.3 Aims** ..... 163

**5.4 Methods** ..... 163

**5.5 Results** ..... 164

**5.5.1 Differentially expressed proteins (DEPs) in placenta homogenate, medium/large STB-EVs and small STB-EVs in Preeclampsia** ..... **164**

**5.5.2 Validation of select proteins in the placenta homogenate, medium/large STB-EVs, and small STB-EVs** ..... **168**

**5.5.3 Functional enrichment of differentially expressed proteins (DEPs) in Preeclampsia** ... **171**

**5.5.4 Correlation between mRNA (transcriptomics) and protein (proteomics) datasets in the placenta, M/L STB-EVs, and S STB-EVs** ..... **175**

**5.6 Discussion** ..... 178

**CHAPTER 6**

**6.1 Abstract** ..... 183

**6.2 Introduction** ..... 184

**6.3 Aims** ..... 185

**6.4 Methods** ..... 185

**6.5 Results** ..... 186

**6.5.1 Identification of critical/hub genes and pathways in preeclampsia (from the transcriptomic and proteomic dataset)** ..... **186**

**6.5.2 Cluster analysis of preeclamptic transcriptomic gene-gene interaction network (PPI) in the placenta tissue, medium/large and small STB-EVs** ..... **190**

**6.5.3 Cluster analysis of preeclamptic transcriptomic gene-gene interaction network (PPI) in placenta tissue, medium/large and small STB-EVs** ..... **197**

**6.5.4 CMap analysis of transcriptomic and proteomic signatures** ..... **202**

**6.6 Discussion** ..... 207

**CHAPTER 7**

**7.1 Final Discussion** ..... 213

**7.2 Summary** ..... **213**

**7.2.1 Aim 1: Identify molecules syncytiotrophoblast membrane extracellular vesicle (STB-EVs) expressed molecules that may be diagnostic of preeclampsia** ..... **214**

**7.2.2 Aim 2: Bioinformatically determine potential mechanisms and molecular PE subtypes** ..... **214**

**7.2.3 Aim 3: Bioinformatically discover repurposed drugs that may be therapeutic in PE** ... **215**

**7.2.4 Future work** ..... **215**

**APPENDIX**

**8.1 List of Publications** ..... 217

**Published Papers** ..... **217**

**Submitted Manuscript** ..... **217**

**Unpublished Manuscript** ..... **217**

**8.2 References** ..... 219

# Abstract

**TITLE:** CHARACTERISATION OF PROTEINS AND RNA EXPRESSED IN SYNCYTIOTROPHOBLAST MEMBRANE EXTRACELLULAR VESICLES (STB-EVs) IN PREECLAMPSIA

**NAME AND COLLEGE:** Dr Toluwalase Ayobami Awoyemi, Hertford college

**DEGREE:** DPhil in Women's and Reproductive Health

**TERM AND YEAR OF SUBMISSION:** Hilary term 2022

**Introduction:** Preeclampsia is a complication of pregnancy that affects 2-8 % of women worldwide. It is one of the leading causes of maternal deaths and premature birth. It is diagnosed by elevated blood pressure (≥ 140/90 mmHg), proteinuria, and/or end-organ damage. Although the precise mechanisms are not fully elucidated, the placenta is involved in this disease process. However, one theory is the role of extracellular vesicles STB-EVs, which are membrane-bound biomolecules that range between 30-1000 nm in size released by the placenta and detected in the circulation. STB-EVs have been reported to be higher in the circulation in PE compared to Normal pregnancy. In addition, the phenotype of the STB-EVs is believed to be different in PE compared to NP. However, it is unclear if the clinical manifestations attributable to STB-EVs in PE are a) because PE STB-EVs are more abundant in circulation, b) because they are of a different phenotype (bigger with a different cargo), or c) a combination of both. This thesis builds on the second premise.

**Aim:** My work explores the possibility that STB-EVs can act as biomarkers and mechanistic and therapeutic targets in PE.

**Methodology:** I have isolated and characterised STB-EVs from the placenta of 8 PE and 6 NP patients via *ex vivo* dual lobe placenta perfusion. I subjected these materials through mass spectrometry, coding RNA, and small RNA sequencing and multi-omics (transcriptomics,

proteomics, and integrated multi-omics) data analysis. This is the first study of its kind in the field.

**Results:** My analysis identified a difference in STB-EV cargoes' transcriptomic and proteomic profiles between preeclampsia (PE) and normal pregnancy (NP). I then identified and verified the differential expression of transcripts (FLNB*, COL17A1, SLC45A4, LEP, HTRA4, PAPP-A2, EBI3, HSD17B1, FSTL3, INHBA, SIGLEC6,* and *CGB3),* microRNA *(hsa-miR-193b-5p, hsa-miR-324-5p, hsa-miR-652-3p, hsa-miR-3196, hsa-miR-9-5p, hsa-miR-421, and hsa-miR-210-3p in the Medium/large STB-EVs)* and proteins *(FLNB (filamin B), COL17A1 (Collagen 17A1), PAPP-A2 (Pappalysin-A2), and SR-BI (Scavenger Receptor Class B Type 1))* for potential use as biomarkers in preeclampsia.

My analysis also identified 1) interesting mechanistic processes such as abnormal protein metabolism, which may be responsible for the clinical and pathological presentation of preeclamptic patients, and 2) molecular clusters that may explain variations in the presentation of PE and potential therapeutic candidates (*ceforamide, thiamine, dexibuprofen*)

**Conclusions:** I performed comprehensive profiling of the transcriptome, proteome and pathways in PE by analysing my three different sample subtypes (placenta, M/L STB-EVs and S STB-EVs). I identified differentially expressed biomolecules (proteins and RNAs) and uncovered mechanistic pathways which may be important in the pathophysiology of PE and could potentially be used in future studies of disease mechanisms and as biomarkers.

# CHAPTER 1

## INTRODUCTION

## 1.1 Background

Preeclampsia is a multisystemic disease of pregnancy characterised by hypertension (systolic blood pressure ≥ 140mmHg / diastolic pressure ≥ 90mmHg), proteinuria (protein/creatinine ratio of 0.3 mg/mmol or more), and/or evidence of maternal acute kidney injury, liver dysfunction, neurological features, haemolysis, or thrombocytopenia, and/or foetal growth restriction and in severe cases, death[1–5]. PE is highly variable in clinical presentation and phenotype[6]. It has a prevalence of 2-8 % globally and poses both short- and long-term adverse morbidity and mortality risk to both the mother and the foetus[7,8]. Diagnosing preeclampsia early in pregnancy has been challenging due to the limitations of current predictive models and biochemical tests (which lack good positive predictive value). The existing tests (Figure 1) perform far better in ruling out rather than ruling in preeclampsia. They are also most effective shortly before the onset of the disease and within a specific time frame (1 or 2 weeks) rather than earlier in pregnancy. This is because the precise mechanisms underlying the disease are incompletely understood- the same reason that no effective treatments are available other than the delivery of the baby and the placenta [9].

It is known that PE can occur in trophoblastic tumours (without the presence of a foetus)[10], that PE is more common in multiple pregnancies (with greater placental mass)[11] and that it has occurred in ectopic pregnancies (excluding the involvement of the uterus)[12]. Finally, delivery of the placenta (irrespective of gestational age) is currently the only cure for the condition. The placenta is, therefore, believed to be central to its pathogenesis. It is thought to cause the disease by releasing soluble factors and extracellular vesicles (STB-EVs) into the maternal circulation to act as mediators and propagators of the disease[13,14].

These placental syncytiotrophoblast-derived EVs, termed syncytiotrophoblast membrane extracellular vesicles, express various biomolecules such as proteins, messenger RNA,

microRNA, transferRNA in their cargo[15,16]. STB-EVs are double-walled spherical structures of placenta origin which can be classified based on their size and biogenesis pathways into medium/large and small STB-EVs[17]. Small STB-EVs are less than or equal to 220 nm in size and formed through multivesicular bodies, whereas medium/large EVs are between 221 nm to 1000 nm and are released directly through the budding of the plasma membrane. The release of syncytiotrophoblast extracellular vesicles (STB-EVs) into the maternal circulation increases with gestation and is further elevated in PE[16,18]. STB-EVs can regulate distant cells such as endothelial cells by depositing the contents of their cargoes[16], affecting immune response[19], and causing vascular dysfunction, platelet activation[19], vasoconstriction, angiogenesis, coagulation, and endothelial activation in pregnancy[20–23]. These expressed biomolecules in EVs combined with their constitutional release as inter-cellular signalling moieties means they also have potential in disease prognosis and monitoring. EVs have been used to diagnose[24,25], pancreatic[26,27], and colorectal[28,29] cancer.

## 1.2 Classification of Preeclampsia

PE has been classified in several ways since it was discovered. The first classification of PE grouped it into placental or maternal categories[30] and another classified into early-onset PE (EOPE-which happens before 34 weeks of gestation) and late-onset PE (LOPE-which happens after 34 weeks of gestation)[31]. The placental and maternal subtypes are perhaps EOPE, and LOPE, respectively and these two categories are believed to have different aetiologies and clinical presentations. A third classification divides it into three; early-onset PE (which happens before 34 weeks of gestation), intermediate-onset (between 34-36 weeks), and late-onset PE (after 36 weeks)[32]. Finally, PE can also be classified into preterm PE (before 37 weeks) and term PE (after 37 weeks)[33].

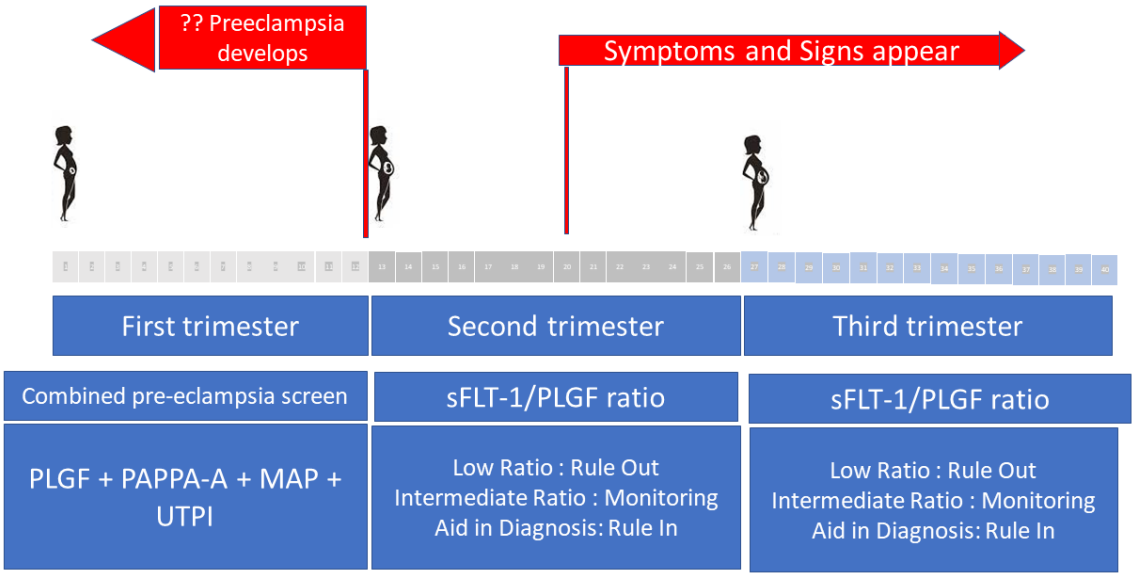



**Figure 1.** The figure shows the timeline of clinical presentation in preeclampsia and the available diagnostic and predictive tests. Preeclampsia develops before the 12$^{th}$ week, but the symptoms do not appear until the 20$^{th}$ week. A combined screening test (placenta growth factor [PLGF], pappalysin A1 [PAPP-A1], mean arterial pressure [MAP], uterine artery pulsatility index [UTPI]) in the first trimester, solubleFLT-1/PLDF ratio in the second and third trimesters have been recommended as screening tools for preeclampsia.

## 1.3 Risk factors of Preeclampsia

Numerous maternal and paternal risk factors have been identified from extensive epidemiological trials. These risk factors have enabled the categorisation of patients into high or moderate to low risk of PE, thereby facilitating the prioritisation of resources. A pregnant woman has an increased risk of PE if the father is a product of a preeclamptic pregnancy (OR-2.1, 95%)[34], or if a man who has already fathered a preeclamptic pregnancy begins a new relationship (crude OR 1.8 (1.2-2.6)[35]. Also, there is an increased risk in conception from donor

insemination compared to natural insemination (OR = 1.4, 95% CI)[36]. Conversely, a change of male partner confers a 1.6% increased risk of developing PE in the female partner[37]. Table 1 summarises the (other) previously described preeclamptic risk factors.

Table 1. Table showing risk factors of preeclampsia

| Risk factors | Mean RR/OR | 95% Confidence interval | Reference |
|---|---|---|---|
| Previous history of preeclampsia | 7.19 | 5.85-8.83 | [38] |
| Antiphospholipid syndrome | 9.72 | 4.34-21.75 | [39] |
| Insulin-dependent diabetes | 3.56 | 2.54-4.99 | [40] |
| Multiple pregnancy | 2.93 | 2.04-4.21 | [39] |
| Nulliparity | 2.91 | 1.28-6.61 | [39] |
| Family history of preeclampsia | 2.90 | 1.70-4.93 | [39] |
| Obesity | 2.47 | 1.66-3.67 | [39] |
| Age > 40 years | 1.96 | 1.34-2.87 | [39] |
| Pre-existing hypertension | 1.38 | 1.01- 1.87 | [39] |
| Smoking during pregnancy | 0.68 | 1.67- 0.69 | [39] |
| Partner related factors | 3.10 | 1.59- 6.73 | [41] |

## 1.4 Complications of Preeclampsia

PE as a multi-systemic disease leads to short- and long-term complications in multiple organs such as the heart, vascular system, kidneys, and brain. PE women have a higher risk of C-section delivery (Mean RR (95% CI) = 3.58 (1.57- 8.12)), induced labour (Mean RR (95% CI) = 5.52 (2.21- 13.83)), preterm delivery before 34 weeks (Mean RR (95% CI) = 3.97(1.55-10.20), longer postpartum hospitalisation (Mean RR (95% CI) = 5.80 (2.12- 15.91)), small for gestational age babies (Mean RR (95% CI) = 2.45 (1.52- 3.95)), neonatal intensive care unit (NICU) admission (Mean RR (95% CI) = 3.34 (1.61- 6.90)), neonatal near miss (Mean RR (95% CI) = 3.65 (1.78- 7.49))[39,42].

## 1.5 Mechanistic theories of Preeclampsia

The pathogenesis of PE is commonly considered a two-stage process (Figure 2), starting with spiral artery remodelling initiating placental dysfunction (stage 1) and ending in the maternal end-organ damage (stage 2) caused by factor X released by the placenta. Factor X is believed to be biomolecules such as proteins, glycoproteins, and syncytiotrophoblast membrane extracellular vesicles (STB-EVs). The other leading theories are:

1) Abnormal spiral artery remodelling and oxidative stress proposed by Brosens et al. and modified by Redman et al. [43,44]

2) Elevation of maternal systemic inflammation proposed by Redman et al. [45]

3) Depletion of vascular endothelial growth factor (VEGF) because of an increase in the anti-angiogenic factors soluble FMS like tyrosine kinase 1 (sFLT-1) by Ahmed et al. [46]

4) Immune mechanisms due to angiotensin 1 autoantibodies (AT1-AA)[47,48]

All theories are believed to lead to a common pathway, maternal endothelial dysfunction.

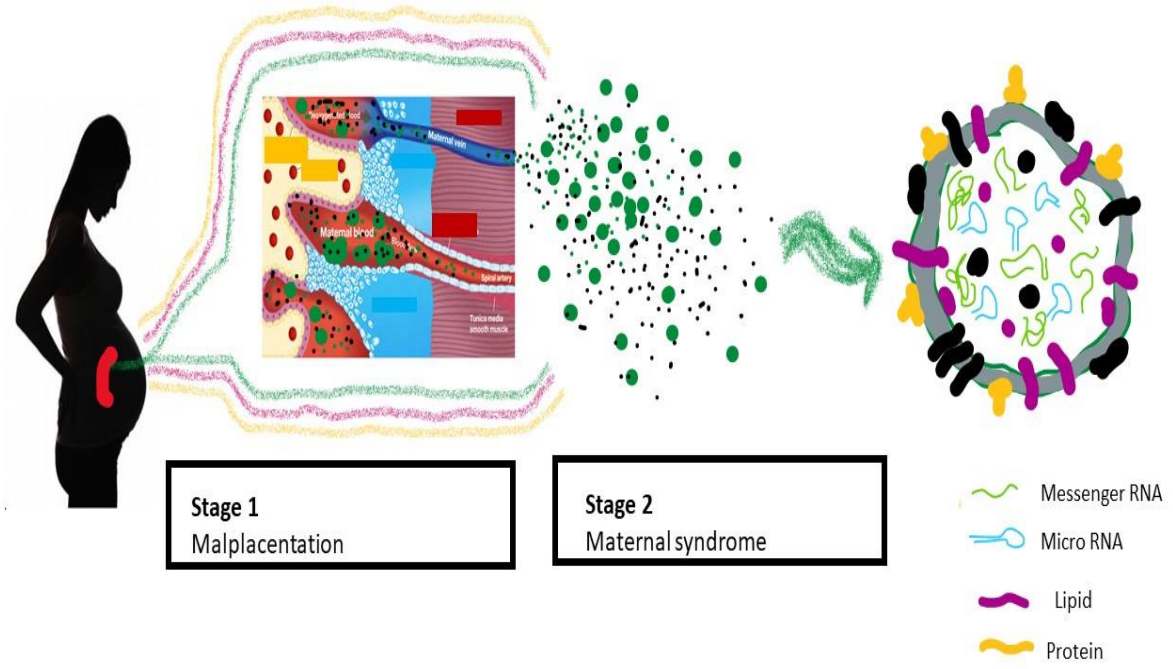



**Figure 2.** Figure summarising the two-stage theories of preeclampsia and the contents of STB-EV cargoes. The two stage theory postulates that there is malplacentation (stage 1) leading to a release of soluble factors and syncytiotrophoblast membrane extracellular vesicles (STB-EVs) into the circulation thus leading to a maternal syndrome. STB-EVs contain biomolecules such as protein, messenger, micro and transfer ribonucleic acid.

*Figure adapted from Pre-eclampsia management with biomarkers Improved pre-eclampsia diagnosis and prognosis of adverse outcome with PLGF and sFlt-1 after week 20 of gestation (Thermofisher)

## 1.6 Syncytiotrophoblast membrane extracellular vesicle (STB-EVs)

STB-EVs are double-walled membrane spherical structures involved in cell-to-cell communications. They are released from the syncytiotrophoblast into the maternal circulation and have various functions in normal pregnancy and disease states (e.g., gestational diabetes and hypertensive diseases of pregnancy). Like other EVs, they interact with recipient cells by either internalisation of the vesicle or by direct interaction between surface molecules on the vesicular and recipient membrane. The nomenclature of STB-EVs has undergone numerous modifications since their discovery. They have been referred to as placenta debris[49], placenta microparticles[50], placenta EVs[51], syncytiotrophoblast microvilli, syncytiotrophoblast microparticles[52], syncytiotrophoblast microvesicles[52], syncytiotrophoblast microvillous membrane[53,54], syncytiotrophoblast-derived microparticles[55], and recently syncytiotrophoblast membrane extracellular vesicles[56,57] (STB-EVs).

### 1.6.1 Classification of syncytiotrophoblast membrane extracellular vesicle (STB-EVs)

Their biogenesis enables the classification of STB-EVs like all EVs into microvesicles, exosomes and apoptotic bodies. However, they can also be classified based on physical characteristics (size) into < 200 nm (small) or > 200 nm (large and/or medium)[58]. For this thesis, the size-based classification was revised to < 220 nm (small) or > 220 nm (large and/or medium) due to the availability of 220 nm instead of a 200 nm filter in our laboratory.

In terms of biogenesis, microvesicles are a larger subtype of EVs, 100-1000 nm in size, produced by out budding of the cell membrane in response to cell activation, stress, or death, while exosomes are smaller sized EVs (30-100 nm) produced from multivesicular bodies. Apoptotic bodies (1 and 5 μm) are a subset of apoptotic extracellular vesicles[59] which also

include smaller ApoEVs, including apoptotic microvesicles (ApoMVs 0.1–1 μm)[60] and exosome-like apoptotic vesicles (< 150 nm)[61]. Apoptotic bodies are formed by apoptotic disassembly, including plasma membrane blebbing, apoptotic membrane protrusion formation, and fragmentation[62]. Apoptotic bodies are associated with cellular death and have not been analysed in this thesis.

## 1.6.2 Isolation and enrichment of trophoblast derived membrane extracellular vesicles

There are two broad categories of trophoblast derived EV isolation; tissue-based methods such as mechanical, placenta explant culture and placental perfusion, which generate STB-EVs, and cell-based methods such as BeWo cell line-derived EVs and trophoblast-derived cell lines (first or the second trimester).

**Mechanical STB-EVs (mSTBM)** is generated by rapidly washing 10 to 20 g of placenta tissue in ice-cold $CaCl_2$ and Kreb's physiological saline. The placenta tissue is placed in ice-cold 0.9% normal saline and mechanically agitated at 0ºC for thirty minutes. This is classically followed by differential centrifugation at 800 g (10 mins) to remove cellular debris, 10,000 g (5 min) to remove larger particles and intracellular debris and a final spin at 100,000 g (1 hour) to generate mechanical STB-Evs (referred to as mSTBM)[63].

**Perfused STB-EVs (pSTBM)** are obtained through *ex vivo* dual lobe placenta perfusion (pSTBM). The foetal (flow rate of 6 to 12 ml/min and pressure of 50 to 90 mmHg) and maternal (flow rate of 10 to 20 ml/min and pressure of 80 to 140 mmHg) vessels of a suitable cotyledon/lobe of the placenta are cannulated and perfused with filtered modified M-199 medium with streptokinase (100,000 IU)[20,64]. The resulting maternal perfusate is then differentially centrifuged at 1500 g (15 mins) to remove cellular debris, 10,000 g (30 mins) for M/L STB-EVs, and 150,000 g (2 hours) for S STB-EVs.

**In vitro explant culture derived STB-EV (eSTB-EV/eSTBM)** involves isolating suitable villous tissue from the placenta, then cutting into thin strips (1-2 mm) and culturing in medium (*DMEM/F-12 medium containing 10% FBS, 5ng/ml EGF; 5 µg/ml insulin; 10 µg/ml transferrin; 20 nM sodium selenite; 400 U/l human chorionic gonadotropin; 100 U/ml penicillin; 100 µg/ml streptomycin and 0.25 µg/ml amphotericin B*) for 24 to 72 hours to facilitate production of STB-EVs then differential ultracentrifugation at 300 g (10 mins), 2,000 g (20 mins), and 10,000 g (30 mins) to remove cellular debris, and 100,000 g (1.5 hours at 4°C) to pellet small vesicles, including exosomes (S STB-EVs)[65].

**Cultured human choriocarcinoma-derived cell line (BeWo) cell line derived EV** derived by culturing BeWo cells in Dulbecco's modified Eagle's medium, heat-inactivated foetal bovine serum (FBS) and exosome free FBS. The culture medium is then collected, and EVs are isolated and enriched using differential centrifugation[66].

**Culture of trophoblast-derived cell line (ATCC No CRL-1584)** (*in 10% Modified Eagle's medium, 10% bovine serum and antibiotics*) for 24 hours in normoxic or hypoxic conditions followed by differential centrifugation[67]; 300 g (5 minutes) and 800 g (5 minutes) to remove cellular debris, and 100,000 g (90 minutes at 4°C) to obtain microparticles. ATCC No CRL-1584 is a villous 3A cytotrophoblast first-trimester placental cell line from American Type Culture Collection (ATCC)[68].

**Isolation of cytotrophoblast (CTBs) from second-trimester human placentas** and culture in 1.5ml serum-free medium containing *DME/H-21, 2% Nutridoma-SP (Roche), 1% sodium pyruvate, 1% HEPES buffer, 1% glutamine plus, 1% penicillin/streptomycin and 0.1% gentamicin* followed by differential centrifugation; 2,000 g (20 mins) and 16,500 g (20 mins), the supernatant was passed through a 0.22 µm filter and centrifuged at 100,000 g (70 min)[69].

Gupta et al., in a comparative study published in 2005, concluded that pSTBM and eSTBM are biologically different from mSTBM and are more physiologically representative[70]. However, pSTB-EVs have a higher EV yield and are relatively cheaper to obtain than eSTB-EVs. Still, they require placenta perfusion knowledge and expertise and have a higher STB-EVs production failure rate (i.e., the proportion of successfully perfused placentas). It is also interesting that all STB-EVs have been enriched with differential ultracentrifugation (dUC) rather than other enrichment methods such as size exclusion chromatography (SEC), density gradient centrifugation (DEC), ultrafiltration, immunoprecipitation, and immunoaffinity beads capture. This may be because of the familiarity of placenta EV researchers with differential ultracentrifugation (dUC), the popularity of differential ultracentrifugation, or the large number of source materials generated from the two most common STB-EV sources; placenta perfusion (as much as 600 ml) and placenta explant culture.

### 1.6.3 Biodistribution of EVs and STB-EVs

Most data of EV biodistribution are from animal models due to challenges that currently lie with their study in humans, such as the safety of fluorescently labelled or radioisotope tagged EVs. Few animal studies have specifically examined pregnancy, but STB-EVs are likely to behave comparably to other EVs.

If we consider the non-pregnant data, in the circulation, EVs (especially small EVs) are rapidly cleared within a few minutes by circulating macrophages and neutrophils[71,72]. Kang et al. extensively reviewed thirty-eight studies and the time course of EVs in twenty different organs when administered into animal models[73]. They found the liver was the principal organ of small-EV localisation with peaks as early as the first hour after administration which persisted for three days[73]. Interestingly, the lungs also peaked in the first hour but diminished subsequently[73]. The kidneys showed low levels of small EVs in the first hour, followed by a

gradual reduction in small EV levels, while the spleen showed moderate levels of small EVs from the 2nd till the 12th hour. To summarise, small EVs are mainly distributed in the liver and lungs. For the other organs studied, the localisation was not as rapid. The bladder showed a peak at 4 hours while the brain, gastrointestinal tract, and the heart gradually and slightly increased up to 24 hours, and the skeletal system had moderate levels of EVs at 24 hours[73].

Large EVs were less studied, but it has been shown that they rapidly localise to the lungs within 1 hour, followed by a gradual decline over 12 hours[73]. The large EVs gradually rose and peaked in the liver in the 24th hour. The kidneys had moderate levels of large EVs, while the brain, heart, and spleen had low to no levels of EVs in them 24 hours post-injection[73]. In summary, the lungs are the main organs where large EVs are localised, followed by the Liver.

In one of the few pregnancy biodistribution studies, Tong et al. evaluated pregnant mice. They noted that medium/large STB-EVs localised to the lungs (after 30 minutes), then the liver and the lungs at 24 hours[74] Interestingly, they noted that the placenta EVs did not target the placenta[74]. They speculated that compared to the non-pregnant state, most STB-EVs are cleared by the kidneys and the lungs rather than just the lungs. They also concluded that this localisation is unlikely to be due to size but rather due to ligand-receptor interaction, some of which have been described by Ngyuen et al., who observed that these STB-EVs are specifically trafficked to the pulmonary interstitial macrophages through outer membrane proteins and integrins (Integrins α3, αV, α5, β1, and β3)[75].

## 1.6.4 Detection of STB-EVs in biofluids

STB-EVs have been found in the plasma (in normal PE, and gestational diabetes mellitus (GDM))[55,76–78] and the urine (in normal and GDM). Extensive literature searches have revealed no detection in other biofluids.

## 1.6.5 Biogenesis of syncytiotrophoblast membrane extracellular vesicle (STB-EVs)

There are two potential explanations for STB-EV generation. The less talked about pathway is the alternate pathway (Figure 3) proposed by Rajakumar et al., which involves shedding small microparticles from deported syncytial aggregates like the release of platelets from circulating megakaryocytes[79].

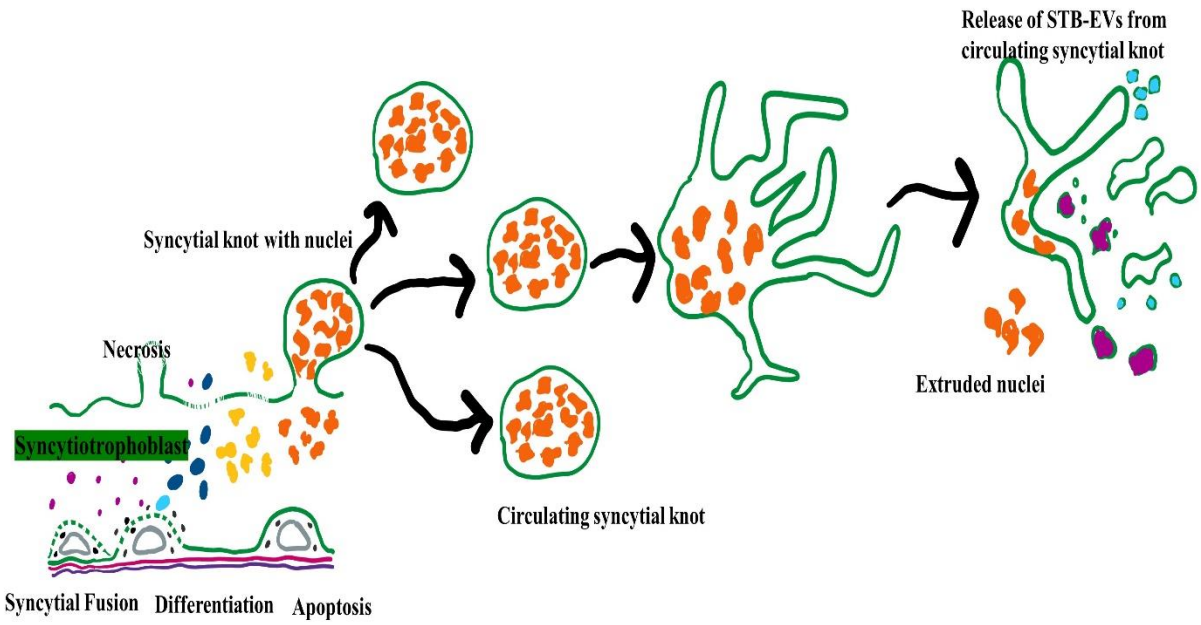



**Figure 3.** Figure showing a schematic representation of the alternate STB-EV biogenesis theory proposed by Rajakumar et al. In preeclampsia, the syncytiotrophoblast is stressed leading to the increased release of multinucleated syncytial knots into the circulation. These circulating syncytial knots further fragment to produce different sized STB-EVs such as M/L STB-EVs and S STB-EVs.

However, the primary biogenetic mechanism (Figure 3), the classic pathway, results in the production of STB-EVs from activated syncytiotrophoblast cells or apoptotic syncytiotrophoblast cells[80,81]. This includes the production of small STB-EVs (including exosomes), medium/large STB-EVs (including microvesicles) or other extracellular vesicles

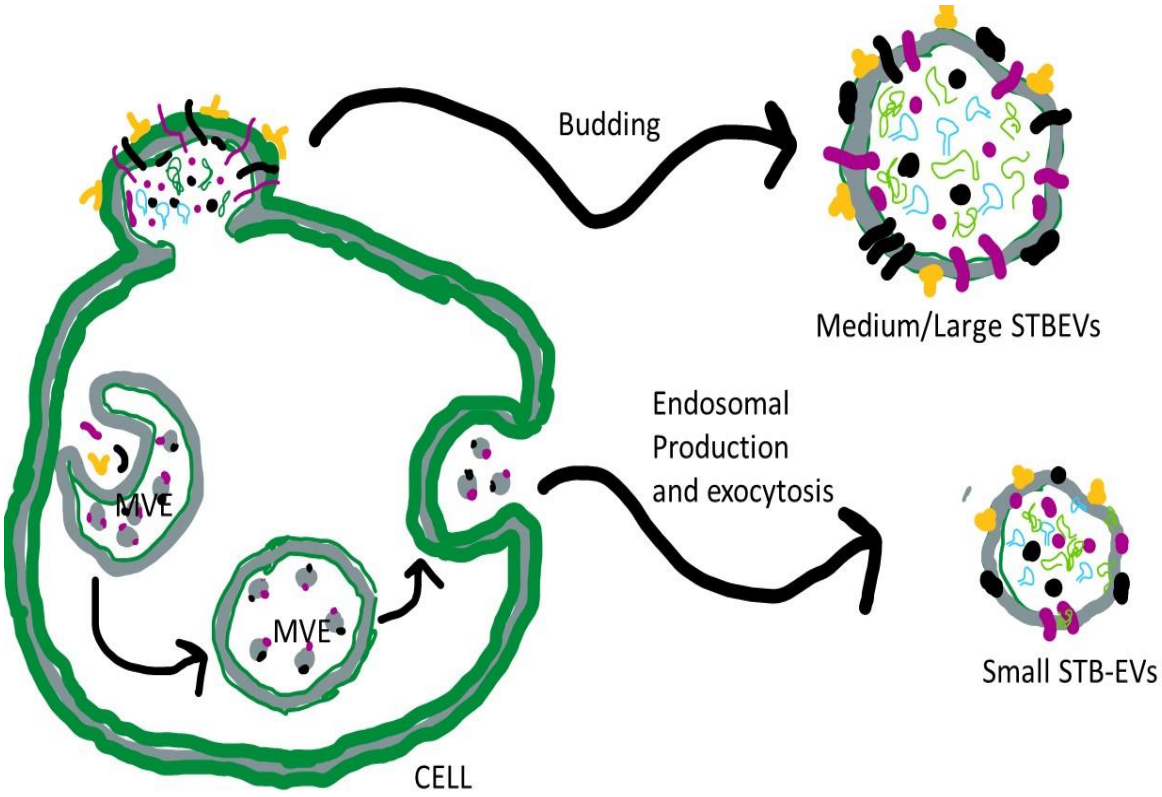



**Figure 4.** Figure showing the biogenesis of exosomes (a subtype of S STB-EVs) from the multivesicular bodies and microvesicles (a subtype of M/L STB-EVs) from blebbing/budding of the plasma membrane.

### 1.6.5.1 S STB-EVs (including exosomes) biogenesis

S STB-EVs (including exosomes) are 30-100 nm-sized extracellular vesicles generated through the ESCRT (Endosomal Complex Required for Transport) dependent or independent endosomal pathways.

In the ESCRT dependent pathway, intracellular early endosomes merge with endocytic vesicles and deport their contents into these endocytic vesicles (Figure 4 and 5) for various downstream processing[82]. Some of the contents are destined to be recycled[83] and are moved to recycling endosomes to be fused with lysosomes. The merged early endosome-endocytic vesicle complex transforms to become late endosomes, also called multi-vesicular bodies (MVBs)[84] or intraluminal vesicles (ILVs). MVBs are formed in two distinct processes. The first involves the organisational of the endosome membrane into specialised units highly enriched for tetraspanins (like CD63-a marker of small STB-EVs (including exosomes)). The enriched tetraspanins facilitate interactions between themselves and gangliosides,[85] transmembrane or cytosolic proteins, cholesterol[86] to form functional membrane microdomains. The second stage required involves four ESCRT (Endosomal Sorting Complex Required for Transportation) multi-protein complexes [83]; ESCRT 0, I, II, and III. All the ESCRTs work in a stepwise manner. ESCRT 0 and ESCRT I subunits cluster ubiquitylated transmembrane cargoes on the microdomains of the limiting membrane of MVBs and recruit ESCRT II and III subcomplexes. ESCRT I and II facilitate membrane budding. ECRT III helps complete membrane budding via ALIX[82], which binds to the tumour susceptibility gene 101 (TSG101) component of the ESCRT I complex and the charged multivesicular body protein 4a (CHMP4) of ESCRT III[87]. ALIX also promotes exosome biogenesis through its interaction with syntenin[88].

In the ESCRT independent pathway (Figure 5), small STB-EVs/exosomes are produced through alternate pathways such as the ceramide pathway (require the generation of ceramide

by neutral type II sphingomyelinase). Ceramide, like ESCRT, allows for the generation of membrane subdomains[89]. The tetraspanins; CD9, CD63, CD81, and CD82 are also involved in the ESCRT independent sorting mechanism based on the observation of defective exosomal biogenesis processes in tetraspanin knockout animal models[90,91]. ALIX and TSG101 are not involved in the ESCRT independent pathway and may thus be absent in this set of exosomes.

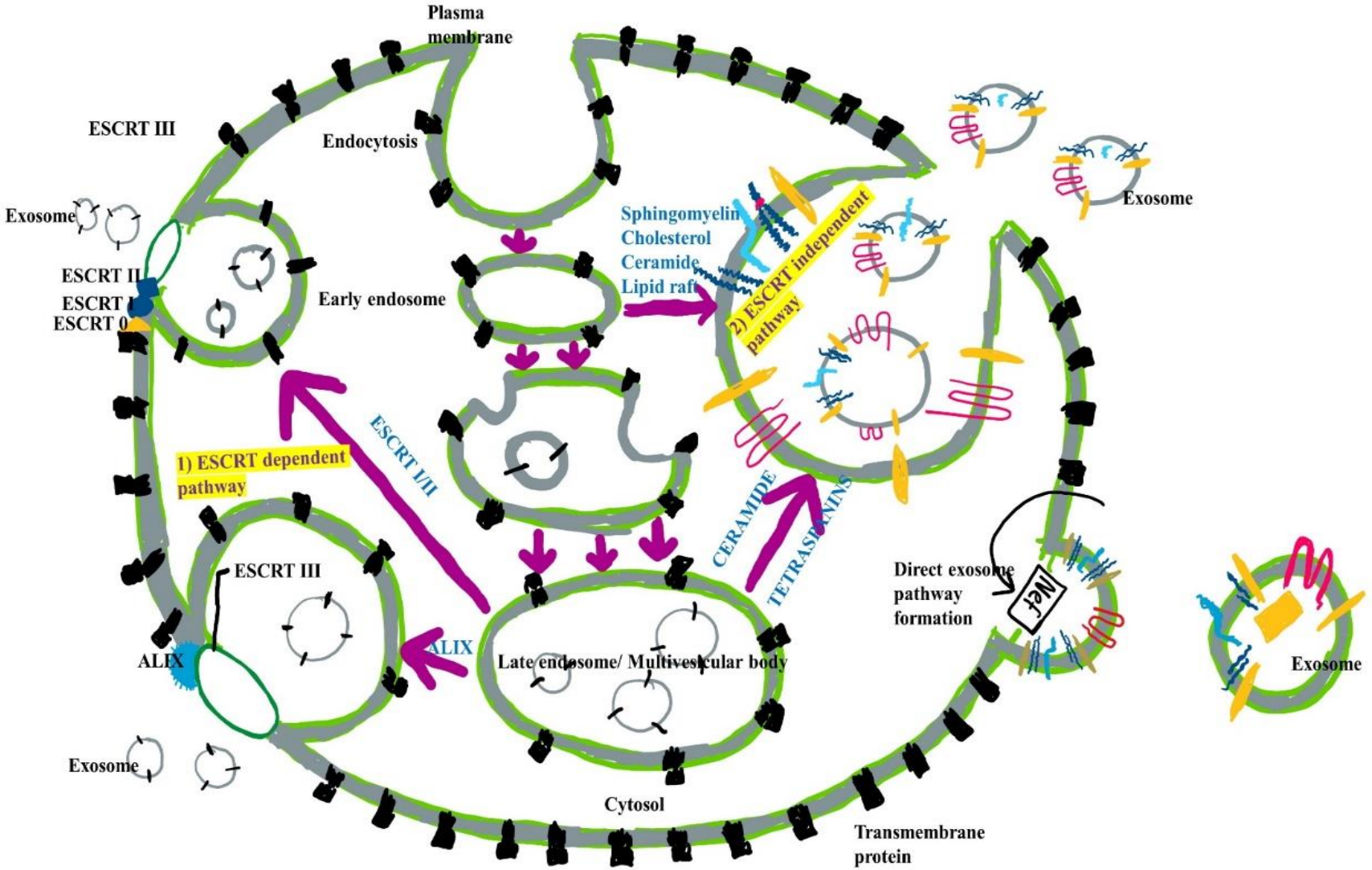



Figure 5. Figure showing ESCRT dependent and independent exosome biogenesis pathways. The ESCRT dependent pathway involves generation of extracellular vesicles via proteins such as ESCRT 0/ I/II/III from late endosomal/multivesicular bodies (MVB) while the ESCRT independent pathway involves generation of extracellular vesicles from MVB by ceramide, cholesterol, spinghomyelin, lipid raft and tetraspanins

### 1.6.5.2 M/L STB-EVs (including microvesicles) biogenesis

In contrast to exosomes, microvesicle's (M/L STB-EVs) biogenesis is less studied. Following a stressful stimulus, calcium influxes into the cells leading to exposure and translocation of phosphatidylserine to the outer membrane leaflet by the enzymes; floppases, flippases, and scramblases[90] (Figure 4). This translocation is followed by outward budding of the plasma membrane and contraction of cytoskeletal structures by actin-myosin interaction to deport the microvesicles (M/L STB-EVs). The biogenesis of microvesicles have been extensively reviewed by others[92]

### 1.6.5.3 Apoptotic bodies

Syncytiotrophoblasts undergoing apoptosis (for several reasons) transform their cellular processes into distinct membrane-enclosed vesicles called apoptotic bodies[93]. These large bodies contain organelles, deoxyribonucleic acid (DNA), histones, and nuclear fragments. Ideally, most apoptotic bodies are phagocytosed by placental macrophages, decidual macrophages, and other live cells to prevent activation of inflammatory or autoimmune responses, and only a few apoptotic bodies spill over into the circulation[94–96].

The size of EVs does not automatically correlate with their biogenesis, and thus I have maintained the size based ISEV nomenclature of M/L STB-EVs and S STB-EVs in this thesis.

### 1.6.6 Preferential targeting and sorting molecules into syncytiotrophoblast membrane extracellular vesicles

Identification of mechanisms that sort molecules into EVs is still largely unclear. No STB-EV-specific mechanisms have been identified, but general mechanisms of EV sorting are likely applicable to STB-EVs.

Cytosolic proteins (such as heat shock (70KDa) protein (HSP70)) are co-sorted with other proteins found ubiquitously on exosomes and glycosylphosphatidylinositol (GPI)-anchored membrane proteins are recruited due to their affinity for lipid domains and rafts. ESCRT complexes sort transmembrane proteins that have been mono-ubiquitinated into intraluminal vesicles (ESCRT dependent pathway) destined to be released as extracellular vesicles.[97,98] Mono- and poly-ubiquitinated proteins can also be sorted independent of ESCRT by sphingolipids, tetraspanins, and ceramide[99,100].

Small RNAs (ribonucleic acid) such as microRNAs contain specific motifs which play a role in preferential exosome sorting[101]. Garcia-Martin et al. identified the presence of unique sequences/sorting motifs (EXOmotifs) enriched up to 80 folds in small EVs. These motifs bind with two RNA binding proteins, Alyref and Fus, to facilitate the sorting[101]. The KRAS-MEK signalling pathway and major vault protein, Y-box binding protein1, hnRNPA2B1, Caveolin-1, neural sphingomyelinase 2 (nSMase2), argonaut 2 are involved in miRNA sorting[102–106]. hnRNPA2B1 is a SUMOylated (small ubiquitin RNA modifier) RNA binding protein that helps identify specific miRNA motifs (GAGAG motif in the 3′ portion of miRNA)[107]. In addition, the microdomains enriched with tetraspanins could concentrate RNA binding proteins such as ESCRT II subcomplex in the membrane sub-domains. Groot et al. [108] have comprehensively reviewed the sorting mechanisms for microRNAs into extracellular vesicles, and an extensive review of general EV sorting mechanisms has been done by Anand et al. [109]

and Villarroya-Beltri et al. [110]. Not much is known about sorting metabolites, lipids, and mRNA or other RNA subtypes asides from microRNA into EVs.

### 1.6.7 Syncytiotrophoblast membrane extracellular vesicle cellular entry mechanisms

Since the discovery that EVs mediate downstream actions in recipient cells, a tremendous amount of interest has risen in identifying the mechanisms of EV uptake by these cells. A few mechanisms (Figure 6) have been identified so far: endocytosis[111], lipid raft mediated endocytosis, clathrin and caveolin-dependent endocytosis[112], RhoA-dependent endocytosis, phagocytosis[113], macropinocytosis[114], and membrane fusion[115]. Endocytosis, a cell's extracellular material absorptive mechanism, occurs through heparan sulphate proteoglycans[116], galectin 5[117], CD91[118], calcium[119], fibronectin[120], or actin, depending on the cellular origin of the EV. Clathrin and caveolin-dependent endocytosis are mediated by dynamin[121] and neuroactive ligand receptors[112]. Lipid raft endocytosis (endocytosis that happens through specialised plasma membrane microdomains) involves glycosphingolipids[122], cholesterol[123], or ERK1/2[124]. Macropinocytosis is mediated through ion pumps (proton pumps or sodium/proton exchangers)[121]. Phagocytosis occurs through phosphoinositide 3-kinases (PI3Ks)[125] or phosphatidylserine121, while membrane fusion is through sodium reabsorption[126]. Concerning STB-EVs, Cronqvist et al. speculated that STB-EV uptake into primary human coronary artery endothelial cells (HCAECs) might be mediated by endocytosis or membrane fusion[127]. At the same time, Vargas et al. observed that villous cytotrophoblast small STB-EVs are taken up by BeWo cells in a syncytin-1 and -2 dependent manner[128]. No extensive study has been done to determine if the mechanisms of uptake of STB-EVs differ from other EVs or if uptake differs between medium, large, and small (STB-) EVs.

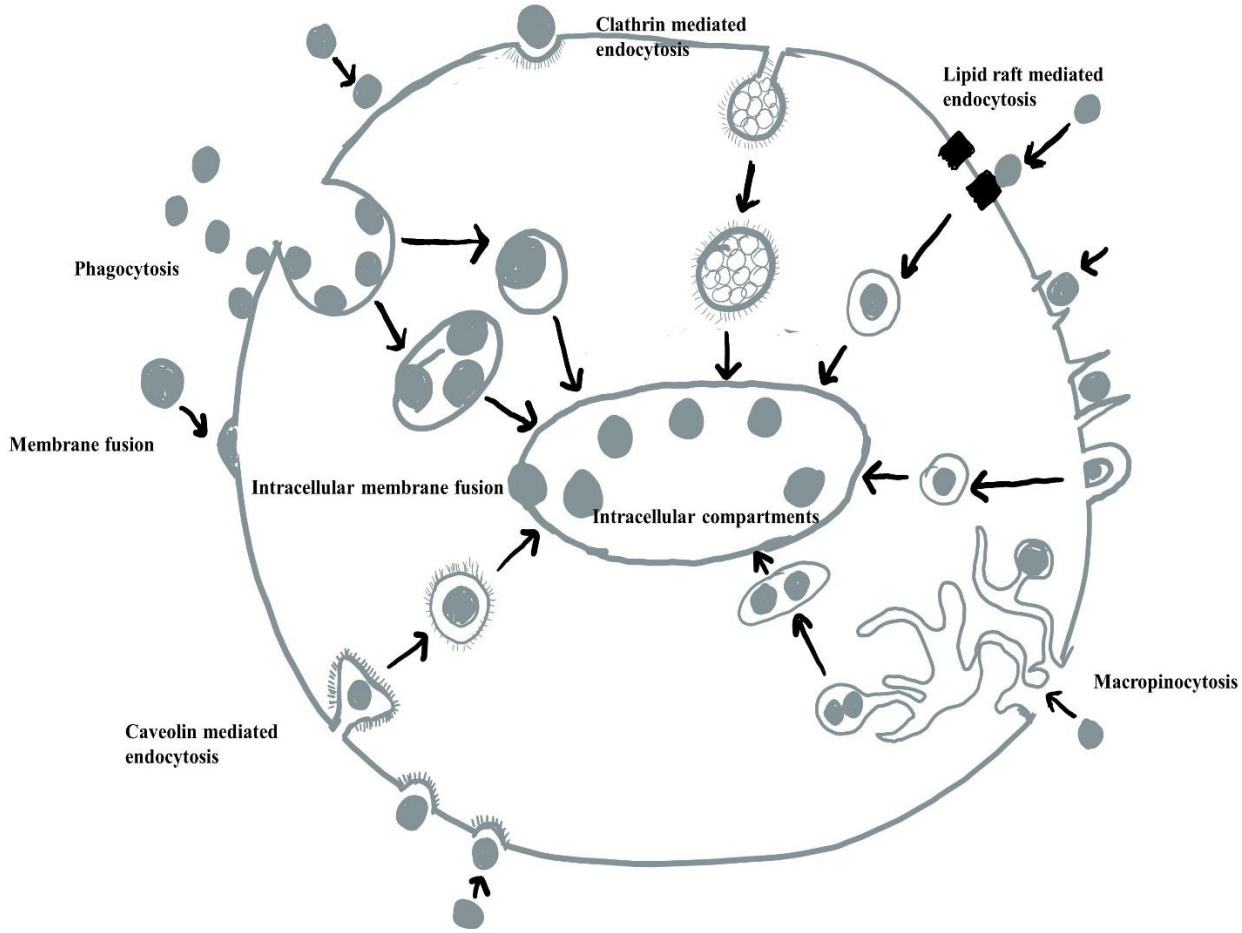



**Figure 6.** Figure showing EV cellular entry mechanisms. EVs from donor cells are internalised by recipient cells via endocytosis, micropinocytosis, membrane fusion, phagocytosis, or membrane fusion. Once internalised, these EVS are absorbed into the intracellular compartments and their contents deposited intracellularly.

## 1.6.8 Diagnostic potential

### 1.6.8.1 Diagnostic potential: syncytiotrophoblast membrane extracellular vesicle expressed diagnostic microRNAs in preeclampsia

MicroRNAs are a sub-class of small non-coding RNAs of 19-24 nucleotides[129]. microRNAs regulate the expression of mRNA by inducing mRNA cleavage or repressing translation[130]. In the circulation, microRNAs can be carried by extracellular vesicles, argonaut 2 (Ago2)

proteins, high-density lipoprotein, and other ribonucleoprotein complexes[131]. In preeclampsia, STB-EV miRNAs have been explored by checking for cell-free microRNA in the circulation (plasma or serum), identifying potential biomarkers, and linking them to the placenta. Srimashki et al summarised most of the previously identified preeclamptic extracellular microRNAs biomarker candidates such as hsa-miR-574-5p, hsa-miR-181a[132], miR-122, miR-758, hsa-miR-517-5p, hsa-miR-520-5p[133], hsa-miR-521, hsa-miR-521, hsa-miR-520h, hsa-miR-542-3p[134], hsa-miR-4313, hsa-miR-23c, hsa-miR-191[135],miR-210, miR-25[136].

### 1.6.8.2 Diagnostic potential: syncytiotrophoblast membrane extracellular vesicle expressed proteins in preeclampsia

Since discovering these EVs, some work has been done to identify differentially expressed proteins on STB-EVs or placenta EVs. Gardiner et al. reported tissue factor (TF) to be upregulated in PE STB-EVs (2 to10 fold increase) with increased TF activity compared to normal pregnancy.

Tanetta et al. noted FLT-1 to be upregulated in PE STB-EVs with multi-colour flow cytometry and Western blot. FLT-1 is an antiangiogenic tyrosine kinase that is membrane-anchored and binds VEGF. Soluble FLT-1, the splice variant of FLT-1, has also been described as upregulated in small STB-EVs by Rajakumar et al. [137]. It is highly expressed in syncytial knots, which are multinucleated, structured near the tips of the placenta villi[137] and found in increased quantities in circulation. Soluble FLT-1 binds freely circulating vascular endothelial factor (VEGF), leading to endothelial dysfunction, vasoconstriction, and reduced endothelial nitric oxide production, all features of PE. Soluble FLT-1 is known to be increased in PE and further increased with severity[138,139]. Rajakumar et al. estimated that more than 25% of the measurable soluble FLT-1 in third-trimester maternal plasma are STB-EV expressed[137].

Our group has previously reported biologically active neprilysin (NEP) as upregulated in PE STB-EVs[140]. NEP is a metalloendopeptidase that inactivates bioactive peptides such as atrial natriuretic peptide (ANP), brain natriuretic peptide (BNP), endothelin, bradykinin, and oxytocin. Similarly, transthyretin, a thyroxine and retinol-binding protein essential in foetal development during early pregnancy[141], is upregulated in placenta nanovesicles, including S STB-EVs[142]. Likewise, I also previously reported the upregulation of a novel glycosylated form of SIGLEC6, a subgroup of the negatively charged carbohydrate-binding lectins in the pericellular matrix of cells on PE STB-EVs[143]. SIGLEC6 regulates cellular activation and clonal expansion of immune cells[144,145].

Tersigni et al. observed human leukocyte antigen-DR isotype 3(HLA-DR 3) to be present on 39% of PE medium/large STB-EV studied and none on NP medium/large STB-EVs. Motta-Mejia et al. found endothelial nitrogen oxide synthase (eNOS), an enzyme that synthesises the potent vasodilator, nitric oxide, to be downregulated with reduced activity in PE STB-EVs compared to NP[146,147]. Finally, placenta protein 13 (PP13) is downregulated in PE STB-EVs compared to normal STB-EVs and may contribute to impaired tolerance and inflammation seen in PE[148].

### 1.6.8.3 Diagnostic potential: syncytiotrophoblast membrane extracellular vesicle expressed diagnostic metabolites, messenger RNA, lipids, and DNA in preeclampsia

No study has been conducted to identify differentially expressed metabolites, messenger RNA, lipids, and DNA in PE STB-EVs compared to NP and would represent an urgent and critical area of further study to help identify the roles of STB-EVs in PE.

## 1.6.9 Mechanisms of action of STB-EVs in preeclampsia

### 1.6.9.1 PE STB-EVs are inflammatory

PE STB-EVs are proinflammatory, but this is true only in EOPE[149,150]. In studies where the phenotypes of STB-EVs are differentiated (i.e., EOPE vs LOPE), LOPE STB-EVs are less likely to produce a proinflammatory phenotype in THP1 cells compared to NP STB-EVs in contrast to EOPE STB-EVs[17]. STB-EVs showed an elaboration of proinflammatory cytokines (tumour necrosis factor (TNF)-α, IL-1, IL-8, IL-6) in neutrophils, B and T cells[151], monocytes[152], which can be inhibited by blocking Toll-like receptor (TLR) signalling or targeting the nuclear factor kappa-light-chain-enhancer of activated B cells (NF-κB)[153].

### 1.6.9.2 PE STB-EVs are anti-angiogenic and cause endothelial dysfunction

Endothelial nitric oxide synthase (eNOS) activity is reduced in PE STB-EVs and may contribute to the vascular dysfunction and hypertension seen in PE[147]. In pregnant animal studies, injection of preeclamptic EVs results in decreased diameter of blood vessels, decreased maternal body weight, increased maternal blood pressure[154], and an increase in circulating sFLT-1[155]. PE STB-EVs enhance cellular oxidative stress by inducing endoplasmic reticulum and mitochondria membrane ruffling and can cause endothelial dysfunction by transferring functional microRNAs or mitochondrial DNA from dysfunctional syncytiotrophoblast[127]. They can bind proangiogenic factors (vascular endothelial growth factor [VEGF], placental growth factor [PLGF], and transforming growth factor beta [TGF-β]), disrupt cultured human umbilical vein endothelial cell (HUVEC) monolayers[156] and inhibit endothelial tube formation *in vitro*, translating to antiangiogenesis[137].

### 1.6.9.3 PE STB-EVs promote abnormal coagulation

Tannetta et al. noted that PE STB-EVs could activate platelet by increasing protein tyrosine phosphorylation which can be halted with aspirin[157]. In addition, they express procoagulant proteins on STB-EVs such as tissue factor (TF)[158], anionic phospholipids (PS)[159] and plasminogen activator inhibitors 1 (PAI-1)[160], which may explain the abnormal coagulation seen in preeclampsia.

## 1.6.10 Challenges of studying/researching STB-EVs in pregnancy and preeclampsia

### 1.6.10.1 Nomenclature and universal STB-EV markers

The field of STB-EVs holds excellent promise as diagnostic, predictive or therapeutic agents in the management of PE. However, there are several challenges (as seen in other EV fields). There is no homogeneity of nomenclature with several variable names to describe the same EVs published in journals. It might be easier to use placenta EVs to denote all EVs from the placenta; STB-EVs, placenta endothelial EVs, cytotrophoblast EVs, and reserve single population names such as STB-EVs or CTB-EVs for EVs of syncytiotrophoblast and cytotrophoblast origins, respectively. A limitation of this newly proposed naming scheme may be that the marker of syncytial origin is still uncertain, with most studies using placenta alkaline phosphatase (PLAP) and a few others using syncytin-1 or-2. PLAP antibodies may also cross-react with other types of circulating alkaline phosphatases like intestinal alkaline phosphatase when used in biofluids. Syncytin-1 is not discriminatory of STB or CTB, while syncytin-2 is expressed only in STB, but both syncytins are expressed in other cells/tissues (human protein atlas). Syncytin-2 expression is reduced in circulating serum-derived PE exosomes[23,128], and due to this, it may also not accurately reflect the circulating levels in diseased and normal

pregnant states. Isthmin-2 seems to be expressed predominantly in the placenta but is also not exclusively syncytiotrophoblast expressed. Undoubtedly, the resolution of these challenges and identifying an ideal marker would enable better comparisons between disease (PE) and control in biofluids such as plasma or urine and accelerate the development of EV based biomarkers.

### 1.6.10.2 Source material

The source material for CTB or STB-EVs is highly variable (can be cell or tissue-derived) as explained in the isolation of STB-EVs section, the only comparative study that evaluated three of the five methods[70] concluded that two methods; perfused STB-EVs and explant STB-EVs represented the most physiological method for the isolation of vesicles. Ultimately, the goal of most STB-EV studies is to translate results to biofluids which are hindered by a lack of consensus on the ideal blood sample type; plasma (EDTA or citrate) or serum. In 2013, the international society of thrombosis and haemostasis recommended citrated plasma as the plasma sample of choice, but this is not strictly adhered to by research labs for logistic and sample availability reasons[161]. The predominant use of serum in clinical circulating STB-EV studies is likely due to their large availability in biobanks compared to plasma samples. Serum may contain unwanted EVs released during clot formation and is thus less preferred to plasma samples. The anticoagulant type and downstream application are also a challenge regarding plasma. Citrated plasma (though the recommended anticoagulant) is less suitable than EDTA for (EV) RNA work, complicating the conundrum[76,162]. In addition to the challenges mentioned above, Coumans et al. have comprehensively identified other methodological challenges and considerations in studying extracellular vesicles in the circulation[76]. It is also time for the placenta EV community to create a data repository for omics studies like oncology to facilitate collaborative research, verification, and translation of research experiments.

## 1.7 Preventive and therapeutic options in Preeclampsia

Therapeutically, the only effective treatment for PE is delivery of the placenta. The commonly used antihypertensive medications (hydralazine, labetalol, methyldopa and nifedipine) are best used to manage the blood pressure and risk of associated complications. At the same time, magnesium sulphate is the most effective preventive therapy for seizures (eclampsia) and promoter of foetal neurodevelopment in preeclamptic patients.

### 1.7.1 Aspirin

The most promising preventive agent in preeclampsia is aspirin, a repurposed drug with anti-inflammatory and analgesic properties. Aspirin is a cyclooxygenase inhibitor that has been shown to reduce the risk of preeclampsia (especially preterm preeclampsia). In a recent systematic review published by the USPSTF (US Preventive Services Task Force), low-dose aspirin (81mg) was found to reduce the risk for preeclampsia, preterm birth, small for gestational age/intrauterine growth restriction, and perinatal mortality in pregnant persons at high risk for preeclampsia[163]. The exact mechanism of aspirin in PE is unknown, but its modest efficacy in PE has been attributed to its effect on platelet aggregation and inflammation, mechanisms abnormal in PE.

### 1.7.2 Sulfasalazine and antioxidants

Like aspirin, sulfasalazine is a repurposed medication with anti-inflammatory properties. Sulfasalazine reduces endothelial dysfunction and promotes a favourable angiogenic profile (a reduction in soluble FLT-1 and an increase in placenta growth factor) by inhibiting the epidermal growth factor receptor (EGFR) pathway[164]. Sulfasalazine has been disappointing in clinical trials with mixed or no significant effects in PE in terms of angiogenic profile and

pregnancy prolongation. There are more trials on the way with a larger sample size and alternate dosing strategy to help re-evaluate its effect.

High-dose folic acid, antioxidants, Vitamin C, B3, and E, have shown promising results in preclinical studies but have failed to show clinical effects in preeclampsia trials[165] or have no complete clinical trial. They were evaluated as preventive and therapeutic agents because PE is a disorder associated with oxidative stress, and thus antioxidants should hypothetically be effective agents.

Melatonin, another antioxidant, reduced oxidative stress in the placenta in preclinical trials[166]. The only melatonin trial done to date showed a modest prolongation of gestation (6 ± 2.3 days) in those with preeclampsia compared to controls and a reduced need for antihypertensive agents among the PE patients on 10 mg melatonin[166].

### 1.7.3 Pravastatin

Pravastatin, an anti-lipidemic medication, results in upregulation of antioxidant pathways and decreased secretion of soluble FLT-1, soluble endoglin, and other antiangiogenic markers[167]. It also upregulates nitric oxide synthase, decrease/resolve inflammation[168,169], hypertension, ventricular remodelling[170], and cardiovascular dysfunction[171]. In preventive studies with pravastatin in humans, mixed results have been obtained, with some showing a minimal or non-significant reduction in the prevention of preeclampsia or foetal mortality.

## 1.7.4 Metformin

Metformin, a repurposed anti-diabetic medication, promotes a favourable angiogenic profile and a reduction of anti-angiogenic markers by inhibiting mitochondrial function[172]. Similarly, there have been mixed results on the ability of metformin to decrease the risk of preeclampsia, with most studies leaning towards a non-significant effect that has hampered its clinical use[173,174].

## 1.7.5 Proton pump inhibitors

Proton pump inhibitors (PPI) are safe in pregnancy and prevent the release of antiangiogenic markers from the placenta in vitro by inhibiting mitochondrial function or/and the epidermal growth factor receptor (EGFR) pathway[175]. They also reduce the production of pro-inflammatory markers and attenuate endothelial dysfunction. In animal models, the PPI esomeprazole has been shown to resolve preeclamptic hypertension. Like pravastatin, epidemiologic and clinical trials show mixed results with a reduction, no meaningful change, or propagation of preeclamptic features depending on the phenotype of preeclampsia (esomeprazole mainly reduces the risk of preterm preeclampsia)[176,177].

## 1.7.6 Nutritional supplements

MitoQ, a mitochondrial antioxidant and dietary supplement, reduces oxidative stress in the placenta in a gestational age-dependent manner. In mouse models, it exacerbates preeclampsia when given earlier in gestation but resolved the preeclampsia phenotype when given later in pregnancy[178]. Polyphenols and flavonoids are antioxidants found in food and plants that also reduce the secretion of soluble FLT-1, resolve preeclamptic symptoms and upregulate antioxidant response in the placental cytotrophoblast in mouse models[179–181].

## 1.7.7 Nanoparticles and nanocarriers

Nanoparticles are becoming increasingly popular drug delivery agents due to their ability to target organs of interest and their safety *in vitro* (depending on the type of nanoparticles) [182]. They can be engineered to localise to the placenta using targeting peptides resulting in a preferential uptake of the therapeutic agents they carry. Polyethene glycol-polylactic acid (PEG-PLA) nanoparticles have been used to precisely deliver soluble FLT-1 small interfering RNA to the placenta with a resulting reduction in placental (mRNA) and serum (protein) sFLT-1 levels[183]. However, some challenges exist, such as concerns about transplacental passage seen in nanoparticles like liposomes[184]. In addition, organic nanoparticles like liposomes may have a less stable drug encapsulation. They can be leaky[185], while inorganic nanoparticles like silica are not biodegradable, and further study on their safety needs to be conducted[185].

## 1.7.8 Other potential therapeutic agents

There are numerous *in vitro*, preclinical, and animal agents and approaches, such as siRNA (against soluble FLT-1 or angiotensinogen)[186], stem cells[187], monoclonal antibodies (eculizumab)[188], anti-thrombin III[189], sildenafil[190] and apheresis[191,192] that are presently being evaluated. The results of these agents would become available in a few years.

## 1.8 Conclusion

Preeclampsia is a multisystemic obstetric disease with diagnostic, mechanistic, and therapeutic challenges. The placenta is believed to be central to its pathology through the release of soluble factors or syncytiotrophoblast membrane extracellular vesicles (STB-EVs). PE STB-EVs are pro-inflammatory, anti-angiogenic, pro-coagulatory, and can cause endothelial dysfunction. Since their discovery, these STB-EVs have been increasingly studied to help explore their use as circulating biopsies in PE, reflecting the placenta and foetus's real-time state. Therapeutically, artificially generated nanoparticles are potential preventive or curative agents due to 1) the abilities of these particles to carry therapeutic agents, 2) targeting specific organs like the placenta and the heart, and 3) the unimpressive results of clinical trials with other medications.

# CHAPTER 2A

## GENERAL AND CHAPTER-SPECIFIC METHODS

## 2.1 General methods

### 2.1.1 Human Subjects

Ethical approval was obtained from the central Oxfordshire research ethics committee C (REFS 07/H0607/74 & 07/H0606/148). I prospectively selected pregnant women undergoing elective caesarean sections before labour onset from the maternity ward at the women's centre, John Radcliffe Hospital, Oxford. Written informed consent was obtained before placenta collection from all participants. The placentas were collected from normal (NP) and preeclamptic (PE) pregnancies and perfused within 10 to 20 minutes of delivery. I defined NP as a singleton pregnancy with no history of preeclampsia, hypertensive disorders, or other complications in pregnancy. Preeclampsia was defined as the co-occurrence of *de novo* hypertension (blood pressure ≥ 140/90 mmHg) and proteinuria (protein/creatinine ratio ≥ 0.3) and/or evidence of maternal acute kidney injury, liver dysfunction, neurological features, haemolysis, or thrombocytopenia, and/or foetal growth restriction after week 20 of gestation according to the International Society for the Study of Hypertension in Pregnancy (ISSHP) [11].

### 2.1.2 Introduction to and clarification of nomenclatures and terminologies used in this thesis

I refer to medium/large STB-EVs (M/L STB-EVs) and small STB-EVs (S STB-EVs) in their crude forms as 10K STB-EV and 150K STB-EV pellets, respectively, during the enrichment and characterisation stages. After confirming that the 10K STB-EV pellets are enriched for EVs within the expected size range (221 to 1000 nm), and 150K STB-EV pellets contain EVs within the expected size range (≤ 220 nm), I renamed the 10K STB-EV pellet and 150K STB-EV pellets to M/L STB-EVs and S STB-EVs, respectively.

## 2.1.3 Enrichment of STB-EVs by placental *ex vivo* dual lobe perfusion and differential ultracentrifugation

Isolation of syncytiotrophoblast extracellular vesicles (STB-EV) and human umbilical vascular endothelial cells involved collection of placentas from normal and preeclamptic women undergoing elective caesarean section before the onset of labour. The placenta was collected during caesarean section and delivered to the laboratory in warm Hanks's solution for immediate processing. An intact peripheral lobe with no visible signs of postpartum villus breakage was identified. Associated umbilical artery and vein of the lobe were cannulated at the chorionic plate and perfused with 0.1 µm filtered tissue culture medium (*Medium 199 with L-glutamine and Earle's salts, containing 0.8% dextran 20, 0.5% bovine serum albumin (BSA) (Sigma UK) and 5000 U/L sodium heparin (Fannin, UK)* at a rate of 5 ml/min. The whole placenta was inverted with the maternal surface facing up and laid in a Perspex water jacket maintained at 37$^{o}$C. The maternal surface was then perfused with pre-formulated tissue culture media medium (*Medium 199 with L-glutamine and Earle's salts, containing 0.8% dextran 20, 0.5%bovine serum albumin (BSA) (Sigma UK)*) through six 1.7 mm foetal feeding tubes (Pennine Healthcare UK) at a controlled rate of 20 ml/min. The lobe was perfused for 20 mins to equilibrate the system, after which the maternal circuit was closed with a volume of perfusion medium of 600 ml (Figure 7). The volume of foetal effluent was continuously measured to ensure the stability of the preparation.

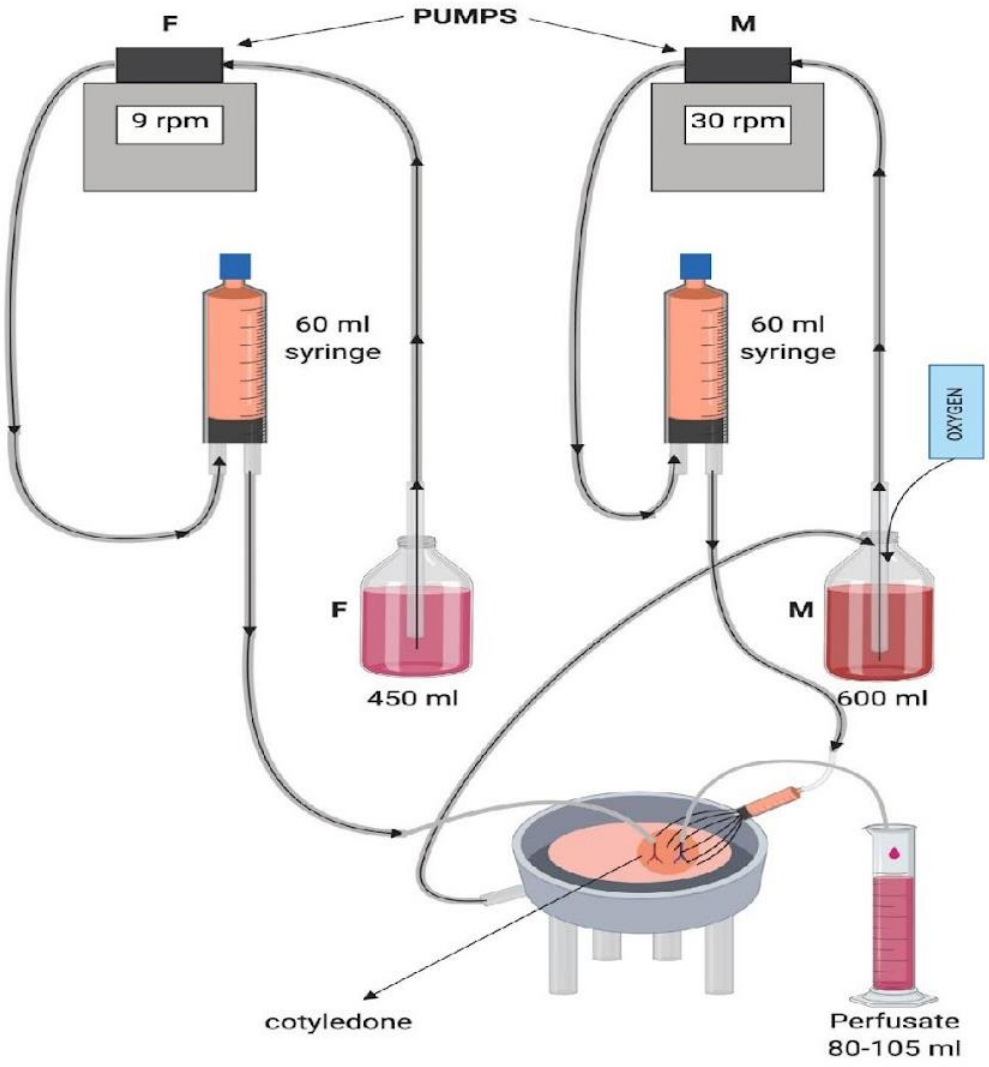



**Figure 7.** Figure showing the *ex vivo* dual lobe perfusion set-up. The placenta perfusion system comprises the foetal circuit (F) on the left and the maternal circuit (M) on the right. The maternal circuit is a closed circuit, the maternal medium moves through the tubes from the maternal medium bottle to perfuse the maternal side of the identified cotyledon. The maternal perfusate is then returned through the tubing to the maternal medium bottle. In contrast the fetal circulation is open, the fetal medium moves through the tubes from the fetal medium bottle to perfuse the fetal side of the identified cotyledon. The fetal perfusate is then measured every twenty minutes to determine flow rate consistency and discarded.

* Adapted with permission from Dr Daniela Iaccarino

At the end of the three-hour perfusion, the placenta perfusate was centrifuged twice at 1,500 g for 10 minutes at 4$^{o}$C (*Beckman Coulter Avanti J-20XP centrifuge using a Beckman Coulter JS-5.3 swing-out rotor*) to remove cell debris (Figure 8). The supernatant was carefully pooled and spun at 10,000 g (10K) in a swing bucket centrifuge (*Beckman L80 ultracentrifuge and Sorvall TST28.39 swing-out rotor*) at 4$^{0}$C for 30 minutes. The 10K STB-EV pellets were washed with filtered phosphate buffer saline (fPBS) followed by resuspension of the 10K STB-EV pellets in fPBS. An aliquot of the resuspended pellets was analysed to identify and characterise STB-EVs. In contrast, the rest were aliquoted to obtain a protein concentration of around 2-5 µg/µl (measured using a Pierce BCA protein assay kit) and immediately stored at -80$^{o}$C. The post-10K supernatant was filtered through a 0.22 µm Millipore stericup filtration device, then spun at 150,000 g for 2 hours (*Beckman L80 ultracentrifuge with a Sorvall TST28.39 swing-out rotor*). The 150K STB-EV pellets were washed, resuspended in fPBS and aliquoted like the 10K STB-EV pellets. This working stock was used for subsequent analysis. My STB-EV enrichment and categorisation process have been deposited on EV Track ([http://www.EVTRACK.org], EV-TRACK ID: EV210382) with a great score of 78%.

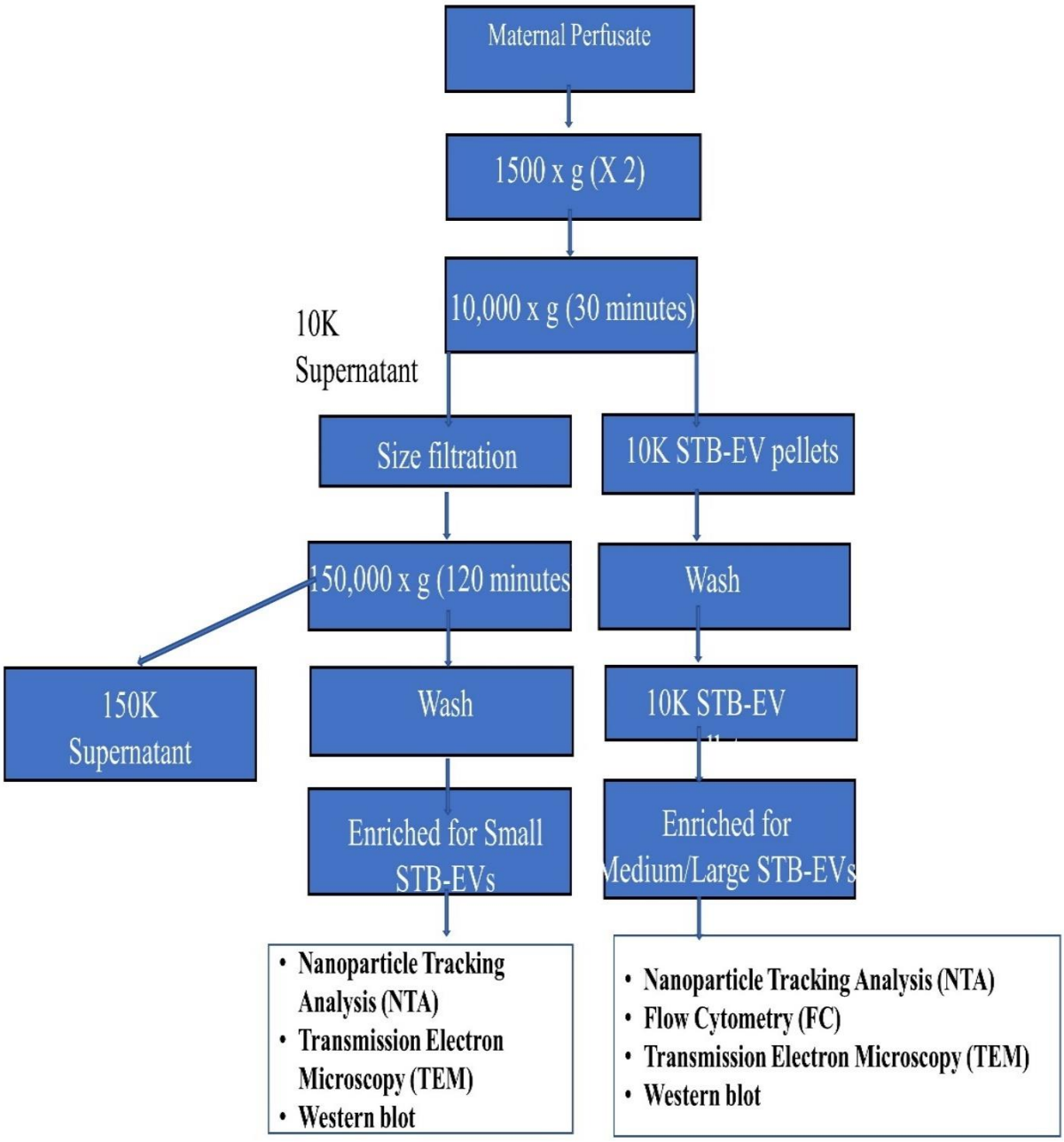



**Figure 8**. Flow chart showing the details of differential ultracentrifugation (10,000 and 150,000 g) performed on the maternal perfusate to obtain M/L STB-EVs and S STB-EVs and the steps involved in characterising these STB-EVs. The pellets from both spins are characterized with nanoparticle trafficking analysis, transmission electron microscopy, flow cytometry, and Western blot.

## 2.1.4 Characterisation of STB-EVs generated by *ex vivo* dual lobe placental perfusion and differential ultracentrifugation

### 2.1.4.1 Transmission electron microscopy

Transmission electron microscopy was outsourced to and performed by Dr. Errin Johnson (Sir William Dunn school of pathology). STB-EV pellets were diluted with fPBS to achieve an STB-EV solution with concentrations between 0.1-0.3 µg/µl. Ten µl of the STB-EV pellet solution was applied to freshly glowing discharged carbon formvar 300 mesh copper grids for 2 mins, blotted with filter paper, and stained with 2% uranyl acetate for 10 seconds, then blotted and air-dried. STB-EV pellets on the grid are negatively stained to enhance the contrast between STB-EV pellets and the background. The grids were imaged using an FEI Tecnai 12 TEM at 120 kV with a Gatan OneView CMOS camera.

### 2.1.4.2 Flow cytometry

Flow cytometric analysis was performed with the help of Dr. Wei Zhang (Nuffield department of Women's and reproductive health). A BD LSR II flow cytometer (BD Biosciences) with a blue, violet, and red laser was used for all sample analyses. Daily quality control (QC) was run using CS&T beads (BD Biosciences). Photomultiplier tube (PMT) voltage determined by the CS&T run was applied to all fluorescent detectors except for the side scatter (SSC), which was determined by Apogee beads mix (1493, Apogee Flow System, UK). The SSC PMT voltage that triggered 0.59 µm silica beads and above was applied to all 10K STB-EV pellets analysed. An SSC threshold of 200 was applied to remove background noise below 0.59 µm silica beads. A flow rate of 10 µl/min was achieved using the TruCount beads (BD science). I calculated the flow rate by dividing the events obtained in the TruCount beads gate by the lot-specific number of beads in each TruCount tube then divided the resulting value by the acquisition time. I diluted the M/L STB-EV samples with fPBS to achieve a 400 events /seconds flow rate.

BD CompBeads (BD Biosciences), recombinant engineered antibodies (REA) compbeads (Miltenyl Biotech), and BODIPY FL N-(2-aminoethyl)-maleimide [505/513 nm] (bioM [Molecular Probes] stained M/L STB-EVs were used for fluorochrome compensation before staining. BioM binds to proteins' cysteine residues and thiol groups, separating stained particles from background noise. Antibodies were titrated independently to achieve optimal staining for STB-EVs and compensation beads to ensure the staining intensity of STB-EVs did not exceed that of the compensation beads. When the compensation beads staining intensity was exceeded by brightly stained events in samples, these events were excluded from downstream analysis. A hundred microliters of diluted 10K STB-EV pellet samples (containing medium/large STB-EVs) were incubated with antibodies at room temperature for 15 minutes before being transferred to an ultrafree 0.22 nm filter unit (Millipore) and centrifuged to remove unbound antibodies at 800 g for two minutes at room temperature. For sample staining, 90 µl of 10K STB-EV pellet were incubated with ten microlitres of Fc receptor blocker (Miltenyl, UK) for ten minutes at $4^{O}C$ and then stained with phycoerythrin (PE) conjugated placenta alkaline phosphatase (PLAP - for syncytiotrophoblast origin), PE Vio770 conjugated anti-classical HLA class I and II ((to exclude co-isolated white blood cell [WBC] EV co-isolation), pacific blue conjugated CD41 (to identify co-isolated platelet EVs) and CD235a (to identify co-isolated red blood cell (RBC) EVs in the dark) for 10 minutes at room temperature. Stained samples were transferred to an ultrafree 0.2 µm filter unit (Millipore) and centrifuged at 800 g for 2-3 minutes to remove unbound antibodies and EVs smaller than the filter pore size. Ninety microliters of fPBS were used to recover 10K STB-EVs retained on the filter membrane. Recovered 10K STB-EVs were further stained with BODIPY FL N-(2-aminoethyl)-maleimide [505/513 nm] (Molecular Probes) at a final concentration of 0.5 nM in the dark at room temperature for 10 minutes before samples were diluted to 500 microlitres and analysed on the flow cytometer to check for events rate. If necessary, subsequent dilutions were made to

achieve a ≤ 400 count/second event rate and reduce swarming. 10K STB-EV pellets were analysed at 10 µl/minute for 10 minutes, and a 100 µl diluted sample was analysed for each patient sample. Controls used for this study include fluorescence minus one (FMO-1) for each fluorochrome and stained samples re-acquired after 2% nonidet P-40 (NP-40) (Sigma) treatment to exclude non-vesicular particles. Data and figures were generated with the Flowjo software version (Tree Star Inc., Ashland, OR). Table 2 shows the instrument parameters used for flow cytometric analysis.

**Table 2.** Table showing the instrument parameters for the BD Bioscience's LSR II flow cytometer.

| Laser | Detector | LP mirror | BP filter | Fluorochrome | Marker/Antigen |
|---|---|---|---|---|---|
| Blue | A | 735 | 780/60 | PE-Vio770 | Classical HLA-I&II |
| | D | 550 | 575/26 | PE | PLAP |
| | E | 505 | 530/30 | BioM | Protein dye |
| | F, SSC | _ | 488/10 | _ | |
| Violet | F | _ | 450/50 | Pacific blue | CD41a, CD235a/b, |

*BP means band pass, BioM means BODIPY FL N-(2-aminoethyl)-maleimide, PE means phycoerythrin, PLAP means placenta alkaline phosphatase, HLA means human leukocyte antigen.

### 2.1.4.3 Nanoparticle tracking analysis

The Nanosight NS500 (instrument equipped with a 405 nm laser (Malvern UK), sCMOS camera, and nanoparticle tracking analysis (NTA) software version 2.3, Build 0033 (Malvern UK)) system calculates the size and concentration of EVs with a modification of the Stokes-

Einstein equation. Laser beams are generated and directed towards the EV samples in the sample chamber through a glass prism where they are refracted at a low angle, leading to the illumination of EVs by the beam of laser. These illuminated EVs are visualized using a conventional video-fitted optical microscope. The light scattered from all EVs in the sample chamber is recorded by the camera, and the NTA software analyses the recordings.

Before sample analysis, instrument performance was checked with silica 100 nm microspheres (Polysciences, Inc.). The samples were diluted in fPBS to a range of 1/10,000 to 1/100,000 as determined by the starting concentration. The samples were automatically injected into the sample chamber with a 1 ml syringe with the following script used for EV measurements: prime, delay: 5, capture: 60, repeat: 4. Images of the analysed samples were captured on camera at a level of 12 (Camera shutter speed; 15 ms and Camera gain; 350). NTA post-acquisition settings were optimised and kept constant between samples. Each video recording was analysed to infer STB-EV size and concentration profile.

### 2.1.4.4 Western blot analysis

I performed Western blots on placental homogenates and STB-EV pellets to further characterise and immune-phenotype. All STB-EVs were probed with placental alkaline phosphatase (PLAP [1.67 µg/µl] at 1:1000 dilution in house antibody), CD63 ([200 µg/µl] at 1:1000 dilution, Sc-59286, Santa Cruz Biotechnology), ALIX ([200 µg/µl] at 1:1000 dilution, Sc-53538, Santa Cruz Biotechnology), and cytochrome C ([200 µg/µl] at 1:1000 dilution, Sc-13156, Santa Cruz Biotechnology) as recommended by the international society for extracellular Vesicles (ISEV)[58]. Placenta alkaline phosphatase antibody is an in-house antibody specific to syncytiotrophoblast-associated or derived proteins (or biomolecules) and denotes placenta origin. ALIX and CD63 are extracellular markers found in all EVs but particularly enriched in 150K STB-EV pellets. Cytochrome C is a negative EV marker found

in all cells and homogenates but not EVs. An equal amount of protein (20- 40 µg) determined by bicinchoninic acid assay (BCA) results was mixed with 4 X Laemmli buffer (*(180 mM Tris-Cl (pH 6.8), 6% SDS, 30% glycerol, 0.3% 2-mercaptoethanol, and 0.0015% bromophenol blue, BioRad)*) with (for PLAP, Cytochrome C, ALIX) or without (for CD63) 5 % β-Mercaptoethanol and diluted to 20 µl with double distilled water (dd $H_20$). The sample mix was then heated at 70$^oC$ for ten minutes, and an equal volume of the sample mix was loaded. Electrophoresis was done under reducing (for PLAP, Cytochrome C, ALIX) and non-reducing (for CD63) conditions on NuPAGE $^{TM}$ 4-12% Bis-Tris Gel 1.0 mm x 10 well gels (Invitrogen by Thermo Fisher Scientific) at 150 V for 1-1.5 hours in a Novex minicell tank (Invitrogen, UK) filled with NuPAGE$^{TM}$ MOPS SDS running buffer (Novex by Life Technologies). Precision plus protein$^{TM}$ dual colour standards (Bio-Rad Laboratories Ltd, Hertfordshire UK) were used as a protein size marker. After protein separation, the separated proteins were transferred to a polyvinylidene (PVDF) membrane (Bio-Rad). The PVDF membrane and gel were sandwiched between four filter paper sheets pre-soaked in anode one buffer solution (*300 mM Tris, 10% methanol pH 10.4*) and two filter paper sheets pre-saturated with anode two buffer solution (*25 mM Tris, 20% methanol pH 10.4*) at the bottom and three filter paper sheets pre-soaked in cathode buffer solution (*25 mM Tris, 40 mM ε-aminohexanoic acid, 20% methanol*) at the top of the gel in a Novex semi-dry transfer apparatus (Life Technologies, UK). The transfer was run at 25 V for 45 minutes. The membranes were blocked for one hour with 5 % Blotto (2BScientific) in 0.1 % TBST (Tris-buffered saline (*20 mM Tris, 137 mM NaCl, pH 7.6) and 1% Tween-20, Sigma*) followed by overnight incubation with the appropriate primary antibodies (PLAP, ALIX, Cytochrome C). After overnight incubation and washing steps with TBST (three times, each for five minutes), the membranes were subsequently incubated with the corresponding secondary antibody, anti-mouse (P044701-2), or anti-rabbit (P044801-2) polyclonal goat immunoglobulins/

horseradish peroxidase (HRP) (1: 2000 dilution, Dako UK Ltd, Cambridgeshire UK) for an hour at room temperature and rinsed three times in TBST for five minutes each time. The membranes were treated with the EZ-ECL chemiluminescence detection kit for HRP (Biological Industries Israel Beit Haemek, Israel) for one minute before being developed using both a gel documentation system (G-Box, Syngene, Cambridge UK) running GeneSys (version 1.5.0.0, Syngene) and a chemiluminescence film (Amersham Hyperfilm™ ECL (enhanced chemiluminescence); GE Healthcare Limited, Buckinghamshire UK) to obtain the band intensity for each lane. Tables 3 and 4 show the list of reagents and antibodies used for Western blot analysis, respectively.

**Table 3.** Table showing the reagents used for Western blot

| Buffers | Power of hydrogen (pH) | Constituents |
|---|---|---|
| 4X Laemmli reducing buffer | 6.8 | 9 parts 4 X Laemmli buffer |
| | | 1 part 2-beta-mercaptoethanol |
| 4X Laemmli non-reducing buffer | | 4 X Laemmli buffer |
| Anode buffer 1 | 10.4 | 300 mM Tris base (36.34 g/L) |
| | | 100 % methanol (20 mL/L) |
| | | 980 ml of $ddH_2O$ |
| Anode buffer 2 | 10.4 | 25 mM Tris base (3.0 g/L) |
| | | 100 % methanol (20 mL/L) |
| | | 980 ml of $ddH_2O$ |
| Cathode buffer | 9.4 | 25 mM Tris base (3.0 g/L) |
| | | 40 nM 6-aminocaproic acid (5.2 g/L) |
| | | 100 % methanol (20 mL/L) |
| | | 980 mL of dH2o |
| 10 X TBS | 8 | NaCl (87.6g) |
| | | Tris base (12.1g) |
| | | 700 ml of $ddH_2O$ |
| TBST | 8 | 10 X TBS (100 mL) |
| | | 0.1 % Tween-20 (1 mL) |
| | | 900 mL of $ddH_2O$ |
| 5% Milk TBST | | 5g of Blotto in 100 mL of TBST |

**Table 4.** Table showing the antibodies used for Western blot

| Antibodies | Concentration | Dilution | Antigen | Specificity | Manufacturer |
|---|---|---|---|---|---|
| Anti-PLAP (NDOG 2) | 1.6 µg/µl | 1/1000 | PLAP | STB-EV | In house antibody |
| Anti-CD63 | 200 µg/µl | 1/1000 | CD63 | STB-EV | Santa Cruz Biotechnology |
| Anti-ALIX | 200 µg/µl | 1/1000 | ALIX | S STB-EV | Cell Signalling |
| Anti-Cytochrome C | 200 µg/µl | 1/500 | Cytochrome C | Placenta homogenate | Santa Cruz Biotechnology |
| Anti-SR-BI | 0.35 µg/µl | 1/1000 | SR-BI | N/A | Abcam |
| Anti-Filamin B | 1.64 µg/µl | 1/1000 | Filamin B | N/A | Insight Biotechnology |
| Anti-PAPP-A2 | 1 µg/µl | 1/2000 | PAPP-A2 | N/A | Abcam |
| Anti-Collagen 17 A1 | 1 µg/µl | 1/1000 | Collagen 17 A1 | N/A | Abcam |
| Polyclonal goat-anti-mouse/rabbit immunoglobulin HRP | | 1/2000 | Mouse and Rabbit Immunoglobulins | N/A | Dako UK Ltd |

## 2.1.5 Cell culture: Human endothelial umbilical vein cells as a positive control for Western blots

Human umbilical vein endothelial cells (HUVEC) were isolated from the human umbilical cord by collagenase digestion of the interior of the umbilical vein. Briefly, placentas were collected from normal pregnant women undergoing elective caesarean section and processed within 10 minutes. The umbilical cord was inspected, and if healthy, the cord was clamped and separated from the placenta. Next, about ten to fifteen centimetres of the cord with no evidence of bleeding or trauma was set aside for HUVEC isolation. The umbilical vein from the cord was identified. The vein was flushed with 20 ml Hanks' solution till the effluent was clear to ensure the patency of the umbilical vein and to get rid of red blood cells. Air was

injected twice to get rid of the Hanks solution. The lower end of the umbilical cord was clamped with artery forceps, and the upper end of the vein was infused with 5 ml of 1X collagenase type IA (1mg/ml) (Sigma, UK). The cord was then incubated at 37$^{o}$C for 15 minutes in 5% $CO_2$ for maximal digestion of the extracellular matrix and the detachment of endothelial cells. During incubation, the cord was intermittently massaged every five minutes. After fifteen minutes, the contents of the umbilical vein were emptied into a ten ml Falcon tube, followed by flushing the cord twice with ten ml of complete endothelial cell medium (Life technologies). The cell suspension was pelleted at 500 g for 5 minutes at room temperature. The pellet was then re-suspended with 2 ml of complete endothelial cell medium and seeded equally into two 1% gelatin-coated T25 cell culture flasks (NUNC $^{TM}$) and topped with 8 ml of complete endothelial cell medium. Cells were left to settle for 2 hours in 5% $CO_2$ and 21% $O_2$, after which the media was changed to get rid of contaminating red blood cells, then every two days until the cells were 89-90% confluent. HUVECs were passaged to make more cells, processed as cell lysates, or stored in liquid nitrogen for future use.

Trypan blue, a dye impermeable to healthy cells but not dead or dying cells, was used to check for viability by direct visual observation under the microscope. Equal volumes of cell suspension and trypan blue (*0.4% w/v solution*) were mixed and loaded on a haemocytometer (superior Marienfled). After verifying the viability of cells, 2 X $10^{6}$ cells were resuspended in 500 microlitres of fPBS and lysed with RIPAs buffer (Thermo Fisher $^{TM}$) buffer using the standard protocol to generate cell lysates.

### 2.1.6 BCA protein assay

Fresh STB-EVs, lysed HUVEC cells, and placenta homogenate were assayed for their protein content using the bicinchoninic acid protein assay kit (BCA) (Pierce). Briefly, bovine serum albumin (BSA) stock (1 mg/ml) was diluted in filtered PBS to give rise to protein concentration standards 1,0.5,0.25,0.125,0.625 mg/ml. STB-EVs, HUVEC lysates, and placenta homogenate samples were diluted in filtered PBS (1: 8 ratio). Twelve and a half microlitres of BSA standards and samples were added to a 96 well plate, followed by 100 microlitres of BCA reagent mix (50:1 ratio of BCA solution and copper II sulphate solution, respectively). Proteins reduce $Cu^{2+}$ to $Cu^{+}$ in an alkaline solution (the biuret reaction), resulting in purple colour, which is read by a spectrophotometer to extrapolate protein concentration based on a standard curve. The 96 well plate was covered in foil and put in the shaker for 5 minutes prior to 30 minutes incubation at 37$^{o}$ C. Reactions were performed in duplicates, and absorbance was read at 562 nm using a FLUOStar OPTIMA (BMG) plate reader.

## 2.2 Methods for mRNA isolation, characterisation, and analysis

### 2.2.1 RNA-sequencing library preparation and sequencing

For sequencing, RNA extraction and sample preparations were performed for placenta tissue (6 NP, 7 PE) with the RNeasy mini kit and STB-EVs (6 NP, 8 PE) with the miRCURY™ RNA isolation kit for biofluids (Exiqon Services, Denmark) based on manufacturer's protocol. An equal amount of STB-EVs based on protein concentration (200 µg) was diluted to 200 µl, and total RNA was extracted from this STB-EV mixture. Thirty milligrams of placenta tissue were mechanically homogenised, and the total RNA was extracted with the appropriate kit.

During extraction, I pre-treated the samples with DNAses to reduce DNA contamination, but the STB-EVs were not pre-treated with RNAses. Due to the elevated nucleases present in the placenta, it will be unlikely for non-vesicular RNAs to be present. In addition, the difficulty in inhibiting nucleases may reduce the yield of RNA isolated from STB-EVs. The extracted RNA was assessed for purity with Nanodrop (NanoDrop 1000 software), and all samples had a 260/280 ratio greater than 1.8. The samples were sent to the Welcome centre for human genetics (WCHG) for sequencing. At WCHG, the RNA was assessed with a bioanalyzer (Agilent Technologies) to determine the concentration and RIN (RNA Integrity Number) values. The RINs were all greater than 8/10 (in the placenta homogenate) but not STB-EV samples with RIN values between 1-3 (Figure 9). It is widely accepted that the RIN values are not applicable for extracellular vesicles due to the fragmented nature of RNA they contain and the absence of 18S and 28S ribosomal RNA peaks[193].

RNA libraries were prepared using the TruSeq RNA library (Illumina). A standard procedure was followed for mRNA sequencing. Briefly, polyadenylated mRNAs were selected from total RNA samples using oligo-dT-conjugated magnetic beads. Polyadenylated RNA samples were immediately converted into stranded Illumina sequencing libraries using 200 bp fragmentation and sequential adapter following the manufacturer's specifications. The resulting cDNA was amplified, enriched, and indexed (12 cycles of amplification) with PCR primers, including an index sequence to allow for multiplexing. All RNA sequences were purified on gels and sequenced on a HiSeq 2500 high output v3 flow cell using paired-end, 75 bp reads (Illumina). Sequencing data have been deposited in the NCBI GEO database (GSE190973) and NCBI's Sequence Read Archive (SRA) database and can be accessed at https://www.ncbi.nlm.nih.gov/geo/query/acc.cgi?acc=GSE190971

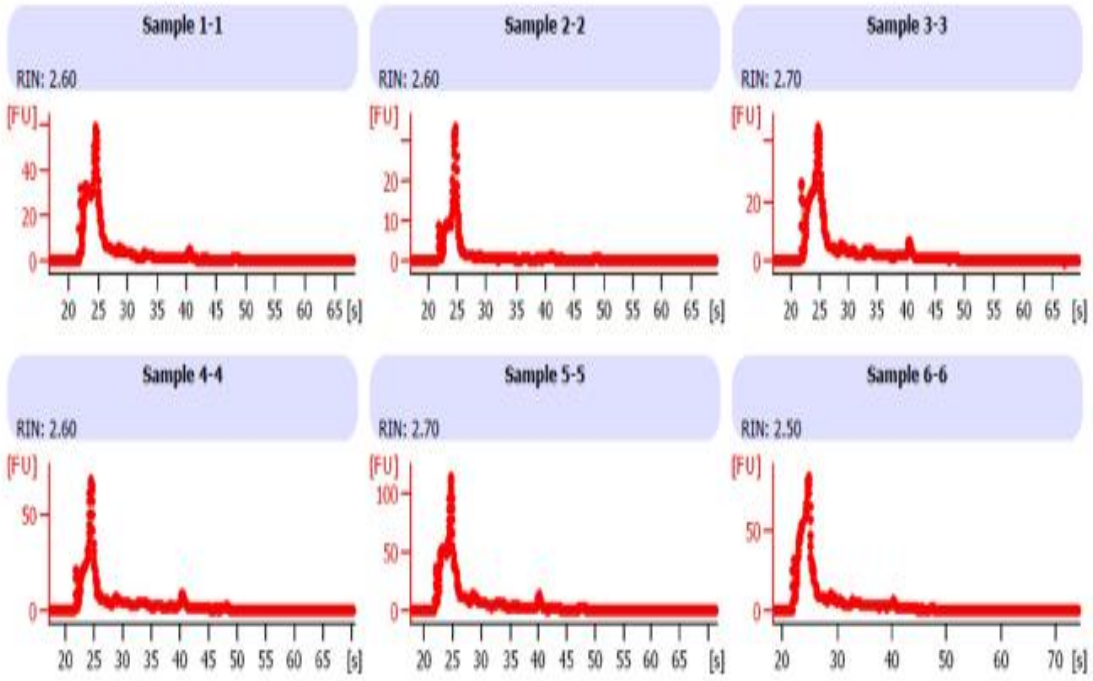



**Figure 9.** Figure showing representative electropherogram for STB-EV samples. As expected, the RNA integrity number (RIN) for all STB-EV samples were less than 3 (details below). The samples were made up of RNA biotypes within the size range of 20-30 base pairs and had RNA integrity number (RIN) values are between 1-3 as expected of extracellular vesicles.

## 2.3 Methods for bioinformatics and statistical analysis of messenger RNA sequences

### 2.3.1 Bioinformatic analysis of messenger RNA sequences

I performed bioinformatics analysis on Galaxy (https://usegalaxy.org/) and (https://usegalaxy.eu/), a project supported in part by the National Science Foundation (NSF), National Human Genome Research Institute Home (NHGRI), the Institute for CyberScience at Penn State, the Huck Institutes of the Life Sciences, and Johns Hopkins University.

Compressed Sanger fastq files generated from the WCHG for placenta tissue and STB-EVs were imputed in the user allocated space on the galaxy project server. I used FastQC[194] (*Galaxy version 0.72+galaxy1*) to obtain overall quality control (QC) metrics and MultiQC[195] ((*Galaxy version 1.9+galaxy1*) to amalgamate the QC metrics before and after trimming of adapters ( trimmomatic[196] [*Galaxy version 0.38.0*]).

I obtained additional QC metrics with Infer Experiment *(Galaxy Version 2.6.4.1),* MarkDuplicates *(Galaxy version 2.18.2.2),* and IdxStats (*Galaxy version 2.0.3*) to assess strandedness, duplicates and chromosomal read mapping, respectively. *Gene Body Coverage (BAM)* Tools (*Galaxy version 2.6.4.3*) was used to assess the gene body coverage. In contrast, the read distribution tool (*Galaxy version 2.6.4.1*) was used to assess the read distribution across features (exons [CDS, 5'UTR,3'UTR], introns and intergenic regions). The QC results were aggregated with MultiQC for ease of interpretation. The trimmed reads for each sample were aligned with the reference Homo sapiens build 38 (hg38) genome obtained from Ensembl with *HISAT 2* (*Galaxy version 2.2.1+galaxy0*). Featurecounts (Galaxy version 2.0.1+galaxy1) were used for each sample to quantify genes based on reads mapped to the provided hg38 reference files. A count matrix was generated with the column join on collection tool (*Galaxy version 0.0.3*) to create a count matrix.

## 2.3.2 Differential expression analysis of messenger RNA data

The DESeq2 package[197] (*v.1.32.0 in R v.4.0.5*) was used to measure the significance of differentially expressed genes between the normal and preeclampsia samples and create plots of the results following the standard protocol and accompanying tutorial. The reported p values were adjusted for multiple testing using Benjamin Hochberg correction and reported as a false-discovery rate. An adjusted p value less than 0.05 was taken as significant. DESeq2 is a

bioinformatic tool for analysing RNA-Seq data count matrix assuming a negative binomial distribution to estimate differential expression. DESeq2 internally corrects for the difference in library size by normalising using the means of ratio. All gene count data were prefiltered to remove all genes with less than five reads across all samples. The data was then visually explored with dimension reduction plots such as principal component analysis and correlation heat maps. Outliers were removed if they clustered away from others and had a correlation score less than 0.8. The DESEQ () function was then run on the newly generated DESeq2 data object (created by the count matrix and the metadata). The DESEQ () function estimates the size factors, estimates the dispersion and performs negative binomial general linear model fitting and computation of Wald statistic. I shrunk the results with 'ashr' to better visualise and rank genes. Ashr is a shrinkage function from the ashr package[198].

Log ratio(M) and average (A) (MA) plots were constructed to visualise the difference between preeclampsia and normal. Typically, the expression of the genes is expected to be consistent between preeclampsia and normal (trumpet-shaped MA plot). Normalised individual gene counts were visualised with ggplot2[199]. The volcano plot was generated with Enhancedvolcano plot, and the enterez ID gene names were obtained with the mygene R package. The differentially expressed mRNAs or small RNAs were screened with the criteria of false discovery rate (FDR) < 0.05 and $|\log_2(\text{Fold change})| \geq 0.75$.

### 2.3.3 Functional enrichment analysis of messenger RNA analysis

Functional gene annotation was performed with the R package, ClusterProfiler[200] (for Gene Ontology [GO] terms[201] and KEGG pathways[202]) and signalling pathway impact analysis (SPIA) with the transcriptome set as the background. Default analytic options and annotation categories were used. Enrichment was done with overrepresentation analysis (ORA) based on

a 2 X 2 contingency table. Based on a hypergeometric distribution, ORA tests overlap between differentially expressed genes and genes in a background (gene set). P value was set at 0.05 after adjusting for multiple testing with Benjamin Hochberg correction. Signalling pathway impact analysis (SPIA)[203] is an enrichment detection tool for KEGG pathways that combines the classic over-representation analysis with the actual perturbation on a given pathway. Gene Ontology and KEGG annotations were chosen based on their popularity in the bioinformatics field and the duration of curation of these databases. Gene Ontology is made up of three categories that classify genes into Cellular Components (CC), Molecular Function (MF), and Biological Processes (BP). The Kyoto encyclopaedia of genes and genomes (KEGG) is a database that contains manually drawn pathway schemas of molecular interaction and reaction networks. The pathways are divided into seven broad categories: *metabolism, genetic information processing, environmental information processing, cellular process, organismal systems, human diseases,* and *drug development*.

## 2.4 Methods for validation of selected mRNA with quantitative polymerase chain reaction (qPCR)

### 2.4.1 Synctiotrophoblast membrane extracellular vesicles (STB-EVs) RNA extraction

Equal quantities of STB-EV samples based on protein concentration and amount were separated and diluted with RNAse free water to make a 200 µl sample mix. The sample mix was loaded on the ExoRnaeasy Maxi Kits (Qiagen) column, and high-quality RNA was extracted. For all STB-EV samples, I spiked with an equal amount of M2 Phage RNA (2 µl of 1: 25 dilutions of 5 nanomolar stock solutions) and external RNA control consortium (ERCC) RNA Spike-in Mix (ThermoFisher Scientific [1 µl of 1: 10,000]) to act as a carrier, increase

RNA extraction efficiency, or/and act as an internal reference gene. RNA quantification and purity were determined as previously described in section 2.2.1.

### 2.4.2 Complementary cDNA synthesis for mRNA synthesis

I generated complementary DNA strands (cDNA) (Figure 10) by reverse transcribing the same quantity of RNA (determined by a bioanalyzer) with the high-capacity cDNA reverse transcription kit (Applied Biosystems, USA). All reactions, including sample thawing, were done on ice. A reaction master mix was constituted using 2 µl 10X RT buffer, 0.8 µl of 100 mM deoxynucleotide triphosphate (dNTP) mix, 2 µl 10X random primers, 1µl multiscribe reverse transcriptase, and 3.2 µl of nuclease-free $H_2O$. Ten microlitres of this master mix were then added to 11 µl RNA samples. This mix was briefly vortexed and centrifuged, followed by reverse transcription reaction with a G-storm$^{TM}$ (G-storm, UK) thermocycler with the following settings: 16$^{o}$C for 30 minutes, 42$^{o}$C for 30 minutes, followed by 85$^{o}$C for five minutes, and a final hold at 4$^{o}$C. For medium/large STB-EVs, the samples were diluted 1: 5 to make a working solution and aliquoted into 120 µl each (for qPCR reaction). For the small STB-EVs, the undiluted samples were aliquoted in 10 µl, and one aliquot was immediately pre-amplified (TaqMan™ PreAmp Master Mix Kit) to be subsequently used in qPCR. In situations where qPCR could not be done on the same day due to the need for preamplification or other reasons, aliquots were kept in the fridge (for < 2 days) - 20$^{o}$C (for less than one month) or – 80$^{o}$C (for greater than one month).

### 2.4.3 Preamplification of complementary DNA samples

As earlier said, the small STB-EVs samples were not adequate and needed to be preamplified. Ten µl of cDNA samples were mixed with 25 µl of TaqMan preamp master mix (2X) and an in-house generated pooled assay mix (0.2X). This mix was briefly vortexed and centrifuged followed by reverse transcription (RT) reaction with a G-storm$^{TM}$ (G-storm, UK) thermocycler with the following settings: 95$^{o}$C for 10 minutes 15 seconds, 95$^{o}$C for 15 seconds, 60$^{o}$C for 4 minutes, 99$^{o}$C for ten minutes, and a final hold at 4$^{o}$C. The reaction was repeated ten times. The samples were then diluted 1: 10 to make a working solution and aliquoted into 120 µl each. Figure 10 shows a description of reverse transcription (RT), and quantitative polymerase chain reaction (qPCR) and Table 5 shows the Taqman expression gene assays used in this project.

### 2.4.4 Quantitative polymerase chain reaction (qPCR) for mRNA validation

Quantitative polymerase chain reaction (qPCR) was done with assistance from Maryam Rahbar and Prassana Logenthiran on Quantstudio$^{TM}$ 3 real-time PCR systems (*Quantstudio$^{TM}$ design and analysis software*), MicroAmp$^{TM}$ optical 96 well reaction plate (N8010560) and optical adhesive film kit (4313663), with the hydrolysis probe based Taqman$^{(R)}$ gene expression assay (Applied Biosystems, USA). The following settings were used: hold 50$^{o}$C for 2 minutes, hold at 95$^{o}$C for 20 seconds, followed by forty cycles of 95$^{o}$C for 1 second and 60$^{o}$C for 20 seconds. Quantitation cycles (Cq) values were generated automatically by the quantstudio design and analysis desktop software. The geometric mean of YWHAZ (*tyrosine 3-monooxygenase/tryptophan 5-monooxygenase activation protein zeta*) and SDHA (*succinate dehydrogenase complex flavoprotein subunit A*) were used as the internal reference genes for the normalisation of all qPCR data. We analysed the qPCR data and calculated fold changes using the $2^{-\Delta\Delta}$Ct method[204]. Data were expressed as fold change, and standard error is denoted as error bars with GraphPad prism software (version 9). Statistical testing was made on the Δ

Ct values using a one-tailed Student t-test, and significance was set at $p < 0.05$. All gene expression assays, their corresponding assay IDs, and amplicon length are listed in table 5.

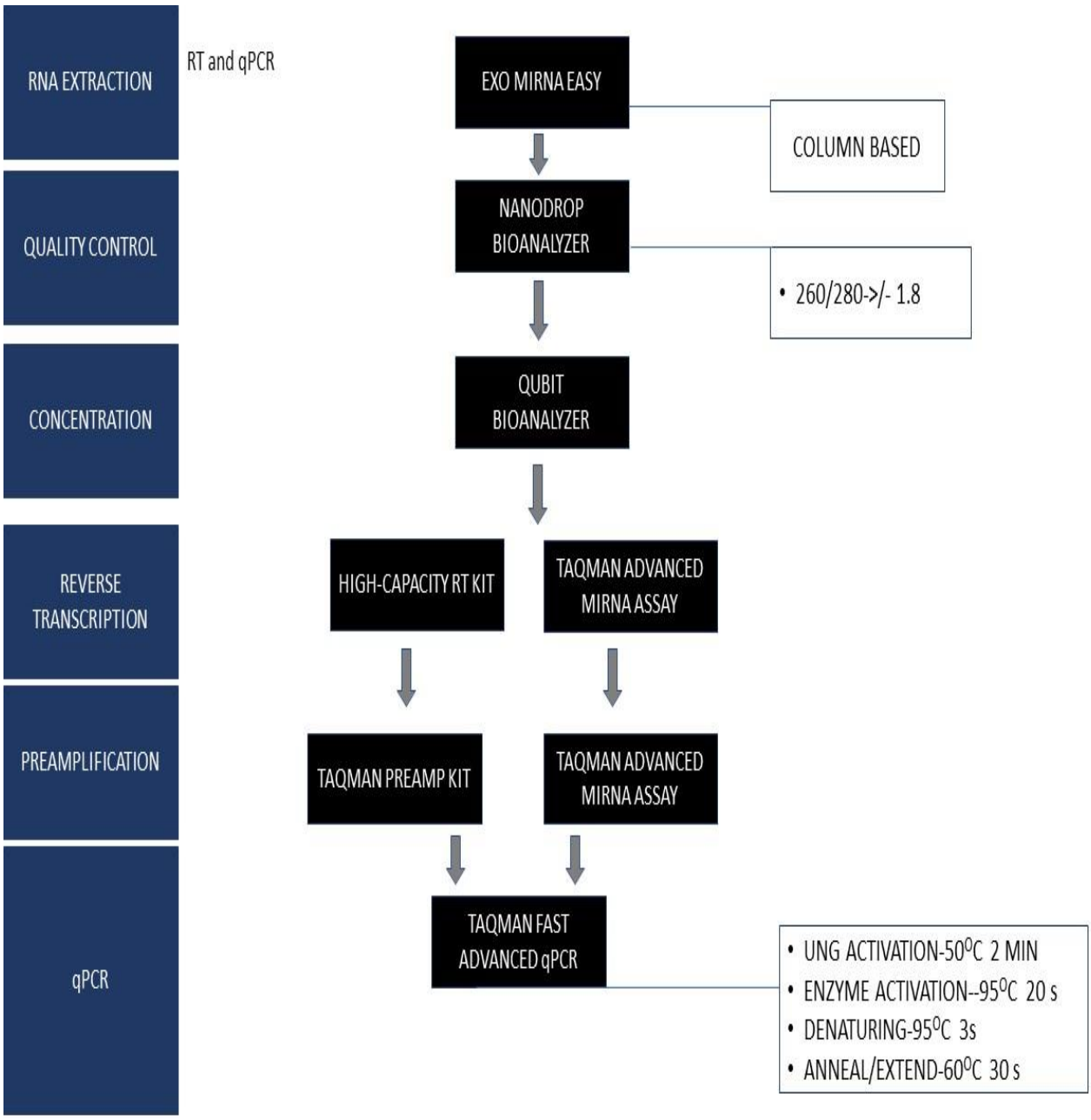



**Figure 10.** Figure showing the steps involved in reverse transcription and quantitative polymerase chain reaction of messenger ribonucleic acid (RNA) and micro ribonucleic acid (RNA). The Taqman Fast advanced qPCR was made up of four steps 1) UNG activation (50°C for 2 minutes), 2) enzyme activation (95°C for 20 seconds), 3) denaturing (95°C for 3 seconds and 4) anneal/extend (60°C for 30 seconds).

**Table 5.** Table showing quantitative polymerase chain reaction (PCR) primers, assay ID and amplicon length.

| Gene Symbol | Assay ID | Amplicon Length |
|---|---|---|
| PAPP-A2 | Hs00535718_m1 | 67 |
| ADAM12 | Hs01106101_m1 | 54 |
| INHBA | Hs01081598_m1 | 61 |
| SIGLEC6 | Hs00971272_g1 | 117 |
| HTRA4 | Hs00538137_m1 | 75 |
| EBI3 | Hs01057148_m1 | 64 |
| FSTL3 | Hs00610505_m1 | 84 |
| HSD17B1 | Hs00166219_g1 | 124 |
| CGB3 | Hs00361224_gh | 55 |
| SDHA | Hs00188166_m1 | 70 |
| ERCC-00071(artificial control) | Ac03459912_a1 | 136 |
| YWHAZ | Hs01122445_g1 | 62 |
| LEP | Hs00174877_m1 | 74 |
| COL17A1 | Hs00990036_m1 | 57 |
| FLNB | Hs00963202_m1 | 100 |
| SLC45A4 | Hs01088148_m1 | 70 |

## 2.5 Methods for microRNA characterisation and analysis

### 2.5.1 RNA-Sequencing library preparation and sequencing

RNA extraction and sample preparations were done for placenta tissue (6 NP, 7 PE) and STB-EVs (6 NP, 8 PE), as earlier stated in section 2.2.1. Using the standard procedure, RNA libraries were prepared with the TruSeq small RNA library preparation kits (Illumina). The 3' and 5' adapters were briefly ligated to the RNA subtype, followed by reverse transcription and library amplification. The amplicons were then gel purified, and the purified construct recovered. Final libraries were concentrated, assessed for size, purity, and concentration with a bioanalyzer, and subsequently normalised to achieve a uniform RNA concentration. Sequencing data have been deposited in the NCBI GEO database (GSE190973) and NCBI's Sequence Read Archive (SRA) database and can be accessed at https://www.ncbi.nlm.nih.gov/geo/query/acc.cgi?acc=GSE190972.

## 2.6 Methods for bioinformatics and statistical analysis of microRNA sequences

### 2.6.1 Bioinformatic analysis of microRNA sequences

I performed bioinformatics analysis for microRNA (Figure 11 and 12) analysis on Oasis 2.0 (*https://oasis.ims.bio/small_rna_classification.php*)[205], a fast, reliable, and easily accessible bioinformatic webtool. Firstly, fastq files were compressed with the accompanying Oasis compressor[205] to facilitate analysis. The compressed files were loaded in the Oasis 2.0 webtool. FastQC (v.0.11.2) was used to obtain quality control (QC) metrics before and after trimming of adapters/barcode [trimmomatic (v.0.32)] and length filtering. Length filtering was set at minimum and maximum length at 15 and 50 nucleotides, respectively. Acceptable mismatches were set at 5% of the read length. Reads were aligned to the human reference genome,

microRNAome, and sRNAome (piwi-interacting RNA, small interfering RNA, small nuclear RNA, and small nucleolar RNA) stored in the Oasis database with STAR (2.4.1d)[206]. Unmapped reads from this step were realigned to the human reference genome (Homo Sapiens hg38) to predict and archive novel microRNAs in the Oasis-Db using Bowtie (v1.0.0). The unmapped read from this second step was mapped to bacterial, archaeal, and viral genomes using Kraken (v.0.15.5-beta)[207] to identify and characterise infectious contaminants. To detect potentially orthologous or cross-species microRNAs reads that could not be classified as humans or infectious contaminants by any of the three steps were realigned to all the non-human microRNAs in miRbase [208]with STAR (v.2.4.1d). All unmapped reads after all four simultaneous steps were subsequently discarded. More information about the default parameter setting for OASIS-db can be found in the accompanying documentation. Quantification of gene expression values was down by STAR quant mode, and exploratory analysis of the results, including visualisation, was done on Oasis. A gene count table was constructed from each gene count.

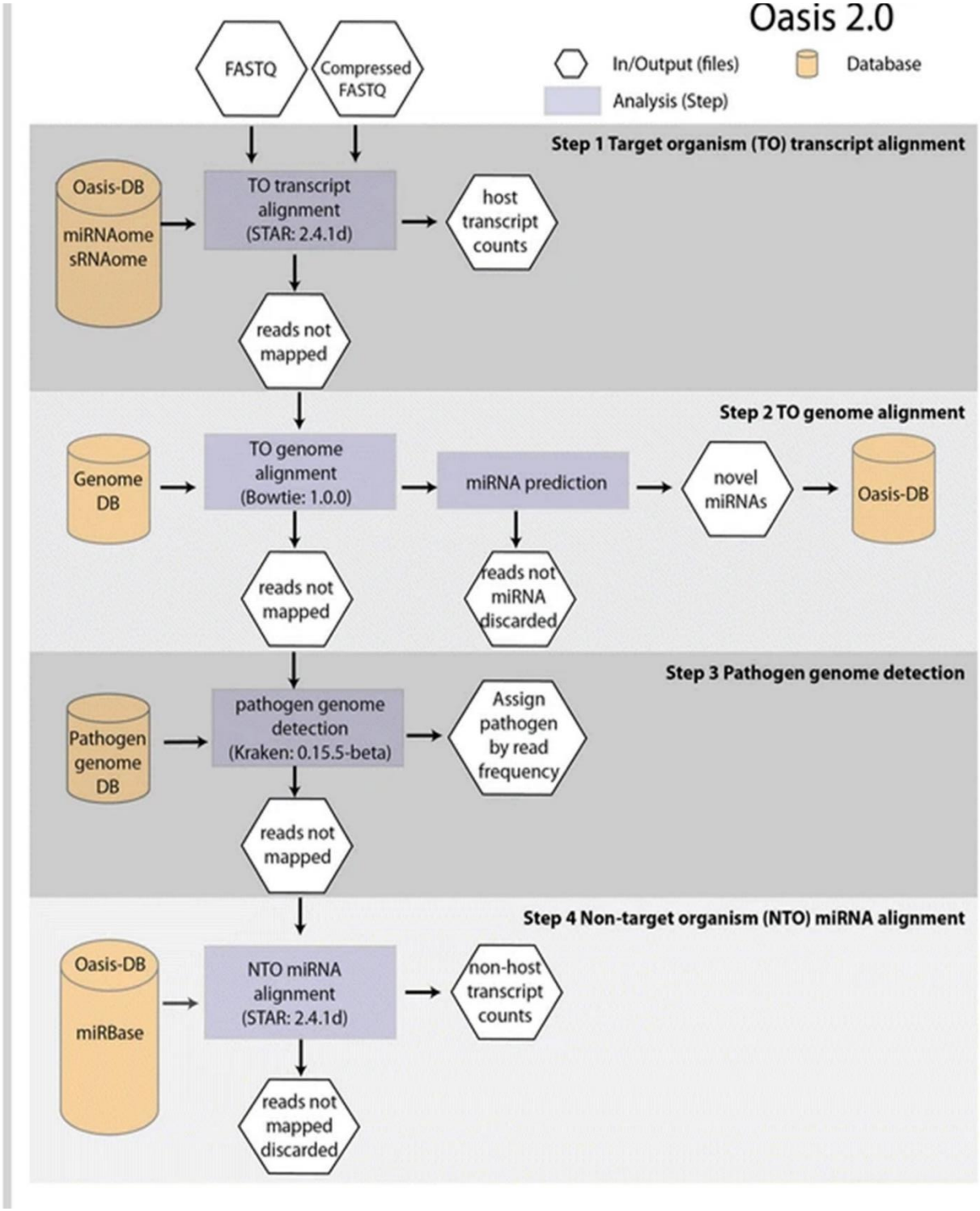



**Figure 11.** Small RNA analysis pipeline adapted from OASIS 2.0[209] showing the four steps involved 1) alignment to the human transcriptome 2) align the reads the human genome 3) alignment to pathogen to get rid of contaminants and 4) alignment to non-target organism miRNAome




**Figure 12**. Figure showing the statistical analysis pipeline used in the analysis of small ribonucleic acid (Small RNA). Differentially expressed micro RNAs were loaded into the DIANA-miRPath v3.0 and the messenger RNA of these microRNA targets predicted. This step was followed by a functional enrichment analysis and identification of significantly overexpressed gene ontology terms or KEGG pathways

## 2.6.2 Differential expression analysis of microRNA data

I used a similar analytic pipeline for the small RNA (particularly microRNA) analysis and mRNA analysis. The DESeq2 package (v.1.32.0 in R v.4.0.5) was used to generate the list of differentially expressed small RNAs between the normal and preeclampsia samples following the standard protocol and accompanying DESeq's tutorial. I adjusted the p values for multiple testing with Benjamin Hochberg and reported these corrected p values as a false discovery rate with significance taken as less than 0.05. In DESeq2, the gene count data were prefiltered to remove all genes with less than five reads across all samples. The data was then visually explored with principal component analysis and Pearson correlation heat maps. Samples were considered outliers if clustered away from others and had a correlation score of less than 0.8. The differentially expressed small RNAs were screened with the criteria of false discovery rate (FDR) $<0.05$ and $|\log_2 (\text{Fold change})| \geq 0.75$.

## 2.6.3 Functional enrichment analysis of microRNA analysis

Due to my specific interest in microRNAs, their ability to regulate transcription, and inadequate functional annotation information on the other small RNA biotypes, I performed functional enrichment analysis on the microRNAs of all samples (placenta and STB-EVs) with DIANA-miRPath v3.0 (http://www.microrna.gr/miRPathv3). The microRNAs were subcategorised into up and downregulated and loaded in DIANA-miRPath v3.0. Up to 100 microRNAs (miRNAs) based on fold change (LFC $\geq 0.75$) and adjusted p value ($< 0.05$) were analysed. This limitation was imposed by the default setting of the tool and the computational intensity of processing large lists of microRNAs. The mRNA targets of the loaded microRNAs were predicted with the microT-CDS algorithm with a microT-threshold of 0.8. The analysis results were fused at the level of categories/pathways to help obtain a more refined result. Furthermore, removal,

summarisation, and visualisation of redundant GO terms were done with REVIGO (http://revigo.irb.hr/).

## 2.7 Methods for validation of selected microRNA with quantitative polymerase chain reaction (qPCR)

### 2.7.1 Complementary cDNA synthesis for microRNA synthesis

Complementary DNA (cDNA) was generated with the TaqMan™ advanced miRNA cDNA synthesis kit (A28007). Before reverse transcribing the RNA samples, I set aside the same quantity of RNA samples and added an equal amount of cel-mir-39 (Integrated DNA technologies, 100 nmoles RNA Oligo) spike-in into each aliquot (as 1 µl per sample of a 0.25 nanomolar working solution All reactions were performed on ice following the manufacturer's protocol. Briefly, the reverse transcription phase was done in four stages 1) polyA tailing, 2) adaptor ligation, 3) reverse transcription, and 4) miR-amplification reaction. MicroRNAs are short nucleotide sequences that do not have a polyA tail, unlike mRNAs. This, in addition to the short sequences, make it challenging to reverse transcribe microRNAs. A polyA tail was artificially added to facilitate reverse transcription to circumvent this. Each reaction was done in a G-storm™ (G-storm, UK) thermocycler with settings provided by the manufacturer. Following reverse transcription, ten µl of reverse-transcribed samples was preamplified. Un preamplified samples were aliquoted and stored in -80$^{o}$C for future use. The preamplified samples were diluted at 1:5 with 0.1X TE buffer and subsequent qPCR reactions. In situations where qPCR could not be done on the same day due to the need for preamplification, aliquots were kept in the fridge (for < 2 days) or - 20$^{o}$C (for less than a month).

## 2.7.2 Quantitative polymerase chain reaction (qPCR)

I selected the following microRNAs to validate based on fold change; hsa-*miR-30b-5p, hsa-miR-221-3p, hsa-miR-222-3p, hsa-miR-324-5p, hsa-miR-194-5p, hsa-miR-519c-3p, hsa-miR-652-3p, hsa-miR-584-5p, hsa-miR-421, hsa-let-7e-5p, hsa-miR-3196, hsa-miR-4488, hsa-miR-4516, hsa-miR-9-5p, hsa-miR-210-3p, and hsa-miR-193b-5p*. I validated these selected differentially expressed microRNAs with quantitative polymerase chain reaction (with help from Maryam Rahbar and Prassana Logenthiran) with the hydrolysis probe-based Taqman® gene expression assay (Applied Biosystems, USA). The Taqman® technology uses a well-described workflow summarised in figure 10. I made a qPCR master mix with 1 µl of 20X Taqman gene expression assay, 10 µl 2X Taqman® gene expression master mix, 7 µl of RNAse free water and added 18 µl of this master mix to 2 µl of preamplified cDNA samples in a 96 well reaction plate (MicroAmp $^{TM}$ optical 96 well reaction Plate) and sealed with a transparent qPCR film (Microamp$^{TM}$ optical adhesive film) to prevent sample loss by evaporation. I carried out forty cycles per reaction using the Quantstudio$^{TM}$ 3 real-time PCR System (Thermofisher), and all microRNAs tested were detected before the 30$^{th}$ cycle. The following settings were used for the qPCR: hold 50$^{o}$C for 2 minutes, hold at 95$^{o}$C for 20 seconds, followed by forty cycles of 95$^{o}$C for 1 second and 60$^{o}$C for 20 seconds acquiring to the FAM $^{TM}$ Channel. Cq values were generated automatically by the Quantstudio design and analysis desktop software (Thermofisher). Raw data obtained from the software was exported as an excel spreadsheet, and all analysis was subsequently performed in Microsoft excel. *Hsa-miR-30d-5p* was used as the internal reference microRNAs to normalise all qPCR data. I chose *hsa-miR-30d-5p* from the sequencing data based on an absent differential expression (FC < than 0.001) between PE and normal and a low standard error (LSE). I then conducted an independent qPCR experiment to validate the stability of *hsa-30d-5p*. qPCR data and fold change (FC) were calculated using the $2^{-\Delta\Delta Ct}$ method[204]. Statistical testing was done on the Δ Ct values using a one-tailed Student

*t-test*, and significance was set at $p < 0.05$. Data visualisation was done with GraphPad Prism software (version 9), expressed as fold change, and standard error denoted as error bars. All miRNA expression assays used and their corresponding assays IDs used in this study are listed in Table 6

**Table 6.** Table showing quantitative polymerase chain reaction (PCR) primers, assay ID and amplicon length.

| MicroRNA | Assay ID |
|---|---|
| Hsa-miR-4516 | 478303_mir |
| Hsa-miR-193b-5p | 478742_mir |
| Hsa-miR-3196 | 483159_mir |
| Hsa-miR-4488 | 478906_mir |
| Hsa-miR-652-3p | 478189_mir |
| Hsa-miR-584-5p | 478167_mir |
| Hsa-miR-194-5p | 477956_mir |
| Hsa-miR-519c-3p | 479495_mir |
| Hsa-miR-324-5p | 483066_mir |
| Hsa-miR-30b-5p | 478007_mir |
| Hsa-miR-221-3p | 477981_mir |
| Hsa-miR-191-5p | 477952_mir |
| Hsa-miR-222-3p | 477982_mir |
| Hsa-miR-30d-3p | 479362_mir |
| Hsa-miR-9-5p | 478214_mir |
| Hsa-let-7e-5p | 478579_mir |
| Hsa-miR-210-3p | 477970_mir |

## 2.8 Methods for protein isolation, characterisation, and analysis

### 2.8.1 Sample preparation for mass spectrometric analysis and bioinformatic analysis of proteomic data from placenta tissue, medium/large, and small STB-EVs

STB-EVs and placental tissue samples were processed for LC-MS (Target Discovery Institute, Oxford). Briefly, STB-EVs and placental tissue samples (10 µg total protein) were reduced with dithiothreitol (DTT) (final concentration 5 mM) for 60 min at room temperature, then alkylated with iodoacetamide (final concentration 20 mM) for 60 min at room temperature. After precipitation with methanol/chloroform, the protein pellet was resuspended in 6 M urea then the urea concentration was reduced to < 1 M with milliQ $H_2O$. Trypsin was added to achieve final trypsin: protein ratio of 1:50, and the samples were digested overnight at 37°C. Peptides were purified on Waters C18 Sep-Pak cartridges according to the manufacturer's instructions. The purified peptides were dried down in a speed vac and resuspended in 2% acetonitrile/0.1% trifluoroacetic acid and diluted 1:20 before injection. Peptides were injected into an LC-MS system comprised of a Dionex ultimate 3000 Nano LC (Liquid Chromatography) and a Thermo Q-Exactive mass spectrometer. Peptides were separated on a 50-cm-long EasySpray column (ES803; Thermo Fisher) with a 75 µm inner diameter and a 60-minute gradient of 2% to 35% acetonitrile in 0.1% formic acid and 5% dimethyl sulfoxide (DMSO) at a flow rate of 250 nl/min. The Top 15 most abundant peaks were fragmented after isolation with a mass window of 1.6 with a resolution of 17,500. The normalised collision energy was 28% (higher collisional dissociation). Raw data was imported and analysed with Progenesis QI (Waters) using standard settings and manually refined retention time alignment. MS/MS data was searched in Mascot (Matrix Science) against a human database (fused Uniprot/Trembl, 03/2018) with oxidation (Met)/deamidation (Gln/Asn) and carbamidomethylation (Cys) fixed as variable modifications. Precursor mass tolerance was set

to 10 parts-per-million (ppm) and fragment tolerance to 0.04 Da. Peptide identifications were FDR (False Discovery Rate) adjusted at 1%, and identifications with Mascot score < 20 were discarded.

Raw label-free quantitation (LFQ) data was imported and analysed in Perseus (Max Planck Institute of Biochemistry). Differential expression was performed by conducting a two-sample independent Student t-test. Multiple testing was corrected via permutation-based FDR (False Discovery Rate) with the default software settings, and significance was < 0.05. G: Profiler (https://biit.cs.ut.ee/gprofiler/gost) was used for functional enrichment analysis of the differentially expressed proteins (DEPs). The enriched pathways/terms from the KEGG database and Gene ontology database; gene ontology biological process (GO: BP), gene ontology molecular function (GO: MF), and gene ontology clinical component (GO: CC) were ascertained for each set of DEPs by applying hypergeometric testing. Multiple testing was corrected by Benjamin Hochberg correction, and the significance level was set to < 0.05.

### 2.8.2 Selection of placenta enriched proteins for Western blot validation

To identify the proteins that could potentially be biomarkers, I created a set of criteria that helped identify proteins that are placenta enriched or specific. Placenta specificity was defined as the sole expression of the protein of interest by the placenta. In contrast, placenta enrichment refers to a protein in which the placenta is one of the top six expressing organs. To achieve this, I combined all DEPs obtained from the placenta, medium/large STB-EVs, and small STB-EVs. I screened them on the publicly available human protein atlas[210], a curated database of experimentally validated protein expression patterns. The identified proteins were then validated by Western blotting.

## 2.8.3 Western Blotting for validation of identified differentially expressed STB-EV proteins in PE

Western blotting was performed as previously described earlier in the methods section. The PVDF membranes was probed for SR-BI (ab52629 [0.35 µg/µl] 1:1000 dilution, monoclonal rabbit, Abcam), Filamin B (GTX387 [1.64 µg/µl] 1: 1000 dilution, monoclonal mouse, Insight biotechnology), PAPP-A2 (ab59100 [1 µg/µl] 1: 2000 dilution polyclonal rabbit, Abcam), Collagen 17 A1 (ab79878 [1 µg/µl] 1: 1000 dilution polyclonal rabbit, Abcam).

Membrane treated with the EZ-ECL chemiluminescence detection kit for HRP (Biological industries Israel Beit Haemek, Israel). The treated PVDF membrane was developed using both a gel documentation system (G Box, Syngene, Cambridge UK) running GeneSys (version 1.5.0.0, Syngene) and a chemiluminescence film (Amersham HyperfilmTM ECL; GE Healthcare Limited, Buckinghamshire UK) and analysed in Fiji. Comparative expression analysis was normalised to the total protein (with Amido black)[211,212]. Statistical testing was performed on the normalised densitometric values using a one-tailed Student t-test, and significance was set at $p < 0.05$. To obtain the band intensity for each lane, I imaged the membranes with both a gel documentation system (G Box, Syngene, Cambridge UK) running GeneSys (version 1.5.0.0, Syngene) and a chemiluminescence film (Amersham HyperfilmTM ECL; GE Healthcare Limited, Buckinghamshire UK). The G Box scanned blots were analysed on Fiji for protein expression, the image was inverted, and the background was determined and subtracted from the band intensity. Following development and imaging of the membranes, the membranes were rinsed in double-distilled $H_2O$ and stained for total protein using amido Black 10 B (Merck) for three minutes with gentle agitation. The membranes were rinsed twice with a decolourising solution (*50% methanol, 7% acetic acid*) and allowed to air-dry overnight in a plastic wrap. The stained membranes were scanned, and total protein was quantified using Fiji[213] software (Version 1.50i, National Institutes of Health, Bethesda, MD, USA). The total

protein was quantified by selecting the area from the 75 KDa marker to the 50 KDa marker for each lane based on the consistency of two observable protein bands in each sample. The lower protein band was used to centre the selection area. The mean grey value was measured for each sample. After accounting for the background signal, the mean grey value for the total protein normalisation strip was used to normalise the protein of interest band intensity. I visualised the data with Graphpad prism software (version 9) as fold change (FC), and error bars denote the standard error of the mean.

## 2.9 Methods for multi-omic correlation analysis

### 2.9.1 MicroRNA-messenger RNA correlation analysis

I was interested in predicting and visualising mRNAs targets of the DE microRNAs that may be important in preeclampsia and which microRNAs may be responsible for the differentially expressed mRNAs in my samples (Figure 13). To do this, I generated normalised expression matrices for microRNAs and mRNAs and analysed them on miRTarVis+ (*http://sehilyi.com/mirtarvisplus/)*[214], a web-based interactive visual analytic tool. The microRNA expression matrices were arbitrarily filtered based on a fold change (FC) of 1.5 and an adjusted p value of 0.05. The mRNA expression data were filtered based on a fold change (FC) of 1.5 and an adjusted p value of 0.005. The filtered data were used to predict microRNA target interactions using the described targetscan prediction algorithm[215,216]. Following prediction, highly correlated microRNA-mRNA pairs were detected with Pearson correlation, mutual information, and maximal information-based nonparametric exploration (MINE). I looked at the top 300 interactions (except for 10K STB-EVs, for which I used the top 1000 interactions to get an adequate number (greater than 100) of interactions). The correlation coefficient cut-off was set at 0.5, and only microRNA-mRNA interactions in the opposite directions were included in the results. I used the same number of interactions for the mutual

information method. In addition, I used a neighbour cut-off score of 3. All other information was the same as for Pearson correlation analysis. Mutual information-based nonparametric exploration (MINE) was performed using the default setting on the webtool. Only microRNA and mRNA identified by all three algorithms were assumed to be the most reliable. Interactions were visualised with a treemap.

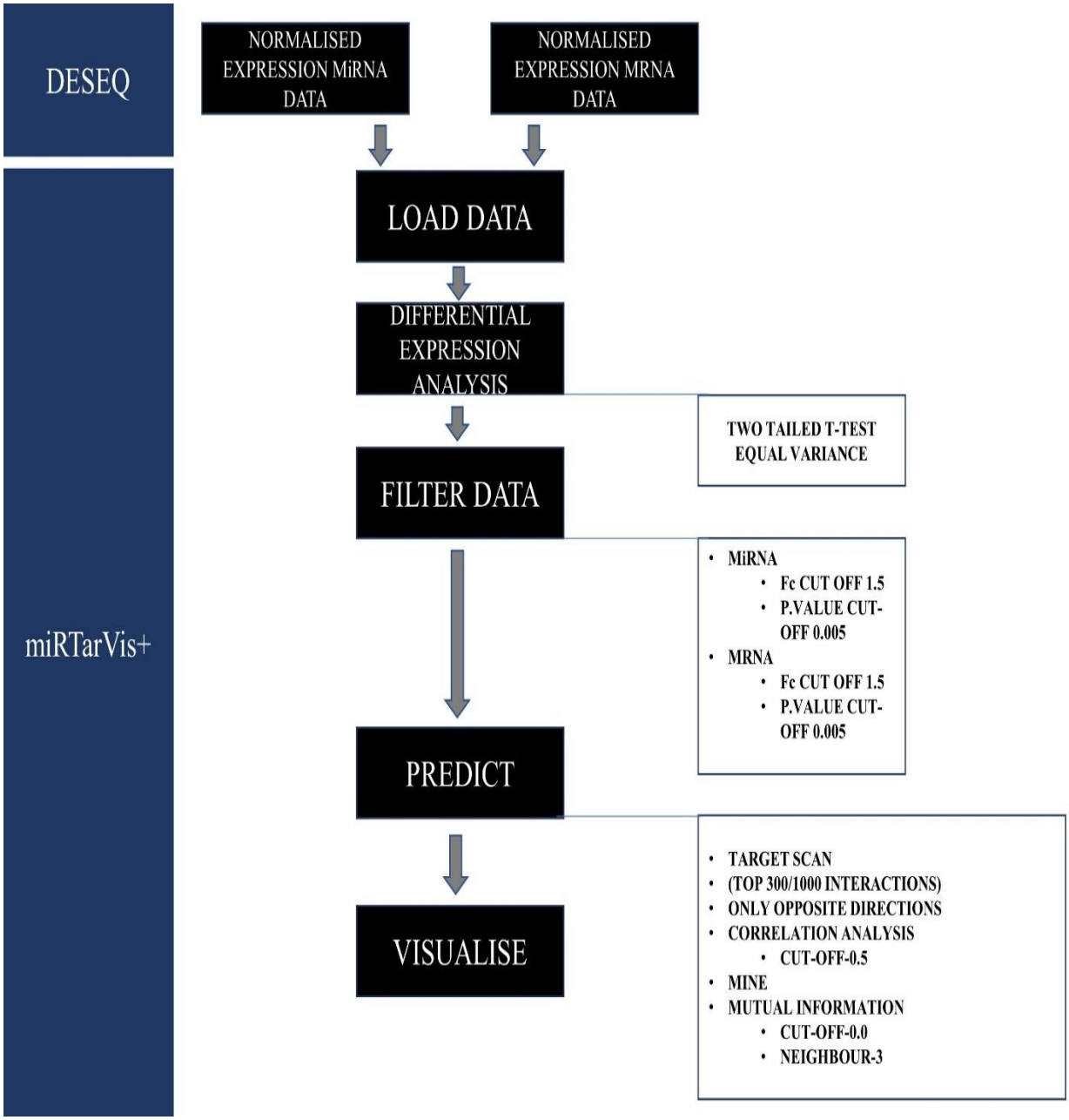



**Figure 13.** Figure showing the microRNA-messenger RNA correlation analysis pipeline. Differentially expression analysis was performed on normalized messenger RNA and microRNA expression data. These differentially expressed molecules were filtered by P value and fold change. The interactions between the differentially expressed messenger RNA and microRNA were predicted and visualised.

### 2.9.2 mRNA-protein correlation analysis

I took three approaches to assess the level of correlation between the mRNA and proteins in our data. Firstly, I evaluated and compared the direction and magnitude of fold change (FC) for all proteins and mRNA detected in our study. Secondly, I evaluated and compared the direction and magnitude of fold change (FC) for only significant proteins compared to all mRNA detected in our study. Finally, I compared the magnitude and direction of fold change (FC) of significant proteins to significant mRNAs. I performed all analyses in R (R v.4.0.5) and assessed all mRNA-protein correlations by calculating the Pearson coefficients. Visualisation of Pearson correlation analysis results was performed with scatter plots.

## 2.10 Methods for modular and clustering network analysis

### 2.10.1 Protein-protein (PPI) and gene-gene interaction (GGI) network construction, hub genes, proteins and pathways, and cluster analysis

I generated and visualised protein-protein (PPI) and gene-gene interaction (GGI) networks for the differentially expressed genes and proteins using the search tool for the retrieval of interacting genes (STRING)[217] plug-in in cytoscape[218] (v.3.8.2). All orphan genes and proteins in the PPI and GGI were pruned to generate a subnetwork consisting only of connected components (i.e., interacting genes or proteins). I confirmed that the network conformed to the power law before downstream analysis. The power law is a statistical concept that denotes the functional proportional relationship between two quantities, where a change in one quantity leads to a proportional change in the other. Critical/hub genes and pathways were bioinformatically determined with the Cytohubba plug-in[219]. Cytohubba ranks genes and proteins (nodes) in a network based on eleven discrete topological analysis methods: *degree, edge percolated component, maximum neighbourhood component, density of maximum*

*neighbourhood component*, *maximal clique centrality*, *bottleneck*, *eccentricity*, *closeness*, *radiality*, *betweenness*, and *stress*. Those genes and proteins identified most often/frequently by these different topological analysis methods were assigned as the critical/hub genes and proteins (top ten selected for each topographical analysis method). To identify essential pathways, the functions of these hub genes and proteins were determined using the online tool g: Profiler[220] with the human transcriptome or proteome (depending on the data) set as the background and the relevant gene ontology terms (biological processes, cellular components, molecular functions) and KEGG pathways identified.

Having identified critical hub genes and proteins using these techniques, I wanted to understand which biological pathways were involved. I identified potential molecular subclasses by breaking down the protein-protein, and gene-gene interaction network into clusters with the MCODE Plug-in (v 1.31 [Bader Lab, University of Toronto]) using the default setting and a node score cut off of 0.2, degree cut off of 2 and K-core of 2 (which allows for the identification of tightly knit clusters). The three highest-scoring clusters were further assessed to identify the biological function based on overrepresentation analysis of gene ontology terms and KEGG pathways with the ClueGO plug-in[221]. ClueGO performs enrichment tests based on hypergeometric distributions, and the p value was corrected for multiple testing using Benjamin-Hochberg correction.

## 2.11 Methods for the discovery of potential therapeutic agents in preeclampsia using connectivity Map Analysis

Using the up and downregulated genes and proteins generated from differential expression analysis, I created a unique disease-based molecular signature. Firstly, the DEGs and DEPs were independently assigned probe IDs with the NetAffxQuery(https://www.affymetrix.com/analysis/netaffx/xmlquery.affx?netaffx=netaffx4_annot). The probe IDs were loaded to CMap (Connectivity Map) (https://www.broadinstitute.org)[222], a database of small molecules, therapeutic agents, and perturbagens (molecules designed to disrupt intracellular processes) and their associated molecular signature. The CMap database can be adapted to identify potential therapeutic agents based on in-silico analysis. The analysis provides enrichment scores from -1 to + 1. Perturbagens with a negative score represents potential therapeutic agents, while perturbagens with a positive enrichment analysis score represent molecules that can theoretically aggravate preeclampsia and should be cautiously used. To increase the confidence in my analysis, I set a filtering threshold with the following parameters, enrichment score greater or equal to ± 0.70 and a p value less than 0.05.

# CHAPTER 2B

## RESULTS OF STUDY POPULATION DESCRIPTION, STB-EVs CHARACTERISATION AND EXPLORATORY ANALYSIS

## 2.12 Results

### 2.12.1 Patient demographics and clinical characteristics

There was a significant difference (Table 7) in the number of pregnancies, with PE women having lower gravidity (mean times of gravidity of 1.24) than NP women (mean times of gravidity of 3.47). Similarly, PE mothers were significantly more likely to be nulliparous than NP women. Furthermore, the average systolic (163.12mmHg) and diastolic (104.62mmHg) blood pressure was significantly higher among the PE cohort. Likewise, there was a significant difference in proteinuria (PE = 2.19 pluses on urine dipstick NP = 0 plus on urine dipstick) and gestation age at delivery (PE = 31.88 weeks' gestation NP = 39.33 weeks' gestation) in PE compared to NP. Finally, PE babies were more likely to be growth restricted with an average birth weight of 1515.31g than normal babies (3671.33g). However, there was no significant difference in maternal age, maternal weight, maternal height, body mass index, previous preterm delivery, smoking status, and the gender of the child.

**Table 7.** Table showing the general characteristics of the study population

| Characteristics | Sub-Classification | Normal Pregnancy | Preeclampsia | P Value |
|---|---|---|---|---|
| Sample size | | 15 | 16 | |
| Maternal age years (mean (SD)) | | 34.07 (5.42) | 34.12 (4.63) | 0.974 |
| Maternal weight kilograms (mean (SD)) | | 76.18 (24.18) | 76.87 (24.39) | 0.938 |
| Maternal height centimetres (mean (SD)) | | 156.27 (32.55) | 162.43 (7.85) | 0.468 |
| Body mass index $kg/m^{-2}$ (mean (SD)) | | 27.7(7.52) | 29.09 (9.4) | 0.653 |
| Body mass index categories (%) | | | | 0.978 |
| | Normal | 6 (40) | 7 (43.8) | |
| | Overweight | 4 (26.7) | 4 (25) | |
| | Obese | 5 (33.3) | 5 (31.2) | |
| Times of gravidity (mean (SD)) | | 3.47 (2.56) | 1.94 (1.24) | 0.041 |
| Systolic blood pressure mmHg (mean (SD)) | | 121.47 (9.49) | 163.12 (14.66) | <0.001 |
| Diastolic blood pressure mmHg (mean (SD)) | | 71.2 (5.56) | 104.62 (7.36) | <0.001 |
| Proteinuria plus(es) (mean (SD)) | | 0 | 2.19 (1.15) | <0.001 |
| Gestational age at delivery in weeks (mean (SD)) | | 39.33 (0.72) | 31.88 (3.52) | <0.001 |

| | | | | |
|---|---|---|---|---|
| Birth weight grams (mean (SD)) | | 3671.33 (568.73) | 1515.31 (726.65) | <0.001 |
| Previous preterm delivery (%) | | 2 (13.3) | 4 (25) | 0.714 |
| Smoking status (%) | | | | 0.295 |
| | Current smoker | 2 (13.3) | 0 (0) | |
| | Non-smoker | 8 (53.3) | 11 (68.8) | |
| | Previous smoker | 5 (33.3) | 5 (31.2) | |
| Times of parity (%) | | | | 0.007 |
| | Multiparity | 7 (46.7) | 1 (6.2) | |
| | Nulliparity | 1 (6.7) | 8 (50) | |
| | Primiparity | 7 (46.7) | 7 (43.8) | |
| Intrauterine growth restriction (IUGR) = Yes (%) | | 0 (0) | 15(93.8) | <0.001 |
| Maternal age greater than 34 (%) | | 8 (53.3) | 6 (37.5) | 0.600 |
| Male new-born gender (%) | | 5 (33.3) | 6 (37.5) | 1.000 |

*Nulliparity, means no previous parous experience, primiparity refers to first time mother and multiparity means mother for at least the second time.

*IUGR means intrauterine growth restriction and refers to a baby below the 5$^{th}$ centile on the growth chart ( based on Obstetrics assessment)

### 2.12.1 Characterisation of STB-EVs by transmission electron microscopy (TEM), nanoparticle tracking analysis (NTA), flow cytometry, and Western blot (WB)

After isolating and enriching STB-EVs, I characterised our sample preparations with TEM, NTA, flow cytometry (FC), and WB. TEM (Figure 14A) showed the typical cup-shaped morphology of extracellular vesicles. In particular, the 10K STB-EV pellet (Figures 14A2, 14A5 and 14A8) showed a size heterogeneity characteristic of M/L STB-EVs (221 to 1000 nm) while the 150K STB-EV pellet (Figures 11A3, 11A6, and 11A9) showed a homogeneous EV size profile (less than or equal to 220 nm). This finding was also replicated by NTA (Figure 14C). The 10K STB-EV (Figure 14C1) pellets had a modal size of 479.4 ± 145.6nm, while the 150K STB-EV (Figure 14C2) pellets had a 205.8 ± 67.7nm. The 10K and 150K STB-EV pellets are hereafter renamed M/L STB-EVs and S STB-EVs, respectively.

WB (Figure 14B) detected PLAP (66 KDa), tetraspanins [CD63 (30–65 KDa), CD81 (20 KDa), and endosomal trafficking proteins, ALIX (95 KDa) and TSG101 (46 KDa). The non-EV marker cytochrome C (12 KDa) was detected in the placenta homogenates but not the STB-EV fractions. Notably, TSG101 and ALIX were more prominent in the S STB-EV fractions than the M/L STB-EV fractions and placenta homogenates.

Flow cytometry (Figure 15,16, and 17) was performed on the M/L STB-EVs due to the sensitivity limit of the flow cytometer. Flow cytometry (Figure 15, 16 and 17) corroborated the WB findings. I found 85 ± 8.3 % (Figure 12C) of qualified events were negative for the following lineage markers (CD41 [platelets] and CD235a [Red blood cells], and then HLA-I and II [white blood cells]). 95 ± 1.2 % of the EVs negative for non-placental markers (listed above) were BODIPY FL N-(2-aminoethyl)-maleimide (bioM) and placental alkaline phosphatase (PLAP) double-positive (Figure 12D). PLAP is a specific marker of syncytiotrophoblast, and so this single EV analysis confirmed that most of the post 10K

samples, within the detection size range, were of placental origin. Flow cytometry showed that our samples were largely vesicular as NP-40 treatment only reduced BODIPY FL N-(2-aminoethyl)-maleimide and PLAP double-positive events by 0.1 ± 0.12% (Figure 12E).

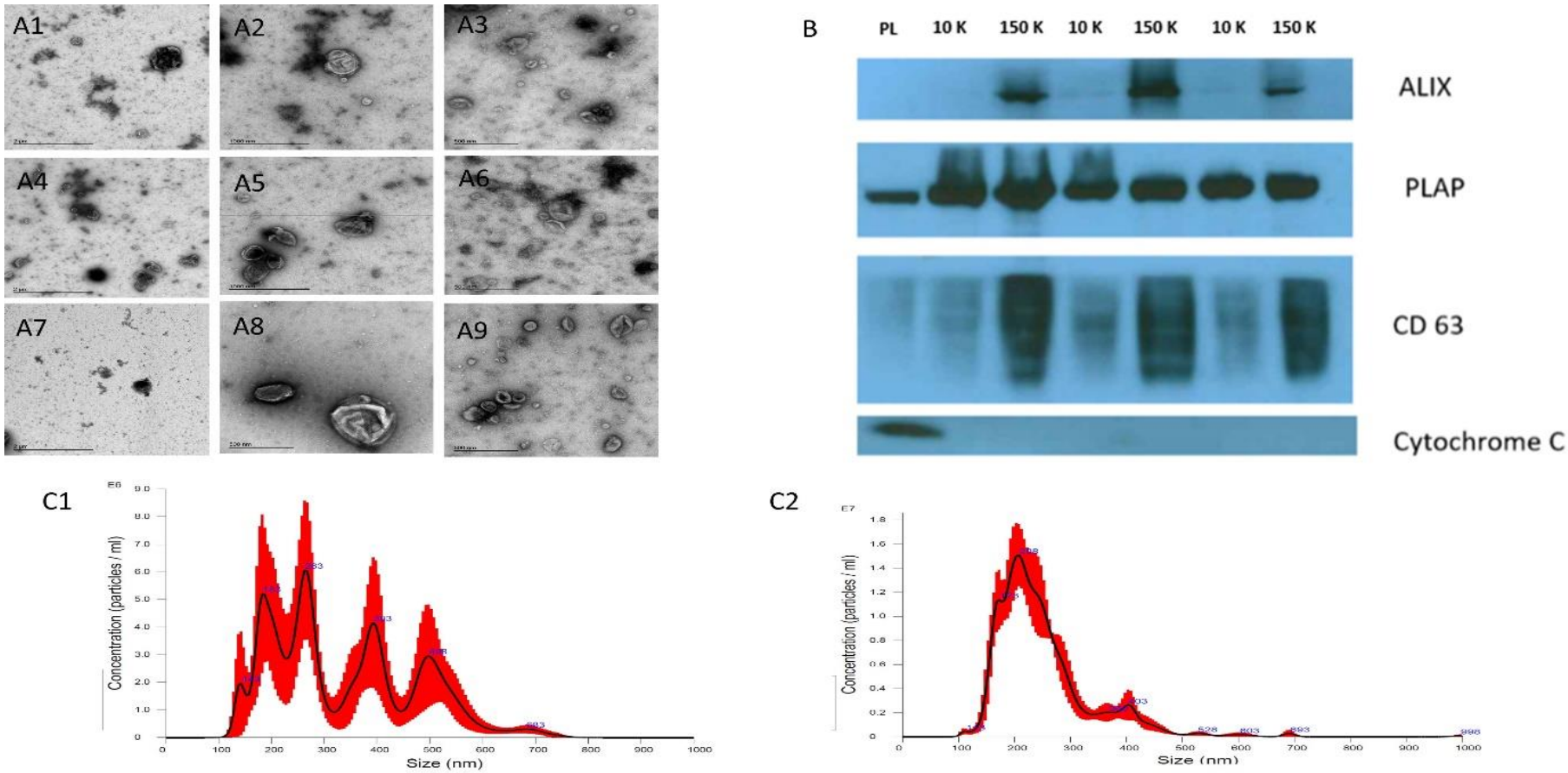





**Figure 14**. STB-EV characterisation. Figure 11A displays representative transmission electron microscopy (TEM) images with wide view (A1, A4, and A7), medium/large STB-EVs (A2, A5, and A8), and small STB-EVs (A3, A6, and A9). Figure B is a Western blot of placenta homogenate (PL), M/L STB-EVs (10K) and S STB-EVs (150K) showing positivity for ALIX, PLAP, CD63 and an absence of cytochrome C in the STB-EV population. Figure 11C shows the NTA results of M/L STB-EVs (C1) and S STB-EVs (C2).

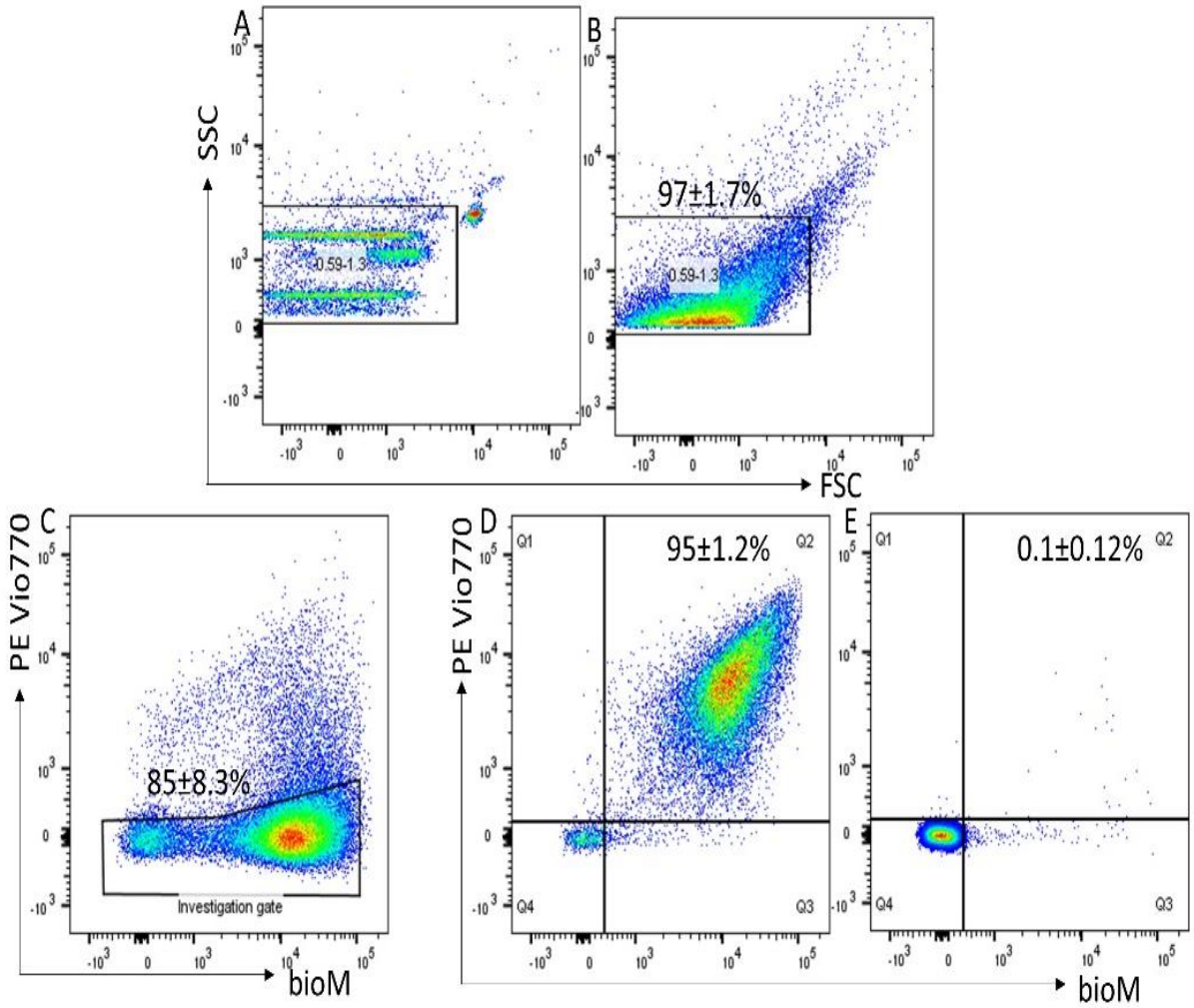



**Figure 15.** Representative flow analysis of M/L STB-EVs in the 10K STB-EV pellet sample. Apogee beads mix were used to set the flow machine's light scatter resolution to 0.59-1.3 mm silica beads (A); Application of SSC and FSC PMTVs determined by apogee beads mix for the analysis of M/L STB-EVs in a 10K sample (B). An investigation gate to include M/L EVs negative for non-placental markers (C); EVs from the investigation gate were further analysed for expression of PLAP and staining by bioM (D). PLAP+ bioM+ EVs sensitive to detergent treatment (E).

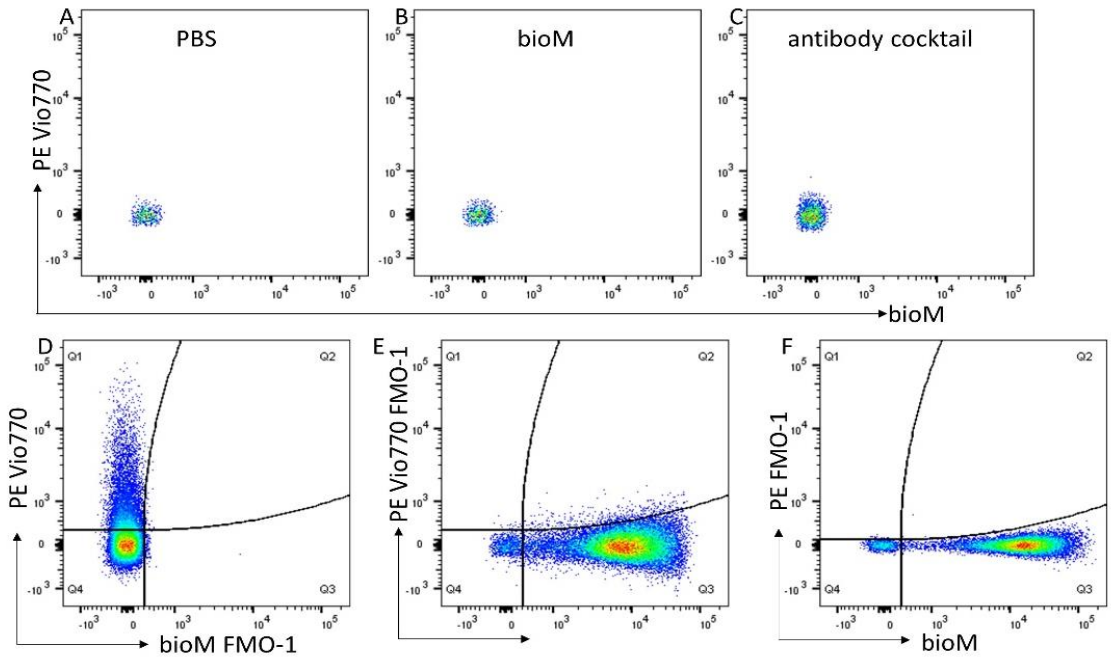



**Figure 16.** Reagent controls, 0.1mm filtered PBS (A); 0.2mm filtered bioM (B) and antibody cocktail (C). Fluorescent minus one (FMO-1) controls, bioM-1 control (D); PE Vio770-1 control (E); PE-1 control (F).

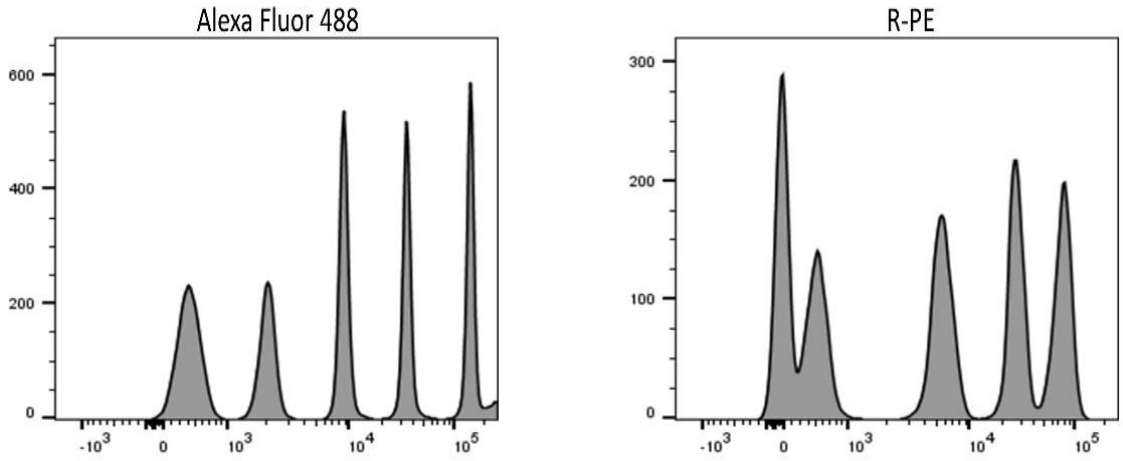



**Figure 17.** Figure showing the fluorescence linearity curve used generated with Quantum ™ MESF (molecules of equivalent soluble fluorochrome) Alexa Fluor 488 and R-PE 9R-phycoerythrin) kits. MESF calculation was calculated using QuickCal v2.3 software from Bangs Laboratories, Inc.

## 2.13 Conclusion

This chapter summarises the general and chapter-specific methods used throughout this thesis. It also contains the descriptive statistics results of the patient population used for this thesis's exploratory/discovery and validation phases. My sample preparation enriched syncytiotrophoblast membrane extracellular vesicles within the expected sized range. They (STB-EVs) also expressed the required extracellular vesicle markers with minimal co-precipitation of other extracellular vesicle sources.

# CHAPTER 3

## RESULTS OF TRANSCRIPTOMIC ANALYSIS OF STB-EVs IN PREECLAMPSIA

## 3.1 Abstract

**Background:** Preeclampsia (PE) is a pregnancy complication affecting 2-8% of pregnancies worldwide and a leading cause of adverse maternal and foetal outcomes, including adverse maternal cardiovascular events later in life. Currently, no effective treatment or diagnostic biomarker(s) exist. Worse still, the causes and mechanisms of placental dysfunction leading to PE are presently not well understood. However, syncytiotrophoblast membrane extracellular vesicles (STB-EVs) have been identified as potentially involved in PE. In this study, I hypothesised that the transcriptome of placental tissue and STB-EVs is different between preeclampsia and normal pregnancy and may act as potential biomarkers and offer mechanistic insights.

**Methods:** I performed RNA-sequencing (RNA-seq) on placental tissue, medium/large and small STB-EVs from PE and NP, followed by bioinformatics analysis to identify targets in PE that could be used in the future for EV based diagnostic tests. Some of the identified biomarkers were validated with real-time polymerase chain reaction. I finalised the analysis by performing an in-silico prediction of STB-EV based mechanistic pathways.

**Results:** My analysis identified a difference in the transcriptomic STB-EVs cargo between preeclampsia (PE) and normal pregnancy (NP). I identified and verified the differential expression of FLNB, *COL17A1, SLC45A4, LEP, HTRA4, PAPP-A2, EBI3, HSD17B1, ARMS2, FSTL3, INHBA, SIGLEC6,* and *CGB3* for potential use as biomarkers in preeclampsia. My analysis also identified interesting mechanistic processes such *as abnormal protein metabolism,* which may be responsible for the clinical and pathological presentation of preeclamptic patients

**Conclusions:** I performed comprehensive profiling of differentially expressed genes and pathways in PE by analysing three different sample subtypes. I believe our strategy increases

the likelihood and confidence that the relevant biomarkers and mechanistic gene pathways I identified are essential in the pathophysiology of PE and could potentially be used in future studies.

## 3.2 Introduction

Preeclampsia (PE) is a multisystemic hypertensive disorder that affects 2-8% of pregnancies worldwide[7]. The direct cause of PE (i.e., mechanisms of placental dysfunction) is still under study, with the only available treatment being the delivery of the placenta[223]. One of the investigated aetiological agents are syncytiotrophoblast membrane extracellular vesicles (STB-EVs), double-walled spherical structures of placenta origin, which can be classified based on their size and biogenesis pathways into medium/large and small STB-EVs [224]. Small STB-EVs are less than or equal to 220nm in size and formed through multivesicular bodies, whereas medium/large EVs are between 221nm to 1000nm and released directly through the budding of the plasma membrane [225]. Their cargo consists of surface proteins, encapsulated proteins, and different subclasses of RNAs such as long noncoding RNAs, messenger RNAs, transfer RNAs, and microRNAs [226], which may be released onto target cells through fusion of membranes and release of content. This ability of STB-EVs further implicates them as potential pathogenic factors in PE. However, the transcriptome of the subtypes of STB-EVs has not been thoroughly explored. Previous studies have identified differentially expressed genes (DEGs) from PE placental tissue such as *Sialic acid-binding Ig-like lectin 6 (SIGLEC6), Vascular endothelial growth factor receptor 1(FLT1), Adrenomedullin (ADM),* and *Pappalysin-2 (PAPP-A2)* [227,228]*, Basic Helix-Loop-Helix Family Member E40 (BHLHE40), Divergent-Paired Related Homeobox (DPRX),* and *HtrA Serine Peptidase 4 (HTRA4)* [229] compared to normal placental tissue. However, to the best of my knowledge, none have explored this in the context of STB-EVs between PE and normal pregnancy (NP).

I hypothesised that 1) the transcriptome of the placenta tissue and STB-EVs are different between PE and NP and 2) analysing these different sample subtypes would allow for more comprehensive and holistic profiling. This comprehensive and integrated approach increases

the probability of detecting relevant biomarkers and mechanistic gene pathways in PE. I performed RNA sequencing (RNA seq) on placental tissue, medium/large and small STB-EVs from PE and NP. My robust analysis provided many potential biomarker and mechanistic targets. It provided some insight into potential mechanisms in preeclampsia that might help inform future extracellular vesicle-based diagnostic tests and mechanistic experiments.

## 3.3 Aims

The aims of this chapter are to:

1. characterise the messenger RNA transcriptomic cargo of PE and NP using next-generation sequencing technologies
2. identify potential biomarkers that may help to diagnose and predict the occurrence of PE in pregnancy earlier
3. identify key regulatory pathways, mechanisms, and networks in PE

## 3.4 Methods

The methods used in this chapter have been described in detail in the Methods section (chapter 2). Briefly, medium/large and small syncytiotrophoblast membrane extracellular vesicles were isolated and enriched by *ex vivo* dual lobe placenta perfusion and differential ultracentrifugation. Biopsies were also obtained from the corresponding placenta specimen. Total RNA was extracted from the samples (placenta homogenate and STB-EVs) and sent for sequencing. The data from the sequenced samples were bioinformatically and statistically analysed to identify differentially expressed genes (DEGs). The functions of these DEGs were bioinformatically identified through functional enrichment analysis for gene ontology terms and KEGG pathways.

## 3.5 Results

### 3.5.1 Differentially expressed genes (DEGs) in placenta homogenate, M/L STB-EVs and S STB-EVs between PE and NP

Comparison between PE and NP placental tissue revealed 580 upregulated and 563 downregulated (total) genes (p-value of < 0.05 [Figures 18A and D]) while in M/L STB-EVs 1,128 were upregulated and 833 were downregulated (p-value of < 0.05 [Figures 18B and E]). In S STB-EVs, 232 were upregulated, and 106 were downregulated (p-value of < 0.05 [Figures 18C and F]). In general, 25 downregulated genes such as *solute carrier family 45 Member 4* (*SLC45A4)* and *dystrobrevin beta (DTNB)* were common to all sample subtypes. Among the upregulated genes, 120 genes were common to all three sample types, *leptin* (*LEP), Epstein-Barr Virus-Induced 3 (EBI3), endoglin (ENG), inhibin subunit beta A (INHBA), FMS related receptor tyrosine kinase 1 (FLT1), filamin B (FLNB),* and *collagen type XVII alpha 1 chain (COL17A1).*

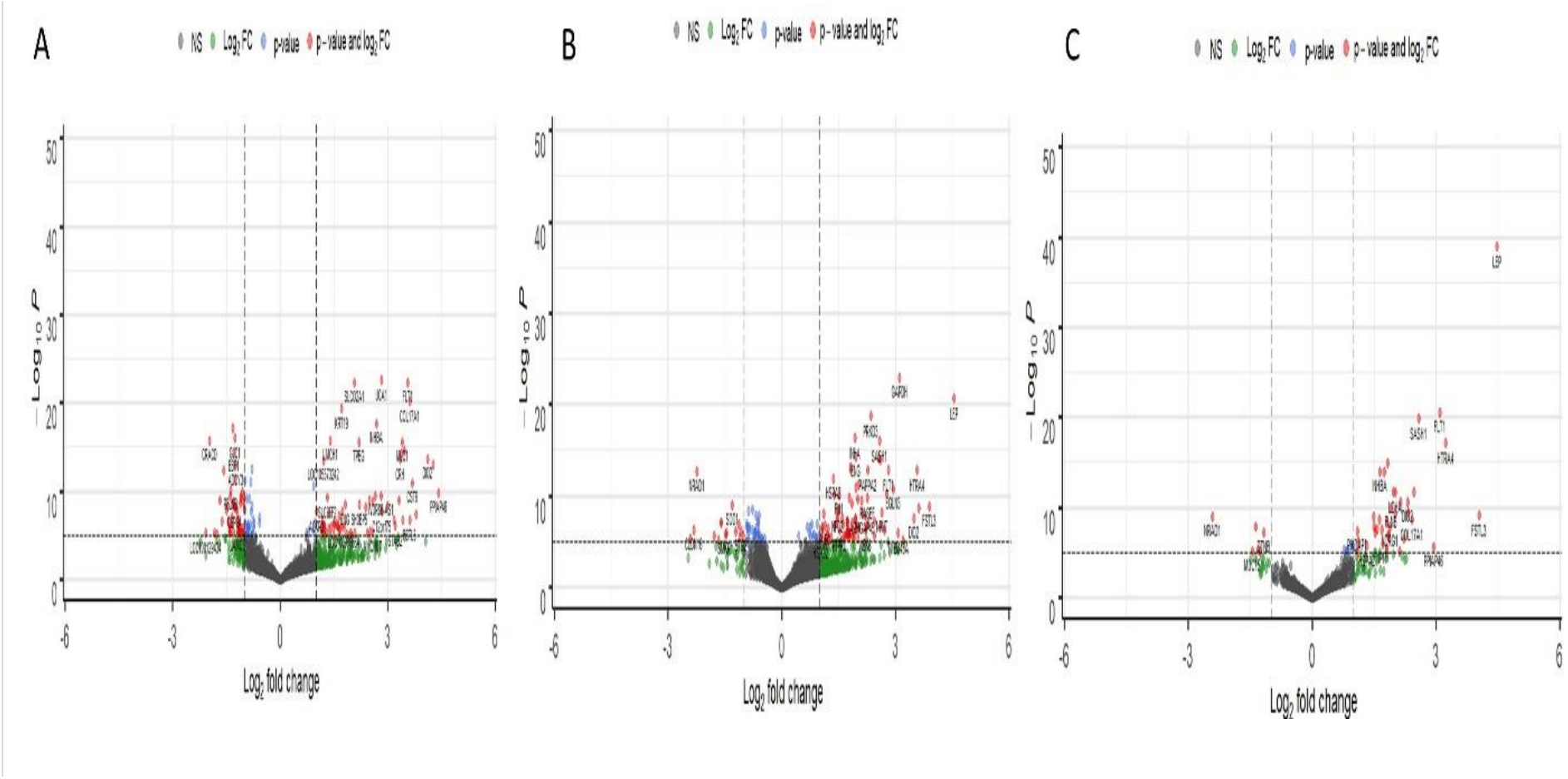



**Figure 18**. Volcano plot and heat maps showing differentially expressed genes in placenta (Figure A and D), medium/large STB-EVs (Figures B and E) and small STB-EVs (Figure C and F). In Figures A, B and C, the most significantly upregulated genes are in the top right quadrant while the most significantly downregulated genes are in the top left quadrant. In Figures D, E and F shows the clear distinction between differentially expressed genes in preeclampsia compared to normal.

## 3.5.2 Quantitative PCR (qPCR) Validation of selected genes

As earlier discussed in the methodology section, I identified the DEGs between common to three sample types based on RNA and protein expression information we found in the human tissue atlas. I selected *HTRA4, PAPP-A2, EBI3, HSD17B1, ARMS2, FSTL3, INHBA, SIGLEC6,* and *CGB3*(Table 8). In addition to these, I selected *FLNB, COL17A1, SLC45A4, LEP,* and *ENG* based on high fold change in our dataset. I performed qPCR analysis of *FLNB, COL17A1, SLC45A4,* and *LEP* in placental lysate and selected *FLNB, COL17A1, SLC45A4, LEP, ENG, HTRA4, PAPP-A2, EBI3, HSD17B1, ARMS2, FSTL3, INHBA, SIGLEC6,* and *CGB3* in both M/L STB-EVs and S STB-EVs. In the placental lysate (Figure 19), *LEP*, *COL17A1*, *SLC45A4*, and *FLNB* were significantly different in PE compared to NP. In the M/L STBEVs (Figures 19 and 20), *LEP*, *SIGLEC6*, *FLNB, COL17A1*, *SLC45A4*, *FSTL3*, and *HTRA 4* were significantly different in PE compared to NP.

In S STB-EVs, (Figure 19 and 20) *FSTL3, HTRA 4, LEP, ENG, INHBA, FLNB, COL17A1, PAPP-A2, ARMS2, SIGLEC6, CGB3, EBI3,* and *SLC45A4* were significantly different. The three sample types, *LEP, COL17A1, SLC45A4, SIGLEC6,* and *FLNB,* were all significantly different between PE and NP, while *LEP, SIGLEC6, FLNB, COL17A1, SLC45A4, FSTL3, and HTRA4* were significant in both M/L and S STB-EVs.

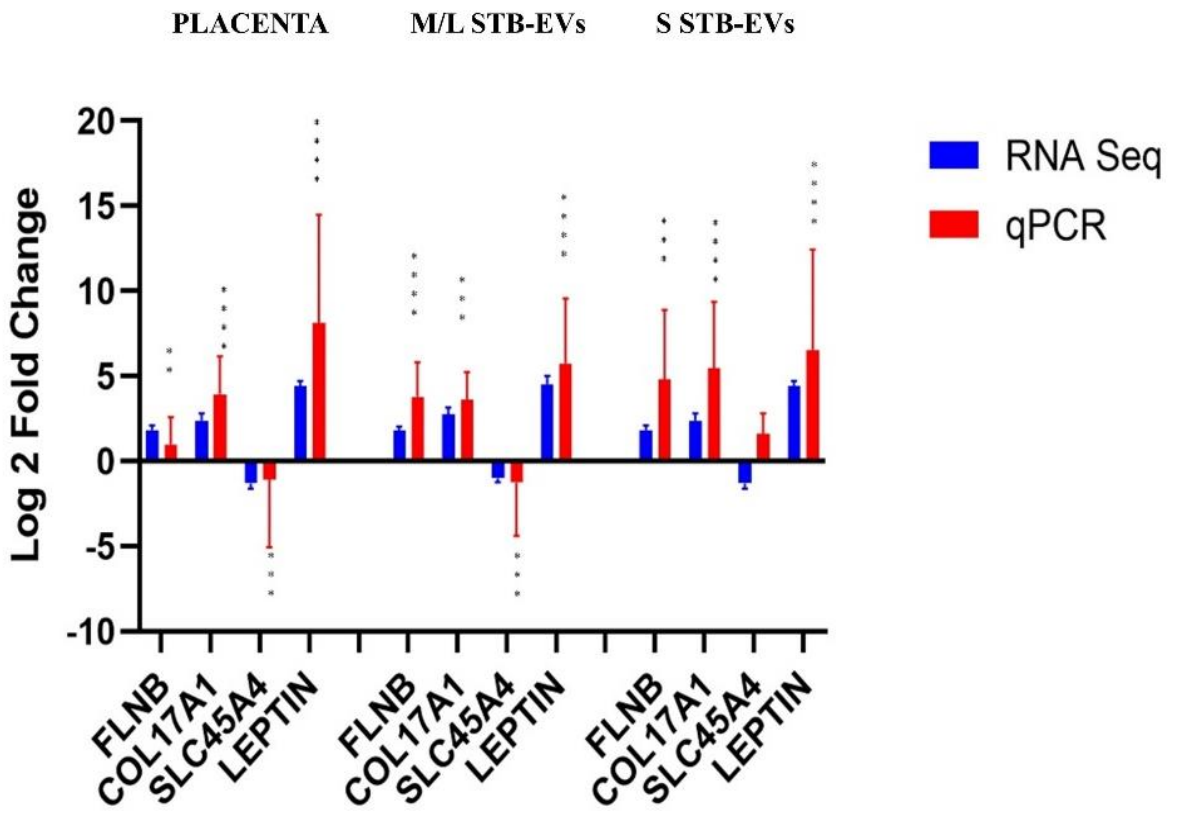



**Figure 19.** Bar graphs showing select differentially expressed genes leptin (LEP), collagen type XVII alpha 1 chain (COL17A1), solute carrier family 45 member 4 (SLC45A4), filamin B (FLNB) and endoglin (ENG) in the placenta, medium/large STB-EVs and small STB-EVs based on qPCR. Data is visualized as mean fold change and error bars represent standard error. *=P <0.05, **=P <0.01, ***=P <0.001, and ****=P 0.0001. Sample size (n) = 6(NP) and 7(PE*)*

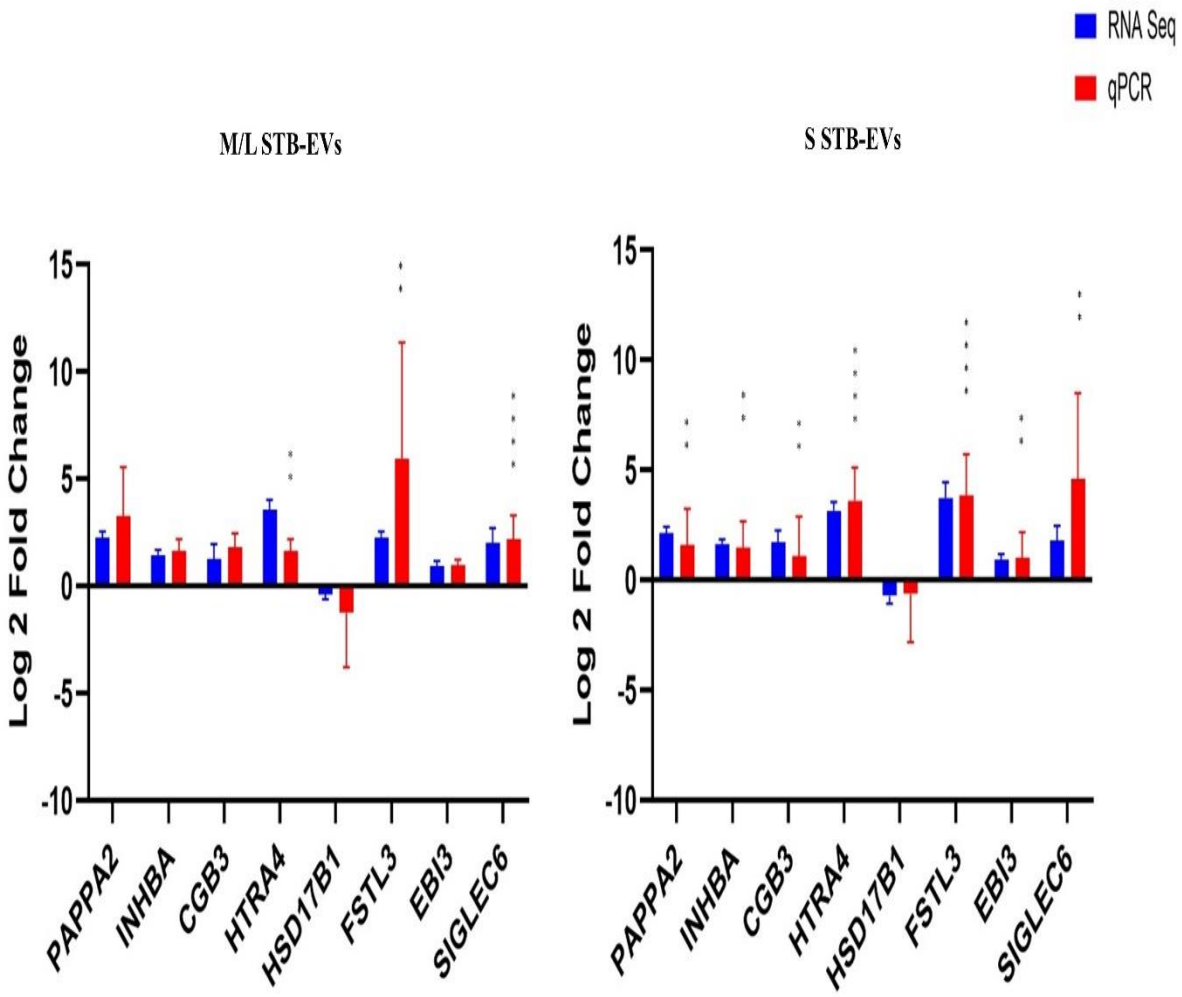



**Figure 20.** Bar graphs showing pappalysin 2 (PAPP-A2), inhibin subunit beta A (INHBA), sialic acid binding Ig like lectin 6 (SIGLEC6), HtrA serine peptidase 4 (HTRA4), Epstein-Barr virus-induced 3 (EBI3), follistatin like 3 (FSTL3), hydroxysteroid 17-beta dehydrogenase 1 (HSD17B1), chorionic gonadotropin 3 (CGB3) and age-related macular degeneration (ARMS2) in medium/large STB-EVs and small STB-EVs based on qPCR. Data is visualized as mean fold change, and error bars represent standard error. *=P <0.05, **=P <0.01, ***=P <0.001, and ****=P 0.0001. Sample size (n) = 4(NP) and 4(PE)

**Table 8.** Table showing the log fold change standard error of verified genes for RNA Seq and quantitative PCR data. LFC means Log 2 fold change and LSE means Log 2 standard error. Significant results are in bold fonts. Sample size for transcriptomics; placenta homogenate (NP = 6 and PE = 7), M/L STB-EVs (NP = 4 and PE = 4) and S- STB-EVs (NP = 6 and PE = 8). Sample size for qPCR; placenta homogenate (NP = 6 and PE = 6), M/L STB-EVs (NP = 6 and PE = 6) and S STB-EVs (NP = 6 and PE = 6).

| | Transcriptomics | | | qPCR | | |
|---|---|---|---|---|---|---|
| Genes | LFC | LSE | P Value | LFC | LSE | P Value |
| M/L STB-EVs (Placenta Specific) | | | | | | |
| PAPP-A2$^{+}$ | 2.27 | 0.28 | <0.0001 | 3.26 | 2.31 | 0.07 |
| INHBA$^{+}$ | 1.45 | 0.24 | <0.0001 | 1.65 | 0.55 | 0.13 |
| CGB3$^{+}$ | 1.28 | 0.69 | <0.01 | 1.82 | 0.65 | 0.16 |
| **HTRA4$^{+}$** | **3.57** | **0.47** | **<0.0001** | **1.65** | **0.55** | **0.02** |
| HSD17B1$^{+}$ | -0.39 | 0.23 | 0.01 | -1.25 | 2.54 | 0.19 |
| **FSTL3+** | **2.27** | **0.28** | **<0.0001** | **5.94** | **5.43** | **0.03** |
| EBI3$^{+}$ | 0.95 | 0.24 | <0.0001 | 1.00 | 0.24 | 0.30 |
| **SIGLEC6$^{+}$** | **2.03** | **0.70** | **<0.01** | **2.17** | **1.14** | **<0.0001** |
| S STB-EVs (Placenta Specific) | | | | | | |
| **PAPP-A2$^{-}$** | **2.12** | **0.31** | **<0.001** | **1.58** | **1.66** | **0.01** |
| **INHBA$^{-}$** | **1.63** | **0.21** | **<0.001** | **1.47** | **1.21** | **<0.01** |
| **CGB3$^{-}$** | **1.69** | **0.56** | **<0.001** | **1.10** | **1.79** | **0.04** |
| **HTRA4$^{-}$** | **3.16** | **0.39** | **<0.001** | **3.61** | **1.50** | **<0.0001** |
| HSD17B1$^{-}$ | -0.73 | 0.34 | <0.01 | -0.64 | 2.18 | 0.08 |
| **FSTL3$^{+}$** | **3.75** | **0.70** | **<0.001** | **3.84** | **1.87** | **<0.001** |
| **EBI3-** | **0.90** | **0.27** | **<0.001** | **1.02** | **1.16** | **0.04** |
| **SIGLEC6-** | **1.81** | **0.67** | **<0.001** | **4.59** | **3.90** | **0.04** |
| Placenta (High Fold Change – not placenta specific) | | | | | | |
| **FILAMIN B$^{+}$** | **1.83** | **0.29** | **<0.0001** | **0.99** | **1.61** | **0.02** |
| **COL17A1$^{+}$** | **2.38** | **0.43** | **<0.0001** | **3.95** | **2.21** | **<0.0001** |
| **SLC45A4$^{+}$** | **-1.32** | **0.29** | **<0.0001** | **-1.08** | **3.99** | **<0.01** |
| **LEPTIN$^{+}$** | **4.40** | **0.32** | **<0.0001** | **8.11** | **6.38** | **<0.0001** |
| M/L STB-EVs (High Fold Change – not placenta specific) | | | | | | |
| **FILAMIN B$^{+}$** | **1.82** | **0.22** | **<0.0001** | **3.78** | **2.03** | **<0.0001** |
| **COL17A1$^{+}$** | **2.77** | **0.39** | **<0.0001** | **3.61** | **1.62** | **<0.01** |
| **SLC45A4$^{+}$** | **-1.02** | **0.23** | **<0.0001** | **-1.27** | **3.12** | **<0.01** |
| **LEPTIN$^{+}$** | **4.54** | **0.48** | **<0.0001** | **5.74** | **3.82** | **<0.0001** |
| S STB-EVs (High Fold Change – not placenta specific) | | | | | | |

| | | | | | | |
|---|---|---|---|---|---|---|
| **FILAMIN B$^{-}$** | **1.83** | **0.29** | **<0.0001** | **4.80** | **4.10** | **0.01** |
| **COL17A1$^{-}$** | **2.38** | **0.43** | **<0.0001** | **5.46** | **3.90** | **0.01** |
| SLC45A4$^{-}$ | -1.32 | 0.29 | **<0.0001** | 1.61 | 1.21 | 0.41 |
| **LEPTIN$^{-}$** | **4.40** | **0.32** | **<0.0001** | **6.53** | **5.91** | **<0.001** |

$^{+}$ = not previously described in PE M/L STB-EVs, $^{-}$ = not previously described in PE S STB-EVs

### 3.5.3 Functional enrichment analysis and signalling pathway impact analysis (SPIA) of differentially expressed genes (DEGs) in Preeclampsia

I performed a functional enrichment analysis (with overrepresentation analysis) on the list of DEGs for placenta tissue, M/L STB-EVs, and S STB-EVs. I also identified functional processes that overlap among the three sample subtypes (Table 9) to understand the role of the identified genes and perhaps STB-EVs in the pathophysiology of preeclampsia.

#### 3.5.3.1 Functionally enriched Gene Ontology Biological processes (GO: BP) in preeclampsia

Some identified processes are congruent with preeclamptic patients' characteristic pathologic and clinical phenotype. Among placenta tissue (Figure 21A), the top three GO: BP terms were *angiogenesis, extracellular matrix organisation,* and *extracellular structure organisation,* while *platelet degranulation, negative regulation of phosphoprotein phosphatase activity,* and *epithelial cell differentiation* were the top overrepresented biological processes among the M/L STB-EVs (Figure 21B). Similarly, the top biological processes for the S STB-EVs (Figure 22A) were *response to hypoxia, decreased oxygen levels, and oxygen levels*. There were 32 similar biological processes between the placenta and S STB-EVs (Figure 22C). These biological processes include *positive regulation of vasculature development, positive regulation of cell adhesion, cellular response to growth factor stimulus, endocrine process, negative regulation of locomotion,* and *response to decreased oxygen levels*. Only one

biological process was similar between the placenta and M/L STB-EVs (*platelet degranulation*), and none was common to all sample types (Table 9).

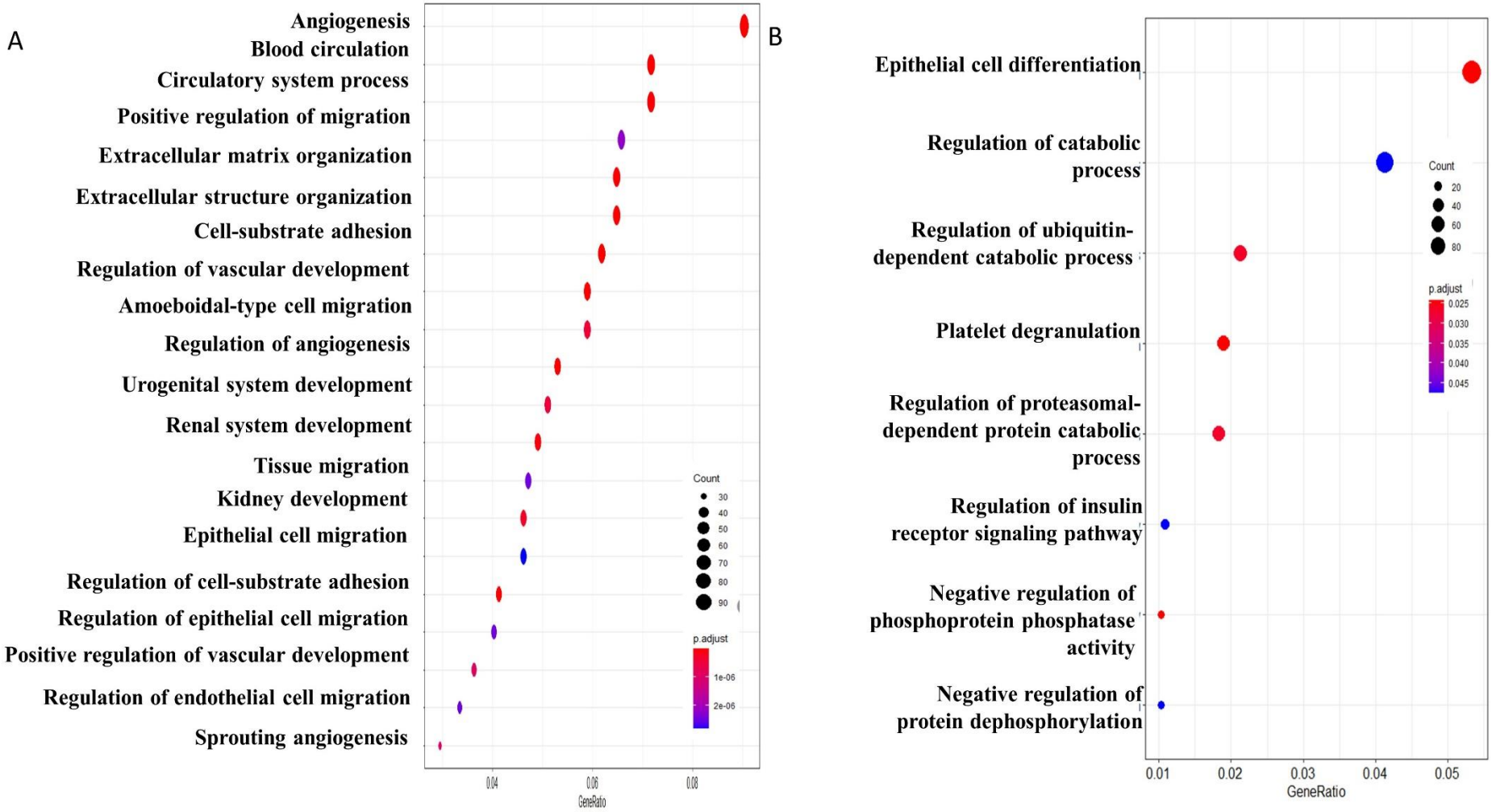



**Figure 21**. Figure showing results of functional enriched biological processes (GO: BP) in the placenta (A), medium/large STB-EVs (B) showing the number of overlapping biological processes between the placenta, medium/large STB-EVs and small STB-EVs.

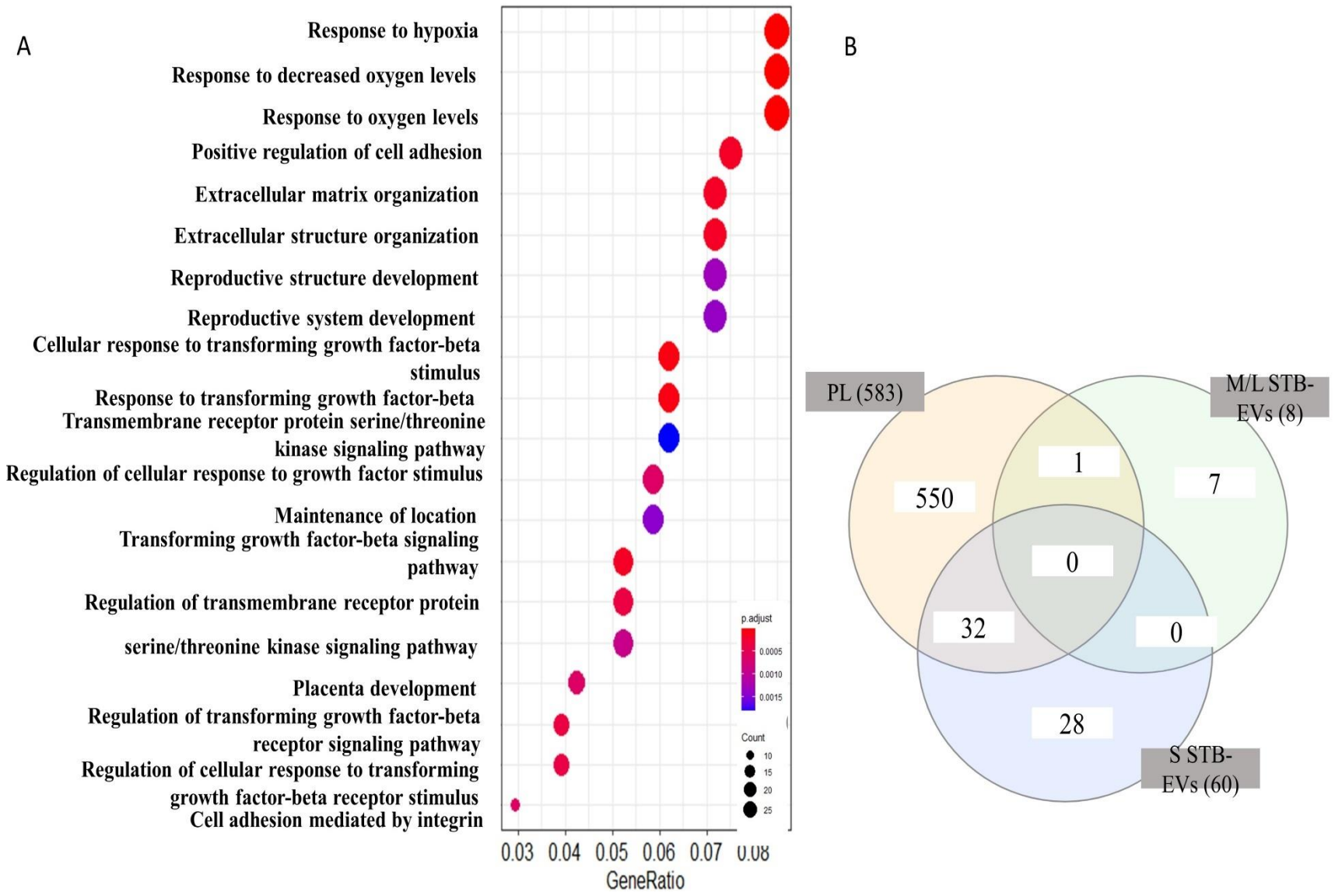



**Figure 22**. Figure showing results of functional enriched biological processes (GO: BP) in small STB-EVs (A) and a combined Venn plot (B) showing the number of overlapping biological processes between the placenta, medium/large STB-EVs and small STB-EVs.

### 3.5.3.2 Functionally enriched Gene Ontology Molecular Function (GO: MF) in preeclampsia

We then assessed the molecular functions of the DEGs. The most overrepresented molecular functions among the placenta homogenate (Figure 23A) were *extracellular matrix structural constituent, growth factor binding,* and *G protein-coupled receptor.* In contrast, we found *phosphatase regulator activity, phosphatidylcholine binding,* and *quaternary ammonium group binding* to be the most overrepresented molecular functions in M/L STB-EVs (Figure 23B) while *cell adhesion molecule binding, integrin binding,* and *cadherin biding,* were the overrepresented among S STB-EVs (Figure 24A). Only *cell adhesion molecule* and *integrin-binding* were common to both placenta and S STB-EVs (Figure 24B, Table 9).

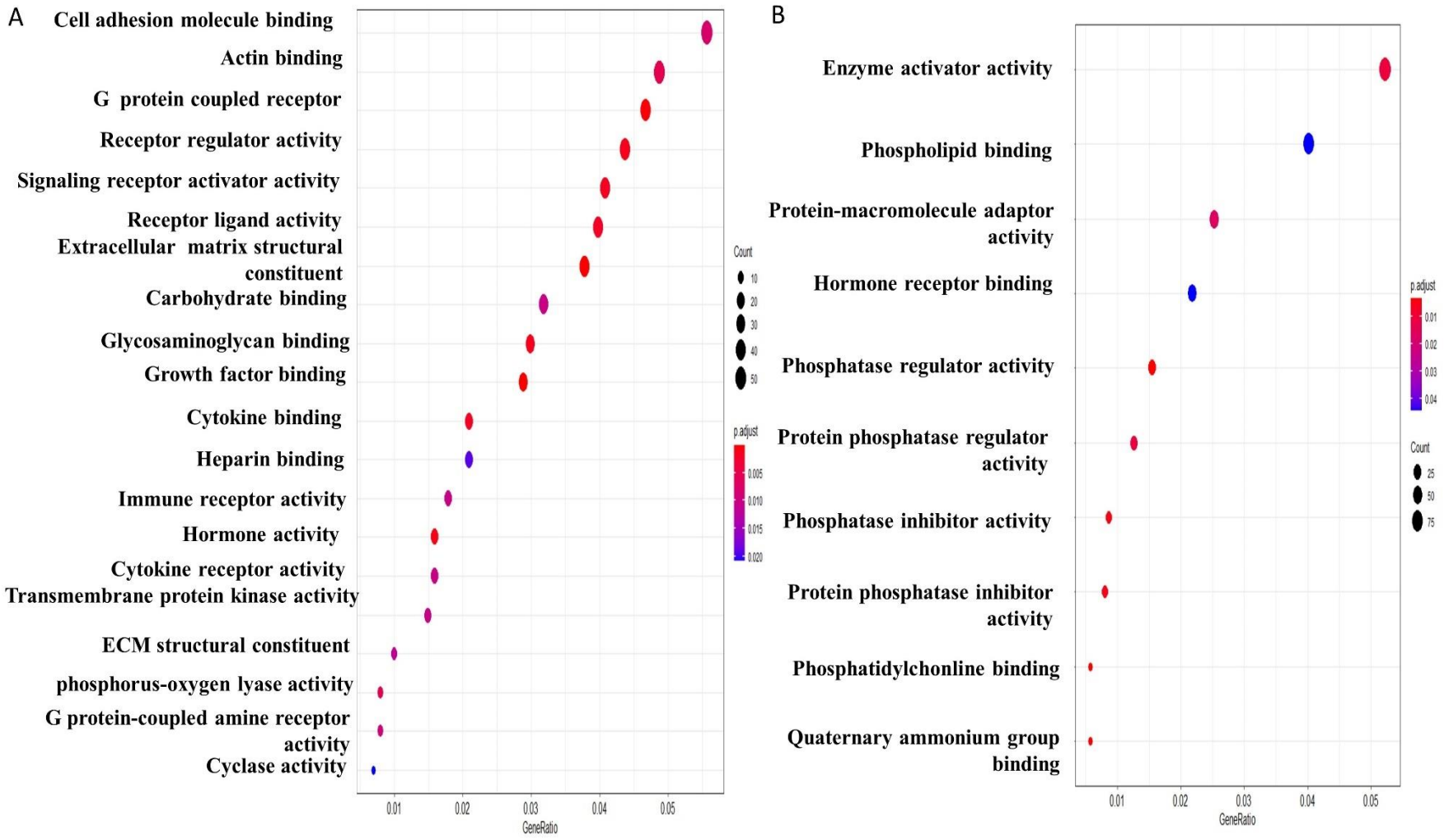



**Figure 23**. Figure showing results of functional enriched molecular functions (GO:MF) in the placenta (Figure A), medium/large STB-EVs (B) showing the number of overlapping biological processes between the placenta, medium/large STB-EVs and small STB-EVs.

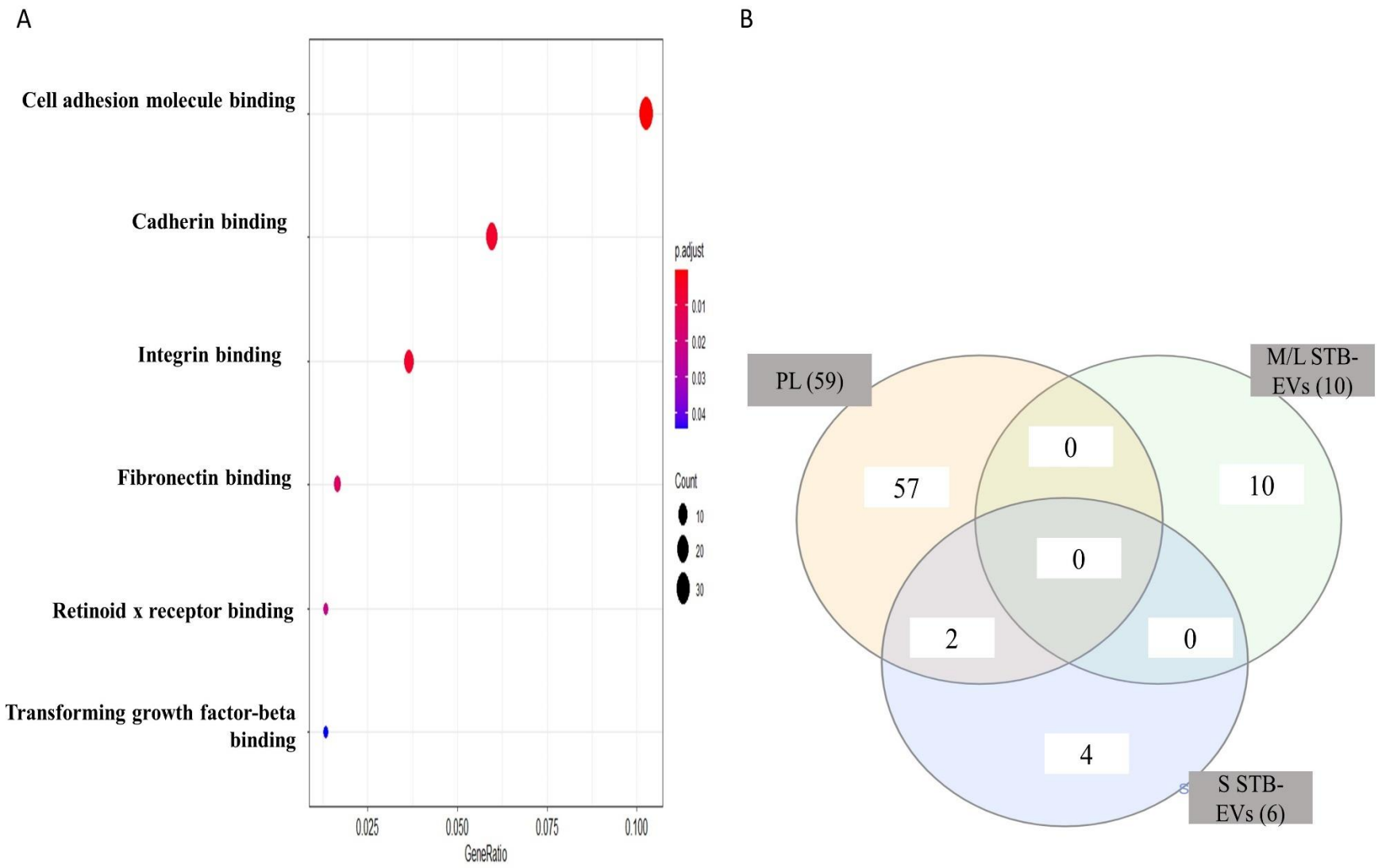



**Figure 24**. Figure showing results of functional enriched molecular functions (GO:MF) in small STB-EVs (A) and a combined Venn plot (B) showing the number of overlapping biological processes between the placenta, medium/large STB-EVs and small STB-EVs.

### 3.5.3.3 Functionally enriched Gene Ontology Cellular Component (GO: CC) in preeclampsia

Likewise, we probed the cellular and subcellular locations of our gene products. The placenta homogenate's most perturbed cellular component terms (Figure 25A) were *collagen-containing extracellular matrix, extracellular matrix,* and *basement membrane. T*he *focal adhesion, cell-substrate junction,* and *actin cytoskeleton* were overrepresented in M/L STB-EVs (Figure 25B). Likewise, the top cellular components of S STB-EVs (Figure 26A) were *cell-substrate junction, focal adhesion,* and *the actin cytoskeleton*. Six cellular components (Figure 26B) were overrepresented among all three sample types. At the same time, four cellular components were common to both placenta and S STB-EVs (collagen-containing extracellular matrix, leading-edge membrane, ruffle membrane, cell-cell junction). One cellular component was common to both M/L and S STB-EVs (vesicle lumen), and one common to the placenta and M/L STB-EVs (platelet alpha granule lumen) (Table 9).

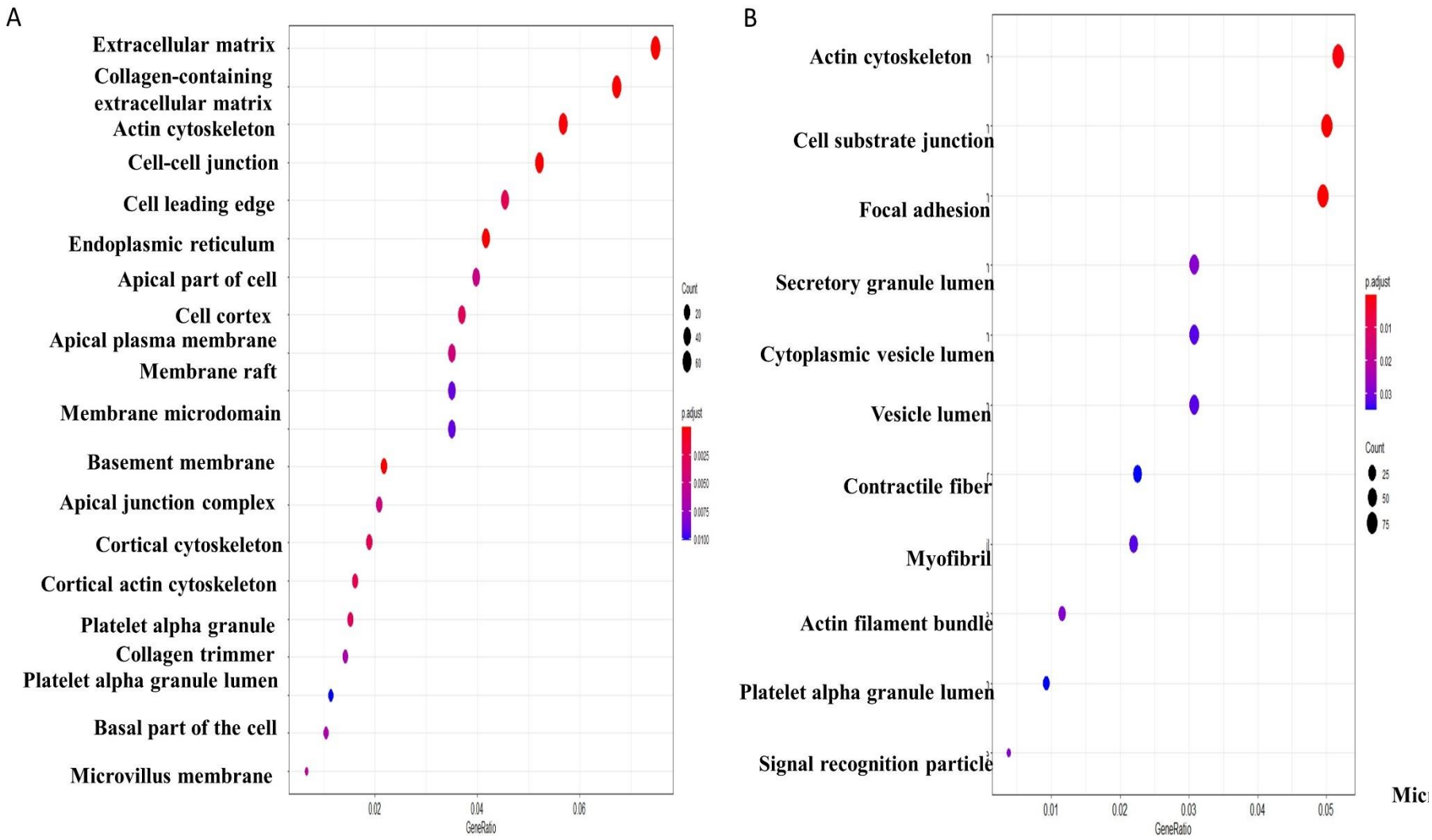



**Figure 25**. Figure showing results of functional enriched cellular components (GO:CC) in the placenta (A), medium/large STB-EVs (B) showing the number of overlapping biological processes between the placenta, medium/large STB-EVs and small STB-EVs.

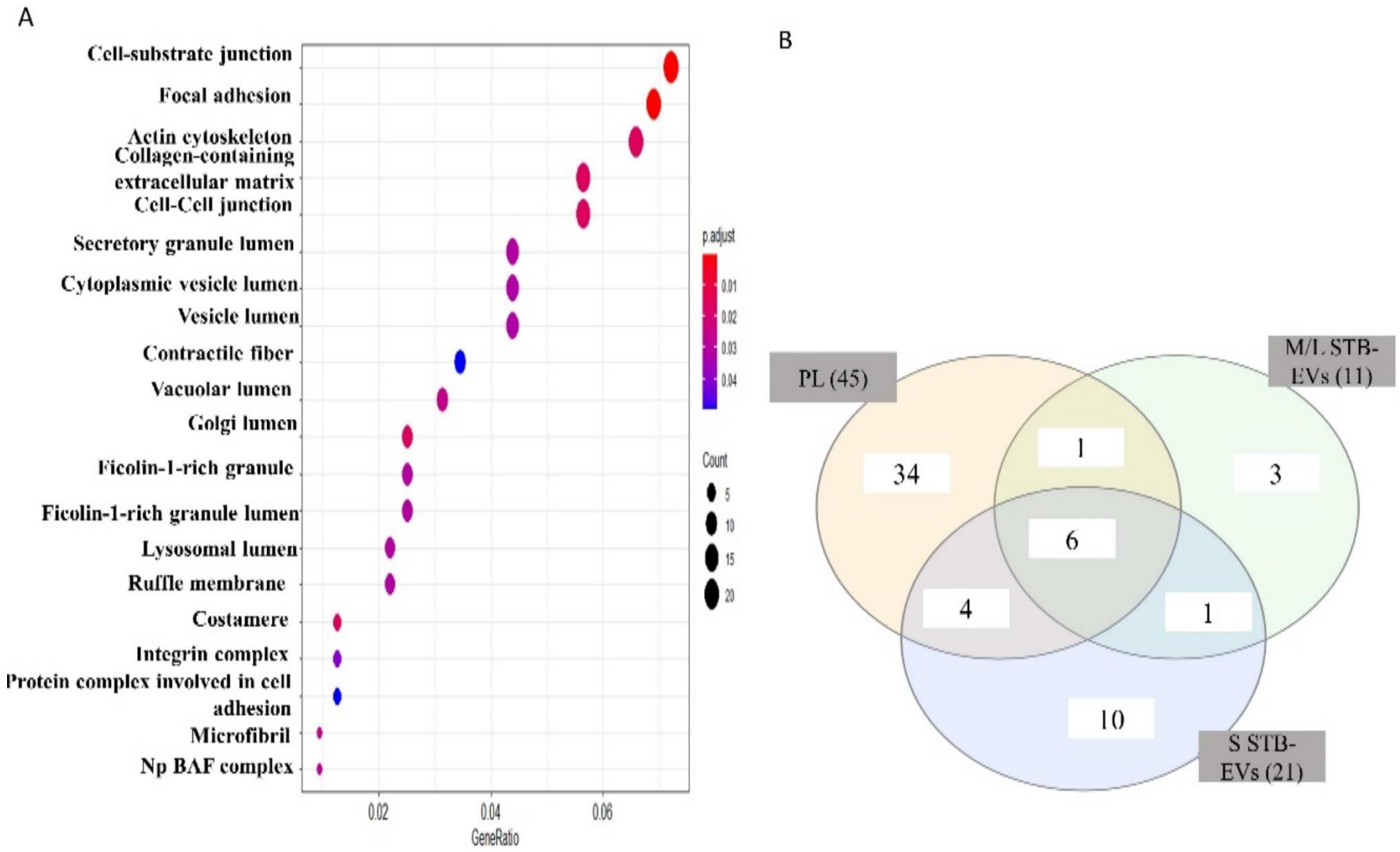



**Figure 26**. Figure showing results of functional enriched cellular components (GO:CC) in small STB-EVs (A) and a combined Venn plot (B) showing the number of overlapping biological processes between the placenta, medium/large STB-EVs and small STB-EVs.

### 3.5.3.4 Functionally enriched KEGG Pathways in Preeclampsia

The KEGG methodology is explained in detail in methods. When performing KEGG analysis, *pathways in cancer, focal adhesion,* and *calcium signalling* represent the most perturbed KEGG pathways among the placenta homogenate (Figure 27A). In contrast, *focal adhesion* was the only significantly overrepresented pathway in M/L STB-EVs (Figure 27B). The top S STB-EV KEGG pathways (Figure 28A) were the *HIF-1 signalling pathway, proteoglycans in cancer,* and *longevity regulation pathway-multiple species. Focal adhesion* was overrepresented among the three sample types. In contrast, the *HIF-1 signalling pathway, proteoglycans in cancer,* and *central carbon metabolism in cancer* were overrepresented in placenta homogenate and S STB-EVs (Figure 28B, Table 9).

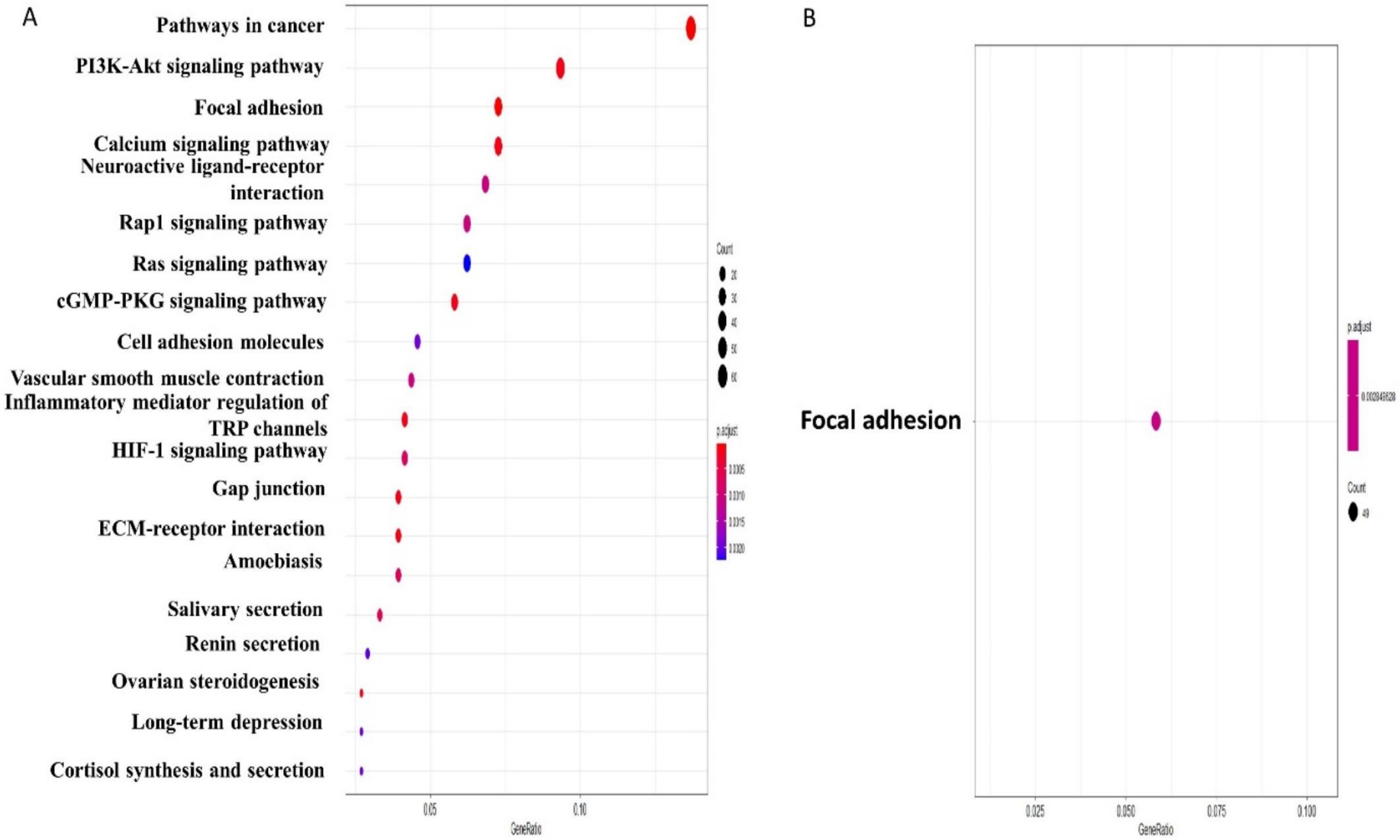



**Figure 27**. Figure showing results of functional enriched KEGG pathways in the placenta (A), medium/large STB-EVs (B) showing the number of overlapping biological processes between the placenta, medium/large STB-EVs and small STB-EVs.

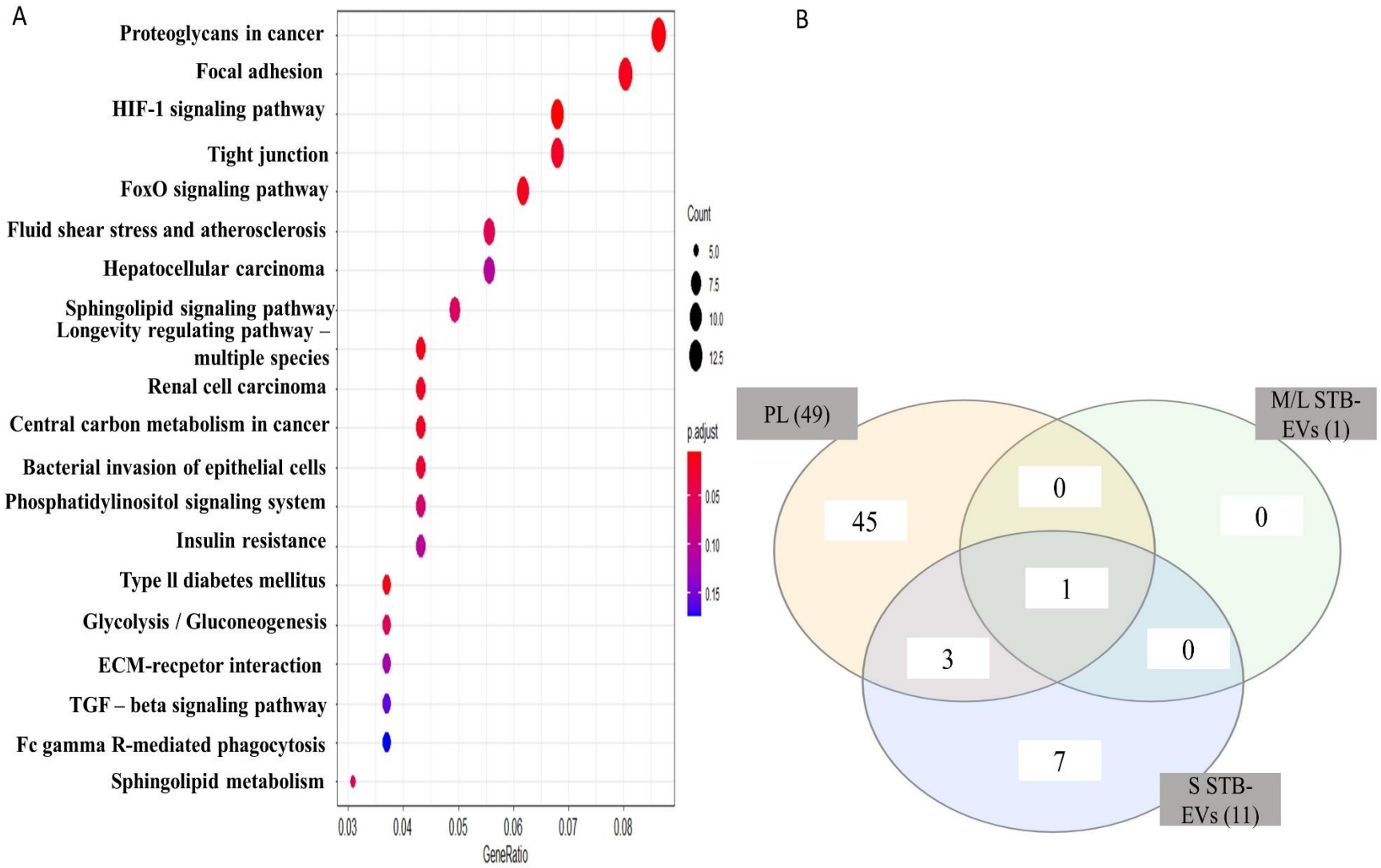



**Figure 28**. Figure showing results of functional enriched KEGG pathways in small STB-EVs (A) and a combined Venn plot (B) showing the number of overlapping biological processes between the placenta, medium/large STB-EVs and small STB-EVs.

### 3.5.3.5 Signalling pathway impact analysis (SPIA) in preeclampsia

Signalling pathway impact analysis of the DEGs in placenta homogenate (Figure 29A) showed *neuroactive ligand-receptor interaction, ECM-receptor interaction, focal adhesion, amoebiasis,* and *gap junction* as the most overrepresented. Of these five, all were inhibited except the *neuroactive ligand-receptor interaction,* which was activated. In contrast, the same analysis on M/L STB-EVs (Figure 29B) revealed two significantly dysregulated pathways, *focal adhesion* and *cytokine-cytokine interaction pathways,* both of which were activated. Similarly, in S STB-EVs (Figure 29C), *adipocytokine, focal adhesion,* and *type II DM* were significantly activated. Among all three sample types (Figure 29D), *focal adhesion* was common to all sample types and potentially highlights a crucial process (Table 9).

A

| SPIA/KEGG Pathway | Adjusted P Value | Status |
|---|---|---|
| Neuroactive ligand-receptor interaction | 0.000 | Activated |
| ECM-receptor interaction | 0.000 | Inhibited |
| Focal adhesion | 0.000 | Inhibited |
| Amoebiasis | 0.000 | Inhibited |
| Gap junction | 0.000 | Inhibited |
| Vascular smooth muscle contraction | 0.001 | Inhibited |
| Pathways in cancer | 0.001 | Inhibited |
| Calcium signaling pathway | 0.001 | Inhibited |
| Salivary secretion | 0.001 | Inhibited |
| Long-term depression | 0.005 | Activated |
| Adipocytokine signaling pathway | 0.006 | Activated |
| Cytokine-cytokine receptor interaction | 0.017 | Activated |
| Small cell lung cancer | 0.041 | Inhibited |

B

| SPIA/KEGG pathway | Adjusted P Value | Status |
|---|---|---|
| Focal adhesion | 0.000 | Activated |
| Cytokine-cytokine receptor interaction | 0.005 | Activated |

C

| SPIA/KEGG Pathways | Adjusted P Value | Status |
|---|---|---|
| Adipocytokine signaling pathway | 0.000 | Activated |
| Focal adhesion | 0.023 | Activated |
| Type II diabetes mellitus | 0.049 | Activated |

D

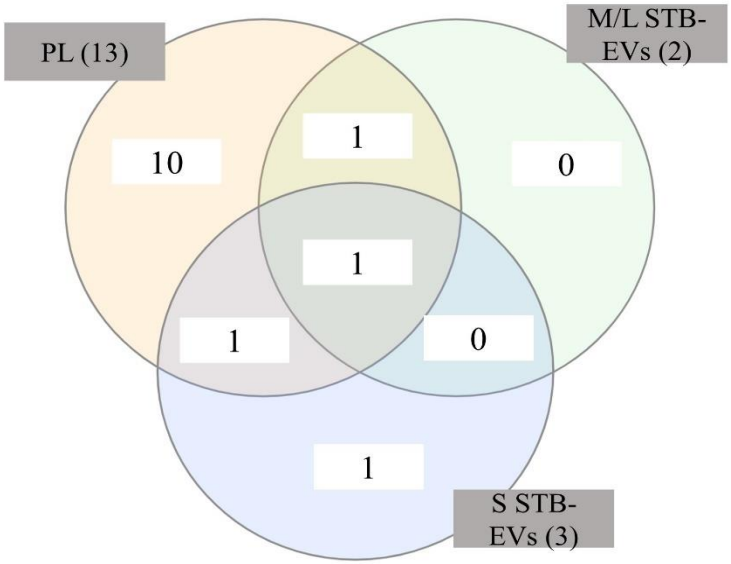



**Figure 29**. Figure showing results of functional enriched SPIA pathways in the placenta (A), medium/large STB-EVs (B) and small STB-EVs (C) and a combined Venn plot showing the number of overlapping SPIA pathways between the placenta, medium/large STB-EVs and small STB-EVs (D).

**Table 9.** List of overlapping differentially expressed proteins in the placenta, medium/large STB-EVs and small STB-EVs

| Sample Type | Gene Ontology terms and KEGG Pathway(s) |
|---|---|
| | Biological Process (BP) |
| PLACENTA and S STB-EVs | Extracellular matrix organization |
| | Extracellular structure organization |
| | Cell-substrate adhesion |
| | Regulation of vasculature development |
| | Regulation of cell-substrate adhesion |
| | Positive regulation of vasculature development |
| | Cell-substrate junction assembly |
| | Cell-matrix adhesion |
| | Cell-substrate junction organization |
| | Positive regulation of angiogenesis |
| | Regulation of cell-matrix adhesion |
| | Positive regulation of cell adhesion |
| | Regulation of cellular response to growth factor stimulus |
| | Negative regulation of locomotion |
| | Endocrine process |
| | Negative regulation of cell-matrix adhesion |
| | Regulation of endocrine process |
| | Transmembrane receptor protein serine/threonine kinase signalling pathway |
| | Positive regulation of phosphatidylinositol 3-kinase signalling |
| | Regulation of transmembrane receptor protein serine/threonine kinase signalling pathway |
| | Endocrine hormone secretion |
| | Response to transforming growth factor beta |
| | Cellular response to transforming growth factor beta stimulus |
| | Response to decreased oxygen levels, |
| | Negative regulation of myeloid leukocyte differentiation |
| | Regulation of phosphatidylinositol 3-kinase signalling |
| | Response to hypoxia |
| | Response to oxygen levels |
| | Maintenance of location |
| | Regulation of gonadotropin secretion |
| | NAD metabolic process |
| | Lipid localization |
| | Molecular Function (MF) |
| PLACENTA and S STB-EVs | Cell adhesion molecule binding, |
| | Integrin binding |
| | Cellular Component (CC) |
| PLACENTA and S STB-EVs | Collagen-containing extracellular matrix |
| | Leading-edge membrane |
| | Ruffle membrane |

| | |
|---|---|
| | Cell-cell junction |
| M/l STB-EVs and S STB-EVs | Vesicle lumen |
| PLACENTA, M/L STB-EVs and S STB-EVs | Actin cytoskeleton |
| | Cytoplasmic vesicle lumen |
| | Secretory granule lumen |
| | Focal adhesion |
| | Cell-substrate junction |
| | Contractile fibre |
| PLACENTA and M/L STB-EVs | Platelet alpha granule lumen |
| KEGG Pathways | |
| PLACENTA and S STB-EVs | ECM-receptor interaction |
| | Inflammatory mediator regulation of TRP channels |
| | HIF-1 signalling pathway |
| | Glycolysis/gluconeogenesis |
| | Central carbon metabolism in cancer |
| | Proteoglycans in cancer |
| PLACENTA, M/L STB-EVs and S STB-EVs | Focal adhesion |

## 3.6 Discussion

Despite significant research efforts, the pathophysiology of preeclampsia (PE) has still not been fully unravelled. In recent years, extracellular vesicles (EVs) have gained interest, particularly their role in the context of PE, their potential to affect functional changes in organs downstream of them, and their ability to act as circulating liquid biopsies revealing data about the donor cells in real-time. STB-EVs have also been found to express several previously identified mechanistic agents and biomarkers such as *SIGLEC6* [230], *FLT1* [231], *MMPs* [232] and may explain the abnormalities in PE, such as endothelial activation and vasoconstriction [233]. The fascinating propensity of EVs, including STB-EVs, to be detected in the circulation and the stability of the molecules they protect in their cargo, especially RNA, formed this study's basis to explore the biomarker potential of STB-EVs [234].

I found 1143, 1961, and 338 genes differentially expressed in placenta tissue, M/L STB-EVs and S STB-EVs, respectively. Some of my findings include *FLT1*, *LEP* [235], *ENG*, *PAPP-A2*

[236], *FSTL3* [237], *PRG2* [237], *INHBA* [238], and other well-known and novel genes well described in the placenta but not STB-EVs. These STB-EV associated mRNA may account for a fraction of some circulating mRNA such as *PAPP-A2*, *LEP*, and *HTRA4* [239] found in increased amounts in PE patients.

I opted to validate *FLNB, COL17A1, SLC45A4, LEP, ENG, HTRA4, PAPP-A2, EBI3, HSD17B1, ARMS2, FSTL3, INHBA, SIGLEC6,* and *CGB3* due to their biomarker potential as earlier described with emphasis on their expression in STB-EVs. Among the subset of genes based on mechanistic interest, *LEP* plays a role in endocrine functions, reproduction, immune function and is produced by the placenta to aid implantation and regulate placental growth [240]. The dysregulation of leptin has been linked to pregnancy complications with higher circulating leptin levels associated with PE [241]. The role of its protein, although not its mRNA, as a potential biomarker has been suggested previously [242]. *COL17A1* is a collagen transmembrane protein involved in extracellular matrix receptor interactions. It has been identified, through mass spectrometry, to be differentially expressed in urine samples from PE. However, it has not been taken forward for its potential as a biomarker [243]. *SLC45A4* is downregulated in PE placentas [229] and promotes glycolysis and autophagy prevention [244], two processes known to be abnormal in PE [245]. *FLNB* is an essential cytoskeletal protein critical in endothelial cell motility and is highly significant and differentially expressed in PE [246].

Interestingly, Wei et al. described the mRNA and protein expression of *FLNB* to be downregulated in PE compared to normal in contrast to this finding [247]. While it is difficult to identify the exact reason, the choice of housekeeping gene may be a reason. Wei et al. used *β actin,* which has been observed to be variable and a potential confounder in other disease states or experimental conditions [248]. In contrast, I used *YWHAZ* and *SDHA* - both more stably expressed genes[249].

*FSTL3* was among the subset of genes with biomarker potential. *FSTL3* glycoprotein is localized to the decidua and highly detected in placental blood vessels, especially in PE [250]. *FSTL3* levels in plasma were higher in women with PE, and elevated plasma levels in the second trimester increased the risk of PE [251]. *HTRA4* is a placental-specific serine protease that stops cell cycle progression and cell differentiation to endothelial cells [252]. Its increased levels in PE may be responsible for endothelial cell dysregulation by disrupting endothelial tube formation and increasing endothelial cell permeability [253].

My analysis also provided mechanistic insights. It identified 618 biological processes, 73 molecular functions, 59 cellular components, 56 KEGG pathways, and 14 SPIA pathways. My findings include some characteristic pathways and GO terms such as *HIF 1 pathway, blood vessel development* [236]*, adipocyte regulation, retinoic acid regulation, hypoxic signalling, associated cytokine pathways* [254]*, PI3/Akt signalling,* and *pathways in cancer* [255]. Nevertheless, I also found several less characterised and new exciting pathways such as *processes involved with protein catabolism and degradation, insulin and other growth factor receptor signalling pathways, nervous system development, ion channel activities, transcription repression,* among others. Interestingly, the signalling pathway impact analysis found that the *focal adhesion pathway* was inhibited in the placenta but ironically activated in both EV subtypes. C*ytokine-cytokine interactions* were activated in M/L STB-EVs, while *type II DM* and *adipocytokine* pathways were activated in S STB-EVs. The risk of PE is known to be increased by 2-4 folds among type II DM patients, and women with a history of PE are more likely to develop type II DM later in life [256]. It would be interesting to explore, in the future, if S STB-EVs play a role in this association or if this association is due to the presence of comorbid conditions common to both PE and DM. Additionally, M/L STB-EVs have been described as proinflammatory, just as identified by my analysis and corroborated by Holder et al. [257].

Finally, *focal adhesion* is critical in the cell-extracellular matrix (ECM) interaction, such as the trophoblast and the ECM, vital in trophoblastic invasion and potentially essential in PE [258]. I found this pathway inhibited in the placenta but interestingly activated in M/L and S STB-EVs. Overall, the differences in the GO terms and pathways among all sample types may portray a difference in roles between the placenta, M/L STB-EVs, and S STB-EVs in the pathogenesis of the disease.

This study is not without limitations that should be considered while interpreting these results. First, while larger than other studies, the sample size is still small, with 13 placenta tissue and 14 STB-EV samples in total (for RNA seq). Secondly, I could not validate more genes due to cost limitations and patient recruitment difficulties due to COVID. It is also challenging to find a gestational age-matched control for PE, particularly the early onset phenotype (< 34 weeks). Therefore, I used term (37 to $41^{+6}$ weeks) controls for the placentae. Notwithstanding, this study has numerous positives, particularly my ability to utilize an integrated approach to identify potential STB-EV mRNA biomarkers, which would help diagnose and prevent PE early. In addition, I teased out some potentially exciting pathways, a few of which raise great mechanistic and comorbidity questions.

# CHAPTER 4

## RESULTS OF MICRORNA TRANSCRIPTOMIC ANALYSIS OF STB-EVs IN PREECLAMPSIA

## 4.1 Abstract

**Background:** Having explored mRNA differences in STB-EV from normal and preeclampsia (PE), I next investigated the potential differences in microRNA.

**Methods:** I performed small RNA sequencing on placental tissue, medium/large and small STB-EVs isolated from PE and NP placentae using *ex vivo* dual lobe perfusion. The sequencing data was bioinformatically analysed to identify differentially regulated microRNAs. Identified microRNAs were validated with quantitative PCR analysis. I completed this analysis by performing an in-silico prediction of STB-EV mechanistic pathways.

**Results:** I identified significant a difference in the STB-EVs microRNA (miRNA) profiles between PE and normal pregnancy (NP). I verified the differential expression of *hsa-miR-193b-5p, hsa-miR-324-5p, hsa-miR-652-3p, hsa-miR-3196, hsa-miR-9-5p, hsa-miR-421,* and *hsa-miR-210-3p* in the medium/large STB-EVs but not small STB-EVs. In silico mechanistic prediction identified novel mechanistic processes (e.g., abnormal protein metabolism) which may contribute to the clinical and pathological presentation of PE.

**Conclusions:** I identified differentially expressed microRNA that may have biomarker potential. The bioinformatic analysis uncovered mechanistic pathways, which may be important in the pathophysiology of PE.

## 4.2 Introduction

Preeclampsia (PE) is a multisystemic disorder of pregnancy that affects 2-8 % of pregnancies globally and confers adverse morbidity and mortality risks to both mother and foetus[8,259]. The diagnosis of PE remains challenging, and the disease mechanism remains elusive[259]. The placenta is believed to be central to its pathogenesis by releasing soluble factors and extracellular vesicles into the maternal circulation to act as mediators and propagators of the disease[13]. Placenta-derived EVs, termed syncytiotrophoblast membrane extracellular vesicles (STB-EVs), express various biomolecules such as proteins, mRNA, microRNA, tRNA in their cargo[13,127]. These EVs include the more studied, small STB-EVs (with a size range of less than 220 nm) and the less well-studied medium/large STB-EVs (221 nm to 1000 nm).

MicroRNAs are a sub-class of small non-coding RNAs of 19-24 nucleotides[129]. MicroRNAs regulate the expression of mRNA by inducing mRNA cleavage or repressing translation[130,260,261]. In the circulation, microRNAs can be carried by extracellular vesicles, argonaut 2 (Ago2) proteins, high-density lipoprotein, and other ribonucleoprotein complexes, as well as circulating freely[131]. Circulating microRNAs have been explored in PE by interrogating cell-free microRNA in the circulation, identifying potential biomarkers and then inferring these to the placenta. Srinivasan et al. recently summarised most of the previously identified preeclamptic extracellular microRNAs biomarker candidates[262]. In addition, Srinivasan et al. also suggested new microRNAs such as *hsa-miR 941, hsa-miR-516b-5p, hsa-mir-let-7b-5p/hsa-miR-155-5p*[262] as being of placental origin. Still, no attention was paid to which subspecies of placenta EVs express these microRNAs, i.e., whether small or medium/large STB-EVs.

In contrast, Wei et al. approached this question using placenta EVs or placenta debris derived from placenta explants rather than *ex vivo* dual lobe placenta perfusion[263].

The biogenesis of EVs may well be more relevant given that medium/large EVs are released because of stress, whilst small EVs appear to be constitutively released. PE is a disease characterised by syncytiotrophoblast stress, and thus medium/large EVs may be more reflective of the placenta's pathology. Finally, most of these studies have examined extracellular RNA (intra and extravesicular) in serum, plasma, or urine rather than focusing on extracellular vesicle RNA. Little to no attention has been paid to medium/large EVs.

I used differential centrifugation to enrich and characterise two subclasses of placenta EVs generated by the *ex vivo* dual lobe perfusion model. These medium/large and small EVs were then separately subjected to small RNA analysis. This analysis uncovered previously unreported microRNAs in PE. Furthermore, I bioinformatically identified disease mechanisms via functional enrichment analysis. To the best of my knowledge, this is the first study to perform small RNA transcriptomic analysis on the originating placental tissue and medium/large and small STB-EVs isolated from the same placental tissue.

## 4.3 Aims

The aims of this chapter are to:

1. characterise the microRNA transcriptomic cargo of PE and NP using next-generation sequencing technologies.
2. Identify potential biomarkers that may help diagnose and predict the occurrence of PE earlier in pregnancy.
3. Identify key regulatory microRNA pathways, mechanisms, and networks in PE.

## 4.4 Methods

The data from the sequenced samples were bioinformatically and statistically analysed to identify differentially expressed microRNAs (DEMs). The functions of these DEMs were bioinformatically identified through functional enrichment analysis for gene ontology terms and KEGG pathways. The methods used in this chapter have been described in detail in the general methods section.

## 4.5 Results

### 4.5.1 General descriptive characteristics of small RNA sequencing in the placenta, medium/large STB-EVs and small STB-EVs

Approximately 9-16 million reads were generated from the sample library, and all reads passed the quality control filter (quality scores above 30 out of 38). The placental reads had a heterogeneous length distribution with two similar peaks around 21-24 nucleotides (the expected size range of MiRNAs) and 31 to 34 nucleotides (size range of small RNA fragments including tRNA halves). The STB-EVs also had two similar peaks, but the 31 to 34 nucleotides peak was more prominent than the 21 to 24 peaks. The placental reads were uniquely mapped to the human small RNAome (hg38) with the Oasis 2.0 pipeline to identify microRNAs, tRNAs, piRNAs, siRNAs and other small RNA species. Of these placental reads (Figure 30), the majority mapped to the rRNA (65-83%), followed by TE and miRNA (8-18%). In contrast, for the STB-EV reads (Figure 23), the majority mapped to tRNA fragments (77-91%), followed by ribosomal RNAs and microRNAs (2-20%).

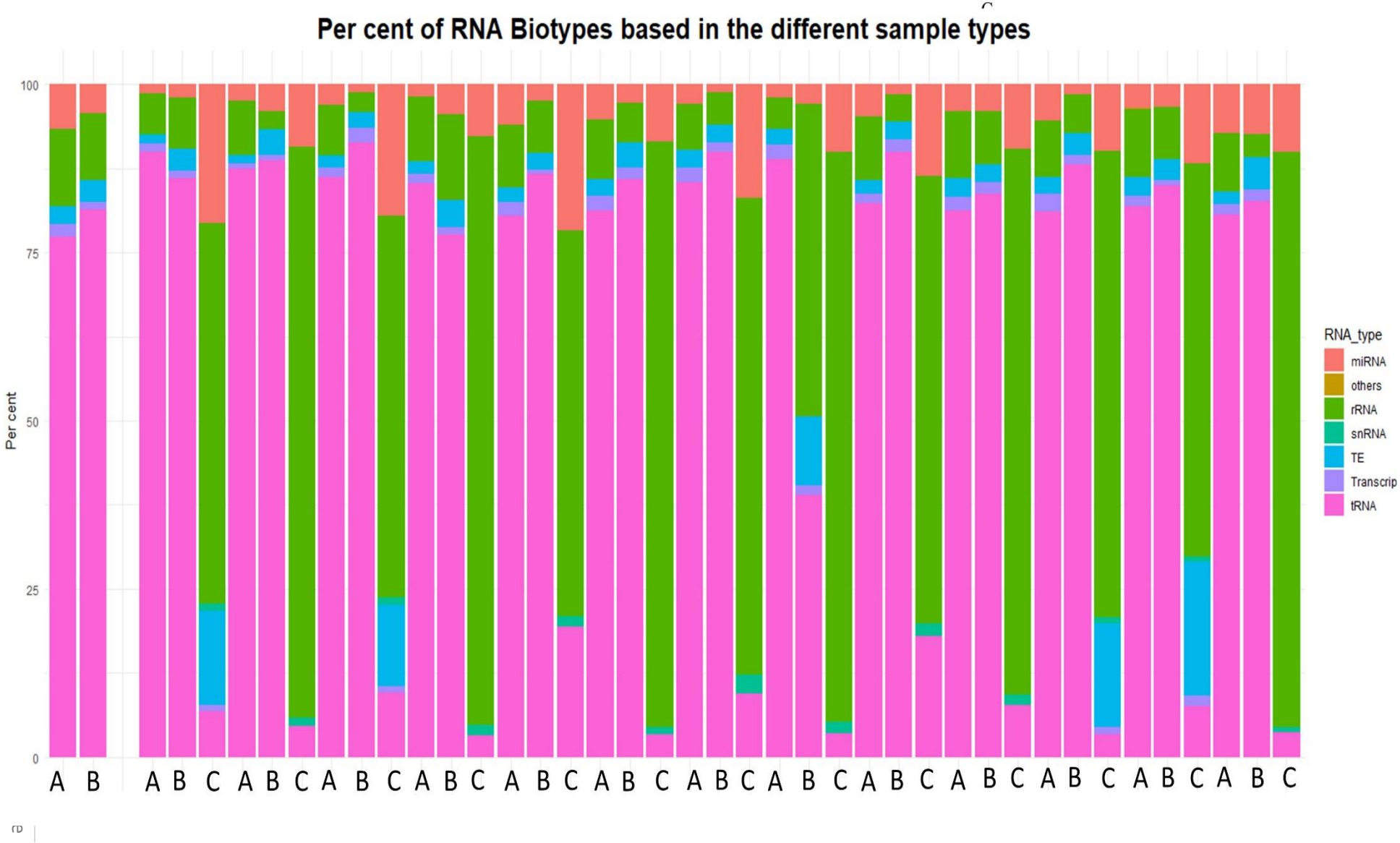



**Figure 30**. Stacked bar chart showing the small RNA biotypes seen in the placenta, medium/large and small syncytiotrophoblast membrane extracellular vesicles. A) is M/L STB-EVs, B) is S STB-EVs and C is Placenta. M/L STB-EVs are predominantly made up of transfer RNAs followed by microRNAs while the placenta mainly consists of ribosomal RNA followed by microRNA

### 4.5.2 Differentially expressed MicroRNAs (DEMs) in Placenta, medium/large STB-EVs, and small STB-EVs in preeclampsia

Comparison between PE and normal pregnancy placental tissue revealed 14 upregulated and 120 downregulated microRNAs (p value of < 0.05 [Figure 31]) while in medium/large STB-EVs, 47 were upregulated and 53 were downregulated (p value of < 0.05 [Figure 32]). Finally, for small STB-EVs, 7 were upregulated, and 9 were downregulated (p value of < 0.05 [Figure 33]). Note that the LFC is more modest in the S STB-EVs. Table 10 shows the top ten DEMs in the placenta, medium/large STB-EVs, and small STB-EVs in Preeclampsia. In general, among the upregulated microRNAs, *hsa-miR-210-3p* and *hsa-miR-193b-5p* were common to all three sample types (Figure 34, Table 11). Seven downregulated microRNAs; *hsa-let-7e-5p, hsa-miR-221-3p, hsa-miR-330-3p, hsa-miR-324-5p, hsa-miR-584-5p, hsa-miR-652-3p, and hsa-miR-1301-3p* were common to all.

**Table 10.** List of differentially expressed microRNAs in the placenta, medium/large STB-EVs, and small STB-EVs. Sample size for transcriptomics; placenta homogenate (NP = 6 and PE = 7) and STB-EVs (NP = 6 and PE = 8).

| MicroRNA | Log2 fold change | Adjusted P Value |
|---|---|---|
| Placenta | | |
| Hsa-miR-210-3p | 1.83 | <0.0001 |
| Hsa-miR-501-5p* | -1.37 | <0.0001 |
| Hsa-miR-377-5p* | -1.37 | <0.0001 |
| Hsa-miR-584-5p* | -1.44 | <0.0001 |
| Hsa-miR-3188* | -1.49 | <0.001 |
| Hsa-miR-652-3p* | -1.51 | <0.0001 |
| Hsa-miR-139-3p* | -1.55 | <0.0001 |
| Hsa-miR-1301-3p | -1.82 | <0.0001 |
| Hsa-miR-3614-5p* | -2.00 | <0.0001 |
| Hsa-miR-6501-5p* | -2.00 | <0.0001 |
| M/L STB-EVs | | |
| Hsa-miR-4488*$^{+}$ | 1.60 | <0.0001 |
| Hsa-miR-3196*$^{+}$ | 1.60 | <0.0001 |
| Hsa-miR-4516*$^{+}$ | 1.50 | <0.0001 |
| Hsa-miR-193b-5p$^{+}$ | 1.50 | <0.0001 |
| Hsa-miR-210-3p$^{+}$ | 1.40 | <0.0001 |
| Hsa-miR-27a-5p$^{+}$ | 1.40 | <0.0001 |
| Hsa-miR-3656*$^{+}$ | 1.20 | <0.001 |
| p-Hsa-miR-113*$^{+}$ | 1.20 | <0.0001 |
| Hsa-miR-652-3p*$^{+}$ | -1.20 | <0.0001 |
| Hsa-miR-324-5p*$^{+}$ | -1.70 | <0.0001 |
| S STB-EVs | | |
| Hsa-miR-210-3p | 1.80 | <0.0001 |
| Hsa-miR-193b-5p | 1.14 | <0.0001 |
| Hsa-miR-10a-5p*$^{-}$ | 0.70 | 0.02 |
| Hsa-miR-324-5p*- | -0.64 | 0.02 |
| Hsa-miR-23a-3p*$^{-}$ | -0.67 | <0.0001 |
| Hsa-miR-1301-3p$^{-}$ | -0.71 | 0.02 |
| Hsa-miR-330-3p*$^{-}$ | -0.82 | 0.01 |
| Hsa-let-7e-5p*$^{-}$ | -0.83 | <0.001 |
| Hsa-miR-584-5p*$^{-}$ | -0.87 | <0.01 |
| Hsa-miR-652-3p*$^{-}$ | -0.96 | <0.001 |

* = not previously described in PE, $^{+}$ = not previously described in PE M/L STB-EVs, $^{-}$ = not previously described in PE S STB-EVs (checked on human microRNA disease database version 3.2)

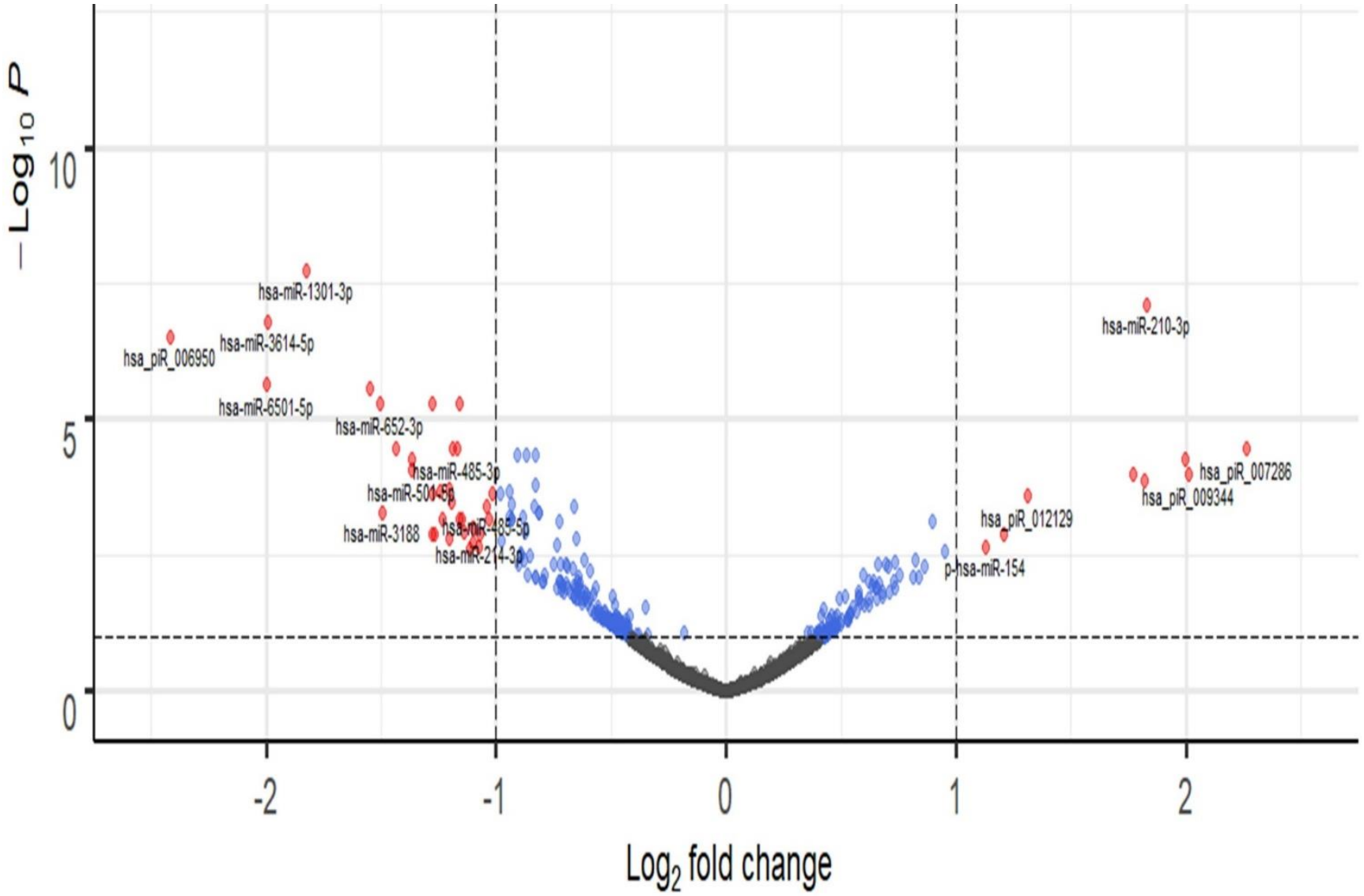



**Figure 31**. Volcano plot showing the differentially expressed small RNAs (microRNAs, piRNAs, siRNAs and SNORDS) in the placenta homogenate. The most upregulated small RNAs are in the top right corner while the most downregulated RNAs are in the top left corner.

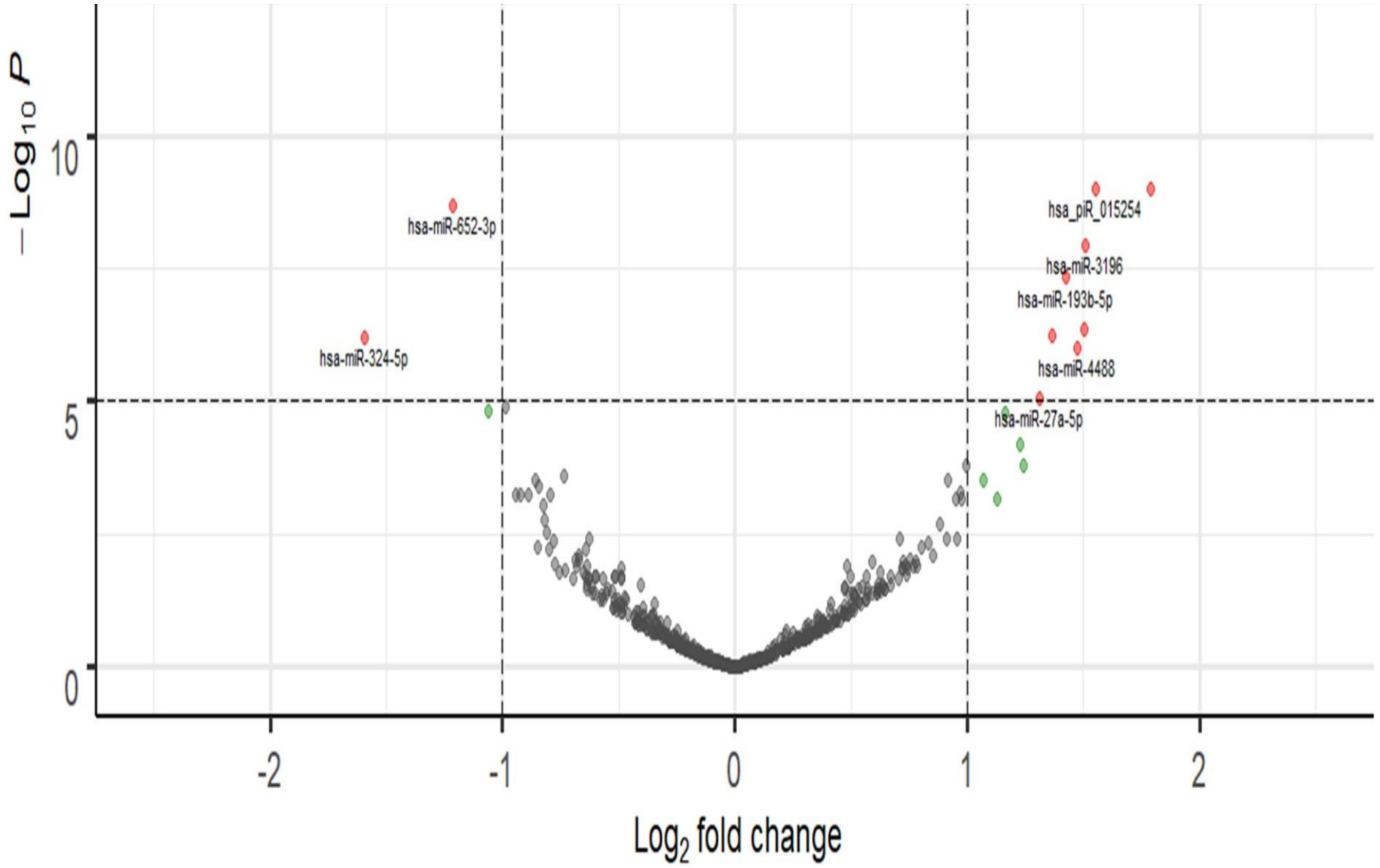



**Figure 32**. Volcano plot showing the differentially expressed small RNAs (microRNAs, piRNAs, siRNAs and SNORDS) in the medium/large STB-EVs. The most upregulated small RNAs are in the top right corner while the most downregulated RNAs are in the top left corner.

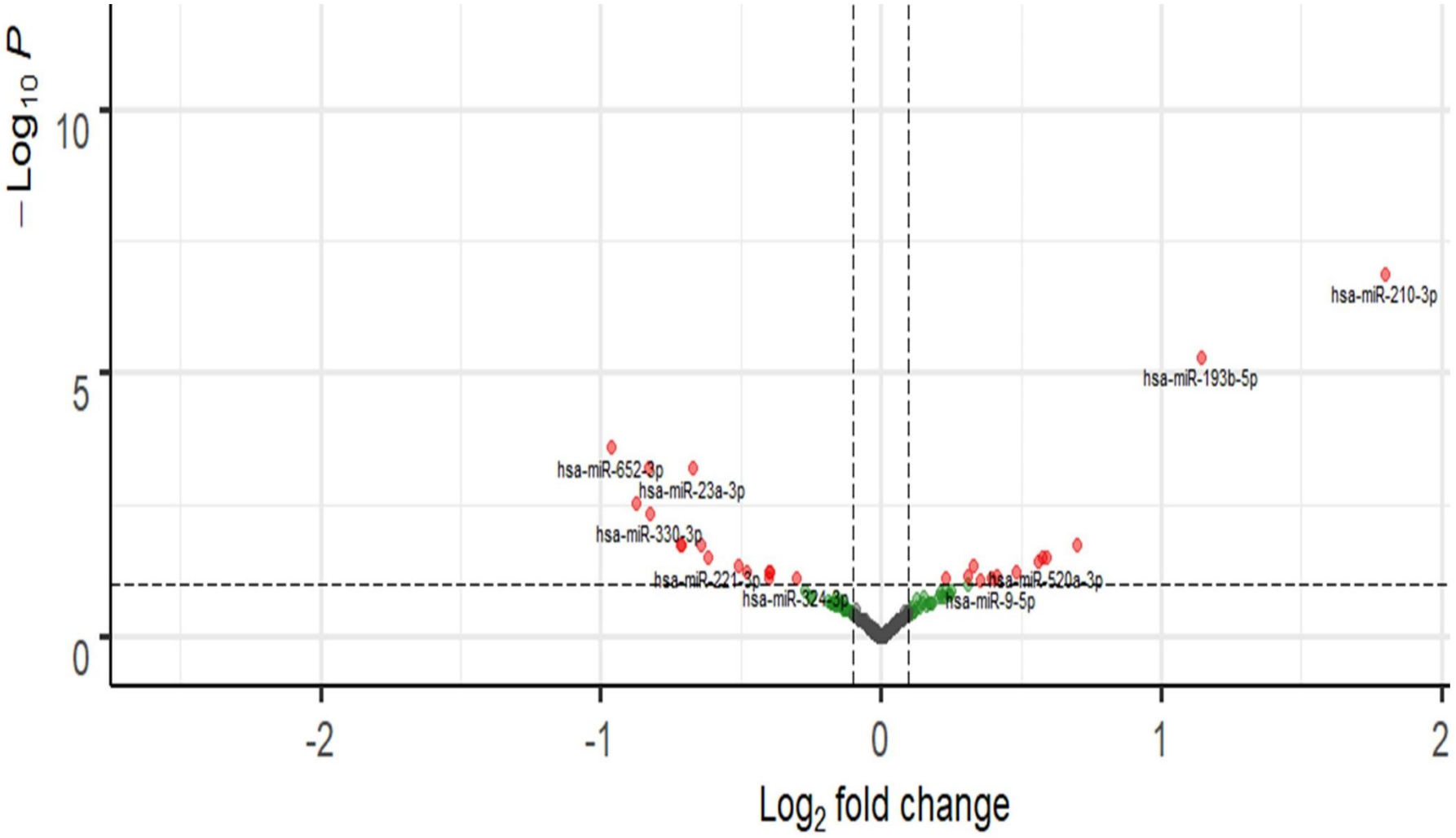



**Figure 33**. Volcano plot showing the differentially expressed small RNAs (microRNAs, piRNAs, siRNAs and SNORDS) in the small STB-EVs. The most upregulated small RNAs are in the top right corner while the most downregulated RNAs are in the top left corner.

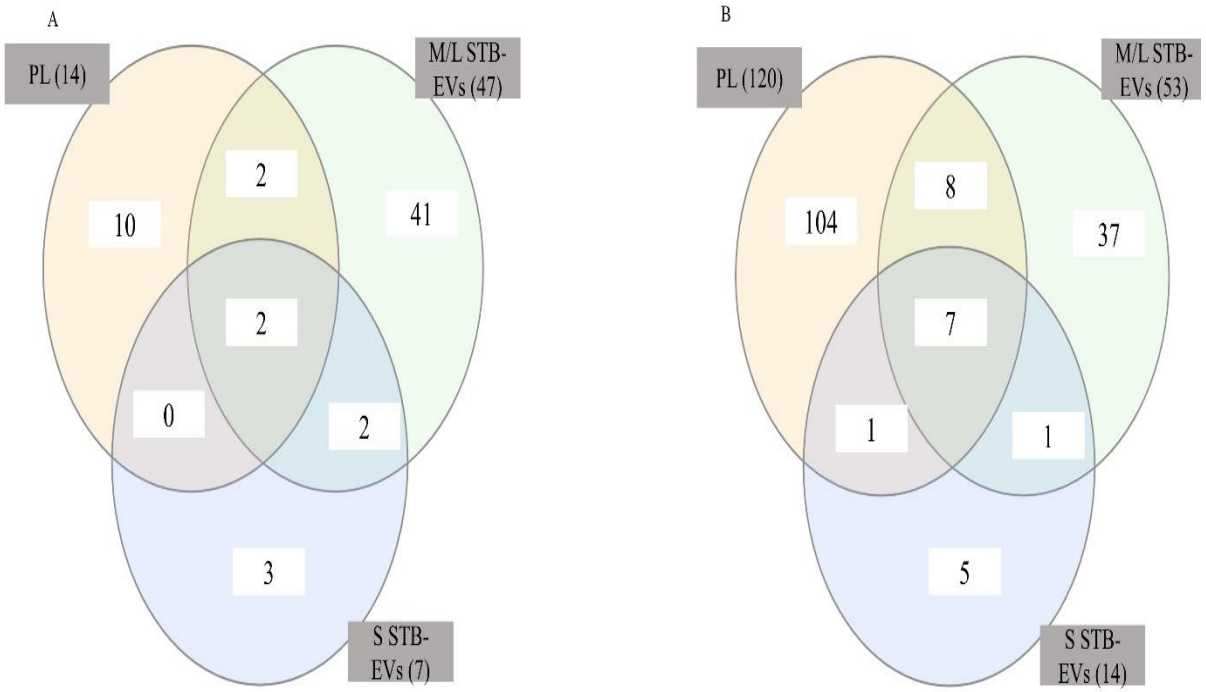



**Figure 34.** Venn diagram showing intersecting upregulated (A) or downregulated (B) differentially expressed microRNAs among the placenta, medium/large STB-EVs and small STB-EVs. *Hsa-miR-210-3p* and *hsa-miR-193b-5p* were upregulated microRNAs common to all three sample types while *hsa-let-7e-5p, hsa-miR-221-3p, hsa-miR-330-3p, hsa-miR-324-5p, hsa-miR-584-5p, hsa-miR-652-3p, and hsa-miR-1301-3p* were downregulated microRNAs common to all.

**Table 11.** Table showing intersecting upregulated (A) or downregulated (B) differentially expressed microRNAs among the placenta, medium/large STB-EVs and small STB-EVs.

| Sample types | Differentially expressed microRNAs (DEMs) |
|---|---|
| Upregulated | |
| M/L STB-EVs and S STB-EVs | Hsa-miR-27a-5p |
| | Hsa-miR-520a-3p |
| M/L STB-EVs, S STB-EVs and PLACENTA | Hsa-miR-210-3p |
| | Hsa-miR-193b-5p |
| PLACENTA and M/L STB-EVs and S STB-EVs | Hsa-miR-365a-3p__Hsa-miR-365b-3p |
| | Hsa-miR-31-5p |
| Downregulated | |
| PLACENTA and S STB-EVs | Hsa-miR-23b-3p |
| PLACENTA and M/L STB-EVs and S STB-EVs | Hsa-let-7e-5p, |
| | Hsa-miR-221-3p |
| | Hsa-miR-330-3p |
| | Hsa-miR-324-5p |
| | Hsa-miR-584-5p |
| | Hsa-miR-652-3p |
| | Hsa-miR-1301-3p |
| PLACENTA and M/L STB-EVs | Hsa-miR-425-5p |
| | Hsa-miR-519b-3p |
| | Hsa-miR-224-3p |
| | Hsa-miR-222-3p |
| | Hsa-miR-194-5p |
| | Hsa-miR-149-5p |
| | Hsa-miR-324-3p |
| | Hsa-miR-877-5p |

## 4.5.3 Quantitative PCR (qPCR) validation of selected microRNAs

As earlier discussed in the methodology section, due to my interest in STB-EVs as potential biomarkers, we selected the most differentially expressed miRNAs (Table 12) from the RNA sequencing data. For medium/large STB-EVs (Figure 35A), of the microRNAs tested *hsa-miR-193b-5p, hsa-miR-324-5p, hsa-miR-652-3p, hsa-miR-3196, hsa-miR-9-5p, hsa-miR-421,* and *hsa-miR-210-3p* were significantly different while for small STB-EVs (Figure 35B) even though *hsa-miR-210-3p, hsa-let-7e-5p, hsa-miR-193b-, hsa-miR-221-3p, hsa-miR-324-5p, hsa-miR-652-3p* ,and *hsa-miR-584-5p* were differentially expressed, none was significantly so.

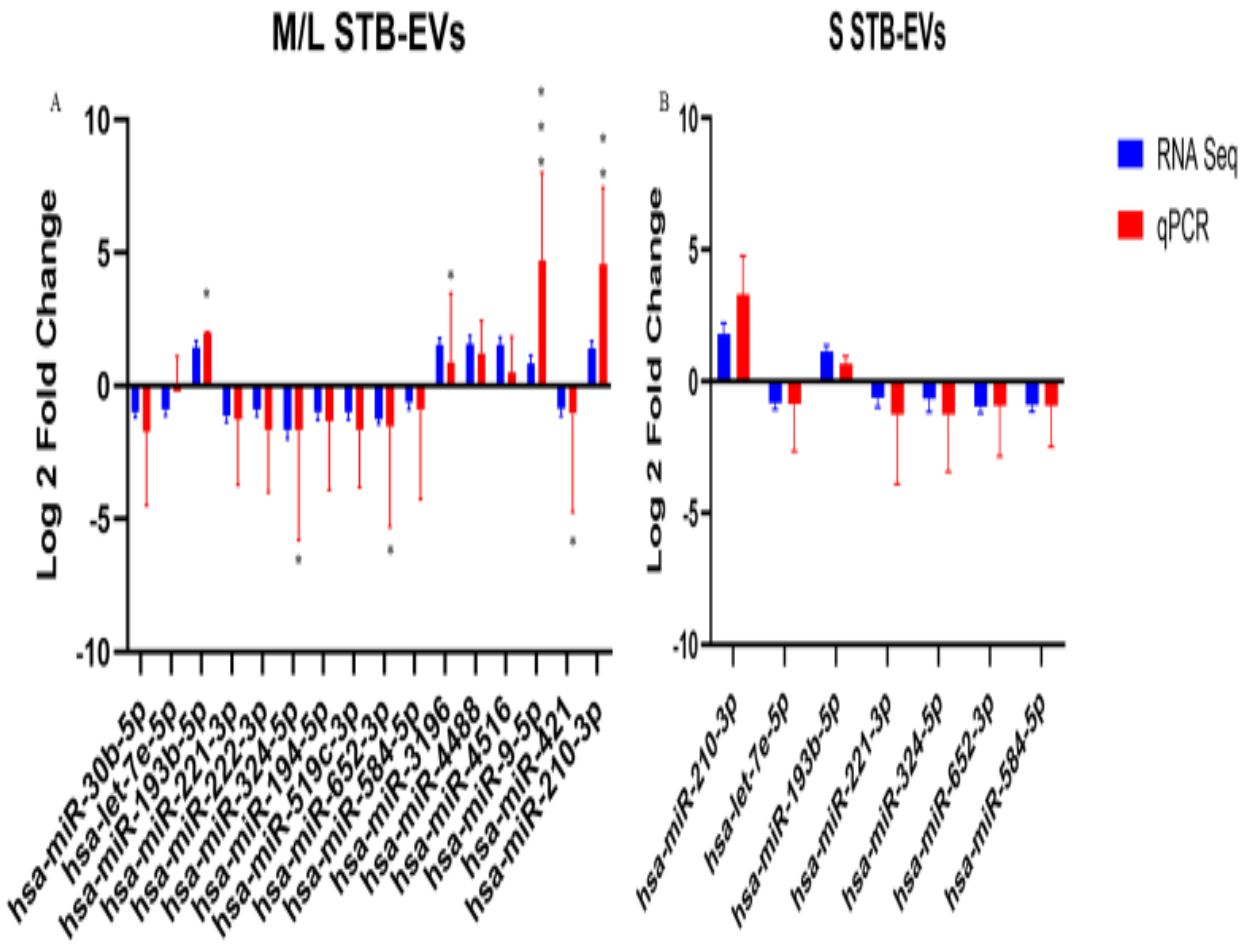



**Figure 35.** Figure showing the validation of select microRNAs from the RNA Seq dataset in a) medium/large STB-EVs and small STB-EVs. The X-axis shows the identity of the select microRNAs, and the Y-axis shows the log2fold change of the qPCR and RNA Seq data. $P < 0.05$ is *, $P < 0.01$ is ** and $P < 0.001$ is *** Sample size for M/L STB-EVs (NP = 4 and PE = 4) and S STB-EVs (NP = 3 and PE = 3)

**Table 12.** Table showing the log fold change (LFC), log fold standard error (LSE) of verified microRNAs for RNA Seq and quantitative PCR data in the placenta (red), medium/large STB-EVs (green), small STB-EVs (blue). Significant qPCR validated results are in bold font. Sample size for qPCR; M/L STB-EVs (NP = 4 and PE = 4) and S STB-EVs (NP = 3 and PE = 3)

| | Transcriptomics | | | qPCR | | |
|---|---|---|---|---|---|---|
| | LFC | LSE | P Value | LFC | LSE | P Value |
| M/L STB-EVs | | | | | | |
| Hsa-miR-30b-5p* | -0.97 | 0.21 | <0.0001 | -1.71 | -2.79 | 0.06 |
| Hsa-let-7e-5p* | -0.89 | 0.22 | <0.0001 | 0.08 | -1.04 | 0.41 |
| **Hsa-miR-193b-5p$^{+}$** | **1.46** | **0.25** | <0.0001 | **2.02** | **-0.02** | **0.04** |
| Hsa-miR-221-3p | -1.12 | 0.24 | <0.0001 | -1.25 | -2.47 | 0.07 |
| Hsa-miR-222-3p* | -0.87 | 0.26 | <0.0001 | -1.66 | -2.33 | 0.06 |
| **Hsa-miR-324-5p*** | **-1.65** | **0.34** | <0.0001 | **-1.66** | **-4.13** | **0.01** |
| Hsa-miR-194-5p* | -1.00 | 0.27 | <0.001 | -1.31 | -2.60 | 0.07 |
| Hsa-miR-519c-3p* | -0.98 | 0.28 | <0.001 | -1.66 | -2.15 | 0.07 |
| **Hsa-miR-652-3p*** | **-1.24** | **0.19** | <0.0001 | **-1.53** | **-3.76** | **0.02** |
| Hsa-miR-584-5p* | -0.63 | 0.25 | 0.01 | -0.90 | -3.36 | 0.07 |
| **Hsa-miR-3196*** | **1.56** | **0.25** | <0.0001 | **0.89** | **-2.60** | **0.04** |
| Hsa-miR-4488* | 1.57 | 0.32 | 0.01 | 1.22 | -1.23 | 0.08 |
| Hsa-miR-4516* | 1.54 | 0.30 | <0.0001 | 0.53 | -1.32 | 0.20 |
| **Hsa-miR-9-5p*** | **0.84** | **0.31** | **<0.01** | **4.73** | **3.30** | **<0.001** |
| **Hsa-miR-421*** | **-0.84** | **0.28** | **<0.01** | **-1.03** | **-3.71** | **0.01** |
| **Hsa-miR-210-3p$^{+}$** | **1.42** | **0.27** | <0.0001 | **4.58** | **2.87** | **<0.01** |
| S STB-EVs | | | | | | |
| Hsa-miR-210-3p | 1.80 | 0.42 | <0.0001 | 3.31 | 1.46 | 0.28 |
| Hsa-let-7e-5p* | -0.83 | 0.23 | <0.0001 | -0.86 | -1.78 | 0.10 |
| Hsa-miR-193b-5p | 1.14 | 0.24 | <0.0001 | 0.67 | -0.29 | 0.40 |
| Hsa-miR-221-3p | -0.62 | 0.35 | 0.03 | -1.26 | -2.63 | 0.06 |
| Hsa-miR-324-5p* | -0.64 | 0.52 | 0.02 | -1.26 | -2.17 | 0.05 |

| | | | | | | |
|---|---|---|---|---|---|---|
| Hsa-miR-652-3p* | -0.96 | 0.23 | <0.0001 | -0.91 | -1.93 | 0.10 |
| Hsa-miR-584-5p* | -0.87 | 0.28 | <0.01 | -0.91 | -1.57 | 0.08 |

* = not previously described in PE, $^{+}$ = not previously described in PE M/L STB-EVs (checked at human microRNA disease database version 3.2)

### 4.5.4 Functional enrichment analysis of differentially expressed microRNAs (DEMs) in Preeclampsia

Given the extensive list of microRNAs obtained from our analysis, it was clear that existing functional enrichment analytical tools were unsatisfactory for understanding the potential interactions (largely because they have not been used to analyse such large numbers of molecules). To circumvent this, I performed functional enrichment analysis (Gene Ontology: biological process, molecular function, cellular components and KEGG pathways) separately on the up and downregulated microRNAs in the placenta, medium/large and small STB-EVs.

There were seven biological processes common to all upregulated microRNAs (Table 11). For the downregulated microRNAs, there were twelve biological processes common to all (see Table 11). Interestingly, three biological processes were influenced by both up and downregulated microRNAs: *neurotrophin TRK receptor signalling pathway, cellular protein modification process,* and *epidermal growth factor receptor signalling pathway*. KEGG pathway analysis (biochemical pathways) showed only the *ECM-receptor interaction* was overrepresented (Table 13) among the three sample types (upregulated microRNA list). In contrast, five KEGG pathways, *ECM-receptor interaction, glycosphingolipid biosynthesis - lacto and neolacto series, morphine addiction, TGF-beta signalling pathway, ErbB signalling pathway,* were common to all sample types (downregulated microRNA list). Interestingly, ECM-receptor interaction was present in up and downregulated microRNA KEGG.

**Table 13.** Table showing the overlapping functional enrichment processes and terms for up and downregulated microRNAs in the placenta homogenate, medium/large STB-EVs and small STB-EVs.

| Upregulated microRNAs | |
|---|---|
| Gene Ontology: Cellular Components | |
| M/L STB-EVs and S STB-EVs | Nucleoplasm |
| PLACENTA, M/L STB-EVs and S STB-EVs | Organelle membrane |
| | Cytosol |
| | Membrane protein complex |
| Gene Ontology: Molecular Function | |
| M/L STB-EVs and S STB-EVs | Translation factor activity |
| | Enzyme regulator activity Cytoskeletal protein binding |
| PLACENTA and M/L STB-EVs and S STB-EVs | Transcription factor binding |
| | Ion binding |
| | Enzyme binding |
| Gene Ontology: Biological Process | |
| M/L STB-EVs and S STB-EVs | Nervous system development |
| | Blood coagulation |
| | Axon guidance |
| | Cell motility |
| | Transcription initiation from RNA polymerase II promoter |
| | Positive regulation of transcription |
| | Cellular nitrogen compound metabolic process |
| | Response to stress |
| | Toll-like receptor TLR1 |
| | Cell death |
| PLACENTA, M/L STB-EVs and S STB-EVs | Transcription |
| | Biosynthetic process |
| | Fc-epsilon receptor signalling pathway |
| | Neurotrophin TRK receptor signalling pathway |
| | Cellular protein modification process |
| | Gene expression |
| | Epidermal growth factor receptor signalling pathway |
| PLACENTA and M/L STB-EVs | Chemical synaptic transmission |

| | |
|---|---|
| | Fibroblast growth factor receptor signalling pathway |
| | Cell-cell signalling |
| KEGG Pathways | |
| PLACENTA and S STB-EVs | Biotin metabolism |
| | Hippo signalling pathway |
| M/L STB-EVs and S STB-EVs | Proteoglycans in cancer |
| | TGF-beta signalling pathway |
| | Lysine degradation |
| PLACENTA, M/L STB-EVs and S STB-EVs | ECM-receptor interaction |
| Downregulated microRNAs | |
| Cellular Components | |
| PLACENTA, M/L STB-EVs and S STB-EVs | Membrane protein complex |
| | Nucleoplasm |
| | Cytosol |
| PLACENTA, M/L STB-EVs and S STB-EVs | Organelle membrane |
| Molecular Function | |
| M/L STB-EVs and S STB-EVs | Translation factor activity |
| PLACENTA, M/L STB-EVs and S STB-EVs | Transcription factor binding |
| | Ion binding |
| | Enzyme binding |
| PLACENTA, M/L STB-EVs and S STB-EVs | Cytoskeletal protein binding |
| PLACENTA and M/L STB-EVs | RNA binding |
| KEGG Pathways | |
| PLACENTA and S STB-EVs | Huntington's disease |
| PLACENTA and M/L STB-EVs | Fatty acid biosynthesis |
| | Proteoglycans in cancer |
| | Mucin type O-Glycan biosynthesis |
| | Hippo signalling pathway |
| | Biosynthesis of unsaturated fatty acids |
| | Glioma |
| | Axon guidance |
| | Wnt signalling pathway |
| | Amoebiasis |
| | Lysine degradation |

| | |
|---|---|
| | Signalling pathways regulating pluripotency of stem cells |
| PLACENTA, M/L STB-EVs and S STB-EVs | ECM-receptor interaction |
| | Glycosphingolipid biosynthesis - lacto and neolacto series |
| | Morphine addiction |
| | ErbB signalling pathway |
| | TGF-beta signalling pathway |

### 4.5.5 MicroRNA and messenger RNA correlation in placenta homogenate, medium/large STB-EVs and small STB-EVs in Preeclampsia

To understand how the alterations in microRNA might influence mRNA expression, I correlated the results of this data with the messenger RNA sequencing presented in Chapter 3. I wanted to explore which of these messenger RNA changes can be explained by the changes in the microRNA profile in our samples. I interrogated the dataset using the freely available web tool called miRTarVIS+. In the placenta, 155 microRNA-mRNA interactions were detected by the three methods used (correlation analysis, mutual information (gain), and MINE - see methods chapters). In medium/large STB-EVs, 57 microRNA-mRNA interactions were identified, which includes the interaction between *hsa-miR-222-3p* (downregulated) and *TPBG* (upregulated) and *PLEKHA2* (upregulated). Similarly, small STB-EVs, 41 microRNA-mRNA interactions were observed, with the most prominent being the interaction between *hsa-let-7e-5p* and 25 upregulated mRNAs, including *ADAMTS1*. Overall, I identified microRNA-mRNA interactions in the placenta (Figure 36), M/L STB-EVs (Figure 37), and S STB-EVs (Figure 38). However, of the qPCR validated M/L STB-EV miRNAs, only two microRNAs (*hsa-miR-324-5p and hsa-miR-421*) had previously validated mRNA targets (Table 14).

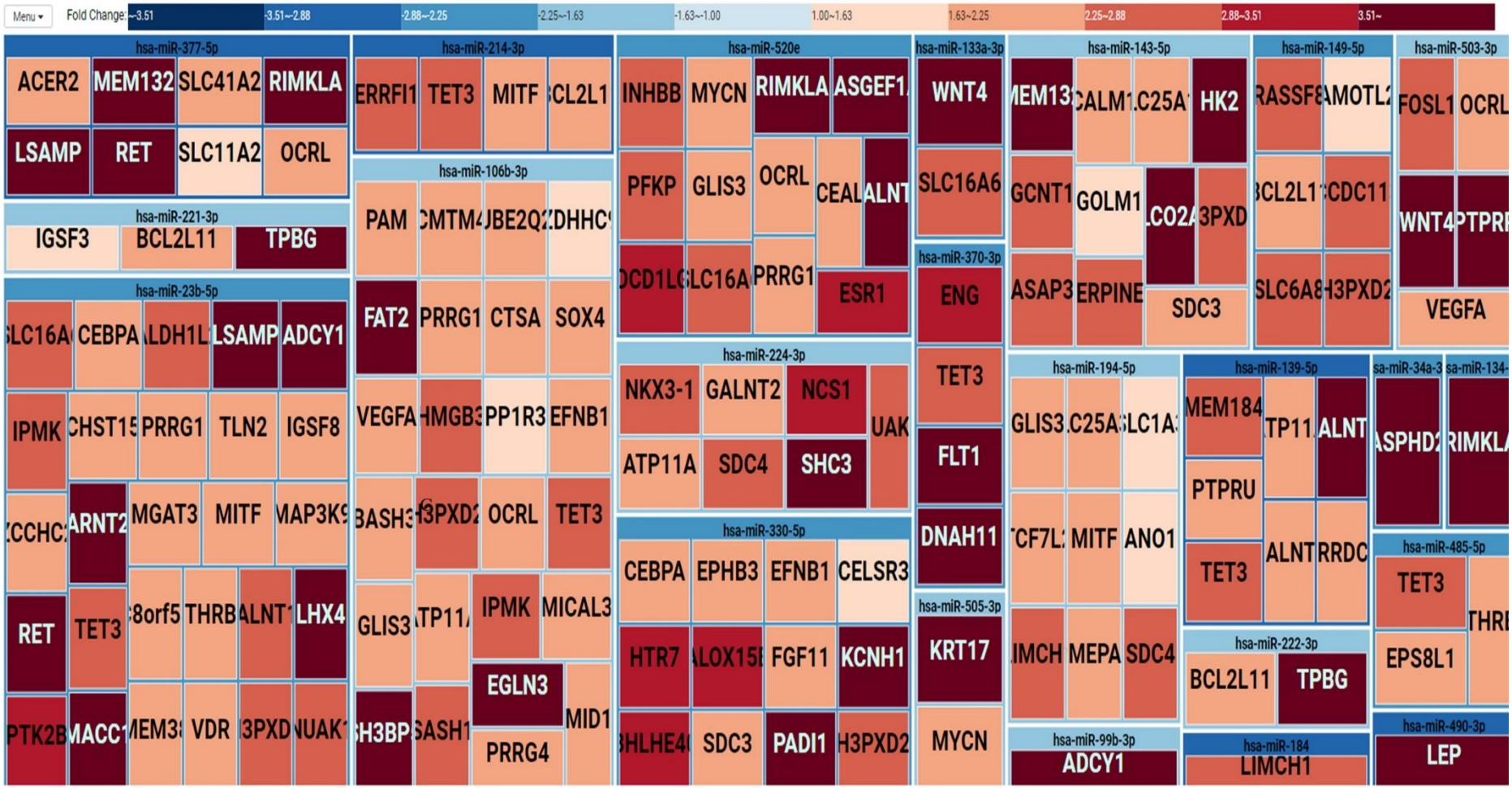



**Figure 36**. Figure showing microRNA-mRNA correlation. Only the 155 microRNA-mRNA interactions identified by all three algorithms were visualised by tree map showing the microRNA-mRNA interactions in the placenta dataset. For the tree map, the mRNA targets are grouped based on the microRNA that is predicted to target them. The rectangles are also colour coded to reflect downregulation (blue) or upregulation (red) of both microRNAs and mRNAs respectively. Each blue rectangle represents the microRNA while the red and orange rectangles represent the messenger RNA controlled for by the microRNA above them.

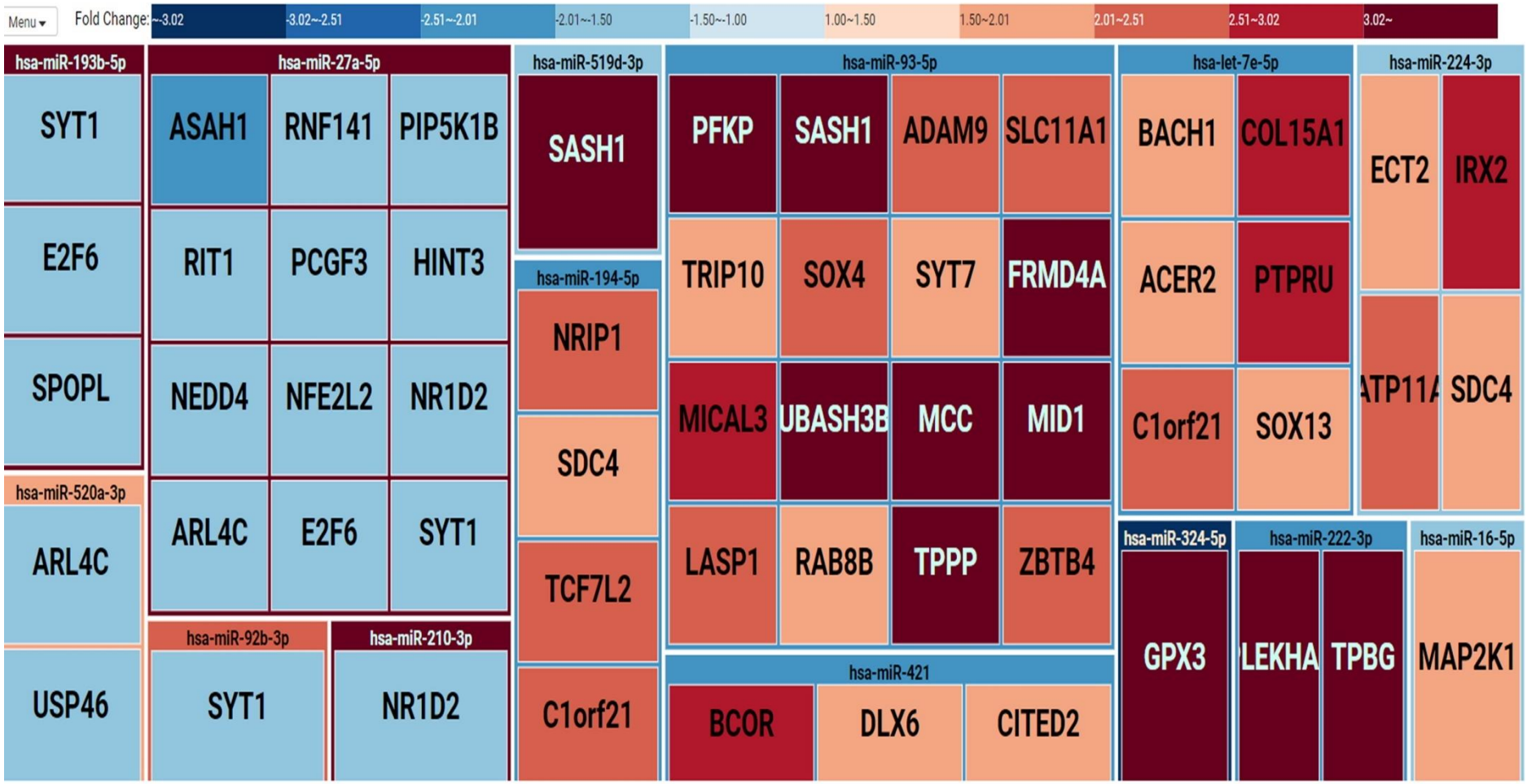



**Figure 37**. Figure showing microRNA-mRNA correlation. Only the 57 microRNA-mRNA interactions identified by all three algorithms were visualised by tree map showing the microRNA-mRNA interactions in the medium/large STB-EVs dataset. For the tree map, the mRNA targets are grouped based on the microRNA that is predicted to target them. The nodes and rectangles are also colour coded to reflect downregulation (blue) or upregulation (red) of both microRNAs and mRNAs respectively. Each strip of blue/red rectangle represents the microRNA while the red and orange/blue big rectangles represent the messenger RNA controlled for by the microRNA above them.

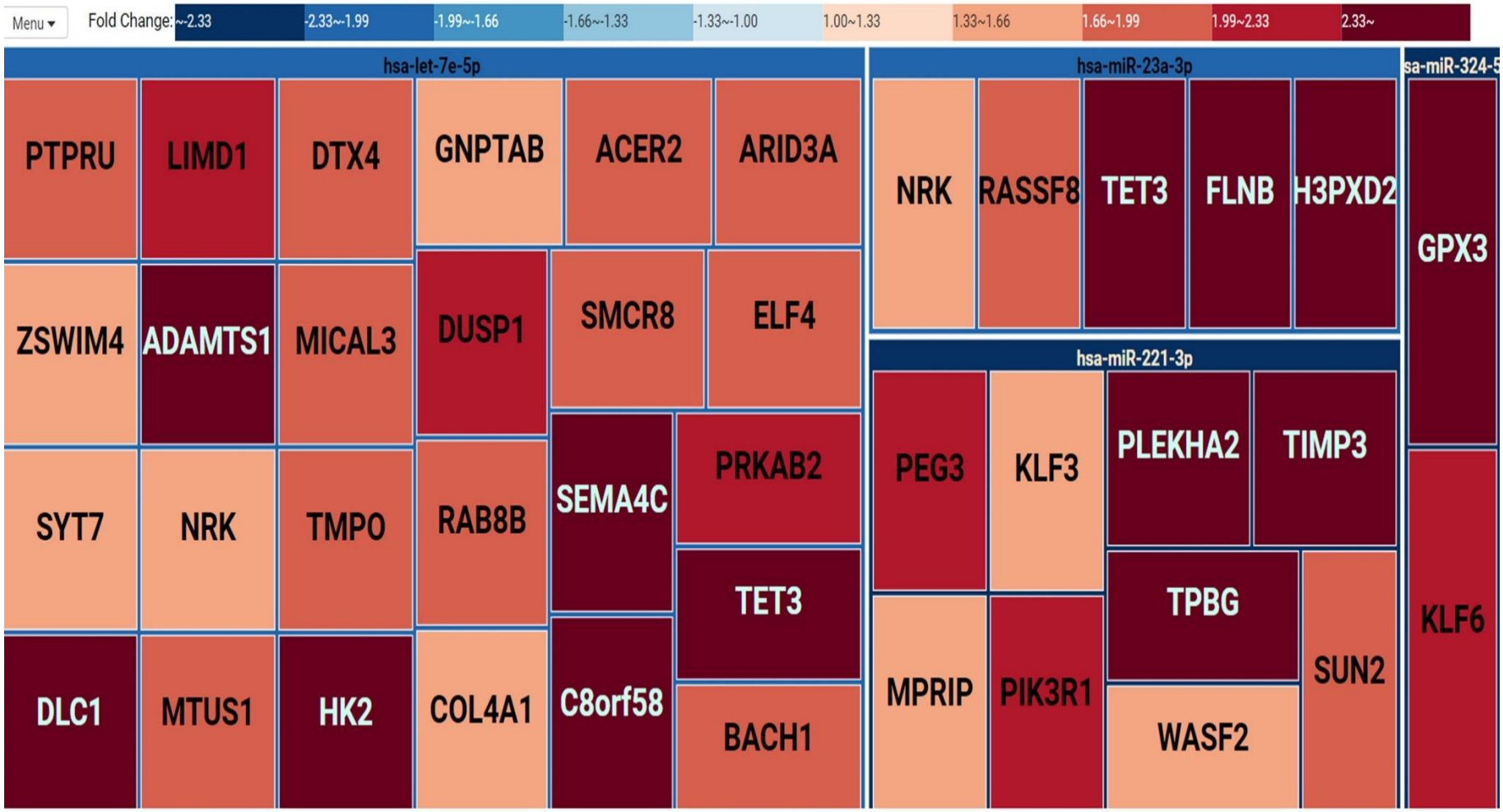



**Figure 38**. Figure showing microRNA-mRNA correlation. Only the 41 microRNA-mRNA interactions identified by all three algorithms were visualised by tree map showing the microRNA-mRNA interactions in the small STB-EVs dataset. For the tree map, the mRNA targets are grouped based on the microRNA that is predicted to target them. The nodes and rectangles are also colour coded to reflect downregulation (blue) or upregulation (red) of both microRNAs and mRNAs respectively. Each small blue rectangle represents the microRNA while the big red and orange rectangles represent the messenger RNA controlled for by the microRNA above them.

**Table 14.** Table showing the validated microRNA-mRNA targets. Validation was by CLIP-Seq, a sequencing technique that identifies microRNAs and targets through their association with the ago silencing complex.

| qPCR validated M/L STB-EV miRNA(s) | mRNA Target (s) | Validation method |
|---|---|---|
| Hsa-miR-324-5p | GPX3 | CLIP-Seq* |
| | MAFB | |
| Hsa-miR-421 | TBC1D22A | CLIP-Seq* |
| | ENAH | |
| | PRKAA2 | |
| | NFIB | |
| | PLS3 | |
| | JARID2 | |
| | AK4 | |

*Source of validation is miRTarBase (www.mirtarbase.cuhk.edu.cn), CLIP-Seq = Crosslinking and immunoprecipitation sequencing

## 4.6 Discussion

In this chapter, I have shown that the microRNA content is different in PE compared to NP. All previous studies (other than the two mentioned below) have assessed circulating microRNA in the plasma or serum, biofluids containing significant contamination from other EV sources. Srinivasan et al. [262] used pooled serum (not the optimum biofluid to interrogate EVs) followed by immunoprecipitation of extracellular markers with the pan EV marker CD63 (although other known EV markers such as CD9 or CD81 were not examined), placenta EVs with PLAP (although PLAP also circulates freely as well as being attached to placental STB-EVs) and anti-AGO2. In addition, there was no morphologic or immunophenotypic evidence as recommended by ISEV to show that these immunoprecipitated molecules were indeed EVs. Another study by Wei et al. [263] described placenta debris (their description) in PE as containing a different microRNA profile than normal. Like Srinivasan et al., they did not subtype the EVs, and their EVs were generated with placental explants rather than *ex vivo* dual lobe placenta perfusion. The difference between the two methods is evident when comparing the small RNA composition of the EVs from the explant culture that they published to the *ex vivo* dual lobe perfusion data we have generated. Chamley et al. reported that most of their EVs were made up of microRNAs, while in our case, most of the small RNA sequences were made up of tRNA half fragments which we have published[264]. Finally, most researchers have focused on exosomes and small STB-EVs rather than medium/large STB-EVs as biomarkers. I concentrated on STB-EVs released by normal and PE placenta isolated from the source organ using *ex vivo* dual lobe placental perfusion. I decided to analyse both small and medium/large STBEVs, given that medium/large STB-EVs are released in response to stress, and preeclampsia is a stress condition.

My analysis identified an extensive list of microRNAs, including some previously identified PE related microRNAs, e.g., miR-210 and miR-193b-5p. I was able to verify some of the most differentially regulated microRNAs in medium/large STB-EVs, but the microRNAs in the small STB-EVs did not reach statistical significance. This finding is at variance with studies that have examined plasma or serum EVs. It may indicate that differences identified in complex biofluids may be because of other contaminating EV sources.

Some of my other findings were also discordant with previous literature. Zhang et al. [265] identified miR-30b-5p to be upregulated in PE placenta and serum, unlike my results which revealed a reduction in this microRNA. Likewise, hsa-miR-584 was found to be upregulated in severe PE placenta by Jiang et al., which I did not observe. Liu et al. found miR- 222-3p to be upregulated in PE plasma[266] and placenta[267] in contrast with this study which found it downregulated in M/L STB-EVs (though not significant). These differences may be due to 1) variations in sample type (plasma vs serum), 2) spatial placenta microRNA expression variability, 3) sampling region[268], 4) technical and methodological variances, 5) analytic differences (RNA Seq (which I performed) compared to microarrays) or 6) might reflect some variability in the phenotype of PE.

Having identified the most differentially expressed microRNA based on the magnitude of fold change, I confirmed these changes by qPCR. I have confirmed some microRNAs as differentially expressed (*hsa-miR-324-5p, hsa-miR-3196, hsa-miR-652-3p hsa-miR-9-5p, and hsa-miR-421*), which, to the best of my knowledge, have not been previously described in preeclampsia. Though hsa-miR-193b-5p (in placenta[269], placenta debris[263]) and hsa-miR-210-3p (in placenta[268], plasma[268,270], serum[136], plasma exosome[271]) have been reported in preeclampsia, they have not been previously reported in perfused M/L STB-EVs. Surprisingly, the identified bioinformatic differences were recapitulated in the placenta and medium/large

STB-EVs, but the interrogation of small EVs showed differences that were not significant. This contrast may be a sample size issue or/and reflect a different role for small STB-EVs.

Having identified and validated key differentially expressed microRNAs, I next wanted to understand their relationship to biological processes that might have disease relevance. I performed in silico prediction of potential mechanisms by which the STB-EV expressed microRNAs may be implicated in PE. My analysis confirmed biological processes known to be abnormal in preeclampsia, such as abnormal *cellular protein modification process*[272], *neurotrophin TRK receptor signalling pathway*[273], *epidermal growth factor receptor signalling pathway*[274], *cell motility*[275], *response to stress*[276], *Fc-epsilon receptor signalling pathway*[277] and *TGF-beta signalling pathway*[278].

I also predicted mRNA targets of differentially expressed microRNA to explore which of the previously described messenger RNA changes (described in Chapter 3) can be explained by the changes in the microRNA profile. Some of these interactions (especially in the M/L STB-EVs) have already been verified by others with CHIP-Seq. Overall, 98% of the microRNA-mRNA interactions consisted of a combination of downregulated microRNAs and upregulated target mRNAs, which would be as expected. The absence of a (microRNA based) explanation for the upregulated mRNA transcripts in the remaining 2% might be because additional mRNA regulatory mechanisms exist in addition to microRNAs. These additional mechanisms may include RNA binding proteins, transcription factors, nonsense-mediated mRNA decay (NMD), other small RNAs, and others[36]. Reassuringly, some of the key differentially expressed genes in PE previously identified by others and us, such as FLT-1, Endoglin, and ADAMTS, were predicted to be targets of the differentially expressed microRNAs in this study (with upregulation of mRNA linked to downregulation of microRNA).

In conclusion, I have identified new STB-EV expressed microRNAs that may be diagnostic in PE. Interestingly, the most prominent differences were seen in the less-studied M/L STB-EVs. This suggests that the previous focus on small STB-EVs might have been misplaced. In addition, I have predicted some potential in silico mechanistic pathways in PE.

# CHAPTER 5

## RESULTS OF PROTEOMIC ANALYSIS OF STB-EVs IN PREECLAMPSIA

## 5.1 Abstract

**Background:** In this chapter, I hypothesised that the proteome of placental tissue and STB-EVs is different between preeclampsia and normal pregnancy and might permit the identification of potential biomarkers and offer mechanistic insights.

**Methods:** I performed mass-spectrometry on placental tissue, medium/large and small STB-EVs isolated from PE and NP placentae using *ex vivo* dual lobe placenta perfusion. Mass-spectrometry was bioinformatically analysed to identify differentially regulated proteins. Identified biomarkers were validated with Western blot. I completed our analysis by performing an in-silico prediction of STB-EV mechanistic pathways.

**Results:** I identified a difference in the STB-EV proteome between PE and normal pregnancy (NP). I discovered and verified differential expression of FLNB (filamin B), *COL17A1 (Collagen 17A1), PAPP-A2 (Pappalysin-A2),* and *SR-BI (Scavenger Receptor Class B Type 1).* In silico mechanistic prediction identified novel mechanistic processes (e.g., abnormal protein metabolism) which may contribute to the clinical and pathological presentation of PE.

**Conclusions:** I performed comprehensive profiling of proteome and pathways in PE by analysing the three different sample subtypes. I identified differentially expressed proteins and uncovered mechanistic pathways which may be important in the pathophysiology of PE and could potentially be used in future studies of disease mechanisms and as biomarkers.

## 5.2 Introduction

Preeclampsia (PE) is a leading cause of maternal death (>75,000 maternal deaths every year) and prematurity (15-20% of all preterm births) worldwide[279]. In the longer term, preeclampsia leads to increased risks of heart failure, coronary heart disease, cardiovascular death, diabetes mellitus (DM) [280], dementia[281], and ischaemic stroke. There are increased risks of bronchopulmonary dysplasia and neurodevelopmental disability in neonates in later life[282].

Predicting PE early in pregnancy has been challenging due to the limitations of current predictive models and biochemical tests (which lack positive predictive value). The existing tests perform far better in ruling out rather than ruling in PE. They are also most effective shortly before the onset of the disease and within a specific period (1 or 2 weeks) rather than earlier in pregnancy. In this chapter, I have attempted to identify potential placenta-derived biomarkers that may address these limitations by capitalising on the biomarker potential of extracellular vesicles and their ubiquitous presence in all body fluids[283].

I have focused on extracellular vesicles released from the placental syncytiotrophoblast (STB) layer, the interface between the foetus and the mother, directly contacting the maternal circulation[284]. I attempted to identify potential molecular targets, mechanisms, and processes of PE through comprehensive proteomics analysis of medium/large (M/L) STB-EVs, and small (S) STB-EVs isolated *ex vivo* and the originating placental tissue from both PE and normal pregnancy.

## 5.3 Aims

The aims of this chapter are to:

1. Characterise the protein cargo of PE and NP using next-generation sequencing technologies.
2. Identify potential biomarkers that may help diagnose and predict the occurrence of PE earlier in pregnancy.
3. Identify critical regulatory protein pathways, mechanisms, and networks in PE.

## 5.4 Methods

The methods used in this chapter have been described in detail in the general methods section. Briefly, medium/large and small syncytiotrophoblast membrane extracellular vesicles were isolated and enriched by *ex vivo* dual lobe perfusion and differential ultracentrifugation. A biopsy sample was also obtained from the corresponding placenta specimen. The samples were sent to the target discovery institute for mass spectrometry, and the generated data was statistically analysed to identify differentially expressed proteins (DEPs) on Perseus. The functions of these DEPs were bioinformatically identified through functional enrichment analysis for gene ontology terms and KEGG pathways.

## 5.5 Results

### 5.5.1 Differentially expressed proteins (DEPs) in placenta homogenate, medium/large STB-EVs and small STB-EVs in Preeclampsia

In total, using mass spectrometry, there were two thousand and twenty-one (2021) proteins identified in the placenta (Figure 38A), one thousand eight hundred and seventy-nine (1879) identified in M/L STB-EVs (Figure 38B) and one thousand eight hundred and eighteen (1818) proteins identified in S STB-EVs (Figure 38C). Of these, fifteen (15) proteins in the placenta, three hundred and four (304) in M/L STB-EVs, and seventy-three (73) in S STB-EVs were differentially expressed between preeclampsia (PE) and normal pregnancy (NP).

In the placenta (Table 15)*, isoform HMG-R of High mobility group protein HMG-I/HMG-Y (HMGA1), Fibrinogen-like protein 1(FGL1), Isoform 1 of Kinesin-like protein KIF2A (KIF2A),* and *Ig kappa chain C region (IGKC)* were the most upregulated proteins based on fold change. Concomitantly, *serum paraoxonase/arylesterase 1 (PON1) and Alpha-1B-glycoprotein (AIBG)* were the only downregulated proteins.

For M/L STB-EVs (Table 15), the most upregulated proteins were the *collagen alpha-1(XVII) chain (COL17A1), isoform 2 of Filamin-B (FLNB),* and *tumour necrosis factor-alpha-induced protein 2 (Fragment) (TNFAIP2)* based on fold change. In contrast, the most downregulated proteins were *sodium-dependent phosphate transporter 1 (SLC20A1), methylthioribose-1-phosphate isomerase (Fragment) (MRI1),* and *prostatic acid phosphatase (Fragment) (ACPP*) based on fold change.

Finally, the S STB-EVs (Table 15) had *solute carrier family 2, facilitated glucose transporter member (SLC2A11), v-type proton ATPase 16 KDa proteolipid subunit (ATP6V0C),* and

*pappalysin 2 (PAPP-A2)* as the most upregulated by fold change while *sodium-dependent phosphate transporter 1 (SLC20A1)* and *isoform 2 of ADP-ribosylation factor GTPase-activating protein (ARFGAP3)* were the most downregulated. There were 25 differentially expressed proteins (DEPs), including *filamin B (FLNB), ERO1-like protein alpha (ERO1A), Endoglin (EGLN), Pappalysin-2 (PAPP-A2), Siglec6 (SIGL6)* shared between M/L STB-EVs and S STB-EVs and only one protein, *isoform 1 of Kinesin-like protein (KIF2A)* shared between the placenta and the M/L STB-EVs. Only one protein *chloride intracellular channel protein 3 (CLIC3)* was found in all three sample types (Table 16).

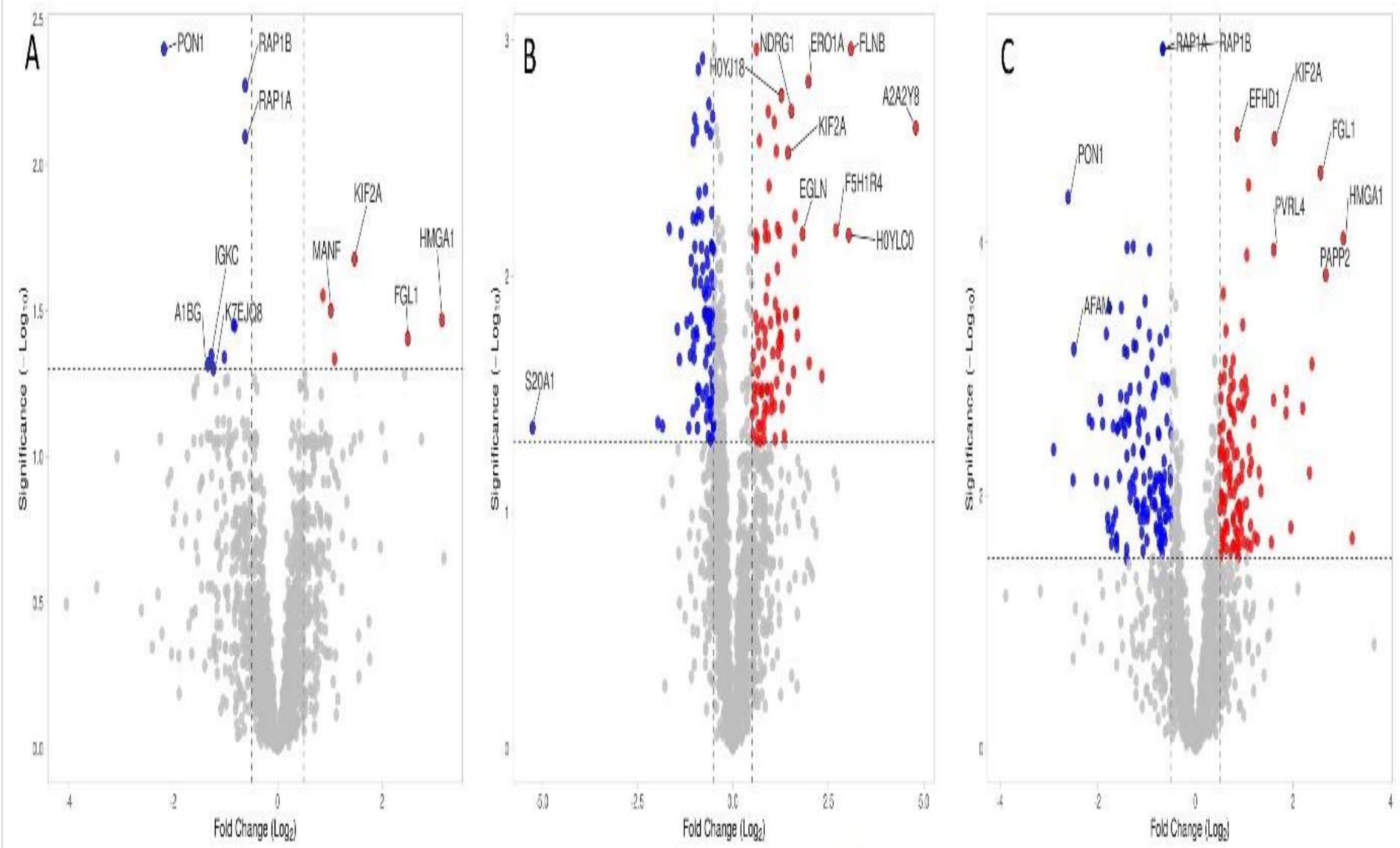



**Figure 39.** Volcano plot differentially expressed proteins in placenta (A), medium/large STB-EVs (B and small STB-EVs (C). Upregulated proteins are marked in red on the upper right quadrant of the plots, while downregulated proteins are displayed in blue on the top left quadrant.

**Table 15.** Top ten differentially expressed proteins in the placenta (red), medium/large STB-EVs (green), small STB-EVs (blue). LFC means log 2 fold change. Add collagen

| Protein | Symbol | LFC | Adjusted P. Value |
|---|---|---|---|
| Placenta | | | |
| Isoform HMG-R of High mobility group protein HMG-I/HMG-Y | HMGA1 | 3.14 | 0.03 |
| Fibrinogen-like protein 1 | FGL1 | 2.49 | 0.04 |
| Isoform 1 of Kinesin-like protein KIF2A | KIF2A | 1.47 | 0.02 |
| Chloride intracellular channel protein 3 | CLIC3 | 1.09 | 0.05 |
| Mesencephalic astrocyte-derived neurotrophic factor | MANF | 1.02 | 0.03 |
| Ig kappa chain V-I region AG | KV101 | -1.02 | 0.05 |
| Haloacid dehalogenase-like hydrolase domain-containing protein 2 (Fragment) | K7EJQ8 | -1.23 | 0.05 |
| Ig kappa chain C region | IGKC | -1.27 | 0.05 |
| Alpha-1B-glycoprotein | A1BG | -1.34 | 0.05 |
| Serum paraoxonase/arylesterase 1 | PON1 | -2.18 | <0.01 |
| Medium/Large STB-EVs | | | |
| Collagen alpha-1(XVII) chain | COL17A1 | 4.79 | <0.01 |
| Isoform 2 of Filamin B | FLNB | 3.09 | <0.01 |
| Tumor necrosis factor apha-inducible protein | TNFAIP2 | 3.03 | <0.01 |
| Minor histocompatibility antigen | HMHA1 | 1.59 | 0.03 |
| Bridging integrator 2 | BIN2 | 2.33 | 0.02 |
| Sodium/potassium-transporting ATPase subunit beta-1 | ATP1B | 1.99 | 0.02 |
| ERO-1 like protein alpha | ERO1L | 1.97 | <0.01 |
| Endoglin | ENG | 1.82 | <0.01 |
| Methylthioribose-1-phosphate isomerase (Fragment) | MRI1 | -1.96 | 0.04 |

| | | | |
|---|---|---|---|
| Sodium-dependent phosphate transporter 1 | S20A1/SLC17A1 | -5.24 | 0.04 |
| Small STB-EVs | | | |
| Solute carrier family 2, facilitated glucose transporter member 11 | SLC2A11 | 8.91 | 0.01 |
| V-type proton ATPase 16 kDa proteolipid subunit | VATL | 7.25 | 0.02 |
| Pappalysin-2 | PAPP2 | 3.76 | 0.02 |
| ERO1-like protein alpha | ERO1A | 3.29 | 0.02 |
| Isoform 2 of Creatine kinase U-type, mitochondrial | KCRU | 3.20 | 0.02 |
| SCARB1 protein | B7ZKQ9 | 2.95 | 0.05 |
| Isoform 2 of Filamin-B | FLNB | 2.92 | 0.02 |
| Solute carrier organic anion transporter family member 2A1 | SO2A1 | 2.86 | 0.02 |
| Isoform 2 of Oligaccharyltransferase complex subunit TC | OSTC | 2.82 | 0.02 |
| SCY1-like protein 2 | SCYL2 | 2.71 | 0.02 |
| Sodium-dependent phosphate transporter 1 | S20A1 | -2.93 | 0.01 |

### 5.5.2 Validation of select proteins in the placenta homogenate, medium/large STB-EVs, and small STB-EVs

I combined all the DEPs identified from the placenta, M/L STB-EVs, and S STB-EVs and selected proteins to validate based on fold change or/and our placenta specificity or enrichment criteria as previously described (see methods). These were pappalysin 2 (*PAPP-A2), collagen 17A1 (COL17A1), filamin B (FLNB),* and *scavenger receptor class B type I (SR-BI/ SCARB1).* Validation was performed by Western blot on all sample types.

In the placenta (Figure 36A and D), *PAPP-A2* (FC =6.39, P Value = 0.0001) and *SR-BI* (FC = 1.72, P Value = 0.04) were all significantly upregulated. *Filamin B* (FC = 2.59, P Value = 0.12)

was upregulated but not significant while *COL17A1* was undetectable. In medium/large STB-EVs (Figure 36B and E), *PAPP-A2* (FC =5.09, P Value = 0.004), *COL17A* (FC =71.21, P Value = 0.002), *FLNB* (FC =7.60, P Value = 0.014) and *SR-BI/SCARB1* (FC =2.28, P Value = 0.018) were all significantly upregulated in PE compared to normal. In S STB-EVs (Figure 36C and F), only *FLNB* (FC =7.73, P Value = 0.003) and *SR-BI/SCARB1* (FC =1.60, P Value = 0.002) were significantly upregulated while *COL17A1*(FC =12.79, P Value = 0.07) and *PAPP-A2* (FC =1.48, P Value = 0.11) were upregulated but not significantly so. None of the four biomarkers validated by Western blot in this study have been previously described to be differentially expressed in PE STB-EVs compared to normal.

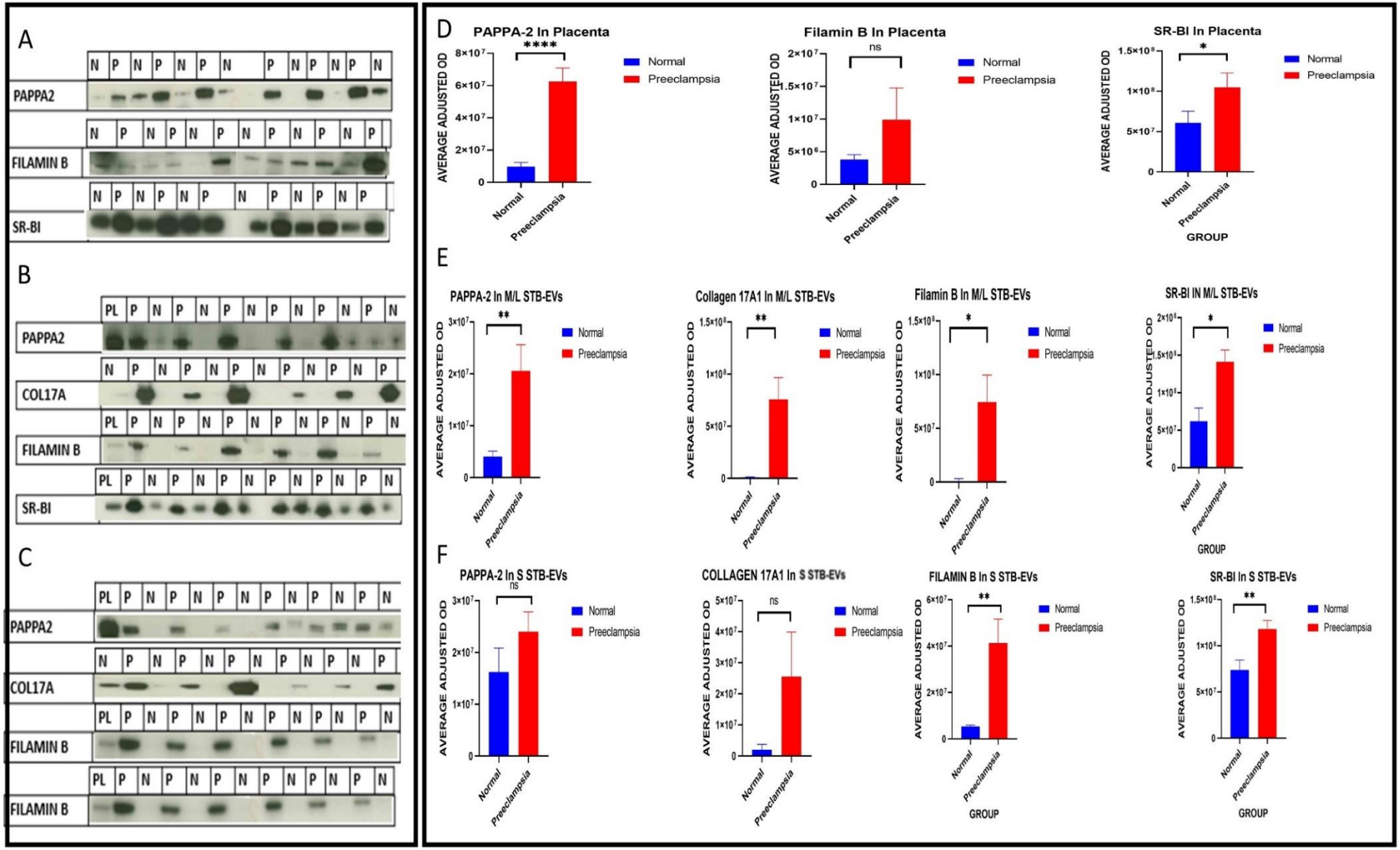



**Figure 40**. Figure showing the results of Western blot and densitometric verification of PAPP-A2, COL17A1, FLNB and SR-BI in the placenta (A and D) M/L STB-EVs (B and E) and S STB-EVs (C and F). Collagen 17A1 did not show up in the placenta homogenate. * means < 0.05, ** means < 0.01, *** means < 0.001, **** means less than 0.001 and ns means non-significant. None of the four biomarkers validated by Western blot in this study have been previously described to be differentially expressed in preeclampsia STB-EVs

### 5.5.3 Functional enrichment of differentially expressed proteins (DEPs) in Preeclampsia

I performed a functional enrichment analysis (with overrepresentation analysis-(ORA)) on the list of differentially expressed proteins for placenta tissue (Figure 37A), medium/large STB-EVs (Figure 37B), and small STB-EVs (Figure 37C) to help better understand their role in preeclampsia (PE). All three sample types (Figures 37B, 37C, and 37D) did not have overlapping gene ontology terms or KEGG pathways. The top biological processes overrepresented in the placenta (Table 17) are essential in *neurotransmitter secretion and transport*. In comparison, the enriched biological processes in the M/L STB-EVs are (Table 17) have a role in *responses to hypoxia*. Finally, *posttranslational protein modification processes* were enriched among small STB-EVs (Table 17) and contained all upregulated proteins. The KEGG pathways, *neurotrophin signalling pathway, spinocerebellar ataxia, Spinocerebellar ataxia, protein processing in endoplasmic reticulum* and *protein processing pathway* were enriched in the placenta, M/L STB-EVs and S STB-EVs (Table 18).

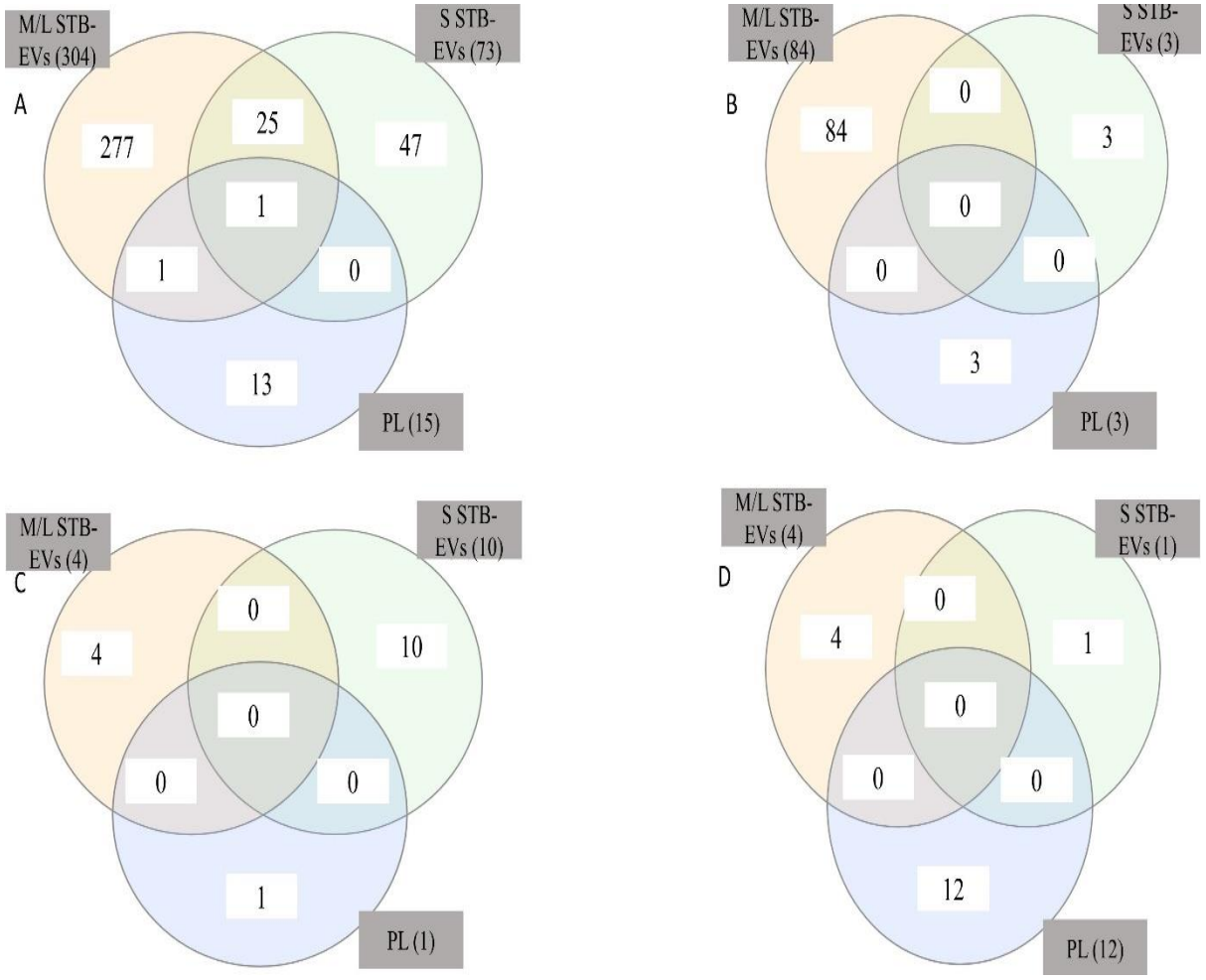



**Figure 41.** Figure showing results of a combined Venn plot showing overlapping DEPs (A), biological processes (B), cellular components (C), and KEGG pathways (D) between the placenta, medium/large STB-EVs and small STB-EVs. The overlapping DEPs are listed in table 17

**Table 16.** List of overlapping differentially expressed proteins in the placenta, medium/large STB-EVs and small STB-EVs

| Sample types | Differentially expressed proteins (DEPs) |
|---|---|
| M/L STB-EVs and PLACENTA | Kinesin-like protein |
| M/L STB-EVs, S STB-EVs and PLACENTA | Chloride intracellular channel protein 3 |
| M/L STB-EVs and S STB-EVs | Filamin B |
| | Endoplasmic Reticulum Oxidoreductase Alpha |
| | X-linked retinitis pigmentosa GTPase regulator interacting protein 1 |
| | Protein NDRG1 |
| | Collagen alpha 1(XVII) chain |
| | Monocyte differentiation antigen CD14 |
| | Trophoblast glycoprotein |
| | Heat shock-related 70 kDa protein 2 |
| | Endoglin |
| | Hippocalcin-like protein 1 |
| | SCARB1 protein |
| | Importin subunit alpha 7 |
| | Protein BCAP |
| | Endothelial protein C receptor |
| | Caveolin |
| | Pappalysin-2 |
| | Phosphatidylinositol 3-kinase regulatory subunit alpha |
| | Keratin, type I cytoskeletal 19 |
| | Siglec6 |
| | Protein disulfide-isomerase |
| | Amine oxidase [flavin-containing] A |
| | Copine-3 |
| | Dolichyl-diphosphooligosaccharide |
| | Sodium-dependent phosphate transporter 1 |
| | Annexin A4 |

**Table 17**. List of Top 3 functionally enriched gene ontology: biological process (GO: BP) in the placenta (red), medium/large STB-EVs (green), small STB-EVs(blue).

| Biological Process (BP) | Adjusted P Values | No of Proteins in BP terms | No of DEP queried | No of DEP found in BP terms |
|---|---|---|---|---|
| Negative regulation of neurotransmitter secretion | 0.02 | 2 | 14 | 2 |
| Negative regulation of synaptic vesicle exocytosis | 0.02 | 2 | 14 | 2 |
| Negative regulation of neurotransmitter transport | 0.05 | 3 | 14 | 2 |
| Response to decreased oxygen levels | 0.00 | 84 | 293 | 30 |
| Cellular response to decreased oxygen levels | 0.00 | 59 | 293 | 24 |
| Cellular ketone metabolic process | 0.00 | 65 | 293 | 26 |
| Peptidyl-asparagine modification | 0.02 | 10 | 73 | 5 |
| Protein N-linked glycosylation via asparagine | 0.02 | 10 | 73 | 5 |
| Protein N-linked glycosylation | 0.02 | 16 | 73 | 6 |

**Table 18.** List of Top 3 functionally enriched KEGG pathways in the placenta (red), medium/large STB-EVs (green) and small STB-EVs (only 1 KEGG-blue).

| KEGG Pathways (KP) | Adjusted P Values | No of Proteins in KP terms | No of DEP queried | No of DEP found in KP terms |
|---|---|---|---|---|
| Neurotrophin signalling pathway | 0.00 | 13 | 14 | 3 |
| Long-term potentiation | 0.01 | 6 | 14 | 2 |
| Renal cell carcinoma | 0.02 | 11 | 14 | 2 |
| Proteasome | 0.00 | 35 | 293 | 17 |
| Spinocerebellar ataxia | 0.00 | 48 | 293 | 21 |
| Alzheimer disease | 0.01 | 94 | 293 | 29 |
| Protein processing in endoplasmic reticulum | 0.02 | 60 | 73 | 10 |

### 5.5.4 Correlation between mRNA (transcriptomics) and protein (proteomics) datasets in the placenta, M/L STB-EVs, and S STB-EVs

I explored the correlation between our proteomics data and transcriptomics data. Only one thousand seven hundred and sixty-five (1765) proteins out of two thousand and twenty-one (2021) were similarly detectable in the transcriptomics data for the placenta tissue. Likewise, thirteen (13) of the fifteen (15) found to be significantly differentially expressed in the proteomics data were also found in the transcriptomic data. Finally, three of the fifteen significantly differentially expressed proteins; *chloride Intracellular Channel 3 (CLIC3), EF-hand domain family member D1 (EFHD)1, and* kinesin *family member 2A (KIF2A)*, were also significantly differentially expressed in the transcriptomic data. In general, there was a poor correlation between the proteomics and transcriptomics in the placenta, R= 0.16, p= 2.3 e-11 (among all detected proteins and RNA [Figure 38A]) and R= 0.31, p= 0.3 (between significantly DEPs and all detected RNA [Figure 38D])

In the M/L STB-EVs proteomics data, one thousand six hundred and forty-nine (1649) proteins out of one thousand eight hundred and seventy-nine (1879) were also present in the transcriptomics data, including two hundred and seventy-four (274) out of three hundred and four (304) significant DEPS. Also, eighty-four (84) of the significant proteins were also found to be significantly differentially expressed in the transcriptomic data. Compared, to the placenta tissue data, the correlation between the transcriptomics data was stronger in the M/L STB-EVs R= 0.45, p= 2.2 e-16 (correlation between all detected proteins and RNA [Figure 38B]) and R= 0.37, p= < 2.2 e-16, (correlation between significantly differentially expressed proteins and whole transcriptomics [Figure 38E]).

In the S STB-EVs, one thousand five hundred and ninety-six (1596) proteins of one thousand eight hundred and eighteen (1818) were detectable in the transcriptomics data, and sixty-seven (67) of the significant proteins were also found in our transcriptomic data. In addition, only twenty (20) of the DEPs were also significantly differentially expressed in the transcriptomic data. The correlation between both data was also low, R= 0.27, p= <2.2 e-16 (correlation between the proteomic and transcriptomic data [Figure 38C]) and R= 0.37, p= < 2.2 e-16 (correlation between significantly DEPs and whole transcriptomics [Figure 38F]).

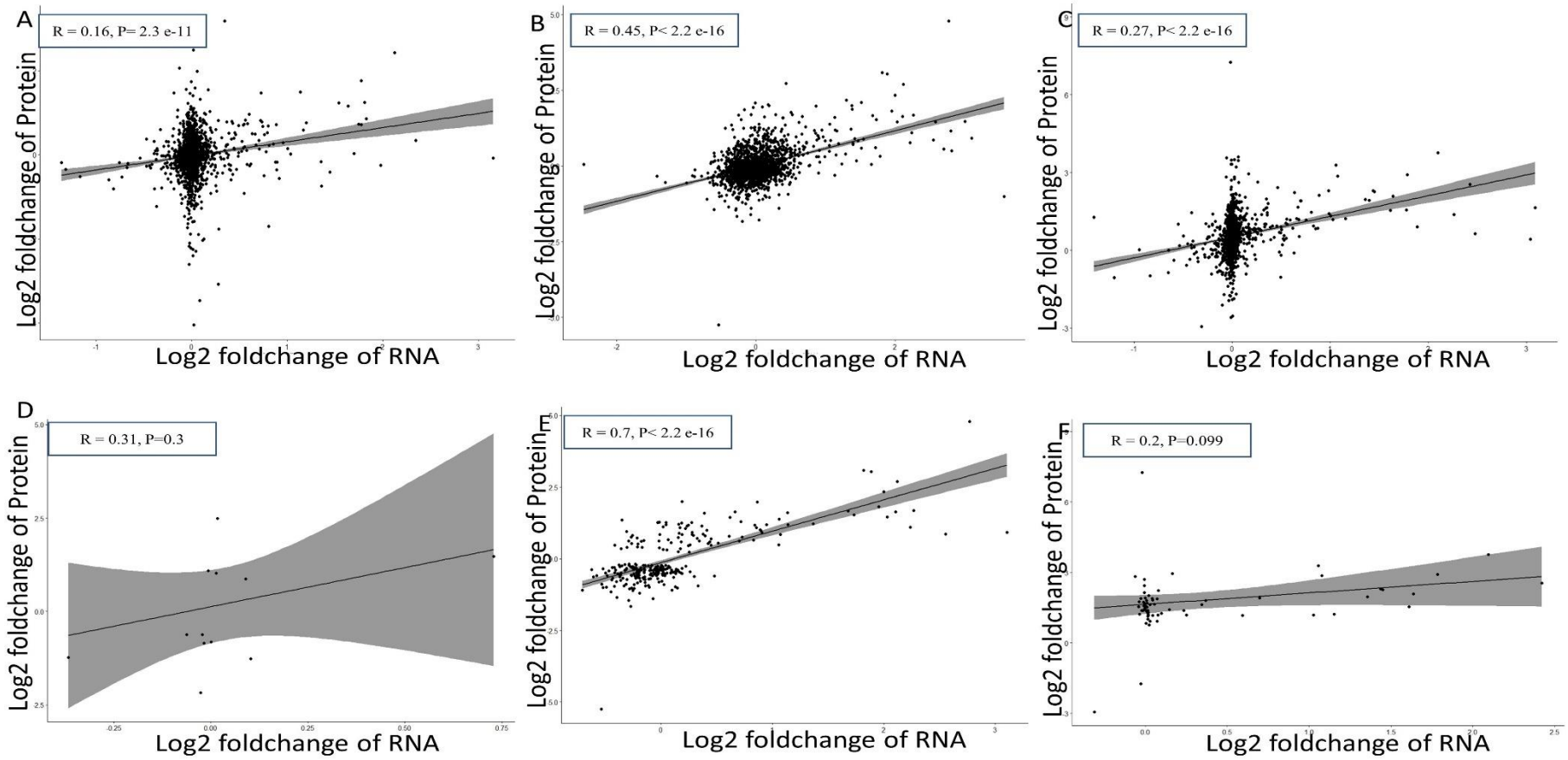



**Figure 41.** Figure showing the correlation between the transcriptomic and proteomics data in the placenta (A and D), medium/large STB-EVs (B and E) and small STB-EVs (C and F). Figure A (significant) represents correlation between all transcripts and proteins in the placenta while figure D (not significant) represents the correlation between differentially expressed proteins and transcripts. Figure B (significant) represents correlation between all transcripts and proteins in the medium/large STB-EVs while figure E (significant) represents the correlation between differentially expressed proteins and transcripts. Figure C (significant) represents correlation between all transcripts and proteins in the small STB-EVs while figure F (not significant) represents the correlation between differentially expressed proteins and transcripts.

## 5.6 Discussion

PE is a pregnancy-specific hypertensive disease that confers severe clinical and economic consequences for both the mother and child[285,286]. However, no biochemical test can reliably predict the development of PE. The use of pro and anti-angiogenic molecules such as placenta growth factor (PLGF), vascular endothelial growth factor (VEGF), soluble endoglin (sENG), and soluble FMS like tyrosine kinase (sFLT-1) as biomarkers of PE have some important limitations. Primarily they have a poor to moderate positive predictive value, and their use is limited to high-risk groups or those with clinically suspected preeclampsia. Interestingly, some of these pro and antiangiogenic markers, tissue factor[287], soluble FLT-1[288], endoglin[289] and neprilysin[290], are expressed on STB-EVs and in higher proportions in PE. I performed a comprehensive proteomic profile to identify potential candidate EV-based biomarkers that were more placental in origin and thus which might have more disease specificity. In addition, we also bioinformatically identified possible mechanistic pathways in preeclampsia.

To my knowledge, this study is the first study to perform proteomics characterisation on all three components simultaneously, including medium/large STB-EVs, small STB-EVs, and placenta tissue from NP and PE. In this study, I found that 304 DEPs, 73 DEPs and 15 DEPs were identified respectively in medium/large STB-EVs, small STB-EVs and placenta tissue from PE compared with normal controls. My analysis found chloride intracellular channel 3 (CLIC3) to be the only differentially expressed (upregulated) protein among all sample types. CLIC3 is expressed in the placenta throughout pregnancy[291] and is upregulated in PE placentas compared to NP, a finding corroborated by our results. However, it has not previously been described in terms of STB-EVs. CLIC3 belongs to the CLIC family and exists in both soluble (enzymatic) and integral forms (ion channel). CLIC3 also recycles activated integrins back to

the plasma membrane and facilitates cell migration and invasion[292], a process that has been identified as abnormal in PE[293].

I pooled the list of differentially expressed proteins from the placenta, M/L STB-EVs, and S STB-EVs. I identified five biomarkers to validate based on fold change *COL17A1*, *Filamin B, scavenger receptor class B type I (SR-BI/ SCARB1)* or/and placenta specificity and enrichment (*PAPP-A2)*. *COL17A1* was differentially expressed in both S STB-EVs and M/L STB-EVs but not detectable in the placenta in both normal and PE. The alpha chain of collagen XVII (COL17A1) is encoded by the *COL17A1* gene, comprising 56 distinct exons. Mutations in the alpha chain have been implicated in non-Herlitz junctional epidermolysis bullosa[294]. Although COL17A1 has not been described in preeclampsia, a protein of the same family, collagen 1, is deposited in higher amounts in the PE placenta and can induce preeclampsia-like symptoms by suppressing the proliferation and invasion of trophoblasts. This suppression was reversible by treating with ERK and B-catenin agonists[295]. Vesicular *COL17A1* has been detected in epithelial cells, prostate cancer cells, serum, urine, and squamous carcinoma cells. However, this thesis is the first to describe the expression and differential expression of *COL17A1* on STB-EVs in PE[296–300].

Likewise, *PAPP-A2* was differentially expressed in both S STB-EVs and M/L STB-EVs. PAPP-A2 cleaves insulin-like growth factor binding protein (IGFBP-5 and, to a lesser extent, IGFBP-3). PAPP-A2's mRNA and protein are differentially expressed in the placenta and maternal serum in PE patients[301–305]. PAPP-A2 has been detected in mesenchymal stem cells, prostatic secretions EVs, serum, and urine exosomes but has not previously been reported in STB-EVs[306].

Filamin B participates in cellular structural mechanics and signals transduction by interacting with ion channels, signalling molecules, transmembrane proteins, and transcription factors[307–

[309]. It also suppresses tumour growth and metastasis[310]. Interestingly, Wei et al. described filamin B as being upregulated [247] in the placenta in contrast to our study. Wei et al. used glyceraldehyde 3-phosphate dehydrogenase (GAPDH) as an internal reference, while I used total protein normalisation to amido black to quantify and compare protein expression. GAPDH is an unreliable internal reference protein, particularly in preeclampsia309,310, which may explain these discordant findings. In addition, I found GAPDH among the most differentially expressed proteins and mRNA in the transcriptomics and proteomics data.

Scavenger receptor class B, type 1 (SCARB1/SR-BI), is most abundant in the adrenal glands, placenta, liver, and brain[313–316]. It is expressed in trophoblasts and placenta endothelium in the placenta, and its levels increase during gestation[317]. It facilitates the uptake of cholesteryl esters from high-density lipoproteins and lipid-soluble vitamins and transthyretin-bound thyroid hormone by placental trophoblast cells[317]. While SR-BI has not been described in preeclampsia, transthyretin has been proposed to have a role in preeclampsia[318,319]. SR-BI was differentially expressed in both M/L STB-EVs and S STB-EVs in this study.

Regarding potential mechanisms of preeclampsia, I found no overlap in the biological processes and KEGG pathways among the three sample types. In the placenta, gene ontology biological processes (GO: BP) involved in *neurotransmitter secretion and transport* were overrepresented, while *platelet activation, MAPK,* and *Rap 1 signalling* pathways were among the detected KEGG pathways. In M/L STB-EVs, *protein modification* and *decreased oxygen level responses* were among the perturbed GO: BP terms. *Alzheimer's* and *Prion disease* were among the identified KEGG pathways. In S STB-EVs, *post-translational modification processes* and *endoplasmic reticulum protein processing* were the principal GO: BP terms and KEGG pathways. Some of these processes and KEGG pathways have been previously described in preeclampsia, while others found in this study are new and warrant further research[320–326].

In conclusion, I have identified new STB-EV bound protein biomarkers significantly differentially expressed in PE compared to normal. These biomarkers are placenta expression enhanced or enriched. The fact that STB-EVs are present in the circulation from early pregnancy through to term and coupled with the knowledge that STB-EV release is enhanced in PE may support further investigation of these proteins as potential biomarkers. In addition, I have explored potential mechanistic pathways that may help decipher some of the mechanisms of PE.

# CHAPTER 6

## RESULTS OF PROTEIN-PROTEIN, GENE-GENE INTERACTION AND CONNECTIVITY MAP (CMap) ANALYSIS OF STB-EVs IN PREECLAMPSIA

## 6.1 Abstract

**Background:** In this chapter, I hypothesised that the PE specific messenger RNA and protein signature of placental tissue and STB-EVs could be interrogated to discover potential molecular subtypes and therapeutic agents.

**Methods:** I created protein-protein interaction (PPI) and gene-gene interaction (GGI) networks from the differentially expressed proteins and messenger RNA from placental tissue, medium/large and small STB-EVs isolated from PE and NP placentae using *ex vivo* dual lobe perfusion. I bioinformatically analysed these PPI and GGI networks (with STRING) to 1) identify critical genes, proteins, and pathways (with Cytohubba and ClueGO), and 2) tease out molecular subtypes and characterise their functions (with MCODE, ClueGO and Cytoscape). Finally, I identified a list of drugs and small molecules that may be repurposed as therapeutic agents in PE using Connectivity Map analysis.

**Results:** I bioinformatically identified critical genes and proteins (glyceraldehyde *3-phosphate dehydrogenase* [*GAPDH], leptin, fibronectin 1, albumin*) and critical pathways (*peptidyl amino acid modification, carbohydrate derivative metabolic process, low oxygen relation process*). I also identified molecular subtypes and potential therapeutic agents (*valdecoxib, bumetanide, ceforanide, arachidonic acid, melatonin*)

**Conclusions:** I identified critical genes, proteins, and pathways involved in preeclampsia and therapeutic agents that may be important in the pathophysiology of PE.

## 6.2 Introduction

Several theories and mechanisms have been proposed to explain PE pathogenesis, summarised in the introduction (chapter 1). Irrespective of the abundance of the theories, the placenta is central to the pathogenesis of preeclampsia. Therapeutically, the only effective treatment for PE is delivery of the placenta[327]. Magnesium sulphate is used to prevent seizures (eclampsia)[328] and facilitate foetal neurodevelopment in preeclamptic patients. In contrast, antihypertensive medications manage blood pressure and the risk of associated complications. The most promising preventive agent in preeclampsia is aspirin, a repurposed drug and I have described other therapeutic and preventive agents in chapter 1.

In this chapter, I have 1) characterised the protein-protein interaction networks of the differentially expressed proteins in the placenta, M/L STB-EVs and S STB-EVs, 2) characterised the gene-gene interaction networks of the differentially expressed genes in the placenta, M/L STB-EVs and S STB-EVs 3) interrogated both networks to identify common themes and 4) used these bioinformatic data to identify candidate therapeutic molecules in preeclampsia.

## 6.3 Aims

The aims of this chapter are to:

1. Construct protein-protein and gene-gene interaction networks using differentially expressed proteins (DEPs) and differentially expressed genes (DEGs).
2. Identify critical proteins, genes and pathways that may explain the mechanisms of preeclampsia.
3. Identify potential therapeutic agents in PE using PE specific molecular signatures from DEPs and DEGs.
4. Integrate PPI and GGI data from the placenta, M/L STB-EVs and S STB-EVs to identify the critical proteins, genes, pathways, and therapeutic agents in PE.

## 6.4 Methods

The methods used in this chapter have been described in detail in the general methods section. Briefly, a protein-protein and gene-gene interaction network were constructed from messenger RNA transcriptomic (Chapter 3) and proteomic (Chapter 5) data with STRING on Cytoscape. Critical genes, proteins and pathway analysis were performed with ClueGO and Cytohubba on Cytoscape. Potential therapeutic agents were identified through Connectivity Map (CMap) analysis.

## 6.5 Results

### 6.5.1 Identification of critical/hub genes and pathways in preeclampsia (from the transcriptomic and proteomic dataset)

I analysed the DEGs and DEPs in the placenta, M/L STB-EVs and S STB-EVs with 11 different clustering methods earlier discussed in the methods section. In the transcriptomic GGI, the hub genes in the placenta were involved in 46 molecular functions, 872 biological processes, 32 cellular components and 66 KEGG pathways. In contrast, in the M/L STB-EVs, the genes are involved in 49 molecular functions, 1004 biological processes, 29 cellular components and 5 KEGG pathways. In the S STB-EVs, there were 54 molecular function pathways, 489 biological processes, 21 cellular components and 6 KEGG pathways connected to the identified hub genes. Figure 42 (A, B and C) shows the hub genes in the placenta, M/L STB-EVs and S STB-EVs.

I performed a similar analysis on the differentially expressed proteins. I excluded the placenta from the hub/critical proteins analysis due to the small quantity of DEPs. Figure 42 (D and E) shows the top ten hub proteins. I assessed the functions of these hub proteins bioinformatically. In the M/L STB-EVs, the proteins were involved in 2 molecular functions, 176 biological processes, 5 cellular components and 7 KEGG pathways. At the same time, in the S STB-EVs, there were 10 molecular function pathways, 12 biological processes, 11 cellular components and 4 KEGG pathways. There were no biological functions overlapping between the STB-EV subtypes.

My analysis identified GAPDH as a hub gene/protein in the placenta (transcriptomics), M/L STB-EVs (transcriptomics), S STB-EVs (transcriptomics) and M/L STB-EVs (proteomics). Leptin (LEP) and fibronectin 1 (FN1) were identified as critical in placenta (transcriptomics),

M/L STB-EVs (transcriptomics), and S STB-EVs (transcriptomics). Finally, albumin was a critical gene/protein in M/L STB-EVs (transcriptomics) and M/L STB-EVs (proteomics).

I then integrated the critical pathways from the transcriptomics and proteomics datasets to help identify pathways common to both datasets. In terms *of biological processes, peptidyl amino acid modification* was common to S STB-EVs (proteomics), M/L STB-EVs (transcriptomics) and S STB-EVs (transcriptomics). In contrast, *carbohydrate derivative metabolic process* was common to S STB-EVs (transcriptomics) and S STB-EVs (transcriptomics). I also found the biological processes involved *in low oxygen-related processes, nitrogen compound and primary metabolic process, and MAPK cascade* in S STB-EVs (proteomics), M/L STB-EVs (transcriptomics) and S STB-EVs (transcriptomics). The *endomembrane system* was a GO: CC term common to S STB-EVs (proteomics), M/L STB-EVs (transcriptomics) and S STB-EVs (transcriptomics). Table 19 lists the overlapping critical/hub GO terms and KEGG pathways.

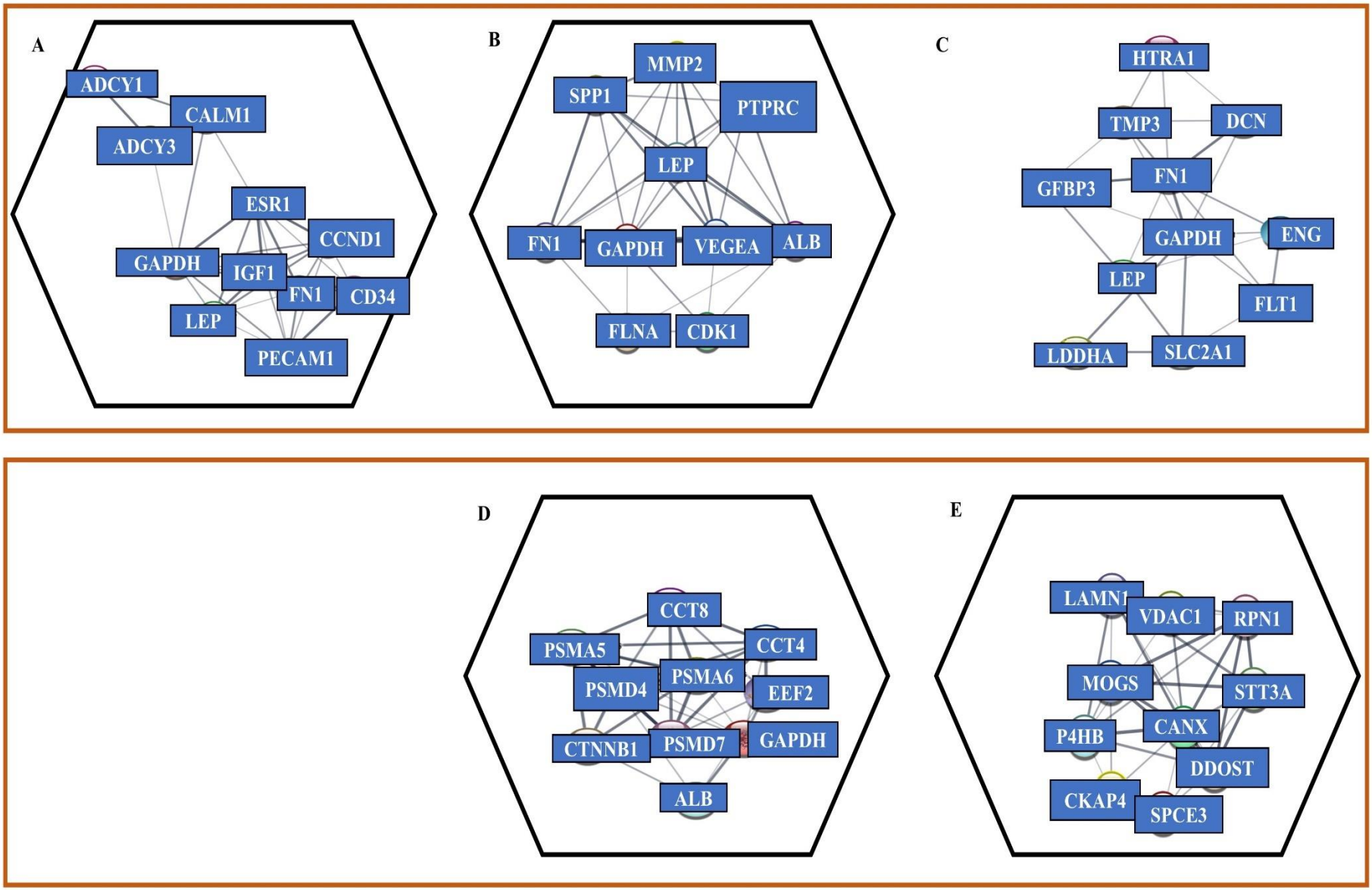



**Figure 42**. Figure showing the identified critical genes and proteins in A) placenta (Transcriptomics), B) M/L STB-EVs (Transcriptomics), C) S STB-EVs (transcriptomics), D) M/L STB-EVs (Proteomics) and S STB-EVs (Proteomics)

**Table 19.** Table showing the overlapping critical/hub Gene Ontology terms (Biological Process, Molecular Function and Cellular Components) and KEGG Pathways from the proteomics and transcriptomic analysis.

| Transcriptomics | Proteomics | Biological Processes (BP) |
|---|---|---|
| M/L STB-EVs, S STB-EVs | S STB-EVs | Peptidyl-amino acid modification |
| S STB-EVs | S STB EVs | Carbohydrate derivative metabolic process |
| | | Response to hypoxia |
| | | Response to decreased oxygen levels |
| | | Regulation of nitrogen compound metabolic process |
| | | Regulation of primary metabolic process |
| | | Response to oxygen levels |
| | | MAPK cascade |
| | | Regulation of macromolecule biosynthetic process |
| | | Regulation of cellular macromolecule biosynthetic process |
| | | Stem cell differentiation |
| | | Regulation of cellular biosynthetic process |
| | | Regulation of biosynthetic process |
| | | Hematopoietic or lymphoid organ development |
| | | Hemopoiesis |
| M/L STB-EVs, S STB-EVs | | Immune system development |
| M/L STB-EVs | | Post-translational protein modification |
| | | Cellular response to stress |
| M/L STB-EVs, S STB-EVs | M/L STB-EVs | Regulation of biological quality |
| | | Positive regulation of DNA metabolic process |
| | | Anatomical structure homeostasis |
| M/L STB-EVs, S STB-EVs | M/L STB-EVs | Cellular macromolecule metabolic process |
| | | Tissue development |
| M/L STB-EVs, S STB-EVs | M/L STB-EVs | Fibronectin binding |
| Transcriptomics | Proteomics | Molecular Function (MF) |
| | | Disordered domain specific binding |
| | | Glycosaminoglycan binding |
| | | Molecular function regulator |
| | | Peptidyl-cysteine S-nitrosylase activity |
| M/L STB-EVs, S STB-EVs | | Glyceraldehyde-3-phosphate dehydrogenase (NAD(P)+) (phosphorylating) activity |

| | | |
|---|---|---|
| | | Glyceraldehyde-3-phosphate dehydrogenase (NAD+) (phosphorylating) activity |
| | | Leptin receptor binding |
| | | Identical protein binding |
| | | Aspartic-type endopeptidase inhibitor activity |
| | | Peptidase regulator activity |
| | | peptide hormone receptor binding |
| M/L STB-EVs, S STB-EVs | M/L STB-EVs | Transferase activity |
| | | Transferring nitrogenous groups |
| Transcriptomics | Proteomics | Cellular Component (CC) |
| M/L STB-EVs, S STB-EVs | S STB-EVs | Endomembrane system |
| | | Extracellular space |
| | | Extracellular vesicle |
| | | GAIT complex |
| | | Extracellular exosome |
| | | Blood microparticle |
| | | Extracellular matrix |
| | | Vesicle |
| | | Extracellular organelle |
| | | Extracellular region |
| M/L STB-EVs, S STB-EVs | | Fibrinogen complex |
| Transcriptomics | Proteomics | KEGG Pathways |
| M/L STB-EVs, S STB-EVs | | Proteoglycans in Cancer |

### 6.5.2 Cluster analysis of preeclamptic transcriptomic gene-gene interaction network (PPI) in the placenta tissue, medium/large and small STB-EVs

In the placenta, cluster analysis recognized twenty-one clusters, but I focused on the top three clusters with the highest scores. Cluster one (Figure 43) had twenty genes and a clustering (mcode) score of twenty, cluster two (Figure 44) had twelve genes, and a mcode score of twelve, cluster three (Figure 45) had thirty-nine genes and a mcode score of 9.79. The genes in cluster one have roles in *signalling pathways and processes*. The genes in cluster two are involved in *blood pressure regulation and maintenance.* Cluster three is involved in endothelial cell proliferation, negative regulation of *inflammatory responses and oxygen regulating signalling processes*.

Likewise, I deconvoluted the M/L STB-EV GGI network and identified the three highest-scoring clusters. The first cluster had thirty-one genes with a mcode score of 14.93. The second cluster had fifteen genes with a score of 14.14, and the third cluster had eleven genes with a score of 11. The top three clusters are depicted in figures 46A, B and C. My functional enrichment analysis did not identify any functionally enriched terms associated with these clusters. Only three clusters were identified in small STB-EVs with three genes and a mcode score of 3 (Figure 47A, B and C). My analysis did not identify any enriched overrepresented functions, and no gene ontology terms or KEGG pathways were identified as overrepresented.

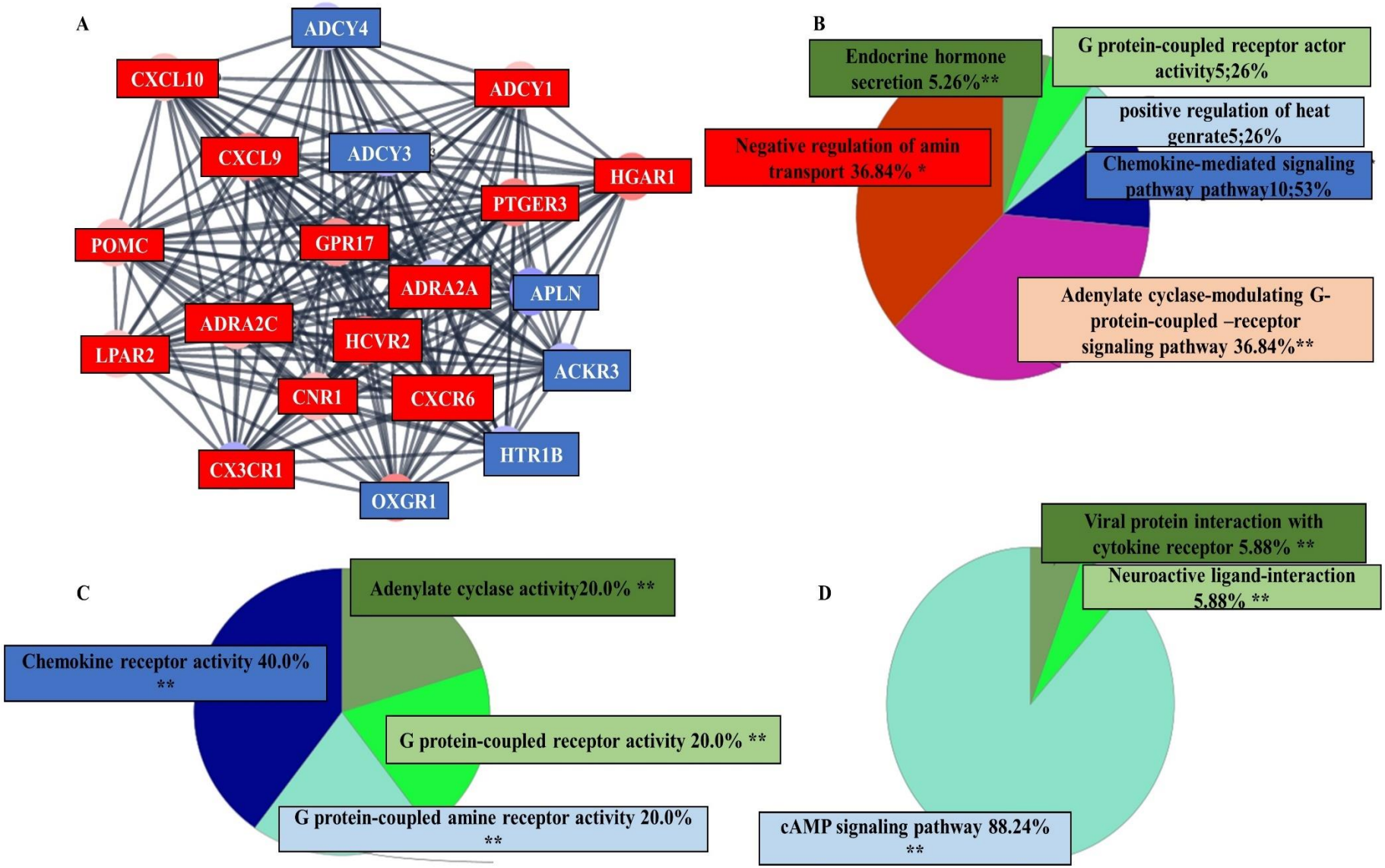



**Figure 43**. Figure showing A) cluster 1 from the placenta gene-gene interaction network analysis and associated B) Gene Ontology: Biological Process, C) Gene Ontology: Molecular Functions, and D) KEGG Pathways

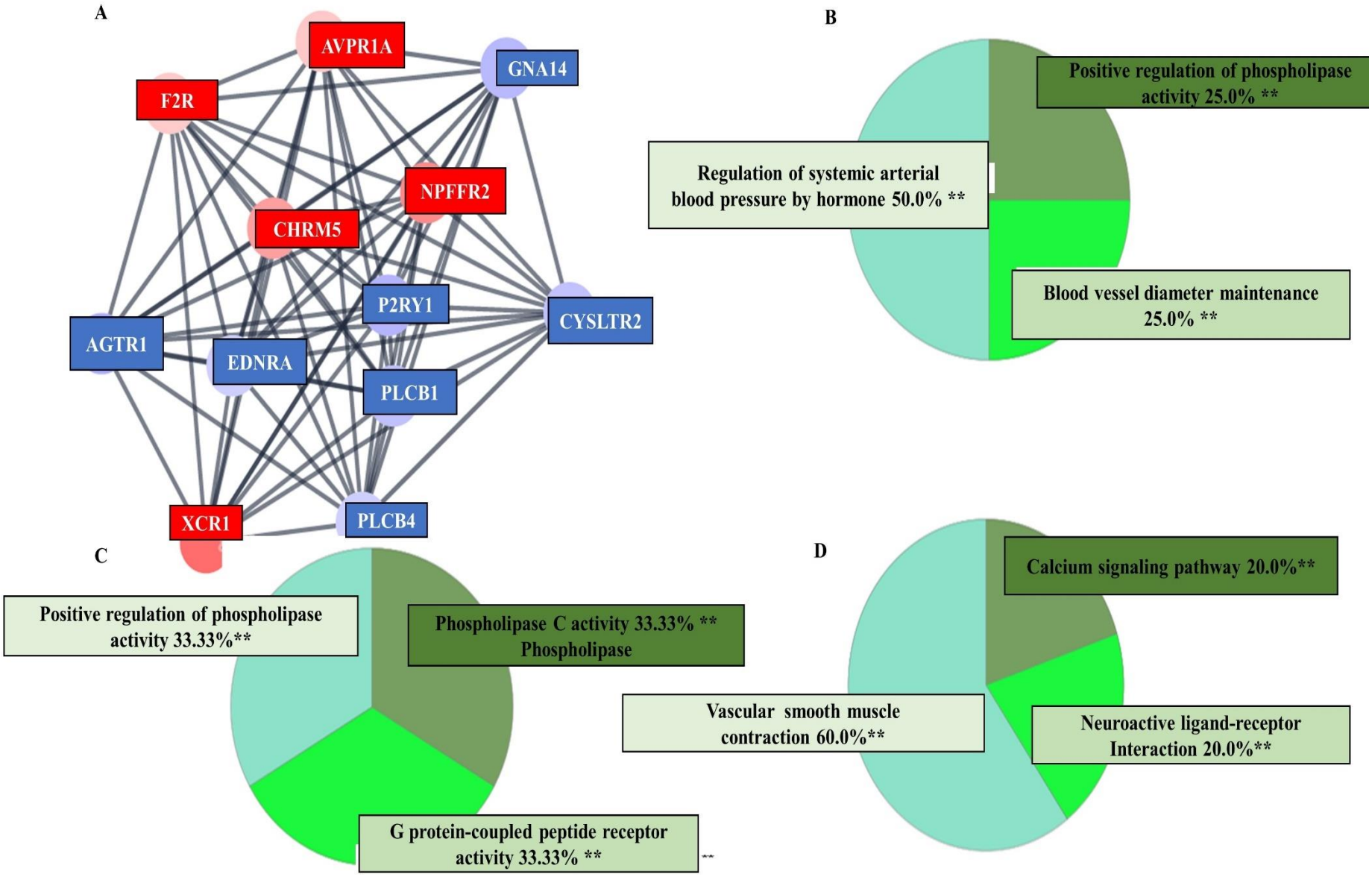



**Figure 44**. Figure showing A) cluster 2 from the M/L STB-EVs gene-gene interaction network analysis and associated B) Gene Ontology: Biological Process, C) Gene Ontology: Molecular Functions, and D) KEGG Pathways

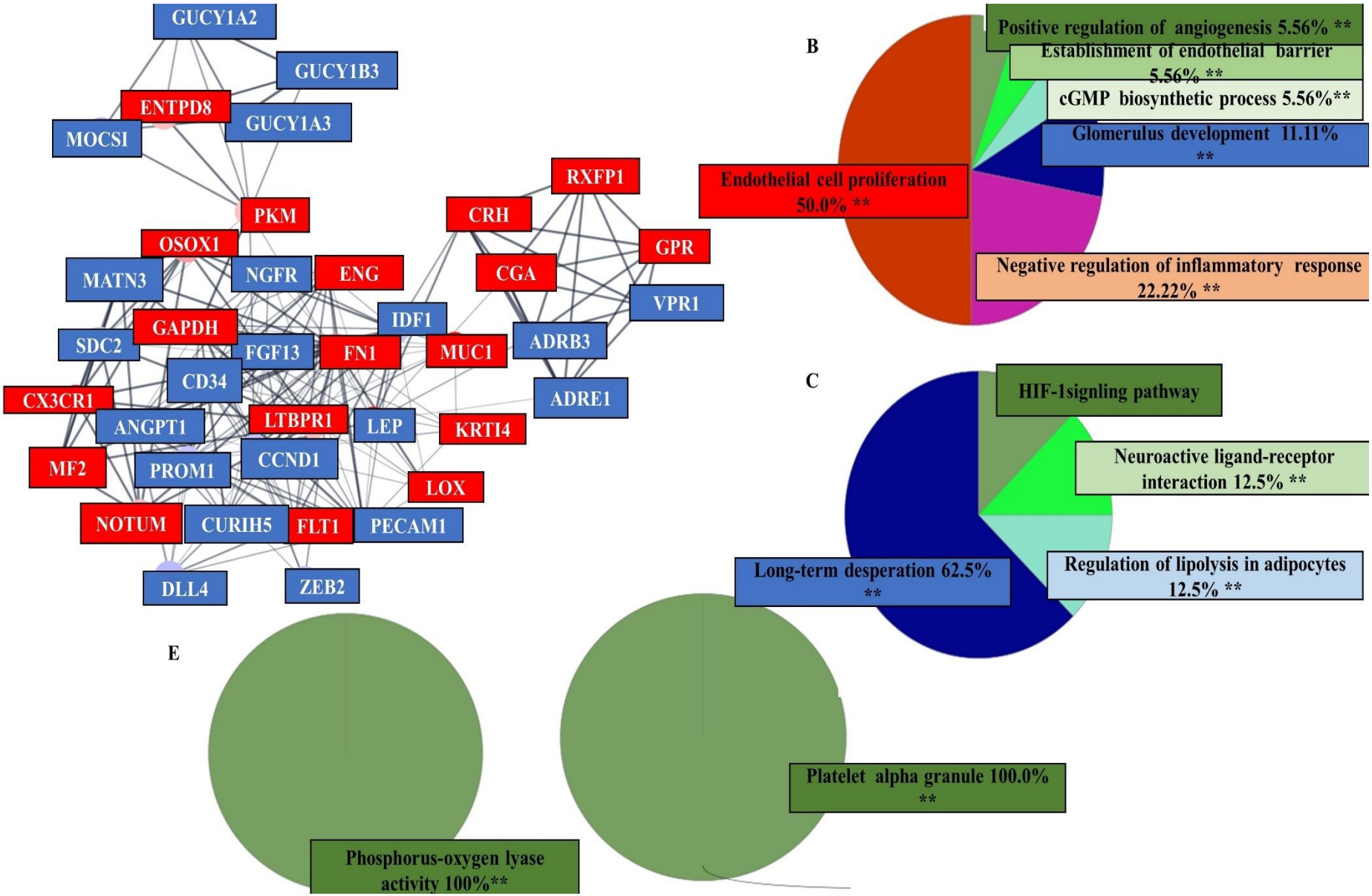



**Figure 45**. Figure showing A) cluster 3 from the M/L STB-EVs gene-gene interaction network analysis and associated B) Gene Ontology: Biological Process, C) Gene Ontology: Molecular Functions, D) Gene Ontology: Cellular Components and E) KEGG Pathways

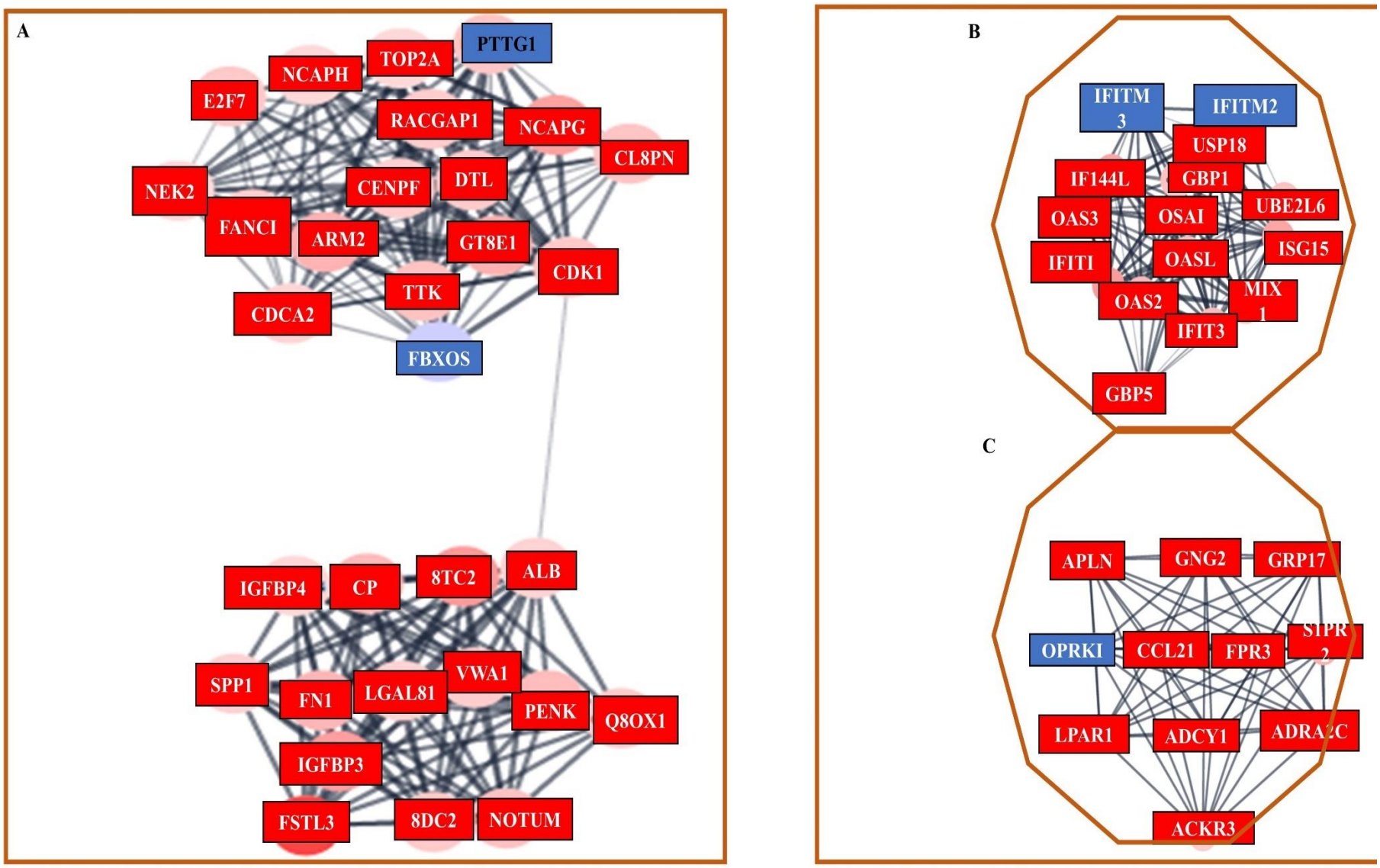



**Figure 46**. Figure showing the genes in the top transcriptomic clusters in M/L STB-EVs (Cluster 1 (A), Cluster 2 (B), Cluster 3 (C)). Red denotes upregulated genes while blue denotes downregulated genes.

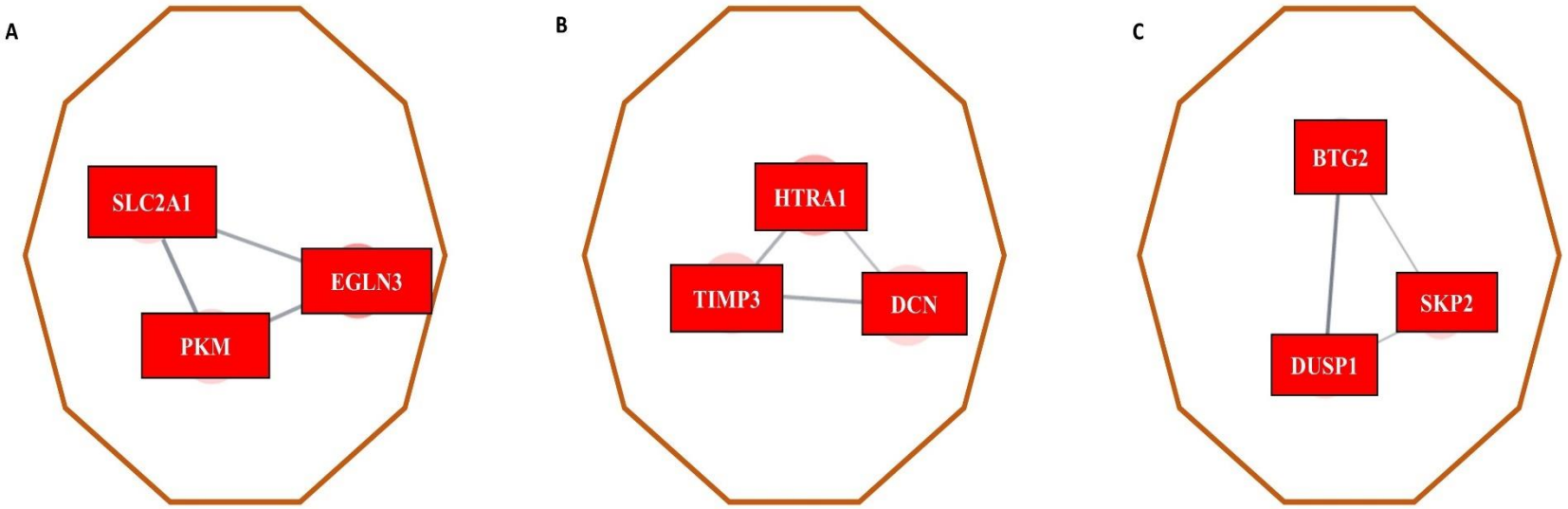



**Figure 47**. Figure showing the genes in the transcriptomic clusters in S STB-EVs (Cluster 1 (A), Cluster 2 (B) and Cluster 3 (C)). Red denotes upregulated genes.

### 6.5.3 Cluster analysis of preeclamptic transcriptomic gene-gene interaction network (PPI) in placenta tissue, medium/large and small STB-EVs

As mentioned earlier, the placenta had fifteen poorly interacting proteins, thus being ineligible for clustering analysis. However, to visualise the connections of the PPI in the placenta, I added 17 proteins known to interact with the identified DEPs and visualised the network (Figure 48).

In the M/L STB-EVs, the top 3 clusters had a clustering score of 23.24, 5.27 and 5 based on their mcode scores, respectively. These three clusters (1,2 & 3) had 30, 23 and 5 proteins within each, respectively. Cluster one (Figure 49) was involved in *proteasome-mediated ubiquitin-dependent* and *other protein-based metabolic or proteasome processes*. The proteins in cluster two (Figure 50A, B and C) are involved in *glucose and carbohydrate metabolic processes*, while cluster three (Figure 50D) had no functionally enriched processes.

There were only two clusters in the S STB-EV PPI network (Figure 51A and B), clusters 1 and 2, with scores of 6.86 and 3, respectively. Both clusters were made up of only upregulated proteins, with cluster 1 containing fifteen proteins and cluster 2 with three proteins. My analysis identified no functionally enriched terms in either of these clusters.

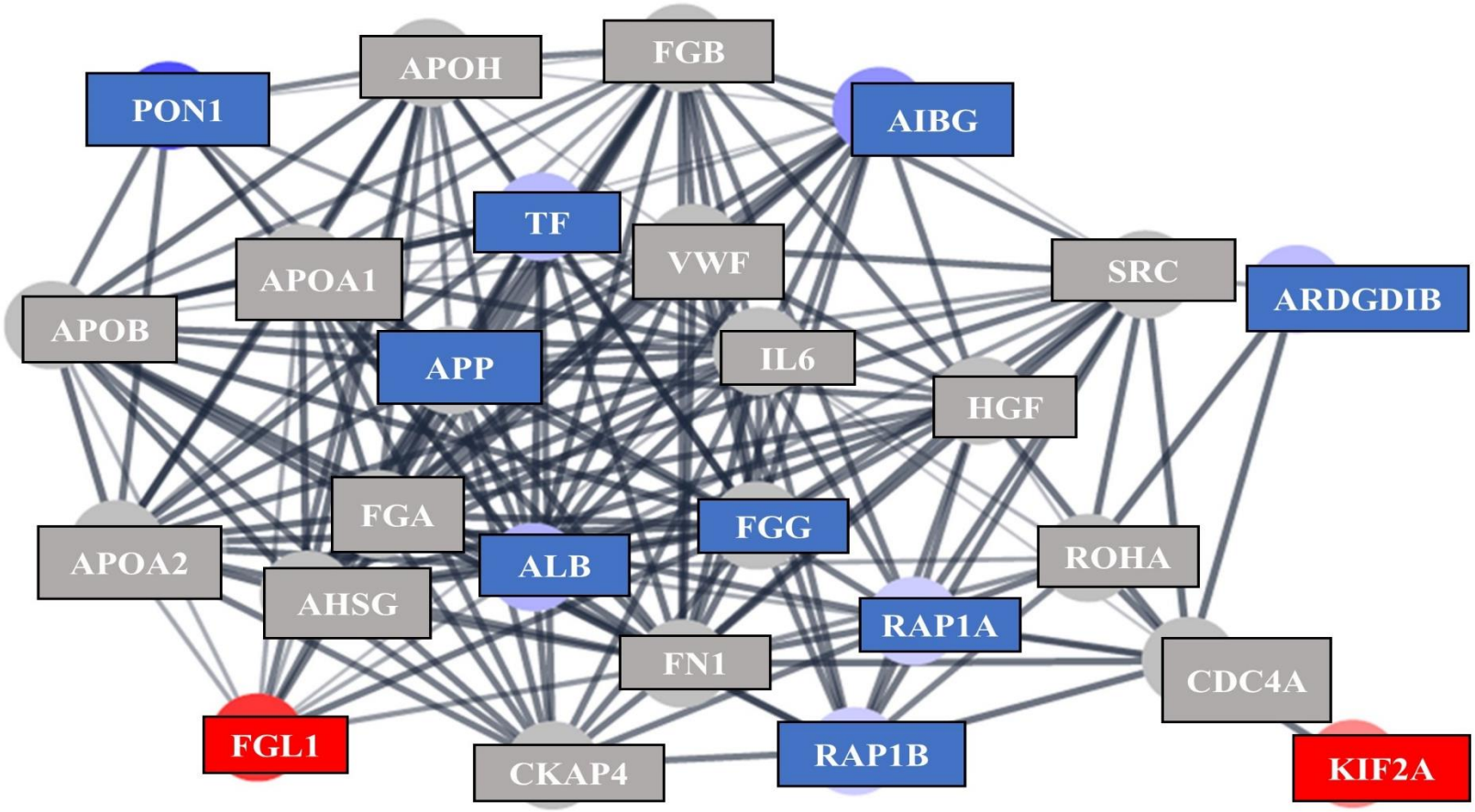



**Figure 48**. Figure showing the proteins in the placenta protein-protein interaction network. Red represents upregulated proteins, blue represents downregulated proteins while grey represents known protein interactors introduced to make the placenta protein-protein interaction network more robust.

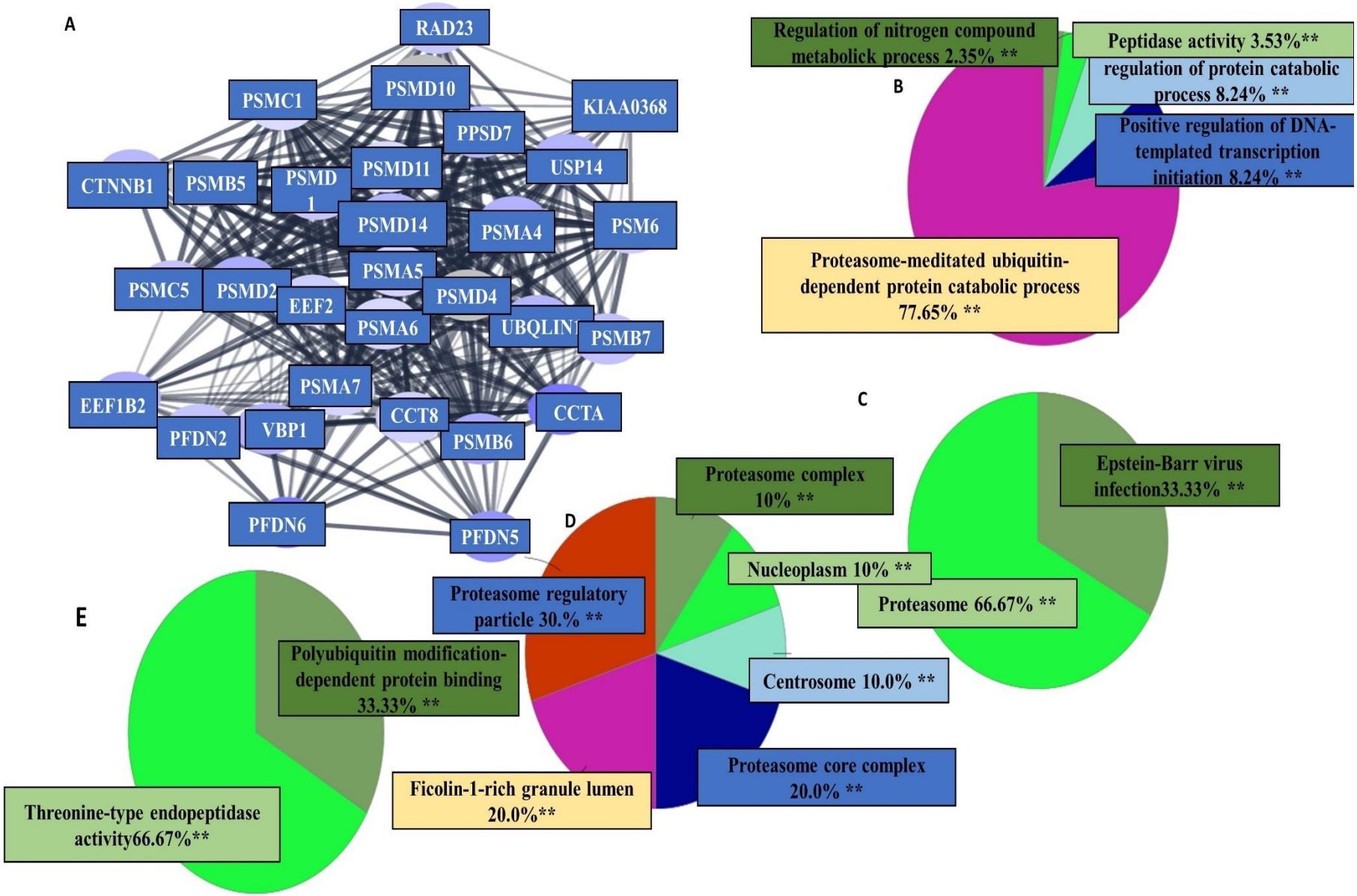



**Figure 49**. Figure showing the differentially expressed proteins in A) cluster 1 from the M/L STB-EVs protein-protein interaction network analysis and associated the B) Gene Ontology: Biological Process, C) Gene Ontology: Molecular Functions, D) Gene Ontology: Cellular Components terms and E) KEGG Pathways

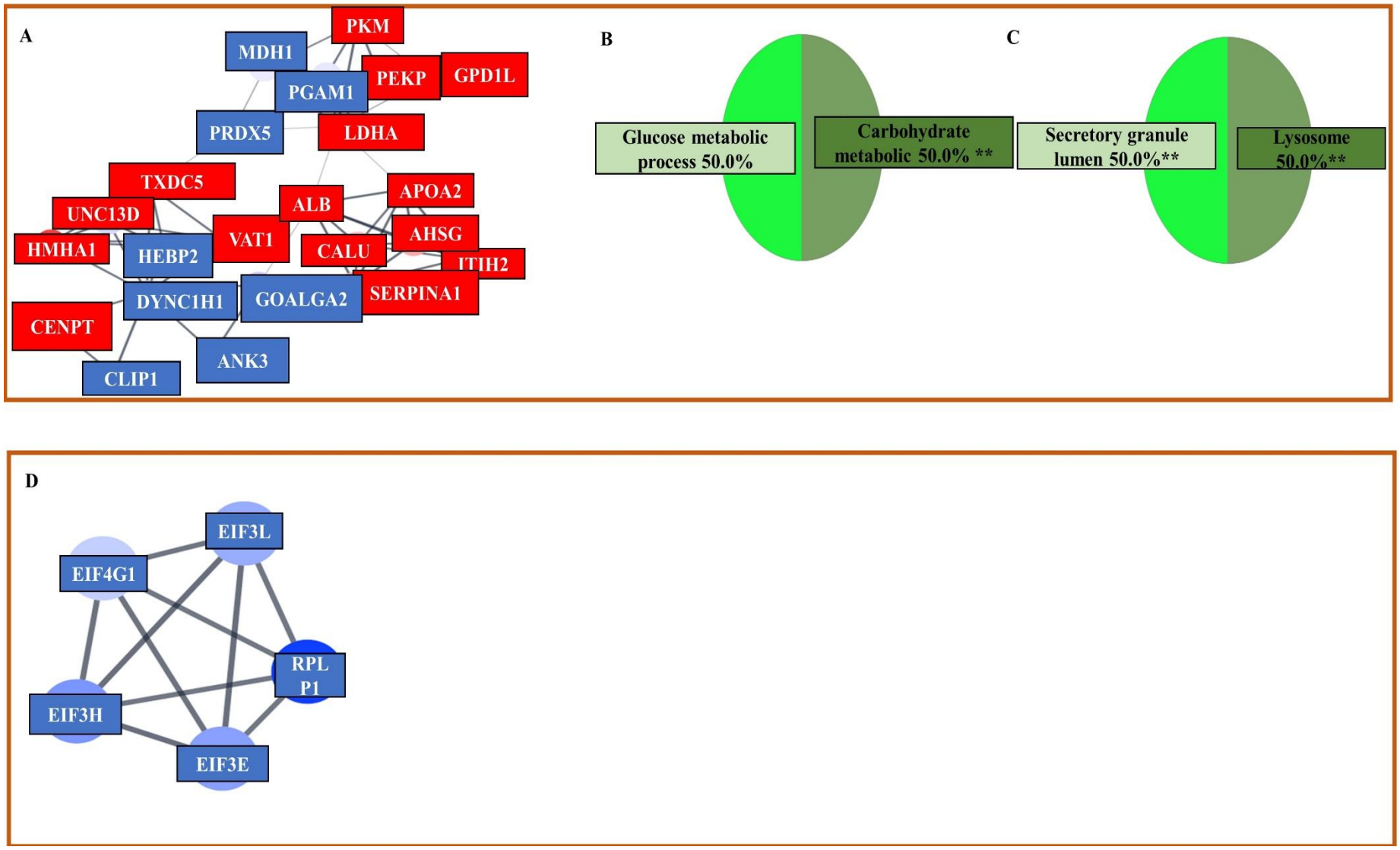





**Figure 50**. Figure showing the differentially expressed proteins in A) Cluster 2 from the M/L STB-EVs protein-protein interaction network analysis and associated B) Gene Ontology: Biological Process, C) Gene Ontology: Cellular Components terms. Figure showing the differentially expressed proteins in D) Cluster 3

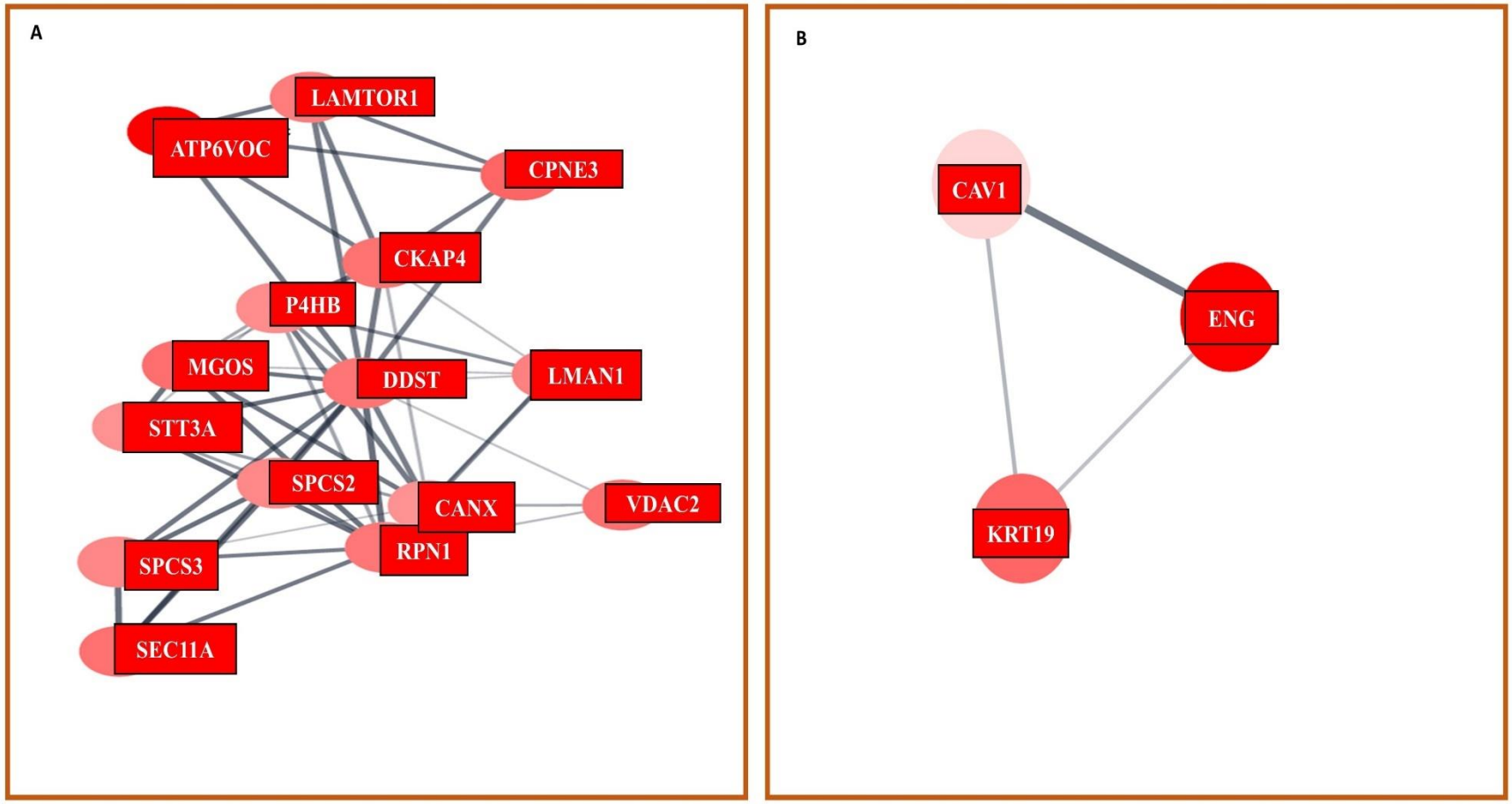



**Figure 51**. Figure showing the differentially expressed proteins in A) Cluster 1 and B) Cluster 2 from the S STB-EVs protein-protein interaction network analysis. Red denotes upregulated proteins

## 6.5.4 CMap analysis of transcriptomic and proteomic signatures

The Broad's institute connectivity map database provides a unique opportunity to identify perturbagens (molecules involved in perturbing function) that are potentially therapeutic (negative enrichment value) or problematic (in disease conditions, e.g., preeclampsia. Table 20 shows a list of identified perturbagens based on the placenta, medium/large and small STB-EVs transcriptomic signatures, filtered based on an enrichment value $\geq \pm 0.70$ and a p value $< 0.05$. The potential therapeutic agents identified by my analysis (by transcriptomic signature) are *valinomycin, valdecoxib (Placenta), bumetanide, ceforanide (M/L STB-EVs), arachidonic acid, melatonin (S STB-EVs)*. In contrast, potentially deleterious medications identified were *hydralazine (placenta), propylthimyacil (M/L STB-EVs), tolazamide (S STB-EVs).*

I performed a similar analysis on the proteomic signatures in all sample types. I concentrated mainly on those with negative enrichment scores as they are likely to be therapeutic. My analysis identified potential therapeutic agents such as *AH-23848*, a thromboxane receptor blocking agent (PL), *thiamine, cephaeline (M/L STB -EVs), perhexiline, progesterone, dexibuprofen (S STB-EVs)*. My analysis also identified *terazosin, timolol, diphenhydramine (Placenta), vorinostat (M/L STB-EVs), pentobutolol, tranexamic acid (S STB-EVs)* as medications that should be used cautiously in PE.

On integration (Table 21 and Figure 52), no perturbagens (with negative or positive enrichment scores) were identified among all sample types. But, in the M/L STB-EVs (proteomics), S STB-EVs (proteomics) and placenta (transcriptomics), *puromycin* was identified as potentially therapeutic. In contrast, *ciclopirox* was identified as potentially harmful in S STB-EVs (placenta) and Placenta (transcriptomics) and S STB-EVs (transcriptomics).

**Table 20.** Table showing results of connectivity map (CMap) analysis from transcriptomic and proteomic data. Molecules with negative enrichment scores represent potential therapeutic agents, while molecules with positive enrichment scores represent drugs that should be used with caution.

| Transcriptomics | | |
|---|---|---|
| CMap name | Enrichment Score | P Value |
| Placenta | | |
| Ciclopirox | 0.99 | <0.001 |
| Withaferin A | 0.93 | <0.001 |
| Proscillaridin | 0.91 | <0.01 |
| Aminoglutethimide | 0.89 | <0.001 |
| Hydralazine | 0.74 | <0.001 |
| Puromycin | -0.92 | <0.001 |
| Mimosine | -0.87 | 0.01 |
| Emetine | -0.81 | <0.001 |
| Valdecoxib | -0.80 | 0.02 |
| SC-560 | -0.76 | 0.03 |
| M/L STB-EVs | | |
| 5252917 | 0.90 | 0.02 |
| Y-27632 | 0.88 | 0.03 |
| Alfaxalone | 0.86 | 0.01 |
| Berberine | 0.85 | <0.0001 |
| Milrinone | 0.84 | 0.01 |
| Cinchonine | -0.98 | <0.0001 |
| Carbimazole | -0.90 | <0.0001 |
| Nadolol | -0.89 | <0.0001 |
| TTNPB | -0.89 | 0.02 |
| Prestwick-1082 | -0.89 | 0.04 |
| S STB-EVs | | |
| AG-012559 | 0.88 | <0.01 |
| Ciclopirox | 0.82 | <0.01 |
| Tolazamide | 0.78 | 0.02 |
| Kinetin | 0.76 | 0.01 |
| (-)-MK-801 | 0.73 | 0.01 |
| Withaferin A | -0.90 | <0.001 |
| Lomustine | -0.79 | <0.01 |
| Melatonin | -0.79 | <0.01 |
| CP-690334-01 | -0.78 | <0.0001 |
| Bumetanide | -0.78 | 0.01 |

| Proteomics | | |
|---|---|---|
| CMap name | Enrichment Score | P Value |
| Placenta | | |
| Isoflupredone | 0.93 | <0.001 |
| Clemastine | 0.90 | <0.01 |
| Iodixanol | 0.89 | <0.01 |
| Prestwick-1082 | 0.87 | <0.01 |
| MK-886 | 0.86 | 0.04 |
| Methylergometrine | -0.87 | <0.001 |
| 8-azaguanine | -0.85 | <0.001 |
| Talampicillin | -0.80 | <0.01 |
| Digoxin | -0.80 | <0.01 |
| Triflusal | -0.78 | 0.02 |
| M/L STB-EVs | | |
| MS-275 | 0.99 | <0.0001 |
| Rifabutin | 0.96 | <0.001 |
| Luteolin | 0.93 | <0.0001 |
| DL-thiorphan | 0.92 | 0.01 |
| Scriptaid | 0.91 | 0.01 |
| STOCK1N-35696 | -0.95 | 0.01 |
| 5182598 | -0.94 | 0.01 |
| Prestwick-983 | -0.89 | <0.01 |
| Thiamine | -0.89 | <0.01 |
| NU-1025 | -0.86 | 0.04 |
| S STB-EVs | | |
| Camptothecin | 0.98 | <0.001 |
| AH-6809 | 0.96 | <0.01 |
| Depudecin | 0.88 | 0.03 |
| Cromoglicic acid | 0.89 | 0.03 |
| Ciclopirox | 0.88 | <0.01 |
| Calmidazolium | -0.96 | 0.01 |
| Terfenadine | -0.86 | 0.01 |
| CAY-10397 | -0.84 | 0.01 |
| Semustine | -0.83 | <0.01 |
| Butoconazole | -0.83 | <0.01 |

**Table 21.** Table showing overlapping small molecules and therapeutics from the proteomics and transcriptomics data. Molecules with negative enrichment scores represent potential therapeutic agents, while molecules with positive enrichment scores represent drugs that should be used with caution.

| NEGATIVE | | |
|---|---|---|
| Transcriptomics | Proteomics | CMAP name |
| M/L STB-EVs, S STB-EVs | | Bumetanide, CP-690334-01, Ikarugamycin |
| M/L STB-EVs, S STB-EVs | M/L STB-EVs | Lomustine |
| S STB-EVs | S STB-EVs | Semustine |
| S STB-EVs | M/L STB-EVs | Primidone |
| | M/L STB-EVs, S STB-EVs | Cephaeline, Anisomycin |
| | Placenta, S STB-EVs | CAY-10397, AH-23848, H-89 |
| Placenta | S STB-EVs | Valinomycin |
| Placenta | M/L STB-EVs, S STB-EVs | Puromycin |
| POSITIVE | | |
| M/L STB-EVs, S STB-EVs | | Rolipram |
| | M/L STB-EVs, S STB-EVs | Camptothecin |
| | Placenta, S STB-EVs | AH-6809, 10-methoxyharmalan, Prestwick-1082 |
| Placenta, S STB-EVs | S STB-EVs | Ciclopirox |

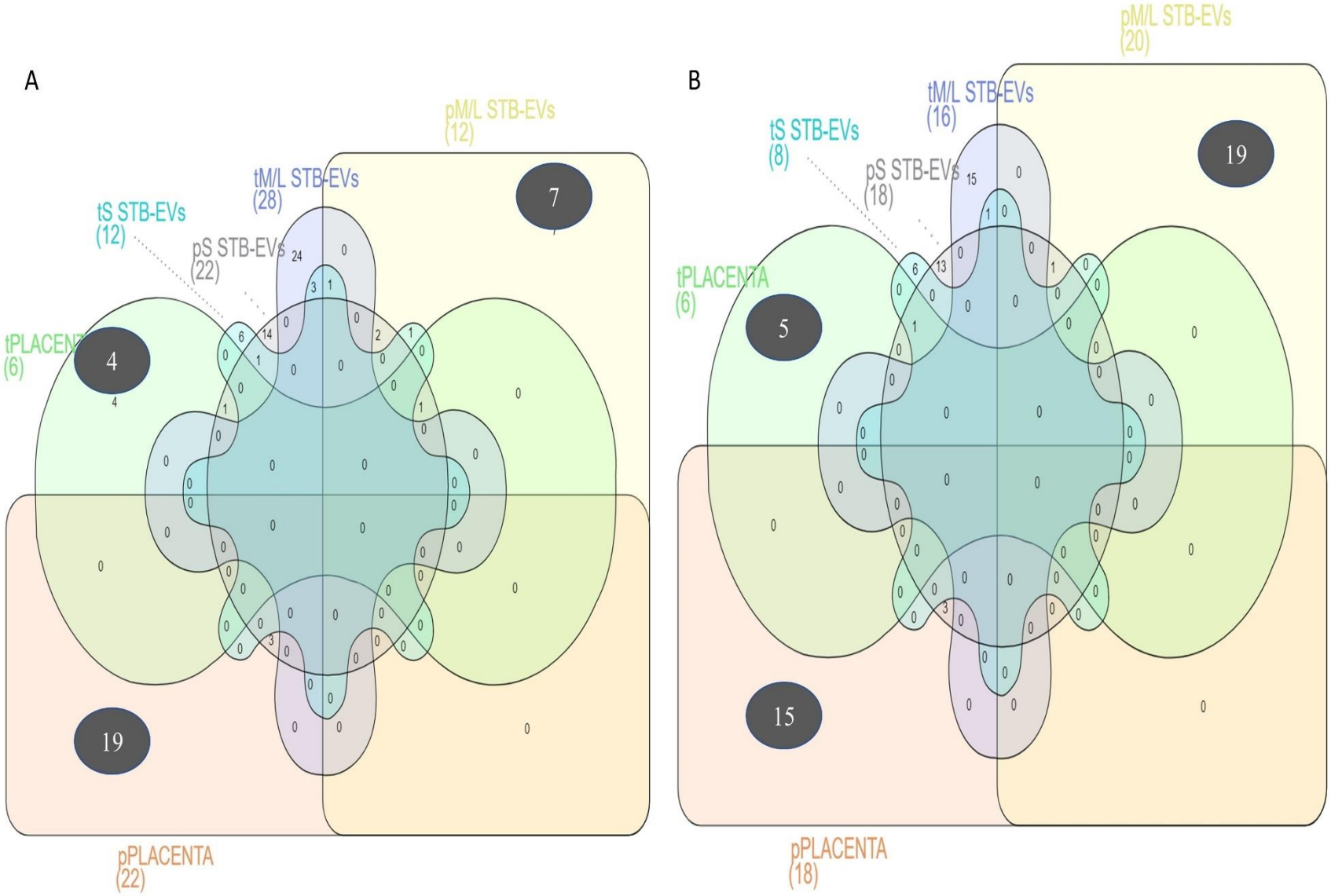



**Figure 52**. Venn diagram showing overlapping CMap small molecules across all datasets. Figure A shows the number of overlapping molecules that are potentially therapeutic while Figure B shows the number of overlapping molecules that are potentially detrimental

## 6.6 Discussion

In this chapter, I have bioinformatically identified hub (critical) genes and attempted to determine their biological relevance. I identified different molecular protein and gene clusters based on the gene-gene and protein-protein interaction network from the transcriptomics and proteomics data, respectively. Hub/critical genes refer to the most connected genes or proteins in either a gene-gene or protein-protein interaction network, i.e., the gene or protein that has the highest interaction with other genes or proteins. They are believed to be fundamental to the integrity of the disease network and thus have relevance in identifying disease modifiable pathways. As commonly practised among bioinformaticians, I arbitrarily chose the first ten hub genes based on clustering scores for the placenta, M/L and S STB-EVs. *GAPDH*, *FN1*, *LEP*, and ALB were all critical genes/proteins based on their presence in at least two sample types after my integrated analysis.

GAPDH is a glycolytic enzyme involved in carbohydrate metabolism, nuclear functions, and innate immunity. GAPDH is expressed in placental tissue in pregnancy, and its level rises to meet the increased metabolic demand in pregnancy. It is often used as a housekeeping gene and endogenous control for gene expression studies[329]. Therefore, using GAPDH as a housekeeping gene in PE is problematic and results presenting GAPDH as a reference should be interpreted with a degree of caution. Fibronectin 1 (FN1) levels in the blood are associated with clinical PE[330–332]. FN1 plays a role in cell-cell interactions, tissue repair, blood coagulation, and cell shape[333]. FN1 participates in the pathogenesis of PE by promoting apoptosis and autophagy in vascular endothelial cells through the PI3K/AKT/mTOR signalling pathway[334].

LEP is involved in energy homeostasis, endocrine functions, immune system regulation and inflammation, angiogenesis, and reproduction. In pregnancy, LEP is involved in the

trophoblast invasion, cellular turnover of the placenta, immune modulator of the placenta, and inflammation[335]. The increased levels of LEP and associated proinflammatory role have been suggested to contribute to the pathogenesis of pregnancy disorders such as PE[336,337]. Some studies have shown no association between LEP and PE[338,339], while others have proposed that LEP may be compensating for the under-perfused placenta by increasing nutrient delivery[340]. LEP has also been reported as a hub gene by Liu et al. [341]. Nevertheless, LEP has been shown to increase throughout gestation with higher levels in PE, but the exact role in the pathogenesis of the disease remains to be determined.

To identify critical pathways based on integrating the datasets (transcriptomics and proteomics), I blended the gene ontology analysis, specific biological processes, molecular functions, cellular components and KEGG pathways for each set of hub genes/proteins. My analysis identified biological processes involved in *protein folding and metabolism* to be dysregulated, among others. Others have reported this pathway to be abnormal in *PE*[342,343]. Protein folding and metabolism dysregulation in PE may be due, in part, to cellular (endoplasmic reticulum) stress secondary to hypoxia leading to accumulation of unfolded proteins in the endoplasmic reticulum. This dysregulation activates a protective response, the unfolded protective response, to reduce ER stress[344]. Cheng et al. identified misfolded amyloid aggregates of transthyretin in preeclamptic placentas. At the same time, Buhimschi et al. also showed congophilia, which is characteristic of protein misfolding and the presence of amyloid precursor protein-derived amyloid-like proteins in the placenta and urine of women with PE[272].

It is also interesting that *organ development, response to hypoxia* and *response to decreased oxygen levels* are some of the abnormal pathways detected by my analysis. It is believed that the hypoxia seen in preeclampsia is responsible for the ER stress though the exact mechanism implicating the unfolded protein response is still under investigation. In addition, no one has

assessed whether the commonly described elevated proteins in PE such as FLT1, soluble FLT1, and endoglin are misfolded.

My analysis also identified ERK1/2 pathways to be critical. ERK1/2 (Extracellular signal-regulated protein kinases 1 and 2) are mitogen-activated protein kinases (MAPK) involved in cell proliferation and apoptosis. D'Oria et al. showed in vitro an intense activation of PKB/Akt and MAPK/ERK in human endothelial cells in response to DCI (D-chiro inositol), molecules found to be increased in preeclampsia[345]. Similarly, Fu et al. showed that NDRG1 (N-myc downstream-regulated gene 1) (increased in preeclampsia) inhibits trophoblast invasion through the ERK/MMP-9[346]. Surprisingly, abnormal regulation of MAPK pathways has also been seen in Alzheimer's disease, another protein folding abnormality disease[347]. My analysis also showed classically described abnormal PE pathways; *regulation of epithelial cell proliferation, regulation of substrate-dependent cell migration, regulation of angiogenesis* and *regulation of vasculature development* being abnormal. An abnormal cellular adhesion process leads to insufficient invasion of the trophoblast into the vessels contributing to the development of PE[348,349].

PE is a highly variable and heterogeneous clinical condition with different clinical presentations and patient characteristics. I explored that these may have identifiable molecular subtypes. I could only ascribe biological relevance to the clusters found in the placenta (transcriptomic) and M/L STB-EVs (proteomics) because the other clusters yielded no functional enrichment results. In the placenta (transcriptomics), Cluster 1 was involved in the *regulation of amine transport and signalling pathways*. cAMP signalling is vital in regulating *PLGF* and *β-HCG*[350,351], both involved in preeclampsia. Clusters 2 genes were involved in *arterial blood pressure* and *vascular smooth muscle control*. Elevated systemic arterial blood is a cardinal feature of preeclampsia and identifying clusters with this biological pathway provides an internal validation for this approach. Cluster 3 genes were associated with *long-*

*term depression,* which is in keeping with the study by Auger et al., which noted that PE women had an increased risk of hospitalization for depression later in life[352].

Finally, I performed a connectivity map analysis on the generated preeclampsia specific molecular signature and bioinformatically identified molecules/therapeutic agents that could be used to treat or reverse PE potentially. Most of the identified therapeutic drugs were teratogenic or not safe in pregnancy. SC-560 and valdecoxib are cyclooxygenase-1 inhibitors with no available safety data in pregnancy. Cyclooxygenase-1 (COX-1) produces baseline levels of prostaglandins that protect the gastrointestinal lining and activate platelets inhibitors. COX-1 has antiinflammatory and anticoagulation effects. Nadolol was identified as a potential therapeutic in M/L STB-EVs. Nadolol is a beta-adrenergic receptor blocking agent with antihypertensive properties. Data about the safety of nadolol in pregnancy is also lacking. Bumetanide, another potential therapeutic we identified, is a loop diuretic with antihypertensive properties but is not recommended for use in preeclampsia due to maternal hypovolemia[353]. My analysis also identified melatonin as a potential therapeutic agent. Only one trial has been conducted on melatonin showed that melatonin improves endothelial dysfunction and prolongs pregnancy in severe PE[166]. It was also found to be safe for the mother and foetus. In this study, melatonin was given from diagnosis and three times daily. The study did not evaluate a difference in effect between day and night dosing or effect before PE diagnosis.

Hydralazine was one of the molecules I predicted could worsen preeclampsia. Hydralazine is presently one of the antihypertensives used to treat severe hypertension in preeclampsia352. Still, its side effects, headache, nausea, and vomiting mimic the symptoms of preeclampsia and thus masquerades the drug's effect. The potential therapeutic agents we uncovered need further research on efficacy and safety in pregnancy.

In conclusion, I have performed a systems-level integrative analysis on the transcriptomic and proteomic profile of the placenta, M/L STB-EVs and S STB-EVs. My analysis has identified potential critical genes, critical pathways, molecular subtypes, and potential therapeutics in preeclampsia. My results may help further understand the pathophysiology of preeclampsia and identify new treatment options.

# CHAPTER 7

## FINAL DISCUSSION

## 7.1 Final Discussion

## 7.2 Summary

I set out to answer three related questions/aims in this thesis, 1) identify molecules syncytiotrophoblast membrane extracellular vesicle (STB-EVs) expressed molecules that may be diagnostic of preeclampsia, 2) bioinformatically determine potential mechanisms of PE and 3) bioinformatically discover repurposed drugs that may be therapeutic in PE. I conducted next-generation sequencing and mass spectrometric analysis on isolated and enriched STB-EVs to identify these STB-EVs expressed molecules. My analysis identified and verified STB-EV biomolecules (proteins, messenger RNA and microRNAs) with diagnostic potentials.

Chapter 1 contains an introduction to preeclampsia and syncytiotrophoblast membrane extracellular vesicles. It highlights the methods of enrichment of STB-EVs, their mechanisms pertaining to PE, their use as circulating biomarkers and biodistribution. I also highlighted the current PE therapeutics advancements with aspirin, sulfasalazine, metformin, and newer treatment modalities.

Chapter 2 detailed the methodology employed in this thesis. I wrote about the process of extracting STB-EVs with *ex vivo* dual lobe perfusion and differential ultracentrifugation, the characterisation of STB-EVs with flow cytometry, Western blot, transmission electron microscopy (TEM), and nanoparticle tracking analysis (NTA) keeping in line with the recommendations by the International Society of Extracellular Vesicles (ISEV).

Chapter 3 contains messenger RNA transcriptomic data analysis results to identify differentially expressed genes and their biological functions. Similarly, in chapters 4 and 5, I showed the results of my analysis on microRNA transcriptomics and proteomics, respectively.

Chapter 6 integrated the results from the messenger RNA transcriptomics and proteomics data sets to facilitate the identification of mechanistic pathways and therapeutic agents.

Ultimately, I answered the three aims in the six chapters of this thesis.

### 7.2.1 Aim 1: Identify molecules syncytiotrophoblast membrane extracellular vesicle (STB-EVs) expressed molecules that may be diagnostic of preeclampsia

Messenger RNA quantitative polymerase chain reaction confirmed the differential expression of FLNB*, COL17A1*, *SLC45A4*, *LEP*, *HTRA4*, *EBI3*, *HSD17B1*, *FSTL3*, *INHBA*, *SIGLEC6*, and *CGB3*. MicroRNA quantitative polymerase chain reaction verified the differential expression of hsa-miR-193b-5p, hsa-miR-324-5p, hsa-miR-652-3p, hsa-miR-3196, hsa-miR-9-5p, hsa-miR-421, and hsa-miR-210-3p in the medium/large STB-EVs. Finally, the Western blot showed FLNB (filamin B), *COL17A1 (Collagen 17A1), PAPP-A2 (Pappalysin-A2),* and *SR-BI (Scavenger Receptor Class B Type 1.)*

### 7.2.2 Aim 2: Bioinformatically determine potential mechanisms and molecular PE subtypes

I integrated all data sets to identify potential critical genes and pathways (*(GAPDH, leptin, fibronectin1* and *albumin))* from my analysis. I found *peptidyl amino acid modification, carbohydrate derivative metabolic process, response to hypoxia and stress, nitrogen compound and primary metabolic process, abnormal protein folding*, and *mitogen-activated protein kinases (MAPK) cascade*. I also identified molecular subtypes from both the proteomic and transcriptomic datasets. *A cluster of genes, e.g., CXCL 10, CXCR1 and ADCY1*, is responsible for *G protein-coupled receptor signalling*, another cluster of genes (including F2R, EDNRA, PLCB4) modulates *arterial blood pressure.* These genes or protein clusters may represent mechanistic and therapeutic targets that later be explored.

### 7.2.3 Aim 3: Bioinformatically discover repurposed drugs that may be therapeutic in PE

I used connectivity map (CMap), a database of thousands of perturbagens, to analyse the placenta specific transcriptomic and proteomic molecular signatures. The analysis identified potential therapeutic agents, including *valinomycin, valdecoxib, bumetanide, ceforanide, arachidonic acid, melatonin, AH-23848,* a thromboxane receptor blocking agent (PL), *thiamine, cephaeline, perhexiline, progesterone, dexibuprofen (S STB-EVs).* I also identified *terazosin, timolol, diphenhydramine, virunostat, pentobutolol, tranexamic acid, hydralazine (placenta), propylthiouracil, tolazamide* as potentially harmful compounds in preeclampsia.

### 7.2.4 Future work

Preeclampsia remains a largely heterogeneous disease whose mechanism is yet fully unravelled. The search for effective PE preventive and therapeutic agents is ongoing with mixed results. Diagnostically, the available tests are best at ruling out PE (excellent negative predictive value) but not so good at ruling in a test (positive predictive value). The next step of this project would be to probe for the identified panel of biomolecules in biofluids such as plasma, serum, or urine initially as diagnostic agents and preferably as predictive molecules. Identification of STB-EV based markers would allow longitudinal profiling of moth the pregnant mother and foetus and perhaps allow personalisation of medical or surgical therapy based on individuals' molecular signatures.

The bioinformatically identified potential mechanisms would also be verified *in vitro* with cellular models or placenta explant models, for example, by treating endothelial cells, cardiomyocytes, or placenta explants with PE STB-EVs and verifying for alterations in pathways responsible for *protein folding, cellular response to hypoxia or stress, regulation of hematopoietic stem cells*. This verification might help unravel the PE mechanisms.

The molecules identified by CMap analysis would also need to be verified *in vitro* to substantiate a biological effect in reversing or cessation of endothelial cell injury and reducing circulating antiangiogenic levels (soluble FLT-1, soluble endoglin), reversal of PE phenotype and pregnancy prolongation.

Finally, I hope this work will add to the existing knowledge on preeclampsia and push the field closer to reducing maternal and foetal morbidity and mortality globally.

## 8.1 List of Publications

### Published Papers

- **Awoyemi T**, Tannetta D, Zhang W, Kandzija N, Motta-Mejia C, Fischer R, Heilig R, Raiss S, Redman C, Vatish M. Glycosylated Siglec-6 expression in syncytiotrophoblast-derived extracellular vesicles from preeclampsia placentas. Biochem Biophys Res Commun. 2020 Dec 17;533(4):838-844. doi: 10.1016/j.bbrc.2020.09.081. Epub 2020 Sep 29. PMID: 32998819.
- **Awoyemi T**, Motta-Mejia C, Zhang W, Kouser L, White K, Kandzija N, Alhamlan FS, Cribbs AP, Tannetta D, Mazey E, Redman C, Kishore U, Vatish M. Syncytiotrophoblast Extracellular Vesicles from Late-Onset Preeclampsia Placentae Suppress Pro-Inflammatory Immune Response in THP-1 Macrophages. Front Immunol. 2021 Jun 7;12:676056. doi: 10.3389/fimmu.2021.676056. PMID: 34163477; PMCID: PMC8215361.

### Submitted Manuscript

- Zhang W, Kandzija N, **Awoyemi T**, Cerdeira, Wang X, Redman C, and Vatish M. Immunological profiling improves analytical specificity for single medium/large extracellular vesicles generated from high-speed centrifugation and allows interrogation of rare extracellular vesicles in minimally processed plasma

### Unpublished Manuscript

- **Awoyemi T**, Zhang W, Rahbar M, Cribbs A, Logentherian P, Jiang S, Cerdeira S, Redman C and Vatish M. Transcriptomic analysis of placenta and its released extracellular vesicles in normal and preeclampsia pregnancies: insights into novel biomarkers and mechanisms of disease

- **Awoyemi T**, Logentherian P, Jiang P, Jiang S, Rahbar M, Cooke W, Zhang W, Cribbs A, Cerdeira S, Redman C, and Vatish M. Micro RNA analysis of placenta and its released extracellular vesicles in normal and preeclampsia pregnancies: insights into novel biomarkers and mechanisms of disease
- **Awoyemi T**, Jiang S, Bjarakadottir, Rahbar M, Lognetherian P, Fischer, Colette G, Zhang W, Cerdeira S, Redman C, and Vatish M. Proteomic analysis of placenta and trophoblast extracellular vesicles in normal and preeclampsia pregnancies: identification of novel biomarkers and insights into disease mechanisms
- **Awoyemi T**, Rahbar M, Redman C, and Vatish M. Integration of transcriptomic and proteomic data of placenta and trophoblast extracellular vesicles in normal and preeclampsia pregnancies: identification of critical pathways, molecular subtypes, and potential therapeutic agents.
- **Awoyemi T**, Cerdeira S, Zhang W, Redman C, and Vatish M. Classification, biogenesis, distribution, roles, and mechanisms of preeclamptic syncytiotrophoblast membrane extracellular vesicles (STB-EVs)

# 8.2 References


1. Brown MA, Magee LA, Kenny LC, et al. Hypertensive disorders of pregnancy: ISSHP classification, diagnosis, and management recommendations for international practice. *Hypertension*. Published online 2018. doi:10.1161/HYPERTENSIONAHA.117.10803

2. Uzan J, Carbonnel M, Piconne O, Asmar R, Ayoubi JM. Pre-eclampsia: pathophysiology, diagnosis, and management. *Vascular Health and Risk Management*. 2011;7:467. doi:10.2147/VHRM.S20181

3. Duley L. The global impact of pre-eclampsia and eclampsia. *Semin Perinatol*. 2009;33(3):130-137. doi:10.1053/J.SEMPERI.2009.02.010

4. Brown MA, Lindheimer MD, de Swiet M, van Assche A, Moutquin JM. The classification and diagnosis of the hypertensive disorders of pregnancy: statement from the International Society for the Study of Hypertension in Pregnancy (ISSHP). *Hypertens Pregnancy*. 2001;20(1). doi:10.1081/PRG-100104165

5. ACOG Practice Bulletin No. 202: Gestational Hypertension and Preeclampsia. *Obstet Gynecol*. 2019;133(1):e1-e25. doi:10.1097/AOG.0000000000003018

6. Roberts JM, Rich-Edwards JW, McElrath TF, Garmire L, Myatt L. Subtypes of Preeclampsia: Recognition and Determining Clinical Usefulness. *Hypertension*. 2021;77:1430-1441. doi:10.1161/HYPERTENSIONAHA.120.14781

7. Lisonkova S, Joseph KS. Incidence of preeclampsia: Risk factors and outcomes associated with early-versus late-onset disease. *American Journal of Obstetrics and Gynecology*. Published online 2013. doi:10.1016/j.ajog.2013.08.019

8. Jeyabalan A. Epidemiology of preeclampsia: impact of obesity. *Nutr Rev*. 2013;71 Suppl 1(0 1). doi:10.1111/NURE.12055

9. Atallah A, Lecarpentier E, Goffinet F, Doret-Dion M, Gaucherand P, Tsatsaris V. Aspirin for Prevention of Preeclampsia. *Drugs*. 2017;77(17):1819-1831. doi:10.1007/S40265-017-0823-0

10. Soto-Wright V, Bernstein M, Goldstein DP, Berkowitz RS. The changing clinical presentation of complete molar pregnancy. *Obstet Gynecol*. 1995;86(5):775-779. doi:10.1016/0029-7844(95)00268-V

11. Bdolah Y, Lam C, Rajakumar A, et al. Twin pregnancy and the risk of preeclampsia: bigger placenta or relative ischemia? *Am J Obstet Gynecol*. 2008;198(4):428.e1-428.e6. doi:10.1016/J.AJOG.2007.10.783

12. Hailu FG, Yihunie GT, Essa AA, Tsega W kindie. Advanced abdominal pregnancy, with live fetus and severe preeclampsia, case report. *BMC Pregnancy Childbirth*. 2017;17(1). doi:10.1186/S12884-017-1437-Y

13. Gathiram P, Moodley J. Pre-eclampsia: its pathogenesis and pathophysiolgy. *Cardiovascular Journal of Africa*. 2016;27(2):71. doi:10.5830/CVJA-2016-009

14. Roberts JM, Escudero C. The placenta in preeclampsia. *Pregnancy Hypertens*. 2012;2(2):72. doi:10.1016/J.PREGHY.2012.01.001

15. Teng F, Fussenegger M. Shedding Light on Extracellular Vesicle Biogenesis and Bioengineering. *Advanced science (Weinheim, Baden-Wurttemberg, Germany)*. 2020;8(1). doi:10.1002/ADVS.202003505

16. Cronqvist T, Tannetta D, Mörgelin M, et al. Syncytiotrophoblast derived extracellular vesicles transfer functional placental miRNAs to primary human endothelial cells. *Scientific Reports 2017 7:1*. 2017;7(1):1-14. doi:10.1038/s41598-017-04468-0

17. Awoyemi T, Motta-Mejia C, Zhang W, et al. Syncytiotrophoblast Extracellular Vesicles From Late-Onset Preeclampsia Placentae Suppress Pro-Inflammatory Immune Response in THP-1 Macrophages. *Front Immunol*. 2021;12. doi:10.3389/FIMMU.2021.676056

18. Germain SJ, Sacks GP, Sooranna SR, Soorana SR, Sargent IL, Redman CW. Systemic inflammatory priming in normal pregnancy and preeclampsia: the role of circulating syncytiotrophoblast microparticles. *J Immunol*. 2007;178(9):5949-5956. doi:10.4049/JIMMUNOL.178.9.5949

19. Ermini L, Ausman J, Melland-Smith M, et al. A Single Sphingomyelin Species Promotes Exosomal Release of Endoglin into the Maternal Circulation in Preeclampsia. *Scientific Reports 2017 7:1*. 2017;7(1):1-16. doi:10.1038/s41598-017-12491-4

20. Tannetta DS, Hunt K, Jones CI, et al. Syncytiotrophoblast Extracellular Vesicles from Pre-Eclampsia Placentas Differentially Affect Platelet Function. *PLOS ONE*. 2015;10(11):e0142538. doi:10.1371/JOURNAL.PONE.0142538

21. Motta-Mejia C, Kandzija N, Zhang W, et al. Placental Vesicles Carry Active Endothelial Nitric Oxide Synthase and Their Activity is Reduced in Preeclampsia. *Hypertension*. 2017;70(2):372-381. doi:10.1161/HYPERTENSIONAHA.117.09321/-/DC1

22. Spaans F, Quon A, Kirschenman R, et al. Role of Lectin-like Oxidized LDL Receptor-1 and Syncytiotrophoblast Extracellular Vesicles in the Vascular Reactivity of Mouse Uterine Arteries During Pregnancy. *Scientific Reports 2020 10:1*. 2020;10(1):1-11. doi:10.1038/s41598-020-63205-2

23. Guller S, Tang Z, Ma YY, di Santo S, Sager R, Schneider H. Protein composition of microparticles shed from human placenta during placental perfusion: Potential role in angiogenesis and fibrinolysis in preeclampsia. *Placenta*. 2011;32(1):63-69. doi:10.1016/j.placenta.2010.10.011

24. Khan S, Bennit HF, Turay D, et al. Early diagnostic value of survivin and its alternative splice variants in breast cancer. *BMC Cancer*. 2014;14(1). doi:10.1186/1471-2407-14-176

25. Wang X, Zhong W, Bu J, et al. Exosomal protein CD82 as a diagnostic biomarker for precision medicine for breast cancer. *Mol Carcinog*. 2019;58(5):674-685. doi:10.1002/MC.22960

26. Kimura H, Yamamoto H, Harada T, et al. CKAP4, a DKK1 Receptor, Is a Biomarker in Exosomes Derived from Pancreatic Cancer and a Molecular Target for Therapy. *Clinical Cancer Research*. 2019;25(6):1936-1947. doi:10.1158/1078-0432.CCR-18-2124

27. Costa-Silva B, Aiello NM, Ocean AJ, et al. Pancreatic cancer exosomes initiate pre-metastatic niche formation in the liver. *Nature Cell Biology*. 2015;17(6). doi:10.1038/ncb3169

28. Yokoyama S, Takeuchi A, Yamaguchi S, et al. Clinical implications of carcinoembryonic antigen distribution in serum exosomal fraction—Measurement by ELISA. *PLoS ONE*. 2017;12(8). doi:10.1371/journal.pone.0183337

29. Giampieri R, Piva F, Occhipinti G, et al. Clinical impact of different exosomes' protein expression in pancreatic ductal carcinoma patients treated with standard first line palliative chemotherapy. *PLoS ONE*. 2019;14(5). doi:10.1371/journal.pone.0215990

30. Ness RB, Roberts JM. Heterogeneous causes constituting the single syndrome of preeclampsia: A hypothesis and its implications. *American Journal of Obstetrics and Gynecology*. Published online 1996. doi:10.1016/S0002-9378(96)70056-X

31. von Dadelszen P, Magee LA, Roberts JM. Subclassification of preeclampsia. *Hypertens Pregnancy*. 2003;22(2):143-148. doi:10.1081/PRG-120021060

32. Boyd HA, Tahir H, Wohlfahrt J, Melbye M. Associations of personal and family preeclampsia history with the risk of early-, intermediate- and late-onset preeclampsia. *Am J Epidemiol*. 2013;178(11):1611-1619. doi:10.1093/AJE/KWT189

33. Phillips JK, Janowiak M, Badger GJ, Bernstein IM. Evidence for Distinct Preterm and Term Phenotypes of Preeclampsia. *J Matern Fetal Neonatal Med*. 2010;23(7):622. doi:10.3109/14767050903258746

34. Esplin MS, Fausett MB, Fraser A, et al. Paternal and maternal components of the predisposition to preeclampsia. *N Engl J Med*. 2001;344(12):867-872. doi:10.1056/NEJM200103223441201

35. Lie RT, Rasmussen S, Brunborg H, Gjessing HK, Lie-Nielsen E, Irgens LM. Fetal and maternal contributions to risk of pre-eclampsia: population based study. *BMJ : British Medical Journal*. 1998;316(7141):1343. doi:10.1136/BMJ.316.7141.1343

36. Hoy J, Venn A, Halliday J, Kovacs G, Waalvvyk K. Perinatal and obstetric outcomes of donor insemination using cryopreserved semen in Victoria, Australia. *Hum Reprod*. 1999;14(7):1760-1764. doi:10.1093/HUMREP/14.7.1760

37. Lie RT, Rasmussen S, Brunborg H, Gjessing HK, Lie-Nielsen E, Irgens LM. Fetal and maternal contributions to risk of pre-eclampsia: population based study. *BMJ : British Medical Journal*. 1998;316(7141):1343. doi:10.1136/BMJ.316.7141.1343

38. Surapaneni T, Patil Bada V, Praveen Kumar Nirmalan C. Risk for Recurrence of Pre-eclampsia in the Subsequent Pregnancy. *Journal of Clinical and Diagnostic Research : JCDR*. 2013;7(12):2889. doi:10.7860/JCDR/2013/7681.3785

39. English FA, Kenny LC, McCarthy FP. Risk factors and effective management of preeclampsia. *Integr Blood Press Control*. 2015;8:7-12. doi:10.2147/IBPC.S50641

40. Diagnosis and Treatment of Hypertension and Pre-eclampsia in Pregnancy in New Zealand. Published online 2018.

41. Shih T, Peneva D, Xu X, et al. The Rising Burden of Preeclampsia in the United States Impacts Both Maternal and Child Health. *Am J Perinatol*. 2016;33(4):329-338. doi:10.1055/S-0035-1564881

42. Mayrink J, Souza RT, Feitosa FE, et al. Incidence and risk factors for Preeclampsia in a cohort of healthy nulliparous pregnant women: a nested case-control study. *Scientific Reports 2019 9:1*. 2019;9(1):1-9. doi:10.1038/s41598-019-46011-3

43. Brosens I. A STUDY OF THE SPIRAL ARTERIES OF THE DECIDUA BASALIS IN NORMOTENSIVE AND HYPERTENSIVE PREGNANCIES. *undefined*. 1964;71(2):222-230. doi:10.1111/J.1471-0528.1964.TB04270.X

44. Redman CWG. Immunological aspects of pre-eclampsia. *Bailliere's clinical obstetrics and gynaecology*. 1992;6(3):601-615. doi:10.1016/S0950-3552(05)80012-4

45. Redman CWG, Sacks GP, Sargent IL. Preeclampsia: An excessive maternal inflammatory response to pregnancy. *American Journal of Obstetrics and Gynecology*. Published online 1999. doi:10.1016/S0002-9378(99)70239-5

46. Ahmed A. Heparin-binding angiogenic growth factors in pregnancy: A review. *Placenta*. 1997;18:215-258. doi:10.1016/S0143-4004(97)80091-4

47. Wallukat G, Homuth V, Fischer T, et al. Patients with preeclampsia develop agonistic autoantibodies against the angiotensin AT1 receptor. *J Clin Invest*. 1999;103(7):945-952. doi:10.1172/JCI4106

48. Dechend R, Viedt C, Müller DN, et al. AT1 receptor agonistic antibodies from preeclamptic patients stimulate NADPH oxidase. *Circulation*. 2003;107(12):1632-1639. doi:10.1161/01.CIR.0000058200.90059.B1

49. Redman CWG, Tannetta DS, Dragovic RA, et al. Review: Does size matter? Placental debris and the pathophysiology of pre-eclampsia. *Placenta*. 2012;33:S48-S54. doi:10.1016/j.placenta.2011.12.006

50. Rusterholz C, Messerli M, Hoesli I, Hahn S. Placental microparticles, DNA, and RNA in preeclampsia. *Hypertension in Pregnancy*. 2010;30(3):364-375. doi:10.3109/10641951003599571

51. Nakahara A, Nair S, Ormazabal V, et al. Circulating Placental Extracellular Vesicles and Their Potential Roles During Pregnancy. *Ochsner J*. 2020;20(4):439-445. doi:10.31486/TOJ.20.0049

52. Gupta AK, Rusterholz C, Huppertz B, et al. A comparative study of the effect of three different syncytiotrophoblast micro-particles preparations on endothelial cells. *Placenta*. 2005;26(1):59-66. doi:10.1016/J.PLACENTA.2004.04.004

53. Aly AS, Khandelwal M, Zhao J, Mehmet AH, Sammel MD, Parry S. Neutrophils are stimulated by syncytiotrophoblast microvillous membranes to generate superoxide radicals in women with preeclampsia. *Am J Obstet Gynecol*. 2004;190(1):252-258. doi:10.1016/J.AJOG.2003.07.003

54. Hoegh AM, Tannetta D, Sargent I, et al. Effect of syncytiotrophoblast microvillous membrane treatment on gene expression in human umbilical vein endothelial cells. *BJOG*. 2006;113(11):1270-1279. doi:10.1111/J.1471-0528.2006.01061.X

55. Chen Y, Huang Y, Jiang R, Teng Y. Syncytiotrophoblast-derived microparticle shedding in early-onset and late-onset severe pre-eclampsia. *International Journal of Gynecology and Obstetrics*. Published online 2012. doi:10.1016/j.ijgo.2012.07.010

56. Dragovic RA, Southcombe JH, Tannetta DS, Redman CWG, Sargent IL. Multicolor flow cytometry and nanoparticle tracking analysis of extracellular vesicles in the plasma of normal pregnant and pre-eclamptic women. *Biol Reprod*. 2013;89(6). doi:10.1095/BIOLREPROD.113.113266

57. Cronqvist T, Saljé K, Familari M, et al. Syncytiotrophoblast vesicles show altered micro-RNA and haemoglobin content after ex-vivo perfusion of placentas with haemoglobin to mimic preeclampsia. *PLoS One*. 2014;9(2). doi:10.1371/JOURNAL.PONE.0090020

58. Théry C, Witwer KW, Aikawa E, et al. Minimal information for studies of extracellular vesicles 2018 (MISEV2018): a position statement of the International Society for Extracellular Vesicles and update of the MISEV2014 guidelines. *Journal of Extracellular Vesicles*. 2018;7(1):1-43. doi:10.1080/20013078.2018.1535750

59. Kerr JFR, Wyllie AH, Currie AR. Apoptosis: a basic biological phenomenon with wide-ranging implications in tissue kinetics. *Br J Cancer*. 1972;26(4):239-257. doi:10.1038/BJC.1972.33

60. Buzas EI, György B, Nagy G, Falus A, Gay S. Emerging role of extracellular vesicles in inflammatory diseases. *Nat Rev Rheumatol*. 2014;10(6):356-364. doi:10.1038/NRRHEUM.2014.19

61. Pavlyukov MS, Yu H, Bastola S, et al. Apoptotic Cell-Derived Extracellular Vesicles Promote Malignancy of Glioblastoma Via Intercellular Transfer of Splicing Factors. *Cancer Cell*. 2018;34(1):119-135.e10. doi:10.1016/J.CCELL.2018.05.012

62. Santavanond JP, Rutter SF, Atkin-Smith GK, Poon IKH. Apoptotic Bodies: Mechanism of Formation, Isolation and Functional Relevance. *Subcell Biochem*. 2021;97:61-88. doi:10.1007/978-3-030-67171-6_4

63. Smith NC, Brush MG, Luckett S. Preparation of human placental villous surface membrane. *Nature 1974 252:5481*. 1974;252(5481):302-303. doi:10.1038/252302b0

64. Schneider H, Panigel M, Dancis J. Transfer across the perfused human placenta of antipyrine, sodium and leucine. *Am J Obstet Gynecol*. 1972;114(6):822-828. doi:10.1016/0002-9378(72)90909-X

65. Tong M, Chamley LW. Isolation and Characterization of Extracellular Vesicles from Ex Vivo Cultured Human Placental Explants. *Methods Mol Biol*. 2018;1710:117-129. doi:10.1007/978-1-4939-7498-6_9

66. Levine L, Habertheuer A, Ram C, et al. Syncytiotrophoblast extracellular microvesicle profiles in maternal circulation for noninvasive diagnosis of preeclampsia. *Scientific Reports 2020 10:1*. 2020;10(1):1-11. doi:10.1038/s41598-020-62193-7

67. Lee SM, Romero R, Lee YJ, Park IS, Park CW, Yoon BH. Systemic inflammatory stimulation by microparticles derived from hypoxic trophoblast as a model for inflammatory response in preeclampsia. *Am J Obstet Gynecol*. 2012;207(4):337.e1-337.e8. doi:10.1016/J.AJOG.2012.06.047

68. Cross CE, Tolba MF, Rondelli CM, Xu M, Abdel-Rahman SZ. Oxidative Stress Alters miRNA and Gene Expression Profiles in Villous First Trimester Trophoblasts. *Biomed Res Int*. 2015;2015. doi:10.1155/2015/257090

69. Taylor SK, Houshdaran S, Robinson JF, et al. Cytotrophoblast extracellular vesicles enhance decidual cell secretion of immune modulators via TNFα. *Development*. 2020;147(17). doi:10.1242/DEV.187013

70. Gupta AK, Rusterholz C, Huppertz B, et al. A comparative study of the effect of three different syncytiotrophoblast micro-particles preparations on endothelial cells. *Placenta*. 2005;26(1):59-66. doi:10.1016/J.PLACENTA.2004.04.004

71. Smyth T, Kullberg M, Malik N, Smith-Jones P, Graner MW, Anchordoquy TJ. Biodistribution and delivery efficiency of unmodified tumor-derived exosomes. *J Control Release*. 2015;199:145-155. doi:10.1016/J.JCONREL.2014.12.013

72. Faruqu FN, Wang JTW, Xu L, et al. Membrane Radiolabelling of Exosomes for Comparative Biodistribution Analysis in Immunocompetent and Immunodeficient Mice - A Novel and Universal Approach. *Theranostics*. 2019;9(6):1666. doi:10.7150/THNO.27891

73. Kang M, Jordan V, Blenkiron C, Chamley LW. Biodistribution of extracellular vesicles following administration into animals: A systematic review. *Journal of Extracellular Vesicles*. 2021;10(8):e12085. doi:10.1002/JEV2.12085

74. Tong M, Chen Q, James JL, Wise MR, Stone PR, Chamley LW. In vivo targets of human placental micro-vesicles vary with exposure time and pregnancy. *Reproduction*. 2017;153(6):835-845. doi:10.1530/REP-16-0615

75. Nguyen SL, Ahn SH, Greenberg JW, et al. Integrins mediate placental extracellular vesicle trafficking to lung and liver in vivo. *Scientific Reports 2021 11:1*. 2021;11(1):1-16. doi:10.1038/s41598-021-82752-w

76. Ostenfeld MS, Jensen SG, Jeppesen DK, et al. miRNA profiling of circulating EpCAM(+) extracellular vesicles: promising biomarkers of colorectal cancer. *J Extracell Vesicles*. 2016;5(1). doi:10.3402/JEV.V5.31488

77. Dragovic RA, Southcombe JH, Tannetta DS, Redman CWG, Sargent IL. Multicolor flow cytometry and nanoparticle tracking analysis of extracellular vesicles in the plasma of normal pregnant and pre-eclamptic women. *Biol Reprod*. 2013;89(6). doi:10.1095/BIOLREPROD.113.113266

78. Herrera-Van Oostdam AS, Toro-Ortíz JC, López JA, et al. Placental exosomes isolated from urine of patients with gestational diabetes exhibit a differential profile expression of microRNAs across gestation. *International Journal of Molecular Medicine*. 2020;46(2):546-560. doi:10.3892/IJMM.2020.4626/HTML

79. Rajakumar A, Cerdeira AS, Rana S, et al. Transcriptionally active syncytial aggregates in the maternal circulation may contribute to circulating soluble fms-like tyrosine kinase 1 in preeclampsia. *Hypertension*. 2012;59(2):256-264. doi:10.1161/HYPERTENSIONAHA.111.182170

80. Goswamia D, Tannetta DS, Magee LA, et al. Excess syncytiotrophoblast microparticle shedding is a feature of early-onset pre-eclampsia, but not normotensive intrauterine growth restriction. *Placenta*. 2006;27(1):56-61. doi:10.1016/J.PLACENTA.2004.11.007

81. Reddy A, Zhong XY, Rusterholz C, et al. The effect of labour and placental separation on the shedding of syncytiotrophoblast microparticles, cell-free DNA and mRNA in normal pregnancy and pre-eclampsia. *Placenta*. 2008;29(11):942-949. doi:10.1016/J.PLACENTA.2008.08.018

82. Hessvik NP, Llorente A. Current knowledge on exosome biogenesis and release. *Cell Mol Life Sci*. 2018;75(2):193-208. doi:10.1007/S00018-017-2595-9

83. Essandoh K, Fan GC. Insights into the Mechanism of Exosome Formation and Secretion. *Mesenchymal Stem Cell Derived Exosomes: The Potential for Translational Nanomedicine*. Published online January 1, 2015:1-19. doi:10.1016/B978-0-12-800164-6.00001-0

84. SOTELO JR, PORTER KR. An Electron Microscope Study of the Rat Ovum. *The Journal of Biophysical and Biochemical Cytology*. 1959;5(2):327. doi:10.1083/JCB.5.2.327

85. Regina Todeschini A, Hakomori S itiroh. Functional role of glycosphingolipids and gangliosides in control of cell adhesion, motility, and growth, through glycosynaptic microdomains. *Biochim Biophys Acta*. 2008;1780(3):421-433. doi:10.1016/J.BBAGEN.2007.10.008

86. Charrin S, Manié S, Thiele C, et al. A physical and functional link between cholesterol and tetraspanins. *Eur J Immunol*. 2003;33(9):2479-2489. doi:10.1002/EJI.200323884

87. McCullough J, Fisher RD, Whitby FG, Sundquist WI, Hill CP. ALIX-CHMP4 interactions in the human ESCRT pathway. *Proc Natl Acad Sci U S A*. 2008;105(22):7687-7691. doi:10.1073/PNAS.0801567105

88. Baietti MF, Zhang Z, Mortier E, et al. Syndecan-syntenin-ALIX regulates the biogenesis of exosomes. *Nat Cell Biol*. 2012;14(7):677-685. doi:10.1038/NCB2502

89. Goñi FM, Alonso A. Effects of ceramide and other simple sphingolipids on membrane lateral structure. *Biochim Biophys Acta*. 2009;1788(1):169-177. doi:10.1016/J.BBAMEM.2008.09.002

90. van Niel G, Charrin S, Simoes S, et al. The tetraspanin CD63 regulates ESCRT-independent and -dependent endosomal sorting during melanogenesis. *Dev Cell*. 2011;21(4):708-721. doi:10.1016/J.DEVCEL.2011.08.019

91. Chairoungdua A, Smith DL, Pochard P, Hull M, Caplan MJ. Exosome release of β-catenin: a novel mechanism that antagonizes Wnt signaling. *J Cell Biol*. 2010;190(6):1079-1091. doi:10.1083/JCB.201002049

92. Tricarico C, Clancy J, D'Souza-Schorey C. Biology and biogenesis of shed microvesicles. *Small GTPases*. 2017;8(4):220-232. doi:10.1080/21541248.2016.1215283

93. Kerr JFR, Wyllie AH, Currie AR. Apoptosis: a basic biological phenomenon with wide-ranging implications in tissue kinetics. *Br J Cancer*. 1972;26(4):239-257. doi:10.1038/BJC.1972.33

94. Elmore S. Apoptosis: A Review of Programmed Cell Death. *Toxicol Pathol*. 2007;35(4):495. doi:10.1080/01926230701320337

95. Taylor RC, Cullen SP, Martin SJ. Apoptosis: controlled demolition at the cellular level. *Nature Reviews Molecular Cell Biology 2008 9:3*. 2008;9(3):231-241. doi:10.1038/nrm2312

96. Erwig LP, Henson PM. Clearance of apoptotic cells by phagocytes. *Cell Death Differ*. 2008;15(2):243-250. doi:10.1038/SJ.CDD.4402184

97. Villarroya-Beltri C, Baixauli F, Gutiérrez-Vázquez C, Sánchez-Madrid F, Mittelbrunn M. Sorting it out: regulation of exosome loading. *Semin Cancer Biol*. 2014;28:3-13. doi:10.1016/J.SEMCANCER.2014.04.009

98. Moreno-Gonzalo O, Villarroya-Beltri C, Sánchez-Madrid F. Post-Translational Modifications of Exosomal Proteins. *Frontiers in Immunology*. 2014;5(AUG). doi:10.3389/FIMMU.2014.00383

99. Yuyama K, Sun H, Mitsutake S, Igarashi Y. Sphingolipid-modulated exosome secretion promotes clearance of amyloid-β by microglia. *J Biol Chem*. 2012;287(14):10977-10989. doi:10.1074/JBC.M111.324616

100. Mittelbrunn M, Gutiérrez-Vázquez C, Villarroya-Beltri C, et al. Unidirectional transfer of microRNA-loaded exosomes from T cells to antigen-presenting cells. *Nature Communications 2011 2:1*. 2011;2(1):1-10. doi:10.1038/ncomms1285

101. Garcia-Martin R, Wang G, Brandão BB, et al. MicroRNA sequence codes for small extracellular vesicle release and cellular retention. *Nature 2021 601:7893*. 2021;601(7893):446-451. doi:10.1038/s41586-021-04234-3

102. Groot M, Lee H. Sorting Mechanisms for MicroRNAs into Extracellular Vesicles and Their Associated Diseases. *Cells*. 2020;9(4). doi:10.3390/CELLS9041044

103. McKenzie AJ, Hoshino D, Hong NH, et al. KRAS-MEK Signaling Controls Ago2 Sorting into Exosomes. *Cell Rep*. 2016;15(5):978-987. doi:10.1016/J.CELREP.2016.03.085

104. Shurtleff MJ, Temoche-Diaz MM, Karfilis K v., Ri S, Schekman R. Y-box protein 1 is required to sort microRNAs into exosomes in cells and in a cell-free reaction. *Elife*. 2016;5(AUGUST). doi:10.7554/ELIFE.19276

105. Cha DJ, Franklin JL, Dou Y, et al. KRAS-dependent sorting of miRNA to exosomes. *Elife*. 2015;4(JULY 2015). doi:10.7554/ELIFE.07197

106. Guduric-Fuchs J, O'Connor A, Camp B, O'Neill CL, Medina RJ, Simpson DA. Selective extracellular vesicle-mediated export of an overlapping set of microRNAs from multiple cell types. *BMC Genomics*. 2012;13(1). doi:10.1186/1471-2164-13-357

107. Villarroya-Beltri C, Gutiérrez-Vázquez C, Sánchez-Cabo F, et al. Sumoylated hnRNPA2B1 controls the sorting of miRNAs into exosomes through binding to specific motifs. *Nature Communications 2013 4:1*. 2013;4(1):1-10. doi:10.1038/ncomms3980

108. Groot M, Lee H. Sorting Mechanisms for MicroRNAs into Extracellular Vesicles and Their Associated Diseases. *Cells*. 2020;9(4). doi:10.3390/CELLS9041044

109. Anand S, Samuel M, Kumar S, Mathivanan S. Ticket to a bubble ride: Cargo sorting into exosomes and extracellular vesicles. *Biochimica et Biophysica Acta (BBA) - Proteins and Proteomics*. 2019;1867(12):140203. doi:10.1016/J.BBAPAP.2019.02.005

110. Villarroya-Beltri C, Baixauli F, Gutiérrez-Vázquez C, Sánchez-Madrid F, Mittelbrunn M. Sorting it out: regulation of exosome loading. *Semin Cancer Biol*. 2014;28:3-13. doi:10.1016/J.SEMCANCER.2014.04.009

111. Christianson HC, Svensson KJ, van Kuppevelt TH, Li JP, Belting M. Cancer cell exosomes depend on cell-surface heparan sulfate proteoglycans for their internalization and functional

activity. *Proc Natl Acad Sci U S A*. 2013;110(43):17380-17385. doi:10.1073/PNAS.1304266110/-/DCSUPPLEMENTAL/PNAS.201304266SI.PDF

112. Escrevente C, Keller S, Altevogt P, Costa J. Interaction and uptake of exosomes by ovarian cancer cells. *BMC Cancer*. 2011;11(1):1-10. doi:10.1186/1471-2407-11-108/FIGURES/6

113. Costa Verdera H, Gitz-Francois JJ, Schiffelers RM, Vader P. Cellular uptake of extracellular vesicles is mediated by clathrin-independent endocytosis and macropinocytosis. *J Control Release*. 2017;266:100-108. doi:10.1016/J.JCONREL.2017.09.019

114. Fitzner D, Schnaars M, van Rossum D, et al. Selective transfer of exosomes from oligodendrocytes to microglia by macropinocytosis. *J Cell Sci*. 2011;124(Pt 3):447-458. doi:10.1242/JCS.074088

115. Parolini I, Federici C, Raggi C, et al. Microenvironmental pH is a key factor for exosome traffic in tumor cells. *J Biol Chem*. 2009;284(49):34211-34222. doi:10.1074/JBC.M109.041152

116. Franzen CA, Simms PE, van Huis AF, Foreman KE, Kuo PC, Gupta GN. Characterization of uptake and internalization of exosomes by bladder cancer cells. *Biomed Res Int*. 2014;2014. doi:10.1155/2014/619829

117. Barrès C, Blanc L, Bette-Bobillo P, et al. Galectin-5 is bound onto the surface of rat reticulocyte exosomes and modulates vesicle uptake by macrophages. *Blood*. 2010;115(3):696-705. doi:10.1182/BLOOD-2009-07-231449

118. Skokos D, Botros HG, Demeure C, et al. Mast cell-derived exosomes induce phenotypic and functional maturation of dendritic cells and elicit specific immune responses in vivo. *J Immunol*. 2003;170(6):3037-3045. doi:10.4049/JIMMUNOL.170.6.3037

119. Hao S, Bai O, Li F, Yuan J, Laferte S, Xiang J. Mature dendritic cells pulsed with exosomes stimulate efficient cytotoxic T-lymphocyte responses and antitumour immunity. *Immunology*. 2007;120(1):90. doi:10.1111/J.1365-2567.2006.02483.X

120. Atay S, Gercel-Taylor C, Taylor DD. Human trophoblast-derived exosomal fibronectin induces pro-inflammatory IL-1β production by macrophages. *Am J Reprod Immunol*. 2011;66(4):259-269. doi:10.1111/J.1600-0897.2011.00995.X

121. Fitzner D, Schnaars M, van Rossum D, et al. Selective transfer of exosomes from oligodendrocytes to microglia by macropinocytosis. *Journal of Cell Science*. 2011;124(3):447-458. doi:10.1242/JCS.074088

122. Izquierdo-Useros N, Naranjo-Gómez M, Archer J, et al. Capture and transfer of HIV-1 particles by mature dendritic cells converges with the exosome-dissemination pathway. *Blood*. 2009;113(12):2732-2741. doi:10.1182/BLOOD-2008-05-158642

123. Montecalvo A, Larregina AT, Shufesky WJ, et al. Mechanism of transfer of functional microRNAs between mouse dendritic cells via exosomes. *Blood*. 2012;119(3):756-766. doi:10.1182/BLOOD-2011-02-338004

124. Svensson KJ, Christianson HC, Wittrup A, et al. Exosome uptake depends on ERK1/2-heat shock protein 27 signaling and lipid Raft-mediated endocytosis negatively regulated by caveolin-1. *J Biol Chem*. 2013;288(24):17713-17724. doi:10.1074/JBC.M112.445403

125. Feng D, Zhao WL, Ye YY, et al. Cellular internalization of exosomes occurs through phagocytosis. *Traffic*. 2010;11(5):675-687. doi:10.1111/J.1600-0854.2010.01041.X

126. Parolini I, Federici C, Raggi C, et al. Microenvironmental pH is a key factor for exosome traffic in tumor cells. *J Biol Chem*. 2009;284(49):34211-34222. doi:10.1074/JBC.M109.041152

127. Cronqvist T, Tannetta D, Mörgelin M, et al. Syncytiotrophoblast derived extracellular vesicles transfer functional placental miRNAs to primary human endothelial cells. *Scientific Reports 2017 7:1*. 2017;7(1):1-14. doi:10.1038/s41598-017-04468-0

128. Vargas A, Zhou S, Eťhier-Chiasson M, et al. Syncytin proteins incorporated in placenta exosomes are important for cell uptake and show variation in abundance in serum exosomes from patients with preeclampsia. *FASEB J*. 2014;28(8):3703-3719. doi:10.1096/FJ.13-239053

129. Norouzi-Barough L, Sarookhani MR, Sharifi M, Moghbelinejad S, Jangjoo S, Salehi R. Molecular mechanisms of drug resistance in ovarian cancer. *J Cell Physiol*. 2018;233(6):4546-4562. doi:10.1002/JCP.26289

130. Acunzo M, Romano G, Wernicke D, Croce CM. MicroRNA and cancer--a brief overview. *Adv Biol Regul*. 2015;57:1-9. doi:10.1016/J.JBIOR.2014.09.013

131. Pös O, Biró O, Szemes T, Nagy B. Circulating cell-free nucleic acids: characteristics and applications. *European Journal of Human Genetics 2018 26:7*. 2018;26(7):937-945. doi:10.1038/s41431-018-0132-4

132. Wu L, Zhou H, Lin H, et al. Circulating microRNAs are elevated in plasma from severe preeclamptic pregnancies. *Reproduction*. 2012;143(3):389-397. doi:10.1530/REP-11-0304

133. Stubert J, Koczan D, Richter DU, et al. miRNA expression profiles determined in maternal sera of patients with HELLP syndrome. *Hypertens Pregnancy*. 2014;33(2):215-235. doi:10.3109/10641955.2013.858743

134. Yang Q, Lu J, Wang S, Li H, Ge Q, Lu Z. Application of next-generation sequencing technology to profile the circulating microRNAs in the serum of preeclampsia versus normal pregnant women. *Clin Chim Acta*. 2011;412(23-24):2167-2173. doi:10.1016/J.CCA.2011.07.029

135. Gunel T, Hosseini MK, Gumusoglu E, Kisakesen HI, Benian A, Aydinli K. Expression profiling of maternal plasma and placenta microRNAs in preeclamptic pregnancies by microarray technology. *Placenta*. 2017;52:77-85. doi:10.1016/J.PLACENTA.2017.02.019

136. Ura B, Feriotto G, Monasta L, Bilel S, Zweyer M, Celeghini C. Potential role of circulating microRNAs as early markers of preeclampsia. *Taiwan J Obstet Gynecol*. 2014;53(2):232-234. doi:10.1016/J.TJOG.2014.03.001

137. Rajakumar A, Cerdeira AS, Rana S, et al. Transcriptionally active syncytial aggregates in the maternal circulation may contribute to circulating soluble fms-like tyrosine kinase 1 in preeclampsia. *Hypertension*. 2012;59(2):256-264. doi:10.1161/HYPERTENSIONAHA.111.182170

138. Ahmad S, Ahmed A. Elevated placental soluble vascular endothelial growth factor receptor-1 inhibits angiogenesis in preeclampsia. *Circ Res*. 2004;95(9):884-891. doi:10.1161/01.RES.0000147365.86159.F5

139. Chaiworapongsa T, Romero R, Kim YM, et al. Plasma soluble vascular endothelial growth factor receptor-1 concentration is elevated prior to the clinical diagnosis of pre-eclampsia. *J Matern Fetal Neonatal Med*. 2005;17(1):3-18. doi:10.1080/14767050400028816

140. Gill M, Motta-Mejia C, Kandzija N, et al. Placental Syncytiotrophoblast-Derived Extracellular Vesicles Carry Active NEP (Neprilysin) and Are Increased in Preeclampsia. *Hypertension*. 2019;73(5):1112-1119. doi:10.1161/HYPERTENSIONAHA.119.12707

141. Landers KA, Mortimer RH, Richard K. Transthyretin and the human placenta. *Placenta*. 2013;34(7):513-517. doi:10.1016/J.PLACENTA.2013.04.013

142. Tong M, Cheng S bin, Chen Q, et al. Aggregated transthyretin is specifically packaged into placental nano-vesicles in preeclampsia. *Scientific Reports 2017 7:1*. 2017;7(1):1-9. doi:10.1038/s41598-017-07017-x

143. Awoyemi T, Tannetta D, Zhang W, et al. Glycosylated Siglec-6 expression in syncytiotrophoblast-derived extracellular vesicles from preeclampsia placentas. *Biochemical and Biophysical Research Communications*. 2020;533(4):838-844. doi:10.1016/J.BBRC.2020.09.081

144. Zhang M, Angata T, Jae YC, Miller M, Broide DH, Varki A. Defining the in vivo function of Siglec-F, a CD33-related Siglec expressed on mouse eosinophils. *Blood*. 2007;109(10):4280-4287. doi:10.1182/BLOOD-2006-08-039255

145. Crocker PR, Paulson JC, Varki A. Siglecs and their roles in the immune system. *Nature Reviews Immunology 2007 7:4*. 2007;7(4):255-266. doi:10.1038/nri2056

146. Sladek SM, Magness RR, Conrad KP. Nitric oxide and pregnancy. *Am J Physiol*. 1997;272(2 Pt 2). doi:10.1152/AJPREGU.1997.272.2.R441

147. Motta-Mejia C, Kandzija N, Zhang W, et al. Placental Vesicles Carry Active Endothelial Nitric Oxide Synthase and Their Activity is Reduced in Preeclampsia. *Hypertension*. 2017;70(2):372-381. doi:10.1161/HYPERTENSIONAHA.117.09321/-/DC1

148. Sammar M, Dragovic R, Meiri H, et al. Reduced placental protein 13 (PP13) in placental derived syncytiotrophoblast extracellular vesicles in preeclampsia - A novel tool to study the impaired cargo transmission of the placenta to the maternal organs. *undefined*. 2018;66:17-25. doi:10.1016/J.PLACENTA.2018.04.013

149. Al-Ofi E, Anumba DOC, Coffelt S. OS006. Functional expression of endogenous ligands of Toll like receptor4 on monocytes and placentae from women during normal pregnancy andpre-eclampsia. *Pregnancy Hypertension: An International Journal of Women's Cardiovascular Health*. 2012;2(3):178. doi:10.1016/J.PREGHY.2012.04.008

150. Bobek G, Surmon L, Mirabito KM, Makris A, Hennessy A. Placental Regulation of Inflammation and Hypoxia after TNF-α Infusion in Mice. *American Journal of Reproductive Immunology*. 2015;74(5):407-418. doi:10.1111/AJI.12417

151. Gupta AK, Rusterholz C, Holzgreve W, Hahn S. Syncytiotrophoblast micro-particles do not induce apoptosis in peripheral T lymphocytes, but differ in their activity depending on the mode of preparation. *J Reprod Immunol*. 2005;68(1-2):15-26. doi:10.1016/J.JRI.2005.05.003

152. Messerli M, May K, Hansson SR, et al. Feto-maternal interactions in pregnancies: placental microparticles activate peripheral blood monocytes. *Placenta*. 2010;31(2):106-112. doi:10.1016/J.PLACENTA.2009.11.011

153. Joerger-Messerli MS, Hoesli IM, Rusterholz C, Lapaire O. Stimulation of monocytes by placental microparticles involves toll-like receptors and nuclear factor kappa-light-chain-enhancer of activated B cells. *Front Immunol*. 2014;5(APR). doi:10.3389/FIMMU.2014.00173

154. Chang X, Yao J, He Q, Liu M, Duan T, Wang K. Exosomes from women with preeclampsia induced vascular dysfunction by delivering sFLT (soluble fms-like tyrosine kinase)-1 and SENG (soluble endoglin) to endothelial cells. *Hypertension*. 2018;72(6):1381-1390. doi:10.1161/HYPERTENSIONAHA.118.11706

155. Nielsen CT, Østergaard O, Johnsen C, Jacobsen S, Heegaard NHH. Distinct features of circulating microparticles and their relationship to clinical manifestations in systemic lupus erythematosus. *Arthritis Rheum*. 2011;63(10):3067-3077. doi:10.1002/ART.30499

156. Tannetta DS, Dragovic RA, Gardiner C, Redman CW, Sargent IL. Characterisation of Syncytiotrophoblast Vesicles in Normal Pregnancy and Pre-Eclampsia: Expression of Flt-1 and Endoglin. *PLOS ONE*. 2013;8(2):e56754. doi:10.1371/JOURNAL.PONE.0056754

157. Tannetta DS, Hunt K, Jones CI, et al. Syncytiotrophoblast Extracellular Vesicles from Pre-Eclampsia Placentas Differentially Affect Platelet Function. *PLOS ONE*. 2015;10(11):e0142538. doi:10.1371/JOURNAL.PONE.0142538

158. Gardiner C, Tannetta DS, Simms CA, Harrison P, Redman CWG, Sargent IL. Syncytiotrophoblast Microvesicles Released from Pre-Eclampsia Placentae Exhibit Increased Tissue Factor Activity. *PLOS ONE*. 2011;6(10):e26313. doi:10.1371/JOURNAL.PONE.0026313

159. Owens AP, MacKman N. Microparticles in hemostasis and thrombosis. *Circ Res*. 2011;108(10):1284-1297. doi:10.1161/CIRCRESAHA.110.233056

160. Guller S, Tang Z, Ma YY, di Santo S, Sager R, Schneider H. Protein composition of microparticles shed from human placenta during placental perfusion: Potential role in angiogenesis and fibrinolysis in preeclampsia. *Placenta*. 2011;32(1):63-69. doi:10.1016/J.PLACENTA.2010.10.011

161. Lacroix R, Judicone C, Mooberry M, et al. Standardization of pre-analytical variables in plasma microparticle determination: results of the International Society on Thrombosis and Haemostasis SSC Collaborative workshop. *J Thromb Haemost*. 2013;11(6):1190-1193. doi:10.1111/JTH.12207

162. Eijndhoven MAJ van, Zijlstra JM, Groenewegen NJ, et al. Plasma vesicle miRNAs for therapy response monitoring in Hodgkin lymphoma patients. *JCI Insight*. 2016;1(19). doi:10.1172/JCI.INSIGHT.89631

163. LeFevre ML. Low-dose aspirin use for the prevention of morbidity and mortality from preeclampsia: U.S. Preventive Services Task Force recommendation statement. *Ann Intern Med*. 2014;161(11):819-826. doi:10.7326/M14-1884

164. Hastie R, Brownfoot FC, Cannon P, et al. Sulfasalazine decreases soluble fms-like tyrosine kinase-1 secretion potentially via inhibition of upstream placental epidermal growth factor receptor signalling. *Placenta*. 2019;87:53-57. doi:10.1016/J.PLACENTA.2019.09.004

165. Roberts JM, Myatt L, Spong CY, et al. Vitamins C and E to prevent complications of pregnancy-associated hypertension. *N Engl J Med*. 2010;362(14):1282-1291. doi:10.1056/NEJMOA0908056

166. Hobson SR, Gurusinghe S, Lim R, et al. Melatonin improves endothelial function in vitro and prolongs pregnancy in women with early-onset preeclampsia. *J Pineal Res*. 2018;65(3). doi:10.1111/JPI.12508

167. Brownfoot FC, Tong S, Hannan NJ, et al. Effects of Pravastatin on Human Placenta, Endothelium, and Women With Severe Preeclampsia. *Hypertension*. 2015;66(3):687-697. doi:10.1161/HYPERTENSIONAHA.115.05445

168. Kumasawa K, Ikawa M, Kidoya H, et al. Pravastatin induces placental growth factor (PGF) and ameliorates preeclampsia in a mouse model. *Proc Natl Acad Sci U S A*. 2011;108(4):1451-1455. doi:10.1073/PNAS.1011293108/-/DCSUPPLEMENTAL

169. Bauer AJ, Banek CT, Needham K, et al. Pravastatin attenuates hypertension, oxidative stress, and angiogenic imbalance in rat model of placental ischemia-induced hypertension. *Hypertension*. 2013;61(5):1103-1110. doi:10.1161/HYPERTENSIONAHA.111.00226

170. Garrett N, Pombo J, Umpierrez M, Clark JE, Simmons M, Girardi G. Pravastatin therapy during preeclampsia prevents long-term adverse health effects in mice. *JCI Insight*. 2018;3(8). doi:10.1172/JCI.INSIGHT.120147

171. Kräker K, O'Driscoll JM, Schütte T, et al. Statins Reverse Postpartum Cardiovascular Dysfunction in a Rat Model of Preeclampsia. *Hypertension*. 2020;75(1):202-210. doi:10.1161/HYPERTENSIONAHA.119.13219

172. Brownfoot FC, Hastie R, Hannan NJ, et al. Metformin as a prevention and treatment for preeclampsia: Effects on soluble fms-like tyrosine kinase 1 and soluble endoglin secretion and endothelial dysfunction. *American Journal of Obstetrics and Gynecology*. 2016;214(3):356.e1-356.e15. doi:10.1016/J.AJOG.2015.12.019/ATTACHMENT/FEC40D1E-DD40-4A3D-8699-2008767E7923/MMC1.PPTX

173. Syngelaki A, Nicolaides KH, Balani J, et al. Metformin versus Placebo in Obese Pregnant Women without Diabetes Mellitus. *New England Journal of Medicine*. 2016;374(5):434-443. doi:10.1056/NEJMOA1509819/SUPPL_FILE/NEJMOA1509819_DISCLOSURES.PDF

174. Alqudah A, McKinley MC, McNally R, et al. Risk of pre-eclampsia in women taking metformin: a systematic review and meta-analysis. *Diabet Med*. 2018;35(2):160-172. doi:10.1111/DME.13523

175. Hastie R, Brownfoot FC, Pritchard N, et al. EGFR (Epidermal Growth Factor Receptor) Signaling and the Mitochondria Regulate sFlt-1 (Soluble FMS-Like Tyrosine Kinase-1) Secretion. *Hypertension*. 2019;73(3):659-670. doi:10.1161/HYPERTENSIONAHA.118.12300

176. Saleh L, Samantar R, Garrelds IM, van den Meiracker AH, Visser W, Danser AHJ. Low Soluble Fms-Like Tyrosine Kinase-1, Endoglin, and Endothelin-1 Levels in Women With Confirmed or Suspected Preeclampsia Using Proton Pump Inhibitors. *Hypertension*. 2017;70(3):594-600. doi:10.1161/HYPERTENSIONAHA.117.09741

177. Hastie R, Bergman L, Cluver CA, et al. Proton pump inhibitors and preeclampsia risk among 157 720 women: A swedish population register-based cohort study. *Hypertension*. 2019;73(5):1097-1103. doi:10.1161/HYPERTENSIONAHA.118.12547

178. Yang Y, Xu P, Zhu F, et al. The Potent Antioxidant MitoQ Protects Against Preeclampsia During Late Gestation but Increases the Risk of Preeclampsia When Administered in Early Pregnancy. *Antioxid Redox Signal*. 2021;34(2):118-136. doi:10.1089/ARS.2019.7891

179. Hannan NJ, Brownfoot FC, Cannon P, et al. Resveratrol inhibits release of soluble fms-like tyrosine kinase (sFlt-1) and soluble endoglin and improves vascular dysfunction - implications as a preeclampsia treatment. *Sci Rep*. 2017;7(1). doi:10.1038/S41598-017-01993-W

180. Williamson RD, McCarthy FP, Manna S, et al. L-(+)-Ergothioneine Significantly Improves the Clinical Characteristics of Preeclampsia in the Reduced Uterine Perfusion Pressure Rat Model. *Hypertension*. Published online 2020:561-568. doi:10.1161/HYPERTENSIONAHA.119.13929

181. da Silva A de S, Nunes DVQ, Carvalho LC dos RM de, et al. Açaí ( Euterpe oleracea Mart) seed extract protects against maternal vascular dysfunction, hypertension, and fetal growth restriction in experimental preeclampsia. *Hypertens Pregnancy*. 2020;39(2):211-219. doi:10.1080/10641955.2020.1754850

182. Keelan JA, Leong JW, Ho D, Iyer KS. Therapeutic and safety considerations of nanoparticle-mediated drug delivery in pregnancy. *Nanomedicine (Lond)*. 2015;10(14):2229-2247. doi:10.2217/NNM.15.48

183. Li L, Yang H, Chen P, et al. Trophoblast-Targeted Nanomedicine Modulates Placental sFLT1 for Preeclampsia Treatment. *Frontiers in Bioengineering and Biotechnology*. 2020;8. doi:10.3389/FBIOE.2020.00064

184. Tüzel-Kox SN, Patel HM, Kox WJ. Uptake of drug-carrier liposomes by placenta: transplacental delivery of drugs and nutrients. *Journal of Pharmacology and Experimental Therapeutics*. 1995;274(1).

185. de Alwis N, Binder NK, Hannan NJ. Pre-eclampsia: Challenges for Nanomedicine Development in Pregnancy. *Trends in Molecular Medicine*. 2021;27(8):824-825. doi:10.1016/J.MOLMED.2021.05.003

186. Haase N, Foster DJ, Cunningham MW, et al. RNA interference therapeutics targeting angiotensinogen ameliorate preeclamptic phenotype in rodent models. *The Journal of Clinical Investigation*. 2020;130(6):2928-2942. doi:10.1172/JCI99417

187. Suvakov S, Richards C, Nikolic V, et al. Emerging Therapeutic Potential of Mesenchymal Stem/Stromal Cells in Preeclampsia. *Current Hypertension Reports*. 2020;22(5):1-13. doi:10.1007/S11906-020-1034-8/TABLES/2

188. Elabd H, Elkholi M, Steinberg L, Acharya A. Eculizumab, a novel potential treatment for acute kidney injury associated with preeclampsia/HELLP syndrome. *BMJ Case Rep*. 2019;12(9). doi:10.1136/BCR-2018-228709

189. Paidas MJ, Tita ATN, Macones GA, et al. Prospective, randomized, double-blind, placebo-controlled evaluation of the Pharmacokinetics, Safety and Efficacy of Recombinant Antithrombin Versus Placebo in Preterm Preeclampsia. *Am J Obstet Gynecol*. 2020;223(5):739.e1-739.e13. doi:10.1016/J.AJOG.2020.08.004

190. Trapani A, Gonçalves LF, Trapani TF, Vieira S, Pires M, Pires MMDS. Perinatal and Hemodynamic Evaluation of Sildenafil Citrate for Preeclampsia Treatment: A Randomized Controlled Trial. *Obstet Gynecol*. 2016;128(2):253-259. doi:10.1097/AOG.0000000000001518

191. Thadhani R, Kisner T, Hagmann H, et al. Pilot study of extracorporeal removal of soluble fms-like tyrosine kinase 1 in preeclampsia. *Circulation*. 2011;124(8):940-950. doi:10.1161/CIRCULATIONAHA.111.034793

192. Thadhani R, Hagmann H, Schaarschmidt W, et al. Removal of soluble fms-like tyrosine kinase-1 by dextran sulfate apheresis in preeclampsia. *Journal of the American Society of Nephrology*. 2016;27(3):903-913. doi:10.1681/ASN.2015020157/-/DCSUPPLEMENTAL

193. Hill AF, Pegtel DM, Lambertz U, et al. ISEV position paper: extracellular vesicle RNA analysis and bioinformatics. *J Extracell Vesicles*. 2013;2(1):22859. doi:10.3402/JEV.V2I0.22859

194. Andrews S. FastQC. *Babraham Bioinformatics*. Published online 2010.

195. Ewels P, Magnusson M, Lundin S, Käller M. MultiQC: summarize analysis results for multiple tools and samples in a single report. *Bioinformatics*. 2016;32(19):3047-3048. doi:10.1093/BIOINFORMATICS/BTW354

196. Bolger AM, Lohse M, Usadel B. Trimmomatic: a flexible trimmer for Illumina sequence data. *Bioinformatics*. 2014;30(15):2114. doi:10.1093/BIOINFORMATICS/BTU170

197. Love MI, Huber W, Anders S. Moderated estimation of fold change and dispersion for RNA-seq data with DESeq2. *Genome Biology*. 2014;15(12):1-21. doi:10.1186/S13059-014-0550-8/FIGURES/9

198. Stephens M. False discovery rates: a new deal. *Biostatistics*. 2017;18(2):275-294. doi:10.1093/BIOSTATISTICS/KXW041

199. Wickham Hadley. *Ggplot2: Elegant Graphics for Data Analysis*. Springer-Verlag ; 2016.

200. Wu T, Hu E, Xu S, et al. clusterProfiler 4.0: A universal enrichment tool for interpreting omics data. *Innovation(China)*. Published online 2021. doi:10.1016/j.xinn.2021.100141

201. Harris MA, Clark J, Ireland A, et al. The Gene Ontology (GO) database and informatics resource. *Nucleic Acids Research*. 2004;32(suppl_1):D258-D261. doi:10.1093/NAR/GKH036

202. Kanehisa M, Sato Y, Kawashima M, Furumichi M, Tanabe M. KEGG as a reference resource for gene and protein annotation. *Nucleic Acids Research*. 2016;44(D1):D457-D462. doi:10.1093/NAR/GKV1070

203. Tarca AL, Draghici S, Khatri P, et al. A novel signaling pathway impact analysis. *Bioinformatics*. 2009;25(1):75. doi:10.1093/BIOINFORMATICS/BTN577

204. Livak KJ, Schmittgen TD. Analysis of relative gene expression data using real-time quantitative PCR and the 2(-Delta Delta C(T)) Method. *Methods*. 2001;25(4):402-408. doi:10.1006/METH.2001.1262

205. Rahman RU, Gautam A, Bethune J, et al. Oasis 2: improved online analysis of small RNA-seq data. *BMC Bioinformatics*. 2018;19(1). doi:10.1186/S12859-018-2047-Z

206. Dobin A, Davis CA, Schlesinger F, et al. STAR: ultrafast universal RNA-seq aligner. *Bioinformatics*. 2013;29(1):15. doi:10.1093/BIOINFORMATICS/BTS635

207. Wood DE, Salzberg SL. Kraken: Ultrafast metagenomic sequence classification using exact alignments. *Genome Biology*. 2014;15(3):1-12. doi:10.1186/GB-2014-15-3-R46/FIGURES/5

208. Griffiths-Jones S, Grocock RJ, van Dongen S, Bateman A, Enright AJ. miRBase: microRNA sequences, targets and gene nomenclature. *Nucleic Acids Res*. 2006;34(Database issue). doi:10.1093/NAR/GKJ112

209. Rahman RU, Gautam A, Bethune J, et al. Oasis 2: Improved online analysis of small RNA-seq data. *BMC Bioinformatics*. 2018;19(1):1-10. doi:10.1186/S12859-018-2047-Z/FIGURES/3

210. Digre A, Lindskog C. The Human Protein Atlas—Spatial localization of the human proteome in health and disease. *Protein Science*. Published online 2021. doi:10.1002/pro.3987

211. Aldridge GM, Podrebarac DM, Greenough WT, Weiler IJ. The use of total protein stains as loading controls: an alternative to high-abundance single-protein controls in semi-quantitative immunoblotting. *J Neurosci Methods*. 2008;172(2):250-254. doi:10.1016/J.JNEUMETH.2008.05.003

212. Lanoix D, St-Pierre J, Lacasse AA, Viau M, Lafond J, Vaillancourt C. Stability of reference proteins in human placenta: general protein stains are the benchmark. *Placenta*. 2012;33(3):151-156. doi:10.1016/J.PLACENTA.2011.12.008

213. Schindelin J, Arganda-Carreras I, Frise E, et al. Fiji: an open-source platform for biological-image analysis. *Nat Methods*. 2012;9(7):676-682. doi:10.1038/NMETH.2019

214. L'Yi S, Jung D, Oh M, et al. miRTarVis+: Web-based interactive visual analytics tool for microRNA target predictions. *Methods*. 2017;124:78-88. doi:10.1016/J.YMETH.2017.06.004

215. Friedman RC, Farh KKH, Burge CB, Bartel DP. Most mammalian mRNAs are conserved targets of microRNAs. *Genome Res*. 2009;19(1):92-105. doi:10.1101/GR.082701.108

216. Grimson A, Farh KKH, Johnston WK, Garrett-Engele P, Lim LP, Bartel DP. MicroRNA targeting specificity in mammals: determinants beyond seed pairing. *Mol Cell*. 2007;27(1):91-105. doi:10.1016/J.MOLCEL.2007.06.017

217. Szklarczyk D, Gable AL, Lyon D, et al. STRING v11: protein-protein association networks with increased coverage, supporting functional discovery in genome-wide experimental datasets. *Nucleic Acids Res*. 2019;47(D1):D607-D613. doi:10.1093/NAR/GKY1131

218. Shannon P, Markiel A, Ozier O, et al. Cytoscape: a software environment for integrated models of biomolecular interaction networks. *Genome Res*. 2003;13(11):2498-2504. doi:10.1101/GR.1239303

219. Chin CH, Chen SH, Wu HH, Ho CW, Ko MT, Lin CY. cytoHubba: Identifying hub objects and sub-networks from complex interactome. *BMC Systems Biology*. 2014;8(4):1-7. doi:10.1186/1752-0509-8-S4-S11/TABLES/4

220. Raudvere U, Kolberg L, Kuzmin I, et al. g:Profiler: a web server for functional enrichment analysis and conversions of gene lists (2019 update). *Nucleic Acids Res*. 2019;47(W1):W191-W198. doi:10.1093/NAR/GKZ369

221. Bindea G, Mlecnik B, Hackl H, et al. ClueGO: a Cytoscape plug-in to decipher functionally grouped gene ontology and pathway annotation networks. *Bioinformatics*. 2009;25(8):1091-1093. doi:10.1093/BIOINFORMATICS/BTP101

222. Lamb J, Crawford ED, Peck D, et al. The connectivity map: Using gene-expression signatures to connect small molecules, genes, and disease. *Science (1979)*. 2006;313(5795):1929-1935. doi:10.1126/SCIENCE.1132939

223. Redman C. Pre-eclampsia: A complex and variable disease. *Pregnancy Hypertens*. 2014;4(3):241-242. doi:10.1016/J.PREGHY.2014.04.009

224. Yáñez-Mó M, Siljander PRM, Andreu Z, et al. Biological properties of extracellular vesicles and their physiological functions. *Journal of Extracellular Vesicles*. Published online 2015. doi:10.3402/jev.v4.27066

225. Théry C, Witwer KW, Aikawa E, et al. Minimal information for studies of extracellular vesicles 2018 (MISEV2018): a position statement of the International Society for Extracellular Vesicles and update of the MISEV2014 guidelines. *Journal of Extracellular Vesicles*. 2018;7(1):1-43. doi:10.1080/20013078.2018.1535750

226. Colombo M, Raposo G, Théry C. Biogenesis, secretion, and intercellular interactions of exosomes and other extracellular vesicles. *Annu Rev Cell Dev Biol*. Published online 2014. doi:10.1146/annurev-cellbio-101512-122326

227. Rumer KK, Uyenishi J, Hoffman MC, Fisher BM, Winn VD. Siglec-6 expression is increased in placentas from pregnancies complicated by preterm preeclampsia. *Reproductive Sciences*. Published online 2013. doi:10.1177/1933719112461185

228. Tsai S, Hardison NE, James AH, et al. Transcriptional profiling of human placentas from pregnancies complicated by preeclampsia reveals disregulation of sialic acid acetylesterase and immune signalling pathways. *Placenta*. Published online 2011. doi:10.1016/j.placenta.2010.11.014

229. Ren Z, Gao Y, Gao Y, et al. Distinct placental molecular processes associated with early-onset and late-onset preeclampsia. *Theranostics*. Published online 2021. doi:10.7150/thno.56141

230. Awoyemi T, Tannetta D, Zhang W, et al. Glycosylated Siglec-6 expression in syncytiotrophoblast-derived extracellular vesicles from preeclampsia placentas. *Biochemical and Biophysical Research Communications*. Published online 2020. doi:10.1016/j.bbrc.2020.09.081

231. Tannetta DS, Dragovic RA, Gardiner C, Redman CW, Sargent IL. Characterisation of Syncytiotrophoblast Vesicles in Normal Pregnancy and Pre-Eclampsia: Expression of Flt-1 and Endoglin. Wang YL, ed. *PLoS ONE*. 2013;8(2):e56754. doi:10.1371/journal.pone.0056754

232. Salomon C, Kobayashi M, Ashman K, Sobrevia L, Mitchell MD, Rice GE. Hypoxia-induced changes in the bioactivity of cytotrophoblast-derived exosomes. *PLoS ONE*. Published online 2013. doi:10.1371/journal.pone.0079636

233. Brown CE, Carty DM, Scotland G. LB01.05: VASCULAR CONSEQUENCES OF PRE-ECLAMPSIA. *Journal of Hypertension*. Published online 2015. doi:10.1097/01.hjh.0000467467.39257.dd

234. Prieto-Vila M, Yoshioka Y, Ochiya T. Biological Functions Driven by mRNAs Carried by Extracellular Vesicles in Cancer. *Frontiers in Cell and Developmental Biology*. Published online 2021. doi:10.3389/fcell.2021.620498

235. Tsai S, Hardison NE, James AH, et al. Transcriptional profiling of human placentas from pregnancies complicated by preeclampsia reveals disregulation of sialic acid acetylesterase

and immune signalling pathways. *Placenta*. 2011;32(2):175-182. doi:10.1016/j.placenta.2010.11.014

236. Guo F, Zhang B, Yang H, et al. Systemic transcriptome comparison between early- And late-onset pre-eclampsia shows distinct pathology and novel biomarkers. *Cell Proliferation*. Published online 2021. doi:10.1111/cpr.12968

237. Gormley M, Ona K, Kapidzic M, Garrido-Gomez T, Zdravkovic T, Fisher SJ. Preeclampsia: novel insights from global RNA profiling of trophoblast subpopulations. *American Journal of Obstetrics and Gynecology*. Published online 2017. doi:10.1016/j.ajog.2017.03.017

238. Brew O, Sullivan MHF, Woodman A. Comparison of normal and pre-eclamptic placental gene expression: A systematic review with meta-analysis. *PLoS ONE*. Published online 2016. doi:10.1371/journal.pone.0161504

239. Munchel S, Rohrback S, Randise-Hinchliff C, et al. Circulating transcripts in maternal blood reflect a molecular signature of early-onset preeclampsia. *Science Translational Medicine*. Published online 2020. doi:10.1126/SCITRANSLMED.AAZ0131

240. Castellucci M, de Matteis R, Meisser A, et al. Leptin modulates extracellular matrix molecules and metalloproteinases: Possible implications for trophoblast invasion. *Molecular Human Reproduction*. Published online 2000. doi:10.1093/molehr/6.10.951

241. Masuyama H, Segawa T, Sumida Y, et al. Different profiles of circulating angiogenic factors and adipocytokines between early- and late-onset pre-eclampsia. *BJOG: An International Journal of Obstetrics and Gynaecology*. Published online 2010. doi:10.1111/j.1471-0528.2009.02453.x

242. Taylor BD, Ness RB, Olsen J, et al. Serum leptin measured in early pregnancy is higher in women with preeclampsia compared with normotensive pregnant women. *Hypertension*. Published online 2015. doi:10.1161/HYPERTENSIONAHA.114.03979

243. Kononikhin AS, Zakharova N v., Sergeeva VA, et al. Differential diagnosis of preeclampsia based on urine peptidome features revealed by high resolution mass spectrometry. *Diagnostics*. Published online 2020. doi:10.3390/diagnostics10121039

244. Chen W, Huang F, Huang J, et al. SLC45A4 promotes glycolysis and prevents AMPK/ULK1-induced autophagy in TP53 mutant pancreatic ductal adenocarcinoma. *Journal of Gene Medicine*. Published online 2021. doi:10.1002/jgm.3364

245. Bloxam DL, Bullen BE, Walters BNJ, Lao TT. Placental glycolysis and energy metabolism in preeclampsia. *American Journal of Obstetrics and Gynecology*. Published online 1987. doi:10.1016/S0002-9378(87)80354-X

246. Tejera E, Bernardes J, Rebelo I. Co-expression network analysis and genetic algorithms for gene prioritization in preeclampsia. *BMC Medical Genomics*. Published online 2013. doi:10.1186/1755-8794-6-51

247. Wei J, Fu Y, Mao X, Jing Y, Guo J, Ye Y. Decreased Filamin b expression regulates trophoblastic cells invasion through ERK/MMP-9 pathway in pre-eclampsia. *Ginekologia Polska*. Published online 2019. doi:10.5603/GP.2019.0006

248. Glare EM, Divjak M, Bailey MJ, Walters EH. β-actin and GAPDH housekeeping gene expression in asthmatic airways is variable and not suitable for normalising mRNA levels. *Thorax*. Published online 2002. doi:10.1136/thorax.57.9.765

249. Meller M, Vadachkoira S, Luthy DA, Williams MA. Evaluation of housekeeping genes in placental comparative expression studies. *Placenta*. 2005;26(8-9):601-607. doi:10.1016/J.PLACENTA.2004.09.009

250. Xie J, Xu Y, Wan L, Wang P, Wang M, Dong M. Involvement of follistatin-like 3 in preeclampsia. *Biochemical and Biophysical Research Communications*. Published online 2018. doi:10.1016/j.bbrc.2018.10.139

251. Founds SA, Ren D, Roberts JM, Jeyabalan A, Powers RW. Follistatin-like 3 across gestation in preeclampsia and uncomplicated pregnancies among lean and obese women. *Reproductive Sciences*. Published online 2015. doi:10.1177/1933719114529372

252. Wang Y, Lim R, Nie G. HtrA4 may play a major role in inhibiting endothelial repair in pregnancy complication preeclampsia. *Scientific Reports*. Published online 2019. doi:10.1038/s41598-019-39565-9

253. Singh H, Zhao M, Chen Q, et al. Human HtrA4 expression is restricted to the placenta, is significantly Up-regulated in early-onset preeclampsia, and high levels of HtrA4 cause endothelial dysfunction. *Journal of Clinical Endocrinology and Metabolism*. Published online 2015. doi:10.1210/jc.2014-3969

254. Benny PA, Alakwaa FM, Schlueter RJ, Lassiter CB, Garmire LX. A review of omics approaches to study preeclampsia. *Placenta*. Published online 2020. doi:10.1016/j.placenta.2020.01.008

255. Li X, Fang Y. Bioinformatics identification of potential genes and pathways in preeclampsia based on functional gene set enrichment analyses. *Experimental and Therapeutic Medicine*. Published online 2019. doi:10.3892/etm.2019.7749

256. Weissgerber TL, Mudd LM. Preeclampsia and Diabetes. *Current Diabetes Reports*. Published online 2015. doi:10.1007/s11892-015-0579-4

257. Baig S, Kothandaraman N, Manikandan J, et al. Proteomic analysis of human placental syncytiotrophoblast microvesicles in preeclampsia. *Clinical Proteomics*. Published online 2014. doi:10.1186/1559-0275-11-40

258. He P, Shao D, Ye M, Zhang G. Analysis of gene expression identifies candidate markers and pathways in pre-eclampsia. *Journal of Obstetrics and Gynaecology*. Published online 2015. doi:10.3109/01443615.2014.990430

259. Hurrell A, Beardmore-Gray A, Duhig K, Webster L, Chappell LC, Shennan AH. Placental growth factor in suspected preterm pre-eclampsia: a review of the evidence and practicalities of implementation. *BJOG*. 2020;127(13):1590-1597. doi:10.1111/1471-0528.16425

260. Raisch J, Darfeuille-Michaud A, Nguyen HTT. Role of microRNAs in the immune system, inflammation and cancer. *World J Gastroenterol*. 2013;19(20):2985-2996. doi:10.3748/WJG.V19.I20.2985

261. Bartel DP. MicroRNAs: target recognition and regulatory functions. *Cell*. 2009;136(2):215-233. doi:10.1016/J.CELL.2009.01.002

262. Srinivasan S, Treacy R, Herrero T, et al. Discovery and Verification of Extracellular miRNA Biomarkers for Non-invasive Prediction of Pre-eclampsia in Asymptomatic Women. *Cell Reports Medicine*. 2020;1(2). doi:10.1016/J.XCRM.2020.100013

263. Wei J, Blenkiron C, Tsai P, et al. Placental trophoblast debris mediated feto-maternal signalling via small RNA delivery: implications for preeclampsia. *Scientific Reports 2017 7:1*. 2017;7(1):1-12. doi:10.1038/s41598-017-14180-8

264. Cooke WR, Cribbs A, Zhang W, et al. Maternal circulating syncytiotrophoblast-derived extracellular vesicles contain biologically active 5'-tRNA halves. *Biochem Biophys Res Commun*. 2019;518(1):107-113. doi:10.1016/J.BBRC.2019.08.015

265. Zhang H, He Y, Wang J xia, et al. miR-30-5p-mediated ferroptosis of trophoblasts is implicated in the pathogenesis of preeclampsia. *Redox Biol*. 2020;29. doi:10.1016/J.REDOX.2019.101402

266. Murphy MSQ, Casselman RC, Tayade C, Smith GN. Differential expression of plasma microRNA in preeclamptic patients at delivery and 1 year postpartum. *Am J Obstet Gynecol*. 2015;213(3):367.e1-367.e9. doi:10.1016/J.AJOG.2015.05.013

267. Liu T, Li W, Zhang J, Zhang Y. MiR-222-3p Inhibits Trophoblast Cell Migration and Alleviates Preeclampsia in Rats Through Inhibiting HDAC6 and Notch1 Signaling. *Reprod Sci*. Published online November 18, 2021. doi:10.1007/S43032-021-00793-Y

268. Xu P, Zhao Y, Liu M, et al. Variations of microRNAs in human placentas and plasma from preeclamptic pregnancy. *Hypertension*. 2014;63(6):1276-1284. doi:10.1161/HYPERTENSIONAHA.113.02647

269. Takizawa T, Ishibashi O, Ohkuchi A, et al. Hydroxysteroid (17-β) dehydrogenase 1 is dysregulated by miR-210 and miR-518c that are aberrantly expressed in preeclamptic placentas: a novel marker for predicting preeclampsia. *Hypertension*. 2012;59(2):265-273. doi:10.1161/HYPERTENSIONAHA.111.180232

270. Sandrim VC, Luizon MR, Palei AC, Tanus-Santos JE, Cavallie RC. Circulating microRNA expression profiles in pre-eclampsia: evidence of increased miR-885-5p levels. *BJOG*. 2016;123(13):2120-2128. doi:10.1111/1471-0528.13903

271. Biró O, Fóthi Á, Alasztics B, Nagy B, Orbán TI, Rigó J. Circulating exosomal and Argonaute-bound microRNAs in preeclampsia. *Gene*. 2019;692:138-144. doi:10.1016/J.GENE.2019.01.012

272. Buhimschi IA, Nayeri UA, Zhao G, et al. Protein misfolding, congophilia, oligomerization, and defective amyloid processing in Preeclampsia. *Science Translational Medicine*. 2014;6(245). doi:10.1126/SCITRANSLMED.3008808/SUPPL_FILE/6-245RA92_TABLE_S6.ZIP

273. D'Angelo A, Ceccanti M, Petrella C, et al. Role of neurotrophins in pregnancy, delivery and postpartum. *Eur J Obstet Gynecol Reprod Biol*. 2020;247:32-41. doi:10.1016/J.EJOGRB.2020.01.046

274. Armant DR, Fritz R, Kilburn BA, et al. Reduced expression of the epidermal growth factor signaling system in preeclampsia. *Placenta*. 2015;36(3):270-278. doi:10.1016/J.PLACENTA.2014.12.006

275. Chen CP, Chen CY, Wu YH, Chen CY. Oxidative stress reduces trophoblast FOXO1 and integrin β3 expression that inhibits cell motility. *Free Radic Biol Med*. 2018;124:189-198. doi:10.1016/J.FREERADBIOMED.2018.06.006

276. Deer E, Vaka VR, McMaster KM, et al. Vascular endothelial mitochondrial oxidative stress in response to preeclampsia: a role for angiotension II type 1 autoantibodies. *Am J Obstet Gynecol MFM*. 2021;3(1). doi:10.1016/J.AJOGMF.2020.100275

277. Zhao M, Li L, Yang X, Cui J, Li H. FN1, FOS, and ITGA5 induce preeclampsia: Abnormal expression and methylation. *Hypertens Pregnancy*. 2017;36(4):302-309. doi:10.1080/10641955.2017.1385795

278. Wu K, Liu F, Wu W, Chen Y, Zhang W. Bioinformatics approach reveals the critical role of TGF-β signaling pathway in pre-eclampsia development. *Eur J Obstet Gynecol Reprod Biol*. 2019;240:130-138. doi:10.1016/J.EJOGRB.2019.06.034

279. PMNCH | Born Too Soon: The Global Action Report on Preterm Birth. *WHO*. Published online 2016. Accessed January 25, 2022. http://www.who.int/pmnch/knowledge/publications/preterm_birth_report/en/

280. Feig DS, Shah BR, Lipscombe LL, et al. Preeclampsia as a Risk Factor for Diabetes: A Population-Based Cohort Study. *PLoS Medicine*. Published online 2013. doi:10.1371/journal.pmed.1001425

281. Basit S, Wohlfahrt J, Boyd HA. Pre-eclampsia and risk of dementia later in life: Nationwide cohort study. *BMJ (Online)*. 2018;363. doi:10.1136/bmj.k4109

282. Saigal S, Doyle LW. An overview of mortality and sequelae of preterm birth from infancy to adulthood. *The Lancet*. 2008;371(9608). doi:10.1016/S0140-6736(08)60136-1

283. Keller S, Ridinger J, Rupp AK, Janssen JWG, Altevogt P. Body fluid derived exosomes as a novel template for clinical diagnostics. *Journal of Translational Medicine*. 2011;9. doi:10.1186/1479-5876-9-86

284. Tannetta D, Masliukaite I, Vatish M, Redman C, Sargent I. Update of syncytiotrophoblast derived extracellular vesicles in normal pregnancy and preeclampsia. *Journal of Reproductive Immunology*. 2017;119:98-106. doi:10.1016/J.JRI.2016.08.008

285. Stevens W, Shih T, Incerti D, et al. Short-term costs of preeclampsia to the United States health care system. *American Journal of Obstetrics and Gynecology*. 2017;217(3). doi:10.1016/j.ajog.2017.04.032

286. Hao J, Hassen D, Hao Q, et al. Maternal and Infant Health Care Costs Related to Preeclampsia. In: *Obstetrics and Gynecology*. Vol 134. ; 2019. doi:10.1097/AOG.0000000000003581

287. Gardiner C, Tannetta DS, Simms CA, Harrison P, Redman CWG, Sargent IL. Syncytiotrophoblast microvesicles released from pre-eclampsia placentae exhibit increased tissue factor activity. *PLoS ONE*. Published online 2011. doi:10.1371/journal.pone.0026313

288. Tong M, Chen Q, James JL, Stone PR, Chamley LW. Micro- and Nano-vesicles from First Trimester Human Placentae Carry Flt-1 and Levels Are Increased in Severe Preeclampsia. *Frontiers in Endocrinology*. 2017;8(JUL):174. doi:10.3389/FENDO.2017.00174

289. Salomon C, Torres MJ, Kobayashi M, et al. A gestational profile of placental exosomes in maternal plasma and their effects on endothelial cell migration. *PLoS ONE*. Published online 2014. doi:10.1371/journal.pone.0098667

290. Gill M, Motta-Mejia C, Kandzija N, et al. Placental syncytiotrophoblast-derived extracellular vesicles carry active NEP (Neprilysin) and are increased in preeclampsia. *Hypertension*. 2019;73(5). doi:10.1161/HYPERTENSIONAHA.119.12707

291. Money TT, King RG, Wong MH, et al. Expression and Cellular Localisation of Chloride Intracellular Channel 3 in Human Placenta and Fetal Membranes. *Placenta*. 2007;28(5-6):429-436. doi:10.1016/J.PLACENTA.2006.08.002

292. Dozynkiewicz MA, Jamieson NB, MacPherson I, et al. Rab25 and CLIC3 Collaborate to Promote Integrin Recycling from Late Endosomes/Lysosomes and Drive Cancer Progression. *Developmental Cell*. 2012;22(1):131. doi:10.1016/J.DEVCEL.2011.11.008

293. KHONG TY, de WOLF F, ROBERTSON WB, BROSENS I. Inadequate maternal vascular response to placentation in pregnancies complicated by pre-eclampsia and by small-for-gestational age infants. *BJOG: An International Journal of Obstetrics & Gynaecology*. 1986;93(10). doi:10.1111/j.1471-0528.1986.tb07830.x

294. Bauer JW, Lanschuetzer C. Type XVII collagen gene mutations in junctional epidermolysis bullosa and prospects for gene therapy. *Clinical and Experimental Dermatology*. 2003;28(1). doi:10.1046/j.1365-2230.2003.01192.x

295. Feng Y, Chen X, Wang H, et al. Collagen I Induces Preeclampsia-Like Symptoms by Suppressing Proliferation and Invasion of Trophoblasts. *Frontiers in Endocrinology*. 2021;12. doi:10.3389/fendo.2021.664766

296. Skogberg G, Lundberg V, Berglund M, et al. Human thymic epithelial primary cells produce exosomes carrying tissue-restricted antigens. *Immunology and Cell Biology*. 2015;93(8). doi:10.1038/icb.2015.33

297. Bruno S, Grange C, Deregibus MC, et al. Mesenchymal stem cell-derived microvesicles protect against acute tubular injury. *Journal of the American Society of Nephrology*. 2009;20(5). doi:10.1681/ASN.2008070798

298. Duijvesz D, Burnum-Johnson KE, Gritsenko MA, et al. Proteomic profiling of exosomes leads to the identification of novel biomarkers for prostate cancer. *PLoS ONE*. 2013;8(12). doi:10.1371/journal.pone.0082589

299. Musante L, Saraswat M, Duriez E, et al. Biochemical and physical characterisation of urinary nanovesicles following CHAPS treatment. *PLoS ONE*. 2012;7(7). doi:10.1371/journal.pone.0037279

300. Garnier D, Magnus N, Meehan B, Kislinger T, Rak J. Qualitative changes in the proteome of extracellular vesicles accompanying cancer cell transition to mesenchymal state. *Experimental Cell Research*. 2013;319(17). doi:10.1016/j.yexcr.2013.08.003

301. Nishizawa H, Pryor-Koishi K, Suzuki M, et al. Increased levels of pregnancy-associated plasma protein-A2 in the serum of pre-eclamptic patients. *Molecular Human Reproduction*. 2008;14(10). doi:10.1093/molehr/gan054

302. Nishizawa H, Pryor-Koishi K, Kato T, Kowa H, Kurahashi H, Udagawa Y. Microarray Analysis of Differentially Expressed Fetal Genes in Placental Tissue Derived from Early and Late Onset Severe Pre-eclampsia. *Placenta*. 2007;28(5-6). doi:10.1016/j.placenta.2006.05.010

303. Winn VD, Gormley M, Paquet AC, et al. Severe preeclampsia-related changes in gene expression at the maternal-fetal interface include sialic acid-binding immunoglobulin-like lectin-6 and pappalysin-2. *Endocrinology*. 2009;150(1):452-462. doi:10.1210/en.2008-0990

304. Várkonyi T, Nagy B, Füle T, et al. Microarray profiling reveals that placental transcriptomes of early-onset HELLP syndrome and preeclampsia are similar. *Placenta*. Published online 2011. doi:10.1016/j.placenta.2010.04.014

305. Whitehead CL, Walker SP, Ye L, et al. Placental specific mRNA in the maternal circulation are globally dysregulated in pregnancies complicated by fetal growth restriction. *Journal of Clinical Endocrinology and Metabolism*. 2013;98(3). doi:10.1210/jc.2012-2468

306. Niada S, Giannasi C, Magagnotti C, Andolfo A, Brini AT. Proteomic analysis of extracellular vesicles and conditioned medium from human adipose-derived stem/stromal cells and dermal fibroblasts. *Journal of Proteomics*. 2021;232. doi:10.1016/j.jprot.2020.104069

307. Stossel TP, Condeelis J, Cooley L, et al. Filamins as integrators of cell mechanics and signalling. *Nature Reviews Molecular Cell Biology*. 2001;2(2). doi:10.1038/35052082

308. Zhou X, Borén J, Akyürek LM. Filamins in Cardiovascular Development. *Trends in Cardiovascular Medicine*. 2007;17(7). doi:10.1016/j.tcm.2007.08.001

309. Zhou AX, Hartwig JH, Akyürek LM. Filamins in cell signaling, transcription and organ development. *Trends in Cell Biology*. 2010;20(2). doi:10.1016/j.tcb.2009.12.001

310. Iguchi Y, Ishihara S, Uchida Y, et al. Filamin B enhances the invasiveness of cancer cells into 3D collagen matrices. *Cell Structure and Function*. 2015;40(2). doi:10.1247/csf.15001

311. Ferguson RE, Carroll HP, Harris A, Maher ER, Selby PJ, Banks RE. Housekeeping proteins: A preliminary study illustrating some limitations as useful references in protein expression studies. *Proteomics*. 2005;5(2). doi:10.1002/pmic.200400941

312. Lanoix D, St-Pierre J, Lacasse AA, Viau M, Lafond J, Vaillancourt C. Stability of reference proteins in human placenta: General protein stains are the benchmark. *Placenta*. 2012;33(3). doi:10.1016/j.placenta.2011.12.008

313. Shen WJ, Azhar S, Kraemer FB. ACTH regulation of adrenal SR-B1. *Frontiers in Endocrinology*. 2016;7(MAY). doi:10.3389/fendo.2016.00042

314. Ganesan LP, Mates JM, Cheplowitz AM, et al. Scavenger receptor B1, the HDL receptor, is expressed abundantly in liver sinusoidal endothelial cells. *Scientific Reports*. 2016;6. doi:10.1038/srep20646

315. Ethier-Chiasson M, Duchesne A, Forest JC, et al. Influence of maternal lipid profile on placental protein expression of LDLr and SR-BI. *Biochemical and Biophysical Research Communications*. 2007;359(1). doi:10.1016/j.bbrc.2007.05.002

316. Husemann J, Silverstein SC. Expression of scavenger receptor class B, type I, by astrocytes and vascular smooth muscle cells in normal adult mouse and human brain and in Alzheimer's

disease brain. *American Journal of Pathology*. 2001;158(3). doi:10.1016/S0002-9440(10)64030-8

317. Landers KA, Li H, Mortimer RH, McLeod DSA, d'Emden MC, Richard K. Transthyretin uptake in placental cells is regulated by the high-density lipoprotein receptor, scavenger receptor class B member 1. *Molecular and Cellular Endocrinology*. 2018;474. doi:10.1016/j.mce.2018.02.014

318. Zhu L, Chen Y, Liu C, et al. Transthyretin as a novel candidate biomarker for preeclampsia. *Experimental and Therapeutic Medicine*. 2014;7(5). doi:10.3892/etm.2014.1558

319. Kalkunte SS, Neubeck S, Norris WE, et al. Transthyretin is dysregulated in preeclampsia, and its native form prevents the onset of disease in a preclinical mouse model. *American Journal of Pathology*. 2013;183(5). doi:10.1016/j.ajpath.2013.07.022

320. Wan Shumei, Peng Ping, Qiao Lin GY. Expression of miR-144, titin-Ab and MAPK signal transduction pathway related proteins in pre-eclampsia patients. *INTERNATIONAL JOURNAL OF CLINICAL AND EXPERIMENTAL MEDICINE*. 2019;11(127):11-20. www.ijcem.com /ISSN:1940-5901/IJCEM0098123

321. Shu C, Liu Z, Cui L, et al. Protein profiling of preeclampsia placental tissues. *PLoS ONE*. 2014;9(11). doi:10.1371/journal.pone.0112890

322. Lee A, Chow L, Skeith L, et al. Platelet Membrane Procoagulation in Preeclampsia. *Blood*. 2020;136(Supplement 1). doi:10.1182/blood-2020-137213

323. Zhang Z, Wang X, Zhang L, Shi Y, Wang J, Yan H. Wnt/β-catenin signaling pathway in trophoblasts and abnormal activation in preeclampsia (Review). *Molecular Medicine Reports*. 2017;16(2). doi:10.3892/mmr.2017.6718

324. Baczyk D, Audette MC, Coyaud E, Raught B, Kingdom JC. Spatiotemporal distribution of small ubiquitin-like modifiers during human placental development and in response to oxidative and inflammatory stress. *Journal of Physiology*. 2018;596(9). doi:10.1113/JP275288

325. VH R, RP W, DE B, BA P, L M. Post-Translational Modifications of the P2X(4) purinergic receptor subtype in the human placenta are altered in preeclampsia. *Placenta*. 2007;28(4):270-277. doi:10.1016/J.PLACENTA.2006.04.008

326. Robajac D, Vanhooren V, Masnikosa R, et al. Preeclampsia transforms membrane N-glycome in human placenta. *Experimental and Molecular Pathology*. 2016;100(1). doi:10.1016/j.yexmp.2015.11.029

327. Dymara-Konopka W, Laskowska M, Oleszczuk J. Preeclampsia - Current Management and Future Approach. *Curr Pharm Biotechnol*. 2018;19(10):786-796. doi:10.2174/1389201019666180925120109

328. Euser AG, Cipolla MJ. Magnesium sulfate for the treatment of eclampsia a brief review. *Stroke*. 2009;40(4):1169-1175. doi:10.1161/STROKEAHA.108.527788

329. Murthi P, Fitzpatrick E, Borg AJ, Donath S, Brennecke SP, Kalionis B. GAPDH, 18S rRNA and YWHAZ are Suitable Endogenous Reference Genes for Relative Gene Expression Studies in Placental Tissues from Human Idiopathic Fetal Growth Restriction. *Placenta*. 2008;29(9):798-801. doi:10.1016/J.PLACENTA.2008.06.007

330. Leeflang MMG, Cnossen JS, van der Post JAM, Mol BWJ, Khan KS, ter Riet G. Accuracy of fibronectin tests for the prediction of pre-eclampsia: a systematic review. *European Journal of Obstetrics and Gynecology and Reproductive Biology*. 2007;133(1):12-19. doi:10.1016/j.ejogrb.2007.01.003

331. Gredmark T, Bergman B, Hellström L. Total fibronectin in maternal plasma as a predictor for preeclampsia. *Gynecologic and Obstetric Investigation*. 1999;47(2):89-94. doi:10.1159/000010069

332. Chavarría ME, Lara-González L, González-Gleason A, Sojo I, Reyes A. Maternal plasma cellular fibronectin concentrations in normal and preeclamptic pregnancies: a longitudinal study for early prediction of preeclampsia. *Am J Obstet Gynecol*. 2002;187(3):595-601. doi:10.1067/mob.2002.123281

333. Schwarzbauer JE, DeSimone DW. Fibronectins, Their Fibrillogenesis, and In Vivo Functions. *Cold Spring Harbor Perspectives in Biology*. 2011;3(7):1-19. doi:10.1101/CSHPERSPECT.A005041

334. Wu H, Liu K, Zhang J. Excess fibronectin 1 participates in pathogenesis of pre-eclampsia by promoting apoptosis and autophagy in vascular endothelial cells. *Mol Hum Reprod*. 2021;27(6). doi:10.1093/MOLEHR/GAAB030

335. Pérez-Pérez A, Toro A, Vilariño-García T, et al. Leptin action in normal and pathological pregnancies. *Journal of Cellular and Molecular Medicine*. 2018;22(2):716. doi:10.1111/JCMM.13369

336. Martínez-Abundis E, González-Ortiz M, Pascoe-González S. Serum leptin levels and the severity of preeclampsia. *Archives of Gynecology and Obstetrics 2000 264:2*. 2000;264(2):71-73. doi:10.1007/S004040000081

337. Taylor BD, Ness RB, Olsen J, et al. Serum leptin measured in early pregnancy is higher in women with preeclampsia compared with normotensive pregnant women. *Hypertension*. 2015;65(3):594-599. doi:10.1161/HYPERTENSIONAHA.114.03979

338. Kaaja R, Laivuori H, Pulkki P, Tikkanen MJ, Hiilesmaa V, Ylikorkala O. Is there any link between insulin resistance and inflammation in established preeclampsia? *Metabolism - Clinical and Experimental*. 2004;53(11):1433-1435. doi:10.1016/J.METABOL.2004.06.009

339. Acromite M, Ziotopoulou M, Orlova C, Mantzoros C. Increased leptin levels in preeclampsia: associations with BMI, estrogen and SHBG levels. *Hormones (Athens)*. 2004;3(1):46-52. doi:10.14310/HORM.2002.11111

340. de Knegt VE, Hedley PL, Kanters JK, et al. The Role of Leptin in Fetal Growth during Pre-Eclampsia. *International Journal of Molecular Sciences*. 2021;22(9). doi:10.3390/IJMS22094569

341. Liu J, Song G, Meng T, Zhao G. Identification of Differentially Expressed Genes and Signaling Pathways in Placenta Tissue of Early-Onset and Late-Onset Pre-Eclamptic Pregnancies by Integrated Bioinformatics Analysis. *Medical Science Monitor : International Medical Journal of Experimental and Clinical Research*. 2020;26:e921997-1. doi:10.12659/MSM.921997

342. Buurma A, Cohen D, Veraar K, et al. Preeclampsia is characterized by placental complement dysregulation. *Hypertension*. 2012;60(5):1332-1337. doi:10.1161/HYPERTENSIONAHA.112.194324

343. Gerasimova EM, Fedotov SA, Kachkin D v., et al. Protein Misfolding during Pregnancy: New Approaches to Preeclampsia Diagnostics. *International Journal of Molecular Sciences*. 2019;20(24). doi:10.3390/IJMS20246183

344. Burton GJ, Yung HW. Endoplasmic reticulum stress in the pathogenesis of early-onset pre-eclampsia. *Pregnancy Hypertension*. 2011;1(1-2):72. doi:10.1016/J.PREGHY.2010.12.002

345. D'Oria R, Laviola L, Giorgino F, Unfer V, Bettocchi S, Scioscia M. PKB/Akt and MAPK/ERK phosphorylation is highly induced by inositols: Novel potential insights in endothelial dysfunction in preeclampsia. *Pregnancy Hypertension*. 2017;10:107-112. doi:10.1016/J.PREGHY.2017.07.001

346. Fu Y, Wei J, Dai X, Ye Y. Increased NDRG1 expression attenuate trophoblast invasion through ERK/MMP-9 pathway in preeclampsia. *Placenta*. 2017;51:76-81. doi:10.1016/J.PLACENTA.2017.01.126

347. Giovannini MG, Cerbai F, Bellucci A, et al. Differential activation of mitogen-activated protein kinase signalling pathways in the hippocampus of CRND8 transgenic mouse, a model of Alzheimer's disease. *Neuroscience*. 2008;153(3):618-633. doi:10.1016/J.NEUROSCIENCE.2008.02.061

348. Lyall F, Bulmer JN, Duffie E, Cousins F, Theriault A, Robson SC. Human trophoblast invasion and spiral artery transformation: the role of PECAM-1 in normal pregnancy, preeclampsia, and fetal growth restriction. *Am J Pathol*. 2001;158(5):1713-1721. doi:10.1016/S0002-9440(10)64127-2

349. Mukherjee I, Dhar R, Singh S, et al. Oxidative stress-induced impairment of trophoblast function causes preeclampsia through the unfolded protein response pathway. *Scientific Reports 2021 11:1*. 2021;11(1):1-20. doi:10.1038/s41598-021-97799-y

350. Depoix C, Tee MK, Taylor RN. Molecular regulation of human placental growth factor (PlGF) gene expression in placental villi and trophoblast cells is mediated via the protein kinase a pathway. *Reprod Sci*. 2011;18(3):219-228. doi:10.1177/1933719110389337

351. Barjaktarovic M, Korevaar TIM, Jaddoe VWV, de Rijke YB, Peeters RP, Steegers EAP. Human chorionic gonadotropin and risk of pre-eclampsia: prospective population-based cohort study. *Ultrasound Obstet Gynecol*. 2019;54(4):477-483. doi:10.1002/UOG.20256

352. Auger N, Low N, Paradis G, Ayoub A, Fraser WD. Preeclampsia and the longitudinal risk of hospitalization for depression at 28 years. *Soc Psychiatry Psychiatr Epidemiol*. 2021;56(3):429-436. doi:10.1007/S00127-020-01920-X

353. BUMETANIDE | Drug | BNF content published by NICE. Accessed January 25, 2022. https://bnf.nice.org.uk/drug/bumetanide.html

354. Paterson-Brown S, Robson SC, Redfern N, Walkinshaw SA, de Swiet M. Hydralazine boluses for the treatment of severe hypertension in pre-eclampsia. *Br J Obstet Gynaecol*. 1994;101(5):409-413. doi:10.1111/J.1471-0528.1994.TB11913.X